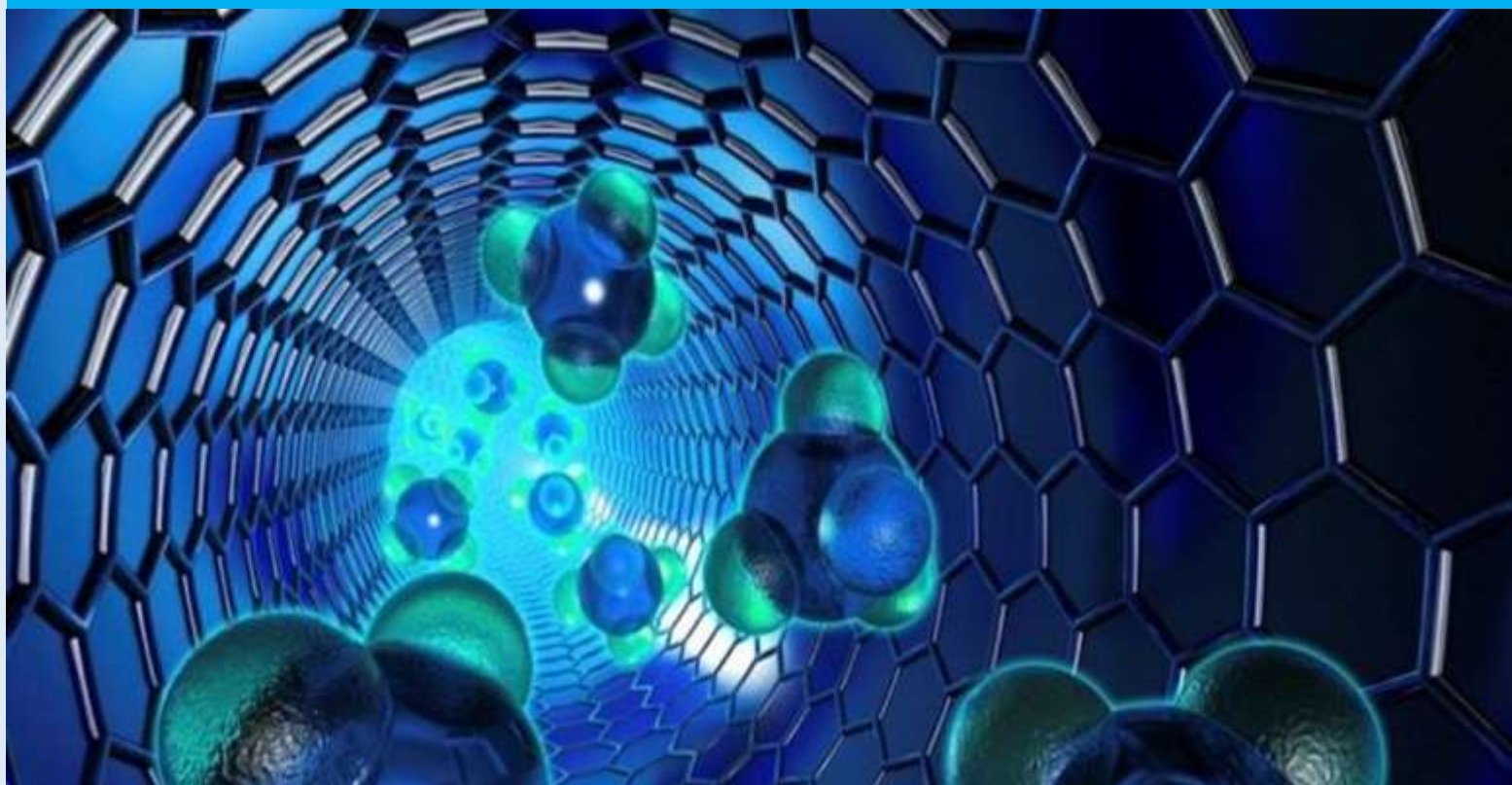


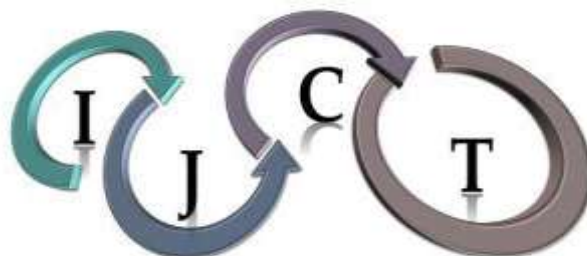
**e-ISSN: 2602-277X**

# *International Journal of Chemistry and Technology*



**Volume: 5, Issue: 2  
E - Journal**

**31 DECEMBER 2021  
<http://dergipark.org.tr/ijct>**



## International Journal of Chemistry and Technology

### JOURNAL INFO

<b>Journal Name</b>	International Journal of Chemistry and Technology
<b>Journal Initial</b>	IJCT
<b>Journal Abbreviation</b>	Int. J. Chem. Technol.
<b>ISSN (Online)</b>	2602-277X
<b>Year of Launching</b>	2017, August
<b>Editor-in-Chief and Managing Editor</b>	Prof. Dr. İbrahim Demirtaş
<b>Editor</b>	Dr. Oğuzhan KOÇER
<b>Manager of Publication</b>	Assist. Prof. Mehmet Akyüz
<b>Scope and Focus</b>	Chemistry, Material Science, Technology
<b>Review Type</b>	Peer Review Double-Blinded
<b>Ethical Rules</b>	Plagiarism check, copyright agreement form, conflict of interest, ethics committee report
<b>Access Type</b>	Open Access
<b>Publication Fee</b>	Free
<b>Article Language</b>	English
<b>Frequency of Publication</b>	Biannually
<b>Publication Issue</b>	June, December
<b>Publisher</b>	Prof. Dr. İbrahim Demirtaş
<b>Web Page</b>	<a href="http://dergipark.org.tr/ijct">http://dergipark.org.tr/ijct</a>
<b>Contact E-mail address</b>	ijctsubmission@gmail.com, ijctsubmission@yahoo.com
<b>Contact Address and Executive address</b>	Department of Chemistry, Faculty of Arts and Sciences, Iğdir University, 76000, Iğdir, Turkey
<b>Contact Telephone</b>	90 532 233 17 38 (Secretary)
<b>Publication Date</b>	31/12/2021
<b>Technical Editor</b>	Assist. Prof. Dr. Evrim BARAN AYDIN
<b>Spelling Editor</b>	MSc. Rabia Acemioğlu
<b>Language (Grammar) Editor</b>	Assist. Prof. Dr. Muhammet KARAMAN, Assist. Prof. Dr. Muhittin KULAK, Dr. Lawali YABO DAMBAGI
<b>Secretary</b>	MSc. Rabia ACEMIOĞLU

All detailed information including instructions for authors, aim and scopes, ethical rules, manuscript evaluation, indexing info, and manuscript template etc. can be found on the main web page of IJCT (<http://dergipark.gov.tr/ijct>).



## International Journal of Chemistry and Technology

**Volume: 5, Issue: 2, Year 2021**

### **Founder of IJCT**

Prof. Dr. Bilal ACEMIOĞLU

### **EDITORIAL BOARD**

#### **Editor-in-Chief**

Prof. Dr. İbrahim DEMİRTAŞ

(Organic Chemistry and Phytochemistry, Iğdır University, Iğdır, Turkey)

#### **Associate Editors**

Prof. Dr. M. Hakkı ALMA  
(Material Science and Technology  
K.Maraş Sütçü İmam/Iğdır University, Turkey)

Prof. Dr. Ekrem KÖKSAL  
(Biochemistry,  
Erzincan Binali Yıldırım University, Erzincan,  
Turkey)

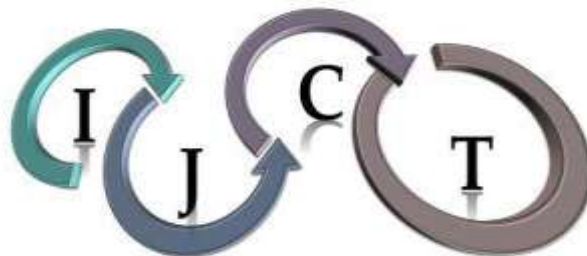
Prof. Dr. Fevzi KILIÇEL  
(Analytical Chemistry,  
Karamanoğlu Mehmet Bey Uni., Karaman, Turkey)

Prof. Dr. Mehmet SÖNMEZ  
(Inorganic Chemistry, Gaziantep  
University, Gaziantep, Turkey)

Prof. Dr. Yuh-Shan HO  
(Chemical and Environmental Engineering,  
Asia University, Taichung City, Taiwan)

Prof. Dr. Yahya GÜZEL  
(Theoretical Chemistry and Polymer Chemistry  
Erciyes University, Kayseri, Turkey)

Prof. Dr. Mustafa ARIK  
(Physical Chemistry,  
Atatürk University, Erzurum, Turkey)



## International Journal of Chemistry and Technology

### Advisory Editorial Board

Prof. Dr. Harun PARLAR  
(Technical University of Munich, München Germany)

Prof. Dr. Shaobin WANG  
(Curtin University, Perth, Australia)

Prof. Dr. Ana Beatriz Rodriguez MORATINOS  
(University of Exramadura, Badajoz, Spain)

Prof. Dr. Jon-Bae KIM  
(College of Health Sciences, South Korea)

Prof. Dr. Rashid AHMAD  
(University of Malakand, Chakdara, Pakistan)

Prof. Dr. Guang-Jie ZHAO  
(Beijing Forestry University, Beijing, China)

Prof. Dr. Jaine H. Hortolan LUIZ  
(Federal University of Alfenas, Unifal-MG, Brazil)

Prof. Dr. Papita DAS  
(Jadavpur University, Jadavpur, India)

Prof. Dr. Vagif ABBASOV  
(Nef-Kimya Prosesleri Institutu, Baku, Azerbaijan)

Prof. Dr. Atiqur RAHMAN  
(Islamic University, Kushita, Bangladesh)

Prof. Dr. Mika SILLANPAA  
(LUT Lappeenranta Uni.y of Technology, Lappeenranta, Finland)

Prof. Dr. Salah AKKAL  
(University of Mentouri Consatntine Consatntine, Algeria)

Prof. Dr. Gilbert Kapche DECCAUX  
(University of Yaounde I, Yaounde, Cameroon)

Prof. Dr. Gelu BOURCEANU  
(Alexandru Ioan Cuza University, Romania)

Prof. Dr. Ahmet ÇAKIR  
(Kilis 7 Aralik University, Kilis, Turkey)

Prof. Dr. M. SALIH AĞIRTAŞ  
(Yüzüncü Yıl University, Van, Turkey)

Prof. Dr. Nufullah SARAÇOĞLU  
(Atatürk University, Erzurum, Turkey)

Prof. Dr. Rahmi KASIMOĞULLARI  
(Dumlupınar University, Kütahya, Turkey)

Prof. Dr. Ahmet Baysar  
(Inonu University, Malatya, Turkey)

Prof. Dr. Hamdi TEMEL  
(Dicle University, Diyarbakır, Turkey)

Prof. Dr. Ö. İrfan KÜFREVİOĞLU  
(Atatürk University, Erzurum, Turkey)

Prof. Dr. Ömer ŞAHİN  
(Siirt University, Siirt, Turkey)

Prof. Dr. Anatoli DIMOGLU  
(Düzce University, Düzce, Turkey)

Prof. Dr. Mehmet UĞURLU  
(Sıtkı Kocman University, Muğla, Turkey)

Prof. Dr. Şükrü BEYDEMİR  
(Anadolu University, Eskişehir, Turkey)

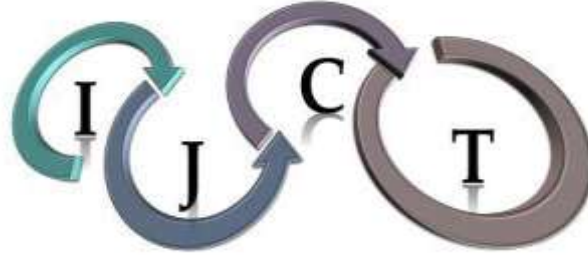
Prof. Dr. Ramazan SOLMAZ  
(Bingol University, Bingöl, Turkey)

Prof. Dr. Mahfuz ELMASTAŞ  
(Health Sciences University, İstanbul, Turkey)

Prof. Dr. Mehmet DOĞAN  
(Balıkesir University, Balıkesir, Turkey)

Prof. Dr. Giray TOPAL  
(Dicle University, Diyarbakır, Turkey)

Prof. Dr. Birgül YAZICI  
(Cukurova University, Adana, Turkey)



## International Journal of Chemistry and Technology

### Advisory Editorial Board

Prof. Dr. Barbaros NALBANTOĞLU  
(Yıldız Technical University, İstanbul, Turkey)

Prof. Dr. Murat ALANYALIOĞLU  
(Atatürk University, Erzurum, Turkey)

Prof. Dr. T. Abdulkadir ÇOBAN  
(Erzincan Binali Yıldırım University, Erzincan Turkey)

Prof. Dr. İsmet KAYA  
(18 Mart University, Çanakklae, Turkey)

Prof. Dr. Serhan URUŞ  
(Sütçü İmam University, K.Maraş, Turkey)

Prof. Dr. Ömer İŞILDAK  
(Gaziosmanpaşa University, Tokat, Turkey)

Prof. Dr. Halim AVCI  
(Kilis 7 Aralık University, Kilis, Turkey)

Prof. Dr. Ahmet TUTAR  
(Sakarya University, Sakarya, Turkey)

Prof. Dr. Duygu EKINCI  
(Atatürk University, Erzurum, Turkey)

Prof. Dr. Metin BÜLBÜL  
(Dumlupınar University, Kütahya, Turkey)

Prof. Dr. Ali KARA  
(Uludağ University, Bursa, Turkey)

Prof. Dr. Murat SARAÇOĞLU  
(Erciyes University, Kayseri, Turkey)

Prof. Dr. Murat SADIKOĞLU  
(Gaziosman Paşa University, Tokat, Turkey)

Prof. Dr. Mustafa KARATAŞ  
(Aksaray University, Aksaray, Turkey)

Assoc. Prof. Dr. Şenay ŞİMŞEK  
(North Dakota State University, Fargo, USA)

Assoc. Prof. Dr. Mahjoub JABLI  
(University of Monastir, Monastir, Tunisia)

Assoc. Prof. Dr. Muhammet KÖSE  
(Sütçü İmam University, K.Maraş, Turkey)

Assoc. Prof. Chin-Hung LAI  
(Chung Shan Medical University, Taiwan)

Assoc. Prof. Niyaz M. MAHMOODI  
(Institute for Color Science and Technology Tehran, Iran)

Assoc. Prof. Dr. Mustafa ÖZDEMİR  
(Süleyman Demirel University, Isparta, Turkey)

Assoc. Prof. Dr. Metin AÇIKYILDIZ  
(Kilis 7 Aralık University, Kilis, Turkey)

Assist. Prof. Masood Ayoub KALOO  
(Govt. Degree College Shopian, J & K, India)

Assist. Prof. Dr. Mutasem Z. BANI-FWAZ  
(King Khalid University, Asir-Abha, Saudi Arabia)

Assist. Prof. Dr. Bakhtiyor RASULEV  
(North Dakota State University, Fargo, USA)

Dr. Zineb TRİBAK  
(Sidi Mohamed Ben Abdellah University, Fez Morocco)

Dr. Sameer Ahmed AWAD  
(University of Anbar, Ramadi, Iraq)

Dr. Ramadan E. ASHERY  
(Damanhour University, Egypt)

## TABLE OF CONTENTS

### Research Articles

---

1. A novel nicotinoyl thiourea manganese complex: synthesis, characterization, and biological activity studies  
Fatma Betül ÖZGERİŞ, Merve YILDIRIM, Arzu GÖRMEZ, Bünyamin ÖZGERİŞ  
Pages: 83-90
2. Biodegradation of chlorpyrifos by bacterial genus *Pseudomonas putida*  
Yakup CUCİ, Sait ÇELİK  
Pages: 91-99
3. Evaluation of zero waste management system and Adana metropolitan municipality zero waste implementation  
Bülent SARI, Hatice Şebnem KÜPELİ, Hakan GÜNEY, Olcayto KESKİNKAN  
Pages: 100-107
4. Comparison of quality properties of the Iranian Saffron (*Crocus sativus* L.) and Saffron grown in macro and micro locations in Turkey  
Hasan ASİL, Ersen GÖKTÜRK  
Pages: 108-116
5. Phytochemical and GCMS analysis on the ethanol extract of *Foeniculum Vulgare* and *Petroselinum crispum* leaves  
Jamaluddeen ABUBAKAR, Great EDO, Nur PASAOGULULARI AYDINLIK  
Pages: 117-124
6. The role of *Lavandula* sp. extract for effective inhibiting the mild steel corrosion in the hydrochloric acid solution  
Demet ÖZKIR  
Pages: 125-132
7. Synthesis, spectral characterization, DFT, and molecular docking studies of 2-((2,3-Dihydrobenzo [b] [1,4] dioxin-6-yl) (1H-indol-1-yl) methyl) phenol compound  
Yeliz ULAŞ  
Pages: 133-140
8. Antioxidant activity of silver nanoparticles synthesized from *Tagetes erecta* L. leaves  
Ramazan ERENLER, Esmâ Nur GEÇER, Nusret GENÇ, Dürdane YANAR  
Pages: 141-146
9. Structural and spectral properties of 4-(4-(1-(4-Hydroxyphenyl)-1-phenylethyl)phenoxy)phthalonitrile: Analysis by TD-DFT method, ADME analysis and docking studies  
Kenan ALTUN, Ümit YILDIKO, Aslıhan Aycan TANRIVERDİ, İsmail ÇAKMAK  
Pages: 147-155

10. Resorcinol derivatives as human acetylcholinesterase inhibitor: An In Vitro and In Silico study  
Uğur GÜLLER  
Pages: 156-161
11. Comparison of chemical composition and nutritive values of some clover species  
İbrahim ERTEKİN  
Pages: 162-166
12. Variation of components in laurel (*Laurus nobilis* L.) fixed oil extracted by different methods  
Musa TÜRKMEN, Oğuzhan KOÇER  
Pages: 167-171
13. Production of organic light-emitting diode with fluorescence featured quinoline derivative  
Mustafa DOĞAN, Ümit ERDEM, Salih ÖKTEN  
Pages: 172-177





## A novel nicotinoyl thiourea manganese complex: synthesis, characterization, and biological activity studies

Fatma Betül ÖZGERİŞ<sup>1</sup>, Merve YILDIRIM<sup>2</sup>, Arzu GÖRMEZ<sup>2</sup>, Bünyamin ÖZGERİŞ<sup>3,\*</sup>

<sup>1</sup> Department of Nutrition and Dietetics, Faculty of Health Science, Ataturk University, Erzurum 25240, Turkey

<sup>2</sup> Department of Molecular Biology and Genetics, Faculty of Science, Erzurum Technical University, Erzurum 25050, Turkey

<sup>3</sup> Department of Basic Sciences, Faculty of Science, Erzurum Technical University, Erzurum 25050, Turkey

Received: 5 May 2020; Revised: 6 July 2021; Accepted: 10 July 2021

\*Corresponding author e-mail: bunyamin.ozgeris@erzurum.edu.tr

**Citation:** Özgeriş, F. B.; Yıldırım, M.; Görmez, A.; Özgeriş, B. *Int. J. Chem. Technol.* 2021, 5 (2), 83-90.

### ABSTRACT

In this study, nicotinoyl thiourea synthesized by starting from nicotinic acid and 3,5-dimethoxy aniline according to the literature. The resulting product was reacted with Manganese (II) acetate tetrahydrate and nicotinoyl thiourea manganese complex was synthesized with a metal-ligand ratio of 1: 1. The chemical structure of newly synthesized metal complex was characterized by FTIR, HRMS, XRD, and elemental analysis. In the second part of the study, the antibacterial and antioxidant activities of the synthesized metal complex were investigated. According to the obtained results, metal complex did not show any antibacterial activity. However, metal complex exhibited strong or equipotent antioxidant properties compared to standard antioxidants in DPPH, ABTS, and Cuprac methods. For this reason, metal complex can be evaluated as an antioxidant agent in food protection and the treatment of many diseases related oxidative stress.

**Keywords:** Thiourea, manganese, metal complex, antibacterial, antioxidant.

### Yeni bir nikotinoyl tiyoüre mangan kompleksi: sentez, karakterizasyon ve biyolojik aktivite çalışmaları

#### ÖZ

Bu çalışmada nikotinoil tiyoüre, nikotinic asit ve 3,5-dimetoksi anilinden başlanarak literatüre göre sentezlenmiştir. Elde edilen ürün Mangan (II) asetat tetrahidrat ile tepkimeye sokularak 1:1 metal-ligand oranıyla nikotinoyl tiyoüre mangan kompleksi sentezlenmiştir. Sentezlenen yeni metal kompleksinin kimyasal yapısı FTIR, HRMS, XRD ve elementel analiz ile karakterize edilmiştir. Çalışmanın ikinci bölümünde sentezlenen metal kompleksin antibakteriyel ve antioksidan aktiviteleri araştırılmıştır. Elde edilen sonuçlara göre metal kompleksi herhangi bir antibakteriyel aktivite göstermemiştir. Bununla birlikte metal kompleksi DPPH, ABTS ve kuprak metodlarında standart antioksidanlara göre güçlü veya eşit potansiyelli antioksidan özellikler sergilemiştir. Bu nedenle, metal kompleksi gıdanın korunması ve oksidatif stres ile ilişkili birçok hastalığın tedavisinde bir antioksidan ajan olarak değerlendirilebilir.

**Anahtar Kelimeler:** Tiyoüre, mangan, metal kompleks, antibakteriyel, antioksidan.

### 1. INTRODUCTION

Thiourea with general formula of  $(R_1R_2N)(R_3R_4N)C=S$  is an important group having a sulphur atom. If the carbonyl group is attached to thiourea, it is called 1-(acyl or aryl) substituent thiourea.<sup>1</sup> Thioureas are important substances for the synthesis of heterocyclics.<sup>2</sup> They can coordinate with transition metals because of using both

oxygen and sulphur atoms.<sup>3</sup> To the best of our knowledge, thiourea derivatives have also a wide spread of usability in the synthetic organic chemistry, agrochemical industries, building blocks in the synthesis of low molecular weight compounds, and pharmaceutical industry because of their activities such as antithyroid, antihemolytic, and antioxidant.<sup>4</sup> The literature includes various derivatives associated with aryl thioureas



having many biological activities such as anti-intestinal nematode<sup>4</sup>, antibacterial and antifungal<sup>5</sup>, hepatitis C virus inhibitor<sup>6</sup>, urease inhibitor<sup>7</sup>, and histamine H<sub>3</sub>, H<sub>4</sub> receptors.<sup>8</sup>

It is known that benzoyl thioureas form complexes with various transition metals such as Ni, Co, Ag and Mn due to carbonyl, thiocarbonyl, and amine groups.<sup>9</sup> Previous studies demonstrate that many metal complexes of benzoyl thioureas have been reported.<sup>10-12</sup> Although benzoyl thioureas and metal complexes are well-known in the literature, there is no experimental data about metal complexes of nicotinoyl thioureas. Nicotinoyl thioureas including a pyridine ring instead of a benzene ring were synthesized in our previously study due to have many biological activity, especially such as antibacterial activity.<sup>13</sup> Therefore, it was aimed to synthesize novel manganese complex of synthesized nicotinoyl thiourea. Antioxidants are important substances for the human body. Free radicals are harmful materials produced by cells. Oxidative stress may occur as a result of the body's inability to effectively remove these free radicals that damage cell and body functions.<sup>13</sup> The principal aim of this study was to synthesize the metal complex and compare the ligand and metal complex in terms of their biological activities. Therefore, we also aimed to comparison of their antibacterial, and antioxidant properties.

## 2. MATERIALS AND METHODS

### 2.1. Chemicals

Nicotinic acid, thionyl chloride (SOCl<sub>2</sub>), potassium thiocyanate (KSCN), Manganese (II) acetate tetrahydrate [Mn(CH<sub>3</sub>COO)<sub>2</sub>·4H<sub>2</sub>O], 3,5-dimethoxyaniline, dms<sub>o</sub>-d<sub>6</sub> and all solvents were bought commercially and it was used just like that. TLC was carried out on silica gel plates with F-254 indicator and compounds were monitored with UV lamp. <sup>1</sup>H and <sup>13</sup>C NMR were recorded on a Bruker 400 MHz instrument and reported in DMSO-*d*<sub>6</sub>. Chemical shifts are reported in ppm by using TMS as an internal standard. The melting points were recorded on an electrothermal melting point apparatus (Electrothermal IA9100) in sealed capillaries and are uncorrected. HRMS were performed on Agilent 6530 Accurate-Mass instrument. FT-IR (Fourier transform) spectra were obtained on a Shimadzu IRTracer-100 spectrometer with GladiATR 10. Elemental analysis (C, H, N) was obtained on a Leco CHNS 932 instrument. XRD spectrum was obtained from GNR Explorer XRD Instrument.

### 2.2. Synthesis of nicotinoyl chloride (2)

This compound (2) was synthesized from nicotinic acid (1) and SOCl<sub>2</sub> as describes previously.<sup>14</sup>

### 2.3. Synthesis of 3-isothiocyanatopyridine (nicotinoyl isothiocyanate) (3)

Compound (3) was synthesized from nicotinoyl chloride (2) and KSCN as describes previously.<sup>15</sup>

### 2.4. Synthesis of N-Nicotinoyl-N'-(3,5-dimethoxyphenyl) thiourea (Ligand) (5)

N-Nicotinoyl-N'-(3,5-dimethoxyphenyl) thiourea (ligand) (5) was synthesized according to the literature.<sup>13</sup> All spectral data are in accordance with the literature.

### 2.5. Synthesis of complex [Mn(L)CH<sub>3</sub>COO]·2H<sub>2</sub>O (6)

Nicotinoyl thiourea (5) (2 eqv.) was dissolved in 15 ml DMF to which a solution of Manganese (II) acetate tetrahydrate (Mn(CH<sub>3</sub>COO)<sub>2</sub>·4H<sub>2</sub>O) (1 eqv.), dissolved in H<sub>2</sub>O (20 ml), was added drop by drop while stirring powerfully, at room temperature. The mixture was refluxed for additional 3 hours, followed by addition of distilled H<sub>2</sub>O (100 ml). After cooling in a refrigerator to 4°C for 24 hours, the dark solid residual was collected by centrifugation and washed three times with distilled water (3 ml). As a result of this procedure, the product was obtained as a deep brown-black powder. Yield; 81%, Mp; >400°C. FT-IR spectrum,  $\nu$ , cm<sup>-1</sup>: 1683 (s) (C=O), 1558 (s) (C=N). Analysis Calculated for C<sub>17</sub>H<sub>22</sub>MnN<sub>3</sub>O<sub>7</sub>S %: C 43.69; H 4.74; N 8.99; S 6.86. Found, %: C 43.72; H 4.72; N 8.96; S 6.88. HR-MS (ES<sup>+</sup>), m/z (calc./found): 467.0559/467.2182.

### 2.6. Antibacterial activity studies

To determine antibacterial activity, agar well diffusion method was applied as described previously.<sup>16</sup> In this context, Mueller Hinton Agar (MHA) were standardized to a cell density of 1.5x10<sup>8</sup>/mL (McFarland No. 0.5), the turbidity of the bacteria was qualified at 600 nm. Wells (6 mm diameter) were burrowed in the plates and these were filled with the samples (100  $\mu$ l). Netilmicin (NET30), Ofloxacin (OFX) and Cefsulodin (CFS) were drew on as positive standard antibiotics, and negative control was 10% (v/v) DMSO solution. The three different concentrations of previously synthesized compound and newly synthesized manganese complex were evaluated against five different bacterial strains. Incubation of the bacterial strains was carried out at 37°C during 24-72 hours. At the end of this period, the diameters of the zones were measured in millimeters. All experiments were done three times according to the described procedure.<sup>16</sup>

### 2.7. Bacterial Strains

As clinical pathogenic bacteria were used *Acinetobacter baumannii* (ATCC 1609), *Enterococcus faecalis* (ATCC 49462), *Escherichia coli* (ATCC 2523), *Methicillin-*

resistant *Staphylococcus aureus* (MRSA) (ATCC 67106), and *Pseudomonas aeruginosa* (ATCC 9027).

## 2.8. Minimum inhibitory concentrations (MICs)

MIC values of the ligand and manganese complex were determined by using sterile 96-well plates. The compounds **5–6** were arranged ranging from 31.25 to 1000  $\mu\text{g/ml}$ , inoculated at 1% (v/v) with an inoculum of  $10^8$  CFU/ml and at 37 °C during 24 hours were incubated. All of this experimental procedure and necessary calculations were prepared according to the manuals. To determine the minimum inhibitory concentration values, lowest concentration of compounds that inhibited visual bacterial growth was then observed.<sup>17, 18</sup>

## 2.9. Antioxidant activity studies

To determine total radical scavenging capacity of the ligand and its manganese complex, 1,1-diphenyl-2-picrylhydrazyl (DPPH<sup>•</sup>) method was used as described earlier. Radical scavenging capacity was compared with butylated hydroxytoluene, trolox, beta carotene, and ascorbic acid.<sup>19</sup> The solution of DPPH<sup>•</sup> was daily prepared and kept in the dark at 4°C. 0.1mM of DPPH fresh solution was prepared in ethanol. After that, an aliquot (0.5 ml) (6.25–200  $\mu\text{g/ml}$ ) was added to test tubes containing 1.5 ml of ligand and its newly synthesized manganese complex in ethanol. With vigorous stirring, resulting mixtures were then incubated in the dark for half an hour. As a result, the absorbance values were measured at 517 nm by spectrophotometer.<sup>20</sup>

2,2'-azinobis-(3-ethylbenzothiazoline-6-sulphonate) radical (ABTS<sup>•+</sup>) scavenging procedure have been improved by Re *et al.*<sup>21</sup> In order to form the ABTS cation radical (ABTS<sup>•+</sup>), 2 mM of ABTS solution in H<sub>2</sub>O was reacted with oxidizing agent of 2.3 mM of potassium persulfate (K<sub>2</sub>S<sub>2</sub>O<sub>8</sub>). Prepared (ABTS<sup>•+</sup>) was soluble in aqueous and organic solvents. To adjust desired absorbance ( $0.700 \pm 0.025$ ) at 734 nm, it was diluted with phosphate buffer (0.1 mM, pH 7.4). Finally, 3 ml of tested samples' solution between 6.25–200  $\mu\text{g/ml}$  concentrations was treated to 1 ml of ABTS<sup>•+</sup> and the resulting absorbance was measured at 734 nm by spectrophotometer.

By using the following equation, the capability to radical scavenge in the DPPH and ABTS<sup>•+</sup> assays was calculated:  $\text{R.S.E (\%)} = [(A.c - A.s) / A.c] \times 100$  where R.S.E is radical scavenging efficacy, A.C is the absorbance value of the control and A.S is the absorbance value of the sample.<sup>22</sup> All calculations were done according to this equations.

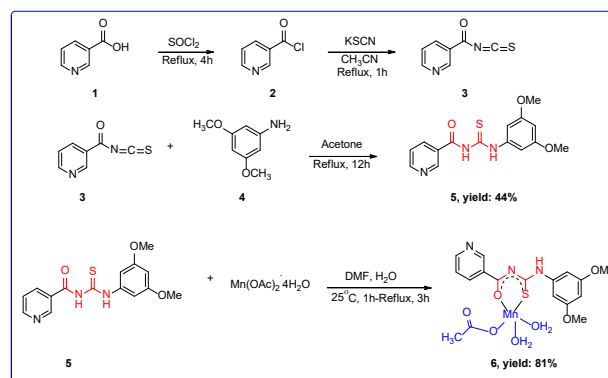
In order to determine the half maximal scavenging concentration of sample (IC<sub>50</sub>), inhibition percentage against all compounds concentrations ( $\mu\text{g/ml}$ ) was plotted.<sup>23</sup>

To determine antioxidant capacity, cupric ions (Cu<sup>2+</sup>) reducing power assay as another method was used to earlier synthesized thiourea and its novel manganese complex. Cu<sup>2+</sup> reducing capability was performed as described earlier.<sup>24</sup> This method is based on the reduction of Cu<sup>2+</sup> to Cu<sup>+</sup>. In this context, copper (II) chloride (CuCl<sub>2</sub>) solution (0.01 M, 0.25 ml), ammonium acetate (CH<sub>3</sub>COONH<sub>4</sub>) buffer solution (1 M, 0.25 ml), and ethanolic neocuproine solution ( $7.5 \times 10^{-3}$  M, 0.25 ml) were transferred to a test tube, which contains compounds **5–6** between 6.25–200  $\mu\text{g/ml}$  concentrations. Distilled water was added to complete the final volume to 2 ml, and then shaken. After half an hour, absorbance values were measured at 450 nm.

## 3. RESULTS AND DISCUSSION

### 3.1. Characterization

In this study, nicotinoyl thiourea (ligand) was synthesized according to the literature.<sup>13</sup> Manganese complex of ligand was synthesized. The synthetic routes are given in Scheme 1. The structure of complex was elucidated by FT-IR, HRMS, elemental analysis, and XRD. Nicotinoyl chloride (**2**) was prepared from nicotinic acid (**1**) according to the literature.<sup>14</sup> Nicotinoyl isothiocyanate (**3**) was synthesized with KSCN<sup>15</sup>, and then reacted with 3,5-dimethoxy aniline (**4**) in acetone at about 65°C to give nicotinoyl thiourea (**5**).<sup>13</sup> The ligand on interaction with Mn(CH<sub>3</sub>COO)<sub>2</sub>·4H<sub>2</sub>O yields manganese complex (**6**) corresponding to the 1:1 metal-ligand ratio.<sup>9, 25</sup> TLC (thin layer chromatography) was used to monitor the reactions. Similar to the literature, the complex is air stable, with deeply dark colored, and insoluble in both H<sub>2</sub>O and most of commercially available the organic solvents but were sparingly soluble in DMSO and DMF.<sup>25</sup> In order to obtain the single crystal of the complex made many attempts but this was unsuccessful. Therefore, we do not use X-ray structure determination.



Scheme 1. Synthetic routes to the target product.

FT-IR spectrum of the ligand (**5**) (nicotinoyl thiourea) displayed the absorption band for the stretching of NH at

3201  $\text{cm}^{-1}$ . A strong band observed in the region of 1682  $\text{cm}^{-1}$  in the FT-IR spectrum of the ligand (**5**) was assigned to the carbonyl group. This C=O band was shifted to the lower frequency range of 1506  $\text{cm}^{-1}$  in the spectra of the complex (**6**), consistent with the coordination of oxygen atom to the manganese ion. Moreover, a strong band observed in the region of 1683  $\text{cm}^{-1}$ . This band was assigned to the C=O stretching vibration of acetate attached to manganese complex. In addition, the characteristic band for C=S appeared at 1161  $\text{cm}^{-1}$  in the spectrum of ligand was shifted to 1153  $\text{cm}^{-1}$  on complexation, indicating relation of sulphur atom in coordination. Moreover, nitrile band formed on complex was observed in the region of 1558  $\text{cm}^{-1}$ . IR spectra of compounds are in agreement with the literature.<sup>26, 27</sup> The XRD pattern of ligand (nicotinoyl thiourea) and its manganese complex exhibits sharp intense peaks throughout the spectrum showing crystalline sample. Additional peaks and shifts in the spectrum are observed when the ligand is attached to manganese (Figure 1).<sup>28</sup>

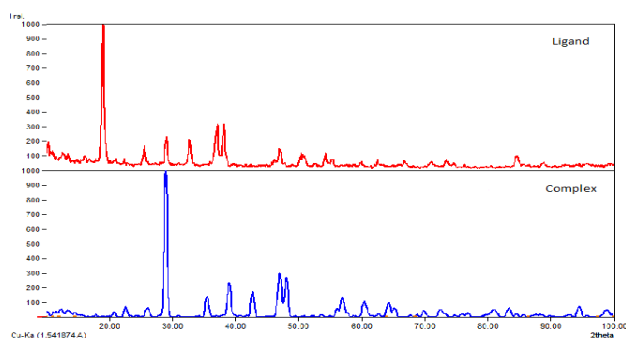


**Figure 1.** XRD pattern of ligand and its complexation with manganese, respectively.

Trial and error method was used to index X-ray diffraction main peaks.<sup>28</sup> Table 1 is shown the crystal size, hkl and 2-theta maximum.

**Table 2.** Antibacterial activity of compounds 5-6.

Bacteria	Compound	Concentrations ( $\mu\text{g/mL}$ ) <sup>a</sup>			MIC <sup>b</sup>	Negative Control <sup>c</sup>	Positive Control <sup>d</sup>		
		1000	500	250			OFX	NET	CFS
<i>Acinetobacter baumannii</i>	5	25	20	18	31.25	-	9	7	8
	6	-	-	-	-				
<i>Enterococcus faecalis</i>	5	28	19	10	31.25	-	11	10	9.5
	6	-	-	-	-				
<i>Escherichia coli</i>	5	29	23	20	31.25	-	9.8	7	7.7
<i>Pseudomonas aureus</i>	5	27	21	17	31.25	-	10	10	9
	6	25	18	15	31.25	-	11	18	9
	6	-	-	-	-				

Evidenced by our previously studies that nicotinoyl thioureas comprising aniline ring having methoxy group at different positions have stronger activity than benzoyl thioureas.<sup>13, 32</sup> It has been determined that compounds containing thiocarbonyl, carbonyl and amine groups have

**Table 1.** XRD peaks and crystal thickness calculated from Scherer's formula

Compound	2-theta maximum	hkl	Crystal size ( $\text{\AA}$ )
Ligand ( <b>5</b> )	18.99	200	5.2
$[\text{Mn}(\text{L})\text{OAc}] \cdot 2\text{H}_2\text{O}$ ( <b>6</b> )	28.99	85	3.08

### 3.2. Biological evaluations

Table 2 is shown the antibacterial activity results for ligand **5** and its manganese complex **6** against five different bacterial strains. Three Gram negative bacteria (*E. coli* ATCC 2523, *A. baumannii* ATCC 1609, and *P. aeruginosa* ATCC 9027) and two Gram positive bacteria (*S. aureus* ATCC 67106, and *E. faecalis* ATCC 49462) were used for antibacterial activity. The results revealed that ligand **5** showed highly strong antibacterial activity against tested bacterial strains<sup>13</sup>, whereas manganese complex did not show any activity.

The MICs of ligand **5** were evaluated at concentration 31.25  $\mu\text{g/ml}$ . The previously synthesized compound **5** inhibited the growth of bacteria with an inhibition zone varying between 25–29 mm, 18–23 mm, and 10–20 mm for concentrations of 1000, 500 and 250  $\mu\text{g} / \text{ml}$ , respectively.<sup>13</sup> A study have shown that the presence of methoxy substituent on benzene reduces the activity due to electron donating group. They have also reported that a pair of electrons that does not participate in bonding are resonating on benzene ring.<sup>29</sup> In another study have determined that the presence of the 4-methoxy group in benzoyl thiourea compounds with aniline groups reduces antibacterial activity (MIC: generally >1000  $\mu\text{g/ml}$ ).<sup>30</sup> Conversely, our compound contains a pyridine ring instead of a benzene ring. Commercially available large number of drugs with antimicrobial, and antioxidant activity in the market contain a pyridine ring.<sup>31</sup>

antibacterial properties especially against gram-negative bacteria<sup>33</sup> because they react with nucleophilic and electrophilic centers of bacterial surface<sup>34</sup> and induce antibacterial activity. Thus, we think that this may be the reason why our ligand shows antibacterial activity. On

the other hand, its manganese complex did not any show antibacterial activity. Notably a report demonstrate that the ligand may be more reactive with the microelements present in the environment or the formed complexes may have an extraordinary coordination that may be inert to cell components. They also concluded that the ligand prepared may be more reactive with microelements essential for bacterial nutrition.<sup>9</sup> Therefore, our manganese complex may not have shown any antibacterial activity because the thiocarbonyl, carbonyl, and amine groups are participated on complexation. This knowledge supports our conclusion why while our ligand has antibacterial activity, our complex does not have antibacterial activity.

Antioxidant properties are very important because of remove harmful effects of free radicals. To determine the free radical scavenging efficacy of various antioxidant materials, DPPH<sup>•</sup> and ABTS<sup>•+</sup> assays have been widely used and these assays are important to screen of antioxidant properties of plant extractions, organic compounds etc. Antioxidant activity of previously synthesized compound **5**<sup>13</sup>, novel manganese complex **6**, and standard antioxidants such as butylated hydroxytoluene, beta carotene, trolox, and ascorbic acid were specified with DPPH<sup>•</sup> and ABTS<sup>•+</sup> assays. Samples were analysed for their antioxidant activity ranging from 6.25–200 µg/ml concentrations. Figure 2 shows a significant decreasing ( $p < 0.05$ ) in the concentration of 1,1-diphenyl-2-picrylhydrazyl (DPPH<sup>•</sup>) radical because of the scavenging ability of previously synthesized thiourea compound by our group, newly synthesized manganese complex, and standards. The scavenging efficacy of samples **5–6** and standards on the 1,1-diphenyl-2-picrylhydrazyl (DPPH<sup>•</sup>) radical reduced in the order of Ascorbic acid > trolox > **6** > **5** > butylated hydroxytoluene > beta carotene, which were 94.95%, 94.41%, 85.36%, 76.69%, 66.03%, 65% at the concentration of 200 µg/ml, respectively. Absorbance values of samples also decreased with an increasing concentration. Figure 2 shows the radical scavenging activity according to the DPPH<sup>•</sup> method. IC<sub>50</sub> values in DPPH<sup>•</sup> method were determined as 4.49 µg/ml ( $r^2$ :

0.9985) for **5**, 4.77 µg/ml ( $r^2$ : 0.9785) for **6**, 4.65 µg/ml ( $r^2$ : 0.9765) for ascorbic acid, 4.69 µg/ml ( $r^2$ : 0.9962) for trolox, 4.59 µg/ml ( $r^2$ : 0.9912) for butylated hydroxytoluene, and 4.65 µg/ml ( $r^2$ : 0.9796) for beta carotene. Radical scavenging efficacy of samples **5–6** and standards in the DPPH<sup>•</sup> method decreased in the following order: **5** > butylated hydroxytoluene > beta carotene > ascorbic acid > trolox > **6**. A lower the IC<sub>50</sub> value indicates a higher the antioxidant activity of samples (Table 3). These results have demonstrated that previously synthesized thiourea compound and its novel manganese complex have equipotent or weak free radical scavenging capabilities compared with standard antioxidants. Samples **5–6** were determined to show effective radical scavenging activity against 2'-azinobis-(3-ethylbenzothiazoline-6-sulphonate) radical (ABTS<sup>•+</sup>) ( $p > 0.001$ ). As can be seen in Figure 2, the samples **5–6** have effective ABTS<sup>•+</sup> radical scavenging activity depending on the concentration (6.25-200 µg/ml). The scavenging efficacy of samples **5–6** and standards on the 2,2'-azinobis-(3-ethylbenzothiazoline-6-sulphonate) (ABTS<sup>•+</sup>) radicals reduced in the order of butylated hydroxytoluene > beta carotene > **6** > ascorbic acid > trolox > **5** > which were 99.72%, 99.66%, 88.08%, 73.86%, 72.44%, 65.72% at the concentration of 200 µg/ml, respectively. Absorbance values of samples **5–6** also decreased with an increasing concentration. IC<sub>50</sub> values for compounds **5–6** were calculated as 5.27 µg/ml ( $r^2$ : 0.9381) for **5**, 4.89 µg/ml ( $r^2$ : 0.9421) for **6**. Additionally, IC<sub>50</sub> values were found as 3.28 µg/ml ( $r^2$ : 0.8094) for butylated hydroxytoluene, 4.94 µg/ml ( $r^2$ : 0.9841) for ascorbic acid, 4.72 µg/ml ( $r^2$ : 0.9795) for trolox, and 3.63 µg/ml ( $r^2$ : 0.9197) for beta carotene (Table 3). The 2,2'-azinobis-(3-ethylbenzothiazoline-6-sulphonate) (ABTS<sup>•+</sup>) scavenging efficacy of samples **5–6** and standards reduced in the following order: butylated hydroxytoluene > beta carotene > trolox > **6** > ascorbic acid > **5**. A lower the IC<sub>50</sub> value indicates a higher the antioxidant activity of samples. It is seen that newly synthesized manganese complex on ABTS<sup>•+</sup> scavenging effect have more stronger than compared to ascorbic acid, while close to butylated hydroxytoluene, beta carotene, and trolox.

**Table 3.** Determination of half maximal concentrations (IC<sub>50</sub>, µg/ml) of compounds **5–6** and standards for DPPH<sup>•</sup> and ABTS<sup>•+</sup> scavenging.

Antioxidant compounds	DPPH <sup>•</sup> scavenging		ABTS <sup>•+</sup> scavenging	
	IC <sub>50</sub>	$r^2$	IC <sub>50</sub>	$r^2$
Ascorbic acid	4.65	0.9765	4.94	0.9841
Trolox	4.69	0.9962	4.72	0.9795
BHT	4.59	0.9912	3.28	0.8094
β-Carotene	4.65	0.9796	3.63	0.9197
<b>5</b>	4.49	0.9985	5.27	0.9381
<b>6</b>	4.77	0.9785	4.89	0.9421



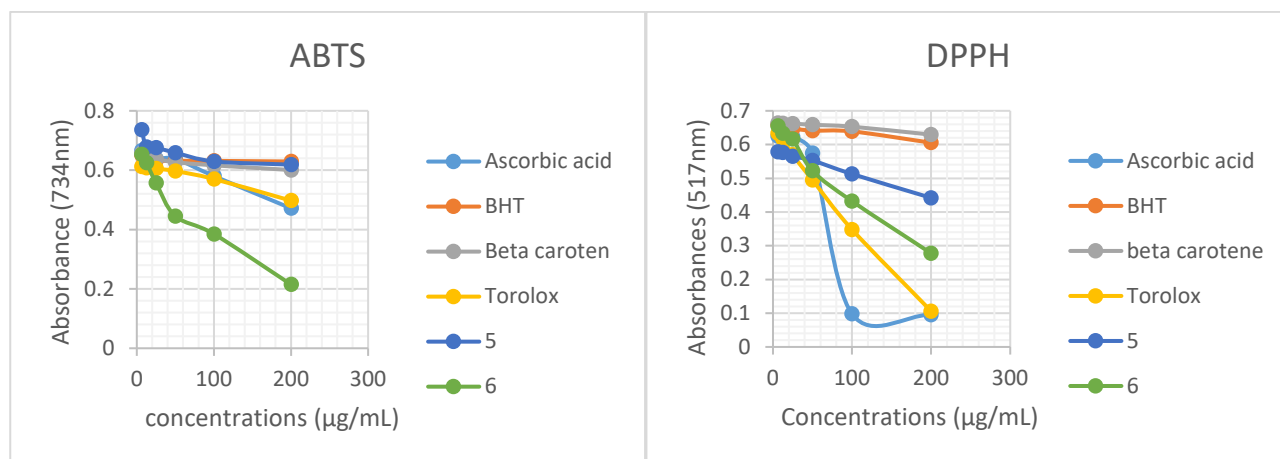


**Figure 2.** ABTS and DPPH free radical scavenging activity of different concentrations (6.25–200 µg/ml) of compound 5–6 and reference antioxidants; Trolox, BHT, β-Carotene and Ascorbic acid (BHT: butylated hydroxytoluene; DPPH: 1,1-diphenyl-2-picrylhydrazyl free radical; ABTS: 2,2'-azino-bis(3-ethylbenzthiazoline-6-sulphonate)).

The values of the CUPRAC method are shown in Table 4. As the oxidizing agent was used the chromogenic neocuproine. Ligand 5 exhibited higher activity than beta carotene and butylated hydroxytoluene, while less active than trolox and ascorbic acid. On the other hand, novel metal complex 6 showed weaker activity than its ligand and all standards. The ascorbic acid solution had the highest CUPRAC value. The reducing power decreased in the order of ascorbic acid > trolox > 5 > butylated hydroxytoluene > beta carotene > 6 for the same concentration (200 µg/ml). The results obtained in DPPH (1,1-diphenyl-2-picrylhydrazyl), ABTS (2,2'-azinobis(3-ethylbenzothiazoline-6-sulphonate)), and CUPRAC (cupric ions ( $\text{Cu}^{2+}$ ) reducing power) method revealed that previously synthesized ligand and its newly synthesized manganese complex have stronger, equipotent or weaker activity than the standards.

**Table 4.** Determination of reducing power of 200 µg/ml concentration of compounds 5–6 and standards by cupric ions ( $\text{Cu}^{2+}$ ) reducing capacity by Cuprac method.

Antioxidants	$\text{Cu}^{2+}$ - $\text{Cu}^+$ reducing	
	$\lambda_{450}^*$	$r^2$
Trolox	$0.517 \pm 0.002$	0.999
BHT	$0.109 \pm 0.001$	0.995
β-Carotene	$0.102 \pm 0.001$	0.997
Ascorbic acid	$3.613 \pm 0.002$	0.974
5	$0.158 \pm 0.004$	0.907
6	$0.079 \pm 0.001$	0.950

To the best of our knowledge from the literature, N,N'-disubstituted and benzoyl thioureas have antioxidant activities and they are an important compounds to inhibit the production of the most well-known oxygen free radicals.<sup>35</sup> In addition, heterocyclic compounds having a pyridine ring exhibit more antioxidant properties compared with benzene ring.<sup>36</sup> We demonstrated this situation in our previously reports.<sup>13, 32</sup> It is known that the central metal atom in metal complexes contributes

positively to antioxidant activity as a result of enhancing the proton donating capacity of the ligand.<sup>37</sup> As with benzoyl or N, N'-disubstituted thioureas, both manganese complex 6 and our previously synthesized nicotinoyl thiourea 5 were determined to have antioxidant activities.

#### 4. CONCLUSIONS

In this study, nicotinoyl thiourea 5, earlier synthesized by our group, was designed as ligand. Its manganese complex 6 has been synthesized for the first time. According to the experimental evaluations, the ligand 5 coordinate to the manganese (II) ion through carbonyl and thiocarbonyl groups of nicotinoyl thiourea. The chemical structure of manganese complex was characterized by FTIR, HRMS, XRD, and elemental analysis. According to these characterizations, the metal:ligand ratio was 1:1. Antibacterial activity studies of these compounds show that earlier synthesized compound 5 have antibacterial activity against all tested bacteria, whereas its manganese complex 6 has not any antibacterial activity. Therefore, while the ligand can be considered as an agent in the treatment of bacterial infections, its manganese complex cannot. In contrast to this situation, manganese complex showed equipotent antioxidant properties compared to standard antioxidants. For this reason, compound 6 can be evaluated as an antioxidant agent in food protection and the treatment of many diseases related oxidative stress. Further research and clinical trials are required to clarify the potential of the compounds in the diseases associated with oxidative stress. Moreover, the synthesis of this complex will lead to the synthesis of more efficient new metal complexes.

#### ACKNOWLEDGEMENTS

We would like to thank High Technology Research Center (YÜTAM, Erzurum Technical University) for XRD measurements and East Anatolia High Technology

Application and Research Center (DAYTAM, Atatürk University) for HRMS analysis. We would like to thank Prof. Dr. Ferhan Tümer for his helpful discussions.

### Conflict on interest

The authors declare that there is no conflict of interest with any person, institution, and company, etc.

### REFERENCES

- Schroeder, D. C. *Chem. Rev.* **1955**, *55* (1), 181-228.
- Murru, S.; Singh, C. B.; Kavala, V.; Patel, B. K. *Tetrahedron* **2008**, *64* (8), 1931-1942.
- Saeed, A.; Flörke, U.; Erben, M. F. *J. Sulphur Chem.* **2014**, *35* (3), 318-355.
- Duan, L. P.; Xue, J.; Xu, L. L.; Zhang, H. B. *Molecules* **2010**, *15* (10), 6941-6947.
- Cunha, S.; Macedo, F. C.; Costa, G. A. N.; Rodrigues, M. T.; Verde, R. B. V.; de Souza Neta, L. C.; Vencato, I.; Lariucci, C.; Sá, F. P. *Monatsh. Chem.* **2007**, *138* (5), 511-516.
- Wyles, D. L.; Kaihara, K. A.; Schooley, R. T. *Antimicrob. Agents Chemother.* **2008**, *52* (5), 1862-1864.
- Brito, T. O.; Souza, A. X.; Mota, Y. C. C.; Morais, V. S. S.; de Souza, L. T.; de Fatima, A.; Macedo, F.; Modolo, L. V. *RSC Adv.* **2015**, *5* (55), 44507-44515.
- Lim, H. D.; Istyastono, E. P.; van de Stolpe, A.; Romeo, G.; Gobbi, S.; Schepers, M.; Lahaye, R.; Menge, W.; Zuiderveld, O. P.; Jongejan, A.; Smits, R. A.; Bakker, R. A.; Haaksma, E. E. J.; Leurs, R.; de Esch, I. J. P. *Bioorg. Med. Chem.* **2009**, *17* (11), 3987-3994.
- Elhusseiny, A. F.; Eldissouky, A.; Al-Hamza, A. M.; Hassan, H. *J. Mol. Struct.* **2015**, *1100*, 530-545.
- Ozpozan, N.; Arslan, H.; Ozpozan, T.; Merdivan, M.; Kulcu, N. *J. Therm. Anal. Calorim.* **2000**, *61* (3), 955-965.
- Ozpozan, N.; Arslan, H.; Ozpozan, T.; Ozdes, N.; Kulcu, N. *Thermochim. Acta* **2000**, *343* (1-2), 127-133.
- Ozpozan, N.; Ozpozan, T.; Arslan, H.; Karipein, F.; Kulcu, N. *Thermochim. Acta* **1999**, *336* (1-2), 97-103.
- Ozgeris, B. *J. Antibiot.* **2021**, *74* (4), 233-243.
- Tumer, F.; Goksu, S.; Secen, H. *Russ Chem Bull.* **2005**, *54* (10), 2466-2467.
- Xue, S.-j.; Guan, Q. *Chinese J. Org. Chem.* **2002**, *22* (9), 646-650.
- CLSI, Performance Standards for Antimicrobial Susceptibility Testing. 27 ed.; Clinical and Laboratory Standards Institute,: Wayne, PA, 2017.
- Gormez, A.; Bozari, S.; Yanmis, D.; Gulluce, M.; Sahin, F.; Agar, G. *Pol. J. Microbiol.* **2015**, *64* (2), 121-127.
- Zgoda, J. R.; Porter, J. R. *Pharm. Biol.* **2001**, *39* (3), 221-225.
- Gülçin, İ. *Life Sci.* **2006**, *78* (8), 803-811.
- Gülçin, İ. *Toxicology* **2006**, *217* (2), 213-220.
- Re, R.; Pellegrini, N.; Proteggente, A.; Pannala, A.; Yang, M.; Rice-Evans, C. *Free Radic. Biol. Med.* **1999**, *26* (9), 1231-1237.
- Gülçin, İ.; Mshvildadze, V.; Gepdiremen, A.; Elias, R. *Phytomedicine* **2006**, *13* (5), 343-351.
- Aksu, K.; Ozgeris, B.; Taslimi, P.; Naderi, A.; Gulcin, I.; Goksu, S. *Arch. Pharm. (Weinheim)* **2016**, *349* (12), 944-954.
- Tohma, H. S.; Gulçin, I. *Int. J. Food Prop.* **2010**, *13* (4), 657-671.
- Nozha, S. G.; Morgan, S. M.; Ahmed, S. E. A.; El-Mogazy, M. A.; Diab, M. A.; El-Sonbati, A. Z.; Abou-Dobara, M. I. *J. Mol. Struct.* **2020**, 129525.
- Selvakumaran, N.; Bhuvanesh, N. S. P.; Karvembu, R. *Dalton Trans.* **2014**, *43* (43), 16395-16410.
- Yeşilkaynak, T. *J. Turkish Chem. Soc. Sect. Chem.* **2016**, *3* (3), 1-14.
- Cullity, B. D., *Elements of X-Ray Diffraction*. 2nd Edition ed.; Addison-Wesley Publishing Company, Inc. : Reading, MA, 1978.
- Rauf, M. K.; Talib, A.; Badshah, A.; Zaib, S.; Shoaib, K.; Shahid, M.; Florke, U.; Imtiaz ud, D.; Iqbal, J. *Eur. J. Med. Chem.* **2013**, *70*, 487-496.
- Obradovic, D.; Nikolic, S.; Milenkovic, I.; Milenkovic, M.; Jovanovic, P.; Savic, V.; Roller, A.; Crnogorac, M. D.; Stanojkovic, T.; Grguric-Sipka, S. *J. Inorg. Biochem.* **2020**, 210.
- Altaf, A. A.; Shahzad, A.; Gul, Z.; Rasool, N.; Badshah, A.; Lal, B.; Khan, E. *J. Drug Des. Med. Chem. (JDDMC)* **2015**, *1* (1), 1-11.



32. Özgeriş, B. *Russ. J. Org. Chem.* **2021**, 57 (3), 422-429.

33. Zhong, Z.; Xing, R.; Liu, S.; Wang, L.; Cai, S.; Li, P. *Carbohydr. Res.* **2008**, 343 (3), 566-570.

34. Ngaini, Z.; Arif, M. A. M.; Hussain, H.; Mei, E. S.; Tang, D.; Kamaluddin, D. H. A. *Phosphorus Sulfur Silicon Relat. Elem.* **2012**, 187 (1), 1-7.

35. Venkatesh, P.; Pandeya, S. N. *Int. J. Chemtech Res.* **2009**, 1 (3), 733-741.

36. Mojarab, M.; Soltani, R.; Aliabadi, A. *Jundishapur J. Nat. Parm. Prod.* **2013**, 8 (3), 125-130.

37. Chen, W. J.; Sun, S. F.; Cao, W.; Liang, Y.; Song, J. R. *J. Ml. Struct.* **2009**, 918 (1-3), 194-197.



## Biodegradation of chlorpyrifos by bacterial genus pseudomonas putida

Yakup CUCİ<sup>1,\*</sup>, Sait ÇELİK<sup>1</sup> Kahramanmaraş Sutcu Imam University, Environmental Engineering Department, 46100, Kahramanmaraş, Turkey

Received: 29 July 2021; Revised: 09 September 2021; Accepted: 10 September 2021

\*Corresponding author e-mail: [cuci@ksu.edu.tr](mailto:cuci@ksu.edu.tr)Citation: Cuci, Y.; Çelik, S. *Int. J. Chem. Technol.* 2021, 5 (2), 91-99.

## ABSTRACT

Chlorpyrifos is an solid organophosphorus pesticide widely used in agriculture. It is relatively stable to hydrolysis in neutral pH and acidic aqueous solutions. Stability decreases with increasing pH. Chlorpyrifos practically insoluble in water, but highly soluble in most organic solvents such as acetone xylene and methyl bromide. It is an effective skin, stomach and respiratory insecticide and is effective against aphids, spider mites, soil bugs and house pests. It is also highly toxic bees and fish. Most pesticides are complex organic molecules and are persistent in the environment, either biota or accumulate in the environment. In pesticide-used areas, the pesticide itself or its residues are transported by rain and irrigation water and mixes into groundwater. The effects caused by the pesticide are closely related to the level of accumulation. During the studies, contamination of chlorpyrifos has been found about 24 km from the site of its application. There are many physico-chemical and biological approaches to remove organophosphorus pesticides from the ecosystem, among them most promising is biodegradation. In this study, the biodegradation potential of chlorpyrifos with *P. Putida* was investigated in the batch stirred reactor. In the optimum conditions, the maximum pesticide removal rate was determined as 1.51 mg g<sup>-1</sup>. d. m.o.h.

**Keywords:** Pesticides, Chlorpyrifos, P. Putida, biodegradation.

## Pseudomonas putida ile chlorpyrifos'un biyodegradasyonu

## ÖZ

Chlorpyrifos tarımda yaygın olarak kullanılan katı bir organofosforlu pestisitir. Chlorpyrifos nötral ve asidik çözeltilerde kararlı olmasına rağmen pH artışı ile kararlılığı azalmaktadır. Chlorpyrifos pratik olarak suda çözünmez fakat aseton ksilen ve metil bromür gibi çoğu organik çözücünde oldukça yüksek miktarda çözünmektedir. Temas, sindirim ve solunum etkili bir insektisit olup yaprak bitleri, kırmızı örümcek, toprak böcekleri ve ev haşerelerine karşı etkilidir. Aynı zamanda arılar ve balıklara karşı da toksiktir. Pestisitler gibi pestisit kalıntıları da çok yönlü ve karmaşık özelliğe sahip olup birikim de yapabilmektedirler. Pestisit kullanılmış alanlarda bu ilacın kendisi veya kalıntıları yağmur ve sulama sularıyla yeraltı sularına karışarak sucul bitki ve hayvanlar için toksik etkiler oluşturmaktadır. Pestisit neden olduğu etkiler canlıdaki birikim düzeyine ve canlının yağ içeriği ile yakından ilişkilidir. Yapılan çalışmalarda Klorpyrifos kontaminasyonu uygulama alanından yaklaşık 24 km uzaklıkta tespit edilmiştir. Organofosforlu bileşiklerin ekosistem giderilmesinde birçok fiziko kimyasal ve biyolojik proses rol oynamaktadır. Ancak bunlar arasında en umut verici yöntemler biyobozunma yöntemleridir. Bu çalışmada chlorpyrifosun *Pseudomonas putida* ile biyodegradasyon potansiyeli incelenmiştir. Optimum şartlarda chlorpyrifosun *P. putida* ile biyodegradasyonunda maksimum pestisit tüketim hızı 1,51 mg/g. K. mo.sa. olarak bulunmuştur.

**Anahtar Kelimeler:** Pestisitler, Chlorpyrifos, P. Putida, biyodegradasyon

## 1. INTRODUCTION

Pesticides (or biocides) are synthetic, organic compounds used to destroy undesirable organisms. The word pesticide is of Latin origin and means a disease-killing substance. These produced substances are completely foreign to nature. These substances, their chemical and

biological change products (metabolites) are of interest not only in terms of their biocidal effects, but also in terms of their targets and effects within the overall ecosystem.<sup>1</sup> More than 10,000 insects, 600 weeds, more than 1500 plant diseases and 1500 species of nematodes are known that can harm humans, animals and plants in varying degrees.

Millions of tons of pesticides have been used in the world, especially in the last 40-45 years. Turkey, which is an agricultural country, has taken its share from this amount. Residues of pesticides have been detected all over the world, including at the poles. Pesticides also adversely affect non-targeted organisms by mixing with air, water and soil during manufacture, storage, marketing and use. When unconscious and careless use is added to this, it is seen that pesticides accumulate at increasing rates in water, soil, plant and animal foods.<sup>2</sup> Pesticides, pesticides that are thrown in our environment aimlessly, unlimitedly and almost uncontrollably, are found in almost all items.<sup>3</sup>

In order to protect natural resources from pollution, it is important to use chemicals used for agricultural purposes in a controlled manner and to prevent further pollution. Some properties of pesticides such as extreme mobility, durability and evaporation cause negative consequences in terms of environmental pollution. In minimizing the pesticide pollution potential, it is also necessary to take into account the expected benefit from pesticide use.<sup>4-6</sup> There is no doubt that agricultural pesticides, which have wide spread routes in the environment, have negative effects on all living things. Pesticides accumulated in water and soil pass into the bodies of creatures such as fish and insects living in these environments. Therefore, birds that feed on these creatures that carry the drug residue are also poisoned. Beneficial insects such as predators and parasitic insects, which have a more sensitive structure, are also highly affected by unconscious spraying.<sup>7</sup> In addition, the uncontrolled use of pesticides causes soil, air, surface and underground water pollution. Controlled use of chemicals used in agriculture is very important to prevent further pollution of these natural resources. As a result of the use of pesticides indiscriminately and in excessive doses without scientific control, negative effects on beneficial living things and other elements of the environment occur as well as pests. However, the most important, perhaps the most important issue for human health is the environmental pollution of the pesticides used and their undesirable effects on the natural balance. While some of these substances have mutagenic and carcinogenic effects in the living body, some of them both accumulate and cause toxic effects in the living body.<sup>8</sup> Artificial chemicals used in agricultural areas are quite durable as a result of their molecular structure and maintain their structural properties under natural conditions. As a result of this stability, they participate in natural cycles thanks to their structure not deteriorating for years. Due to their structural durability, they cause significant pollution in soil, water, groundwater and surface waters.<sup>9</sup>

The most important feature sought in pesticides is that they are very toxic and effective against harmful animals and organisms. In addition, it is expected to be less toxic or harmless to warm-blooded animals, especially humans. However, among the drugs produced so far,

those with these qualities are very few. For this reason, it should be accepted that pesticides are poisonous to humans and all other living things as a general rule. Because it is clear that drugs with biological activity will cause some potential dangers and cause some undesirable problems such as environmental contamination as a result of their use, and this has been well established recently.<sup>7</sup>

Agrochemicals are applied directly to the soil surface or into the soil, on the plant, or on the seedlings in the form of seed spraying. A significant part of the drug thrown on the plant falls into the soil. Drugs that fall into the soil can move in the soil over time, depending on factors such as soil type, solubility, permanence and climate.<sup>10</sup> After the pesticides applied to the plant, soil or seed for agricultural struggle have fulfilled their lethal effects, some of the pesticides are absorbed by the various organs of the plant, and the remaining part is distributed in the application area in the form of removal from the soil, retention in the soil and transformation into other compounds.<sup>11</sup>

The structure, mode of action and properties of the active substances of pesticides are different from each other. Pesticide active substances that contaminate the plant surface stay there for a certain period of time, some of them enter the plant, and some dissolve in water and translocate into the plant through roots, leaves or branches. In this way, the effective substances of pesticides found with the plant gradually decrease over time with removal mechanisms such as being washed with rain, leaking, dripping, being carried by the wind, evaporation, oxidation under the sun, hydrolyzed by high humidity, or decomposing by mixing with plant secretions after completing their activities. The important point here is that the existing pesticide residues are present in all kinds of foodstuffs at a level that will not harm human, animal and environmental health before coming to the market for consumption. For this reason, each drug is subjected to toxicological and pharmacological trials before being put on the market. These trials are carried out on experimental animals in the form of feeding with medicated product for a short period of 2-3 months and for a long period of at least 2 years.<sup>12</sup> The effects caused by pesticides are closely related to the accumulation level and the oil content of the living thing.<sup>13</sup>

Artificial organic pesticides are usually produced as concentrated (technical) substances. The active ingredient content of a formulated commercial pesticide can vary between 1 and 95 percent by weight and is applied as powder, granule, solution, emulsion or wettable fine powder.<sup>10</sup> According to the researches, the way of application of the drug contributes to the environmental pollution as well as the efficiency. It is obligatory to work on the use of other drugs that do not

form pesticide residues and to continue this struggle with biological methods.<sup>14</sup>

Biological degradation of pesticides is under the influence of factors that affect normal microbial activity in soil. As is well known, these factors are temperature, moisture content, organic matter present, pH, etc. are factors. Most pesticides are new compounds for soil microorganisms. Therefore, biodegradation is slow at first due to the lack of adaptation of microorganisms. Some polar groups such as -OH, -COO, -NH<sub>2</sub> and -NO<sub>2</sub> contained in pesticide molecules form the action points for organisms. Studies show that the pesticide concentration in the soil decreases with the addition of easily decomposable organic materials.<sup>1</sup> While microorganisms have an effect on pesticide concentrations due to their activities, pesticides also greatly affect the biological activity and microbial composition of the soil. The main purpose of metabolic processes in the world of microorganisms is energy production and cell synthesis. The vast majority of organic materials are capable of meeting these two purposes of heterotrophic bacteria. However, the most striking feature of microorganisms is that they go through an acclimation process. In other words, if substances that are resistant to biological decomposition are applied slowly and in very low concentrations to a certain microorganism species, it is certain that microorganism species that have adapted to them over time and can use these substances as energy and nutrients will develop.<sup>15</sup> Fallmann and co-workers<sup>16</sup> investigated the applicability of the Photo-Fenton method to treat pesticide-containing waters in their study. They successfully applied this Photo-Fenton process including Fe<sup>+2</sup>/H<sub>2</sub>O<sub>2</sub>/UV-V to 10 commercial pesticide mixtures. Experiments with a single pesticide yielded notable differences in reaction rates, although each pesticide degraded. Aksu (2005)<sup>17</sup> states that biosorption studies are also carried out for pesticides, and that it is possible to remove some pesticides with a few microorganism species including bacteria and fungi.

Bellinaso and co-workers<sup>18</sup> investigated the biodegradation of trifluralin herbicide with bacteria isolated from soil. They found that five bacteria isolated from the soil could be used in the biodegradation of trifluralin, and three of these isolated bacteria increased the degradation of trifluralin by more than 20%. Sanchez and co-workers<sup>19</sup>, in their study investigating the effect of sewage sludge on pesticide biodegradation in soil, found that the biodegradation of pesticide residues caused changes in the microorganism population of the soil.

In this study, it was aimed to biodegrade free *P. putida* and chlorpyrifos pesticide in cut cup. Substrate consumption is a result of the activities of microorganisms and reactions in cell metabolism. In the study, pesticide biodegradation occurred in aerobic environment with microorganism species were

determined. For this reason, the maximum growth rate and pesticide removal of the microorganism were determined without acclimatization and after acclimatization of the selected pesticide in aerobic environment. In addition, the possibility of acclimatized bacteria to use this pesticide as a single substrate was determined.

## 2. MATERIALS AND METHODS

After *P. putida* bacteria are grown in media containing chlorpyrifos pesticide, the effects of temperature, initial pH, agitation speed, initial pesticide concentration and different media parameters on microorganism growth and pesticide consumption rates were examined in batch system, and optimum temperature, initial pH, shaking speed were examined. and initial pesticide concentrations were determined. Determining the amount and types of degradation products of chlorpyrifos pesticide, which was exposed to physical and microbiological effects throughout the entire experimental study, was excluded from the scope of this study due to the difficulties encountered in the analysis.

In order to obtain a lower concentration solution from the stock solutions by dilution, the stock solutions were taken from the deep freezer and kept under laboratory conditions enough for their temperature to reach room temperature. Standard solutions were prepared separately at concentrations of 10, 20, 30, 40 and 50 mg L<sup>-1</sup> by diluting the stock solutions at room temperature.

### 2.1. Preparation of samples for gas chromatography analysis

It is very important to determine the exact and precise amounts of pesticides in pesticide analysis. (Table 1) Since the pesticide concentrations to be found as a result of the analysis are generally low, pesticide analysis is difficult. Quantitative analysis of pesticides by gas chromatography; It is done by obtaining chromatograms of pesticide standards prepared at known concentrations in gas chromatography and by comparing the peak length (or peak area) of the solution with unknown concentration and the peak length (or peak area) of the solution with known concentration.<sup>20</sup>

For this, standard pesticide solutions prepared at different concentrations were injected into gas chromatography and chromatograms were obtained. Peak areas or peak sizes obtained for pesticides from the chromatograms were plotted against pesticide concentration. Thus, a calibration curve was obtained for each pesticide.

Pesticide concentration in the samples was determined by calculating the pesticide amount corresponding to this peak area or height by substituting the peak area or peak size of the sample in the equation obtained from the calibration curve.

**Table 1.** Optimum determination conditions in gas chromatography of Chlorpyrifos insecticide

<b>Detector</b>	Flame Ionization Detector (FID)
<b>Column</b>	Restek Brand Rtx-5MS (Crossbond 5% diphenyl 95% dimethyl polysiloxane) programmable temperature 350 °C, decomposition temperature 330 °C
<b>Column Dimensions</b>	0.25 mm inner diameter - 30 m length
<b>Temperatures</b>	
Injection Unit	300 °C
Column	280 °C
Detector	300 °C
<b>Gas Flow Rates</b>	
Air	330 ml min <sup>-1</sup>
Hydrogen	33 mL min <sup>-1</sup>
Carrier Gas (N <sub>2</sub> )	1.4 mL min <sup>-1</sup> (10 lb/in <sup>2</sup> )
Carrier Gas + Reference Gas	30 mL min <sup>-1</sup>
<b>Injection Technique</b>	
Split	1/25
Recorder	0.5
Paper Speed AT	64
Retention Time	5,17 min

## 2.2. Microorganism production

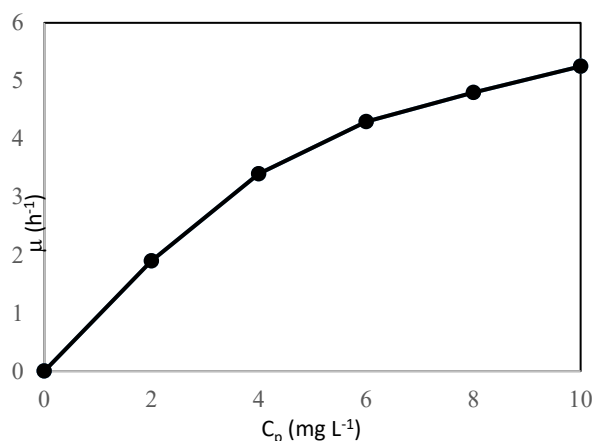
The *P. putida* used in the study was obtained from the American Type Culture Collection. NRRL B-252 coded *P. putida* from the American Type Culture Collection (A.T.C.C) was produced in the laboratory for use in studies. The composition of the rich broth used in the production of *P. putida* is given in Table 2.

**Table 2.** Composition of rich broth used in the production of *P. putida*.

Glucose	3
Yeast extract	2
bacteriological peptone	2
K <sub>2</sub> HPO <sub>4</sub>	1
KH <sub>2</sub> PO <sub>4</sub>	1
(NH <sub>4</sub> ) <sub>2</sub> .SO <sub>4</sub>	1
MgSO <sub>4</sub> .7H <sub>2</sub> O	0.5

Bacterial culture brought in lyophilized form was first produced in petri dishes containing solid nutrient medium with agar and in tubes containing slanted agar in an oven at 30 °C and then transferred from these media to rich liquid nutrient media containing glucose. 100 ml of the medium with the composition given in Table 2 was added to 250 ml flasks, and the mouths of the flasks were closed with cotton plugs and aluminum foil. The media prepared for sterilization in this way were sterilized by keeping them in an autoclave at 121 °C for 45 minutes. Bacteria were inoculated at a ratio of 1/10 to the medium prepared by sterilization. Then, *P. putida* was grown by keeping it in an orbital incubator operating at 30 °C and

100 rpm stirring speed for 72 hours. In order to demonstrate the effect of substrate inhibition on the microorganism used in the study, the amount of glucose was changed between 3-10 g in a pesticide-free medium. According to the data obtained, it can be seen from Figure 1 that glucose alone does not have an inhibitory effect on the growth of *P. putida*.

**Figure 1.** The effect of initial glucose amount on the specific growth rate of *P. putida* (T=30 °C, X<sub>0</sub>= 10 mL, MS=100 rpm)

## 2.3. Acclimatization of the microorganism to the pesticide-containing environment

Accustoming microorganisms to toxic organic compounds such as pesticides is an important process that must be done in order to increase microbial activity. The acclimatization time ranges from a few hours to a few weeks, depending on the nature of the vaccine used.<sup>21</sup> Accordingly, a series of experiments were conducted to acclimate *P. putida* to pesticides.

The acclimatization of the microorganism to the pesticide was carried out gradually. First, liquid nutrient media containing 3 g L<sup>-1</sup> glucose + 0.01 g L<sup>-1</sup> pesticide were prepared, and cultures grown in 3 g L<sup>-1</sup> glucose medium were planted in the prepared liquid nutrient medium. After the growth was observed, acclimation of the microorganism was continued. The acclimation process is similar in media containing 1 g L<sup>-1</sup> glucose + 0.01 g L<sup>-1</sup> pesticide, 0.5 g L<sup>-1</sup> glucose + 0.01 g L<sup>-1</sup> pesticide and 0.0 g L<sup>-1</sup> glucose + 0.01 g L<sup>-1</sup> pesticide and then transferred to the biodegradation medium. By determining the amount of increase in the mass of microorganisms in the solution during the acclimatization period, it was decided that the acclimatization process of the microorganism to the pesticide environment was realized.

The composition of the nutrient medium used in biodegradation studies is given in Table 2. Biodegradation experiments were carried out by adding the microorganism produced after the acclimatization process to this medium at a ratio of 1/10. Pesticide was added to the solution prepared according to the



composition in Table 3, in varying amounts depending on the nature of the experiment.

**Table 3.** Nutrient media used in biodegradation studies.

Glucose	0.5
K <sub>2</sub> HPO <sub>4</sub>	1
KH <sub>2</sub> PO <sub>4</sub>	1
(NH <sub>4</sub> ) <sub>2</sub> SO <sub>4</sub>	1
MgSO <sub>4</sub> ·7H <sub>2</sub> O	0.5

In order to prevent all kinds of infections that may occur in the working environment, all the studies with living organisms should be carried out under sterile conditions. The flasks, tubes and pipettes containing the nutrient medium were sterilized by keeping them in an autoclave at 121 °C for 45 minutes. The environment where the sowing process was carried out was chemically sterilized with ethyl alcohol before sowing and a UV lamp was used for a certain period of time. The sowings were made in such a way that sterilization would not deteriorate in the presence of the burner flame. Tubes and flasks containing solid and liquid nutrient media produced in active form were stored in a refrigerator at 4 °C. The microorganism stored in the refrigerator was transferred to new nutrient media once every 15 days to maintain the activity of the microorganism.

#### 2.4. Preparation of pesticide solutions

In the biodegradation of Chlorpyrifos pesticide with *P. putida*, a stock pesticide solution was prepared from Sarban 4 E and Folicor WP 25 pesticides at a concentration of 2000 mg L<sup>-1</sup> on the basis of active substance. Pesticide solution was added to the nutrient medium with the help of a pipette to form the desired concentration from these stock solutions.<sup>22</sup>

#### 2.5. Reproduction Studies in Mixed Pot Working in Batch Order

Reproduction studies in batch order were carried out in 250 mL flasks in which 100 mL of medium was left. Pesticide biodegradation studies were carried out by placing these flasks used in biodegradation in orbital incubators that can operate at constant temperature and mixing speed. In reproductive studies in batch order; After mixing 50 mL of medium with 10 mL of microorganism, the required amount of stock pesticide solution was added to the medium+microorganism solution of this mixture to contain pesticide at the determined concentration. Then the working volume was completed to 100 mL with distilled water. Except for the microorganism concentration, the pH of the prepared experimental setup was adjusted separately and a sample was taken from the mixture to determine the initial pesticide concentration and stored in the refrigerator. Then, the growth medium, whose pH was adjusted, was sterilized in an autoclave at 121 °C for 45 minutes. 10 mL vaccine (*P. putida*) was added to the pesticide-containing

medium prepared for production by sterilization, and it was kept in an orbital incubator at constant temperature and stirring speed for 72 hours. After the growth was completed, the microorganisms were separated from the liquid medium by centrifugation at 5000-6000 rpm for 3 minutes. Dry microorganism concentration was determined by keeping the microorganisms in an oven at 60 °C for 12 hours on tared aluminum foil. The liquid part was immediately extracted with dichloromethane for pesticide determination and stored in a deep freezer until analysis.

### 3. RESULTS AND DISCUSSION

The biodegradation of *P. putida* bacteria and chlorpyrifos was investigated in batch stirred reactors. Glucose, selected as the substrate, was used as an additional carbon source to the pesticide. In the experiments, the effects of parameters such as initial pH, temperature and initial pesticide concentration on substrate consumption and microorganism production rates and productivity were investigated in batch system with free *P. putida*.

#### 3.1. Effect of initial pH

The initial pH is an important parameter for the specific growth rate of *P. putida* and its effect on the pesticide consumption rate in a growth medium containing chlorpyrifos. Hydrogen ion concentration significantly affects the activities and growth of microorganisms. Each microorganism has an optimum pH range where it shows maximum activity. In order to maximize the activities of organisms, the pH of the environment must be kept under control at an optimum value. By keeping the mixing speed, temperature and chlorpyrifos concentration constant, the amount of change in the microorganism concentration in different initial pH values (pH= 3-9) is given in Figure 2.

As a result of the studies carried out in the media containing chlorpyrifos pesticide and prepared at different initial pH values, it was observed that the growth rate of *P. putida* decreased in the media with pH values lower than pH = 8 and with high pH values.

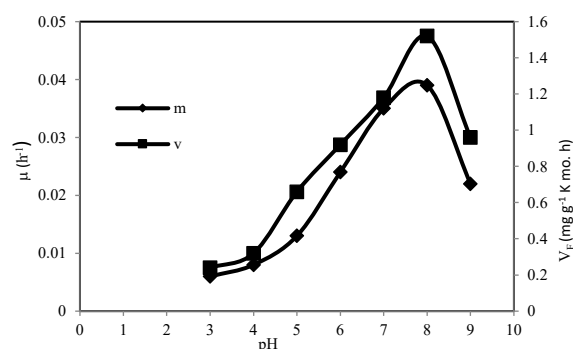


**Figure 2.** The effect of the initial pH' mm on the specific growth and pesticide consumption rate of the microorganism.



### 3.2. Effect of temperature

One of the most important parameters affecting the growth of microorganisms and accordingly the rate of substrate consumption is temperature. The effect of temperature on the growth of *P. putida* in a breeding medium containing Chlorpyrifos pesticide was investigated in the range of 20-35 °C.

In Figure 3, the effect of temperature on the specific growth and chlorpyrifos pesticide consumption rate of *P. putida* is given. From Figure 3, it is seen that the optimum temperature determined for the growth of *P. putida* bacteria and maximum consumption of chlorpyrifos pesticide in the pesticide environment is 30 °C.

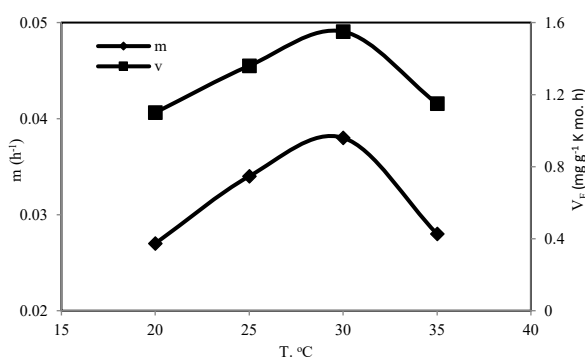


**Figure 3.** The effect of temperature on the specific growth and pesticide consumption rates of the microorganism. (*P. Putida*, pH = 8,0, C<sub>F0</sub> = 50 mg L<sup>-1</sup>, X<sub>0</sub> = 10 mL; MS = 100 rpm)

Temperature is especially effective on the enzyme systems of microorganisms. As can be seen from Figure 3, it is seen that low temperatures have an inhibiting effect on the growth of *P. putida* and decrease the growth rate of this microorganism. It is known that the enzyme system of microorganisms deteriorates at high temperatures. Above the optimum temperature, microorganism growth decreases with the increase in temperature, and as a result, microorganism death occurs with excessive increase. At higher temperatures than the optimum temperature (30 °C), lower microbial specific growth rates and pesticide consumption rates were obtained at higher temperatures, since microorganisms lost their metabolic activities due to the deterioration of the enzyme structures in the microorganism.

### 3.3. Effect of initial chlorpyrifos concentration

One of the most important parameters affecting the growth rate and substrate consumption rate of microorganisms in biodegradation studies is the initial substrate concentration. In order to investigate the effect of the initial concentration of the substrate on the growth of *P. putida* and the biodegradation of chlorpyrifos pesticide, the effect of the initial chlorpyrifos pesticide concentration on the growth and chlorpyrifos consumption rate of *P. putida* bacteria in experimental studies carried out at constant temperature and mixing

speed. 25-500 mg L<sup>-1</sup> initial pesticide concentration and the results are given in Figure 4 and Table 3. It can be seen from Figure 4 that the maximum specific growth rate for *P. putida* microorganism is obtained when the initial substrate concentration is 50 mg/L at optimum constant temperature and stirring speed. It can be clearly seen from Figure 4 that the growth rate of microorganisms decreases rapidly when the initial pesticide concentration rises above 50 mg L<sup>-1</sup>. Pesticide concentration above 50 mg/L causes substrate inhibition, and pesticide concentrations greater than 50 mg L<sup>-1</sup> cause a rapid decrease in the specific growth rate of microorganisms. The reason for this inhibition is that excessive pesticide disrupts the bacterial structure and prevents their cellular functions.

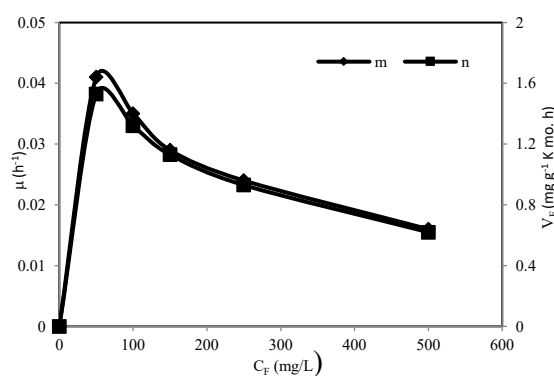


**Figure 4.** Effect of initial pesticide concentration on microorganism specific growth and pesticide consumption rates. (*P. Putida*, pH = 8, T = 30 °C, X<sub>0</sub> = 10 mL, KH = 100 rpm)

**Table 3.** Maximum microorganism concentrations, % pesticide consumption values and doubling times obtained at different pesticide concentrations (*P. putida*)

C <sub>F0</sub> (mg/L)	X <sub>m</sub> G k.mo/L	% Cosuption	t <sub>d</sub> (h)
52.31	0.675	68.01	17.5
101.41	0.575	61.61	20.9
146.47	0.554	50.16	24.2
207.84	0.450	41.68	26.3
264.63	0.340	33.85	32.34
533.41	0.176	14.64	53.3

The decomposition of organic substances in the metabolic processes of microorganisms affects the amount of oxygen in the waters. Microorganisms decompose the organic substances in the water. In the presence of toxic substances in the environment, the activities of microorganisms slow down and thus the decomposition of organic substances is prevented. During the decomposition of organic substances, a dynamic balance occurs between the active microorganisms present in the water and the degradable organic matter. Depending on the concentration of organic matter in the water, an oxygen consumption proportional to the microorganism concentration occurs. When Table 3 is examined, it is seen that the percentage of pesticide consumption decreases continuously after 50

mg L<sup>-1</sup> pesticide concentration, while the microorganism doubling time (td) increases.

In optimum conditions where the initial pH is 8, the temperature is 30 °C and the initial pesticide concentration is 52.31 mg L<sup>-1</sup>, the specific growth rate of the microorganism is 0.0395 h<sup>-1</sup>, the pesticide consumption rate is 1.51 mg pesticide/g k. B.C. h, and the percentage of pesticide consumption was found to be 68.01% at the end of 24.

When the pesticide is used as the sole carbon source, it is the substrate pesticide that inhibits growth. However, when a carbon source other than pesticide is used, both the pesticide and other carbon source may inhibit growth. The data were evaluated in terms of both substrate and toxic compound inhibition, and the compatibility of substrate and toxic compound inhibition with the Monod equation given below was investigated. In this equation,  $\mu_m$  represents the maximum growth rate (h<sup>-1</sup>), and  $K_s$  the saturation constant (g L<sup>-1</sup> or mg L<sup>-1</sup>).

$$\mu = \frac{\mu_m C}{K_s + C} \quad (1)$$

It was determined that non-competitive substrate inhibition (Halden's equation) best describes the system. It is written as the Halden equation.

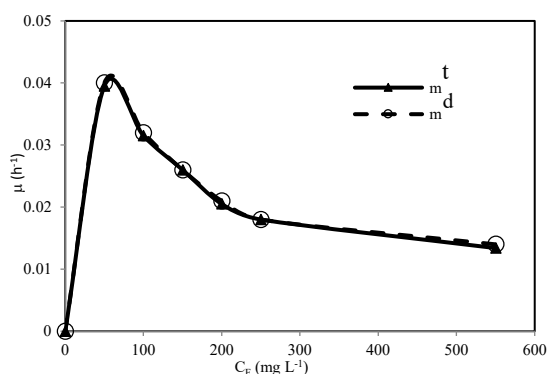


**Figure 5.** Comparison of microorganism specific growth rate values calculated from the experimental and Monod equations

$$\mu = \frac{\mu_m}{(1 + \frac{K_s}{C})(1 + \frac{C}{K_i})} \quad (2)$$

Here,  $K_i$  is the inhibition constant (mg/g/L) and  $K_i \gg K_s$  is the equation as follows;

$$\mu = \frac{\mu_m C}{K_s(1 + \frac{C}{K_i})} \quad (3)$$

In Figure 4, the microorganism specific growth rate values calculated by experimental and nonlinear regression method were compared. The constants in Equation 2 were calculated as the maximum microorganism growth rate  $q_{max} = 0.054$  h<sup>-1</sup> the saturation constant  $K_s = 3.62$  mg L<sup>-1</sup> and the inhibition constant  $K_i = 171.71$  mg L<sup>-1</sup>.

### 3.4. Effect of mixing speed

Mixing is necessary to increase microbial growth by ensuring that the microorganism is in good contact with the nutrient medium. The mixing speed is also one of the important parameters that affect the growth and substrate consumption rates of the microorganism. The mixing speed in the biodegradation of Chlorpyrifos pesticide was investigated in the range of 50-150 rpm. Microorganism concentration in the medium and chlorpyrifos pesticide concentrations remaining in the medium were determined for each mixing speed value, and the effect of mixing speed on the specific growth and pesticide consumption rates of the microorganism is given in Figure 5 below. As can be seen from Figure 5, optimum microorganism concentration and pesticide consumption were obtained at a stirring speed of 100 rpm. A reduction in both the microorganism concentration and the degraded chlorpyrifos concentration was observed at mixing speeds lower and higher than 100 rpm.

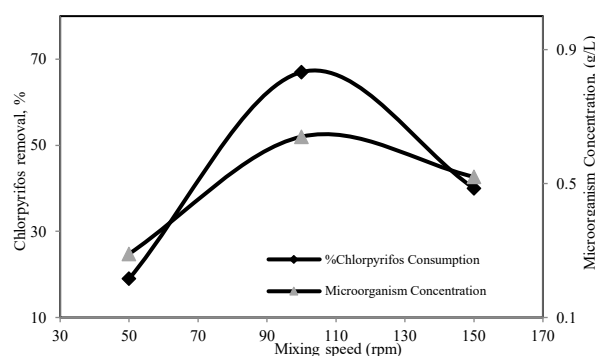


**Figure 6.** Comparison of microorganism specific growth rate calculated from the experimental and Monod equations

## 4. CONCLUSIONS

It is aimed to obtain a smooth and as high a peak area as possible for the peaks of the substance analyzed in gas chromatography. For this, while developing a gas chromatography method for the study, different columns and detectors were tried. The optimum injection, column and detector temperatures were investigated for each column and detector tested. As a result of these studies, flame ionization detector (FID) and Rtx-5MS capillary column were used for chlorpyrifos pesticide. Various temperature programs were applied to the column in order to obtain peaks resulting in a higher peak area by ensuring the separation of the pesticide from its solvent in the column. As a result of increasing the column temperatures according to a program, the baseline of the detector increased continuously until the end of the analysis with the injection, so it was decided to work with constant column temperatures.

The sample volume injected into the injection unit is generally between 0.5-1  $\mu$ L for capillary columns. For this reason, the injection volume was applied as 1  $\mu$ L in

the studies. The sample, which turns into steam due to the temperature of the injection unit, is dragged to the column by the nitrogen gas. Pesticide analyzes could not be performed properly because the pesticide could not be separated when the whole injected sample was dragged into the girth (splitless). For this purpose, the method in which only part of the sample injected into the injection unit is used and the other part is thrown out (split) has been tried and very good and clear separation peaks that can be used in the analysis of pesticides have been obtained.

As a result of these studies, a calibration curve was created within the framework of the optimum analysis conditions obtained for chlorpyrifos in gas chromatography. The correlation of the obtained calibration curve did not fall below 99%. Since the sensitivity of the detectors to the determined substances changes over time, calibration charts were reconstructed at the beginning and end of the analysis.

It has been understood that the composition of the biodegradation media greatly affects the consumption of pesticides, and it has been understood that when another carbon source is present in the environment, the bacteria prefer the other carbon source, which is easier to use, instead of consuming the pesticide. In experimental studies, where glucose was used as the sole carbon source and the inhibition effect of glucose on microorganism growth rate was examined, it was observed that glucose did not inhibit microorganism growth (Figure 1).

In the batch system, the effects of system parameters such as pH, temperature and initial pesticide concentration on the specific growth and substrate consumption rate of the microorganism were investigated. 8, optimum temperature was determined as 30 °C and optimum initial pesticide concentration was determined as 50 mg L<sup>-1</sup>. Under these conditions; The maximum microorganism specific growth rate obtained in the biodegradation of chlorpyrifos with *P. putida* was 0.0395 h<sup>-1</sup> and the pesticide consumption rate was 1.51 mg g<sup>-1</sup> k.mo.h.

It was observed that excessive toxic component inhibition was effective at concentrations higher than 50 mg L<sup>-1</sup> pesticide concentration. Maximum microorganism growth rate ( $\mu_{max}$ ) for Chlorpyrifos, *P. putida*; 0.054 h<sup>-1</sup>, saturation constant (Ks); 3.62 mg L<sup>-1</sup> and inhibition constant, (KI); It was found to be 171, 71 mg L<sup>-1</sup>. In the biodegradation of pesticides in living systems in batch order; By working with mixed cultures, the increasing and decreasing effects of pesticides on the growth rate can be examined. This study, which is done in a batch mixing vessel, can be studied in continuous, filled and semi-batch reaction vessels.

#### ACKNOWLEDGEMENTS

This article has been produced from the doctoral thesis titled "Investigation of biodegradation and effects of

sunlight, temperature and microorganisms on some pesticides" which was submitted to the Fırat University, Institute of Natural and Applied Sciences, Department of Environmental Engineering in September, 2005.

#### Conflict of interests

*I declares that there is no a conflict of interest with any person, institute, company, etc.*

#### REFERENCES

- Haktanır, K. A. Ü. *Ziraat Fakültesi, T. no:107*, **1985**, Ankara.
- Barlas, N. *Tübitak* **1996**. Project: YDABÇAG 217/A.
- Güler, Ç.; Uz, H.; Sur, H. *TSE Standard Ekonomik ve Teknik Dergi*, **1998**, 440(37), 54-59.
- Ünlü, K.; Özenirler, G.; Sözüdoğru, S. *Turkish J Eng Env Sci.*, **1997**, 21, 189-202.
- William, M.D.; Coates, J.A.; Garcia, K.L.; Signorella, L.L.; Delfino, J.J. *J. Chromatogr. A*, **1993**, 643, 341-350.
- Yıldırım, E. *Tarımsal Zararlılarla Mücadele Yöntemleri ve Kullanılan İlaçlar*. Atatürk Üniv. Ziraat Fak. Yayınları, No:219, Erzurum, 350 s. 2008.
- Baltensweiler, W. Z. *Ang. Ent.*, **1985**, 99:77-85.
- Güler, Ç.; Uz, H.; Sur, H. *TSE Standard Ekonomik ve Teknik Dergi*, **1998**, 440(37), 54-59.
- Gürman, A. *Kimya Mühendisliği Dergisi*, **1993**, 138. Sayı.
- Öztürk, S. *Tarım İlaçları*, Hasat Yayıncılık, İstanbul. 1990.
- Ecevit, O.; Bayraklı, F. *Pestisit kalıntı sorunu ve Önemi, Çölleşen Dünya ve Türkiye Örneği*, T.C. A.Ü. Çevre Sorunları Araştırma Merkezi, Erzurum. 13-17 Mayıs, 1985.
- Güvener, A. *Pestisit Kalıntı Sorunları*, I. Ulusal Zirai Mücadele İlaçları Sempozyumu, DİE, Ankara.27-29 Kasım, 1980.
- Türkiye Çevre Vakfı, 1995, *Türkiye'nin Çevre Sorunları '95*, Altıncı Baskı, Önder Matbaa, Ankara, 1995.
- Ayas, Z.; Barlas, N.; Kolankaya, D. *Aquat. Toxicol.* **1997**, 39(2)171-181.

15. İnce, N.; Bekbölet, M. *Türkiye’de Pestisit Tüketimine İlişkin Kirlenme Öncelikleri*, Türkiye’de Çevre Kirlenmesi Öncelikleri Sempozyumu, 21-22 Mayıs, İstanbul, 1991.
16. Falmann, H.; Krutzler, T.; Bauer, R.; Malato, S.; Blanco, J. *Catal. Today*, **1999**, 54, 309-319.
17. Aksu, Z. *Process Biochem* **2005.**, 40, 997-1026.
18. Bellinaso, M. L.; Greer, C. W.; Peralba, M. C. C.; Henriques, J.A.P; Gaylarde, C.C. *FEMS Microbiol. Ecol.* **2003**, 43, 191-194.
19. Sanchez, M.E.; Estrada, I.B.; Martinez O.; Martin-Villacorta, J.; Aller, A.; Moran, A. *Chemosphere*, **2004**, 57, 673-679.
20. Tutarlı, A. Elazığ’da Tarımsal Mücadele Amacıyla Kullanılan Pestisitlerin Topraktaki Kalıntılarının Araştırılması, Master's Dissertation, F.Ü. Fen Bilimleri Enstitüsü, Elâzığ, 1991.
21. Buitron, G.; Koeffed, A.; Capdeville, B. *Environ Technol*, **993**, 14, 227-236.
22. Barlas, N. *Tübitak* **1996**. Project: YDABÇAG 217/A.



## Evaluation of zero waste management system and Adana metropolitan municipality zero waste implementation

Bülent SARI<sup>1,\*</sup>, Hatice Şebnem KÜPELİ<sup>2</sup>, Hakan GÜNEY<sup>3</sup>,  
 Olcayto KESKİNKAN<sup>1</sup>

<sup>1</sup>Cukurova University, Faculty of Engineering, Department of Environmental Engineering, Adana, Turkey

<sup>2</sup>Adana Metropolitan Municipality, Adana

<sup>3</sup>Toros University, Vocational School, Mersin, Turkey

Received: 8 September 2021; Revised: 15 September 2021; Accepted: 19 September 2021

\*Corresponding author e-mail: bsari@cu.edu.tr

**Citation:** Sarı, B.; Küpeli, H. Ş.; Güney, H.; Keskinan, O. *Int. J. Chem. Technol.* 2021, 5 (2), 100-107.

### ABSTRACT

In this study, policies and regulations about the operation of the system in the world and in Turkey regarding the necessity of transitioning to the Zero Waste Management System as a waste management system were examined and a literature review was made about the studies on this subject. In line with the information obtained, the implementation of the system in the administrative service units of Adana Metropolitan Municipality was evaluated. For this purpose, the amounts of recyclable wastes and non-recyclable wastes collected separately in the service buildings, taking into account the 12-month period, were determined. In this process, a total of 137992 kg of waste was collected. 119009 kg of these wastes were included in the urban waste collection system and sent to the integrated solid waste disposal facility, while 21983 kg was delivered to licensed companies as recyclable waste. With the transition to the Zero Waste Management System, it has been determined that the amount of waste going to the integrated solid waste disposal site has decreased by 16% in a 12-month period. In addition, as a result of the statistical studies on waste data, it was determined that the recyclable wastes and the non-recyclable wastes in the 95% confidence interval showed a statistically significant difference according to the service units ( $p < 0.05$ ).

**Keywords:** Solid Waste, Zero Waste, Waste Separation, Recycling, Adana Metropolitan Municipality.

### 1. INTRODUCTION

The "disposable" culture, which developed with the rapid urbanization, economic and industrial developments, and

### Sıfır atık yönetim sistemi ve Adana büyükşehir belediyesi sıfır atık uygulamasının değerlendirilmesi

#### ÖZ

Bu çalışmada atık yönetim sistemi olarak Sıfır Atık Yönetim Sistemi'ne geçilmesinin gerekliliği ile ilgili Dünya'da ve Türkiye'de sistemin işleyişi hakkında politikalar, mevzuatlar incelenerek bu konuda yapılan çalışmalarla ilgili literatür taraması yapılmıştır. Elde edilen bilgiler doğrultusunda Adana Büyükşehir Belediyesine ait idari hizmet birimlerinde sistemin uygulanması değerlendirilmiştir. Bu amaçla hizmet binalarında 12 aylık dönem dikkate alınarak geri dönüştürülebilir atıklar (GDM) ile geri dönüşümü mümkün olmayan atıkların (GDMO) ayrı ayrı toplanan miktarları tespit edilmiştir. Bu süreçte toplam 137992 kg atık toplanmıştır. Bu atıkların 119009 kg'ı kentsel atık toplama sistemine dahil edilip entegre katı atık bertaraf tesisine gönderilirken, 21983 kg'ı GDM olarak lisanslı firmalara teslim edilmiştir. Sıfır Atık Yönetim Sistemine geçilmesiyle entegre katı atık bertaraf sahasına giden atık miktarının 12 aylık süreçte %16 azaldığı tespit edilmiştir. Ayrıca atık verilerine dair istatistiksel çalışmalar neticesinde %95 güven aralığında GDM ve GDMO'ların hizmet birimlerine göre istatistiksel olarak anlamlı bir farklılık gösterdiği tespit edilmiştir ( $p < 0.05$ ).

**Anahtar Kelimeler:** Katı Atık, Sıfır Atık, Atık Ayırma, Geri Kazanım, Adana Büyükşehir Belediyesi.

the rise in living standards due to the increasing population in developing countries, has significantly changed both the waste production rate and the waste composition. However, considering the lack of



awareness in the society about waste diversity and waste separation, the inadequacy of waste collection-transport organization and the difficulties experienced in financial resources, it is becoming more and more difficult for municipalities that are responsible for waste management in cities to provide an effective and efficient service to the residents of the city.<sup>1</sup> Ensuring an effective, systematic and efficient waste management from the formation of the waste to its final disposal depends on the good implementation of waste management.<sup>2</sup> In this context, Zero Waste Management System (ZWMS), which is one of the waste management systems, which aims to prevent and reduce waste at its source, and to ensure its reuse when this is not possible, has gained great importance throughout the world.

The term zero waste was first used by Paul Palmer in the name of Zero Waste Systems Inc-ZWS, which was founded in the 1970s in Oakland, California, United States and obtains raw materials from chemicals. The meaning used today appeared for the first time in the late 1990s<sup>3</sup>. Over time, many countries and organizations around the world have adopted the concept of zero waste. Zero waste is a waste management approach that is based on sustainability in the world of production, pushes individuals to act responsibly in living and usage areas, thus aiming to produce as little waste as possible. Zero waste management hierarchy forms the basis of ZWMS. This hierarchy; It consists of four steps: (a) reject what you do not need and reduce your needs, (b) reuse what you consume, (c) recycle what you cannot refuse, reduce and reuse, and (d) compost/decompose the rest.<sup>4</sup>

When the methods used in the world for ZWMS are examined, six themes that can be applied in the life cycle stages of production and consumption systems and aiming to reduce waste generation are suggested. These six themes are; design for zero waste, smart waste control and reduction planning, smart waste collection, high-value mixed waste treatment, industrial collaboration, waste-to-source and recycling.<sup>5</sup>

Design for zero waste focuses on using less material for the product and easy assembly/disassembly of the product at end-of-life. To serve this purpose in the manufacturing industry, disassembly product designs and additive manufacturing technologies are being developed. Disassembly (reverse assembly) is the process of systematically separating the parts that make up a product, and the fact that the product can be disassembled makes great contributions to protecting the environment by facilitating its repair/renewal and recycling.<sup>6</sup> Smart waste controls consist of hardware and software solutions that analyze waste volumes, automatically sort waste, and evaluate opportunities to divert waste through waste reduction, recycling or reuse. Waste collection efficiency includes modern smart waste collection systems, smart waste bins monitored by an integrated sensor network, trucks, maps and a data

management center, as well as using new technology providers including geographic information systems, data access networks, sensors and the internet of things. Mixed waste treatment refers to systems that accept mixed solid waste streams and then separate the designated recyclable materials through a combination of manual and mechanical separation. Industrial cooperation, on the other hand, has been respected in recent years as a cooperation structure where companies come together and the waste of one is the raw material for the other.<sup>5</sup> Industrial collaboration is a field of research that focuses on developing digital technologies that identify wastes suitable for resource matches and facilitate these exchanges between different companies in a particular area or region.<sup>7</sup>

In our country, ZWMS was first implemented in the Ministry of Environment and Urbanization (MEU) and the Presidential Complex and the studies on its spread to the whole country are increasingly continuing. In this context, the "Zero Waste Implementation Guide", prepared to guide the implementation of ZWMS, is available on the MEU's website. In addition, with the Zero Waste Regulation published in the Official Gazette dated 12.07.2019 and numbered 30829, the responsibilities of public/private institutions and organizations were determined. In order to implement ZWMS with a sustainable and professional approach; the roadmap, which consists of 7 stages: determining the focal point, determining the current situation, planning, needs and supply, training, implementation and evaluation, was created by the MEU.<sup>8</sup>

In this study, the effectiveness of ZWMS in Adana Metropolitan Municipality (AMM) scale was tried to be revealed. In this context, the ZWMS applied in AMM service units has been examined and evaluated. In the study, the wastes generated in AMM were divided into two categories as "recyclable waste (RW)" and "non-recyclable waste (NRW)". Wastes were collected at source as RW and NRW, and the waste data from each service unit was recorded. The waste data obtained were evaluated with the help of descriptive statistics, parametric test ANOVA and non-parametric test Kruskal Wallis-H. It is thought that the results of the study will contribute to the spread of ZWMS applications.

## 2. MATERIALS AND METHODS

### 2.1. AMM and Its Affiliates

AMM, selected for the study, provides services in Adana Province and 15 districts with its 24 Departments, 103 Branch Offices and 9239 personnel. AMM service buildings consist of the general administration building (historical town hall), the central building, the additional service building and various campuses located in suitable places for the needs of the city. The service units



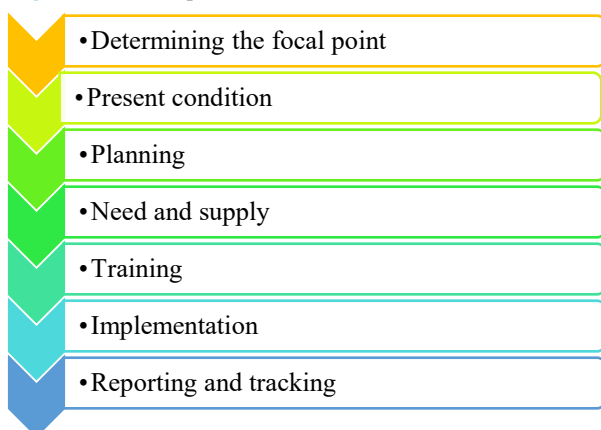
examined within the scope of the study and where ZWMS is applied are given below:

- AMM Headquarters and Additional Service Buildings
- Municipal Houses Additional Service Building
- Department of Agricultural Rural Services
- Department of Culture and Social Affairs
- Transportation Department Bus Branch Office
- Municipal Police Department
- Department of Parks and Gardens

## 2.2. ZWMS Review at AMM

The ZWMS, which is being implemented in AMM, has been examined roadmap covering the stages presented in Figure 1 according to Ministry of Environment and Urbanization applications, Zero Waste Regulation legislation and taking into account the relevant literature.

Figure 1. Roadmap of ZWMS<sup>8</sup>



## 2.3. Obtaining the Essential Oils mixtures Statistical Evaluation of ZVMS at AMM

SPSS 22 V. package program was used for statistical analysis of waste data. One-way analysis of variance (ANOVA) used in the study is used to compare the means of more than two groups.<sup>9</sup> In order to apply this analysis; data should consist of quantitative variables, distribution of data should be normal, group variances should be relatively homogeneous.<sup>10</sup> The distribution of data was evaluated with the Kolmogorov - Smirnov test.<sup>11,12</sup> Levene test was used to test the homogeneity of group variances.<sup>13</sup> If there is a difference between the groups in the comparison of group means, Duncan test, which is one of the multiple comparison tests, was used to determine which group had the greater effect.<sup>14</sup> Another test used in the study is the Kruskal-Wallis-H test. This test, which is a non-parametric test, is used when there is a problem in the assumptions of one-way analysis of variance.<sup>15</sup> If there is a statistically significant difference between the groups, the Bonferroni-corrected Mann Whitney-U Test, which is preferred in pairwise

comparisons, was used to determine between which groups this difference was.<sup>16</sup>

## 3. RESULT AND DISCUSSION

### 3.1. ZWMS Review at AMM

Feasibility studies for the Zero Waste Management System started in AMM service buildings in 2018, and it was put into practice as of March 2019. In order to realize ZWMS in AMM with a sustainable and professional approach, a roadmap consisting of 7 stages was taken as a basis: focus, current situation, planning, needs and procurement, training, implementation, reporting and follow-up. In order to carry out all the work and operations related to ZWMS, the Waste Management Branch Directorate under the Environmental Protection and Control Department has been determined as the focal point. The types of wastes coming out of the administrative service units are generally paper-cardboard wastes in the current situation. After paper, the most common type of waste is plastic, glass and metal (water bottles, glass juice bottles, metal beverage bottles, etc.). There is no food leftovers because of there is no cafeteria in the service buildings. Since the personnel meets their nutritional needs from outside, there is only packaging waste of food. In addition, in the case of bringing fruit and vegetables from home, fruit peels and tea and coffee pulp are waste as a result of frequent beverage consumption in offices. There are also napkins, wet wipes, etc. in the garbage cans in the toilets. wastes are generated. The number of RW and NRW boxes to be delivered to the service units were determined by the focal point personnel, taking into account the floor plan, number of rooms and corridor lengths of each service building, as presented in Table 1.

Table 1. Binary Collection System Boxes Distributed to Service Units

Service Units	RW Box (pcs)	NRW Box (pcs)
AMM Headquarters and Additional Service Buildings	100	100
Belediye Evleri-Additional Service Building	30	30
Department of Agricultural Rural Services	6	6
Department of Culture and Social Affairs	5	5
Transportation Department Bus Branch Office	6	6
Municipal Police Department	5	5
Department of Parks and Gardens	6	6

Following the planning stage, by the staff of the Waste Management Branch (focus point) for the employees of the institution in the training hall of the AMM main

service building; training was provided on prevention of waste generation, minimizing waste if prevention is not possible, prioritizing reuse, separate collection of waste at source, recycling/recovery of waste, and project process (Figure 2).



Figure 2. Images Of The Training Phase In AMM

In the service buildings of the institution, a dual collection system has been established in the offices in accordance with the ZWMS. According to this system, RWs are collected in blue boxes and NRWs are collected in gray boxes. The filled boxes are weighed and the waste data is recorded. The wastes coming out of the blue boxes are stored in the temporary storage area determined in the service units and sent to the collection and sorting facilities from there. The wastes collected in gray boxes are included in the urban garbage collection system and delivered to the ITC (Invest Trading & Consulting AG) Solid Waste Disposal Facility, which serves under the responsibility of AMM.

Since it is not possible to create an area that will allow to collect each type of waste in separate categories in AMM service units, a dual collection system is applied in the offices. However, as can be seen in Figure 3, a “Zero Waste Corner” has been created on the ground floor of the service building, which is called the Main Building, where it can be easily reached by the staff and visitors. Boxes suitable for collecting waste were placed in eight different categories: brown for organic waste, black for non-recyclable waste, purple for bread residues, blue for paper-cardboard waste, yellow for plastic waste, green for glass waste, gray for metal waste, white for food residues. In addition, a red-colored box was placed for battery waste and implementation was started in this region. With this application, it is aimed to raise awareness of the personnel and citizens visiting the institution by drawing their attention on the subject.

Temporary storage areas have been created within the service units in order to keep the wastes safely before they are delivered to the processing facilities. The cleaning personnel perform the occupancy checks of the collection equipment, emptying and cleaning the waste bins, changing the bags according to the color scale, weighing the collected wastes, and delivering them to the temporary storage area



Figure 3. AMM Waste Collection Equipment

In order to register, document and monitor the places to apply ZWMS and to ensure the traceability of the wastes managed within the scope of the system, the Integrated

Environmental Information System (IEIS), which is an online system created by the MEU, has been registered as AMM and service units have been added. The amount of waste collected from the buildings on a monthly basis by the Waste Management Branch is reported to the IEIS. It is possible to say that the roadmap and similar methods chosen for the implementation of ZWMS in AMM strengthen the sustainable environmental policy and support social awareness in waste management.

### 3.2. Calculation of Waste Amounts in Service Units Affiliated to AMM

Waste calculation results generated within the scope of ZWMS in AMM service units between October 2019 and September 2020 are given in Table 2 on a monthly basis. The working period is also included in the fight against the Covid-19 epidemic of the world and our country. Especially in March-April-May 2020, the decrease in the amount of waste and the change in the amount of waste during the period can be explained by our country's full closure, alternate and flexible working practices within the scope of the epidemic.

**Table 2.** Amount of Waste Collected in All Service Units by Month

Months	RW (kg)	NRW (kg)	Total (kg)	Recovery rate (%)
October 2019	1735	10130	11865	14.60
November 2019	1228	9110	10338	11.88
December 2019	1620	9791	11411	14.20
January 2020	1550	10500	12050	13.58
February 2020	1525	10220	11745	13.00
March 2020	1185	7925	9110	13.00
April 2020	1520	7590	9110	16.70
May 2020	1480	9422	10902	13.58
June 2020	2950	10256	13206	22.40
July 2020	2015	10920	12935	15.58
August 2020	3070	10235	13305	23.07
September 2020	2105	9910	12015	17.52
Total	21983	116009	137992	16

The recovery rates of wastes in the selected period are given in Figure 4. As seen in Figure 4, the highest recovery rate is in August with 23.07%, followed by June with 22.40%.

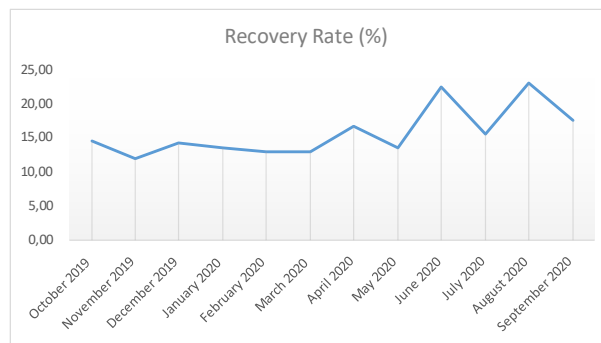


**Figure 4.** Monthly Waste Recovery Rates in All Service Units Applying ZWMS

Erdur (2019) reported that the amount of recyclable waste removed from the garbage with the implementation of the ZWMS project in the administrative service buildings of Süleymanpaşa Municipality was 18.04% in the first month of the project, while it was 27.03% in the twelfth month.<sup>17</sup> With ZWMS, it was stated that by learning which materials should not be thrown away, a decrease in the amount of waste and an increase in recyclable wastes were observed with the formation of zero waste awareness in the personnel. In general, fluctuations are observed in the recovery rates of the service units obtained in this study (Figure 4). The reason for this is the fact that the staff has been transferred to a rotating/flexible working system in order to protect the health of the employees of the institution in many service units, with the Covid-19 virus epidemic appearing in our country for the first time on March 11, 2020, and as a result, the number of daily working people has decreased. In addition, it has been evaluated that factors such as the increase in the use of disposable materials such as masks due to the change in habits during the epidemic period, the increase in the use of napkins and wet wipes in the garbage cans in the toilets, along with the increase in the habit of hand washing, caused fluctuations in the amount of waste and recycling rates.

### 3.3. Statistical Evaluation of Waste Data

Descriptive statistics on waste data from AMM service units are presented in Table 3. According to Table 3, while the average RW collected in all service units during a year is 1831.92 kg, the average NRW is 9667.42 kg. The Kolmogorov-Smirnov test and Levene test results of the collected waste data are given in Table 4. According to Table 4, it was observed that the RW data did not conform to the normal distribution at the 95% confidence interval ( $p < 0.05$ ) and their variances were not homogeneous ( $p < 0.05$ ). It was observed that the NRW data conformed to the normal distribution at the 95% confidence interval ( $p > 0.05$ ) and their variances were homogeneous ( $p > 0.05$ ).



**Table 3.** Descriptive Statistics on Waste Data in AMM Service Units

Descriptive Statistics	RW (kg)	NRW (kg)
N	12	12
Mean	1831.92	9667.42
Standard error of mean	176.74	291.89
Median	1585.00	10020.00
Mode	1185.00**	7590.00**
Standard deviation	612.25	1011.15
Variance	374853.17	1022437.35
Minimum	1185.00	7590.00
Maximum	3070.00	10920.00

\*\* : Multiple modes are available. The smallest value is shown.

**Table 4.** Kolmogorov- Smirnov Test and Levene Test Results of Waste Types

Tests	Type of Waste	Test Statistics	p
Kolmogorov- Smirnov	RW	0.22	0.00*
	NRW	0.08	0.20
Levene	RW	12.43	0.00*
	NRW	2.18	0.06

\*: p<0.05

ANOVA test was used because NRW data provided the assumptions of normality and homogeneity of variances, and Kruskal-Wallis-H test was applied because RW data did not provide assumptions. Obtained results are given in Table 5. According to Table 5, NRWs and RWs show a statistically significant difference in 95% confidence interval according to service units (p<0.05). According to the Duncan test result applied to the NRW data to find out which service unit or units these differences originate from, it was seen that this difference was mostly in the Central Building and Additional Service Buildings. The result of the Mann-Whitney U test with Bonferroni correction applied to the RW data is given graphically in Figure 5. In Figure 5, the differences between service units are shown in orange. Considering the average rank of the service units, it is seen that the 1st service unit, called the Central Building and Additional Service Buildings, has higher RW than the other service units.

**Table 5.** ANOVA and Kruskal-Wallis-H test results

Tests	Test Statistics	p
NRW - ANOVA	12.57	0.00*
RW - Kruskal-Wallis-H	49.18	0.00*

In this study, the wastes from the service units of AMM were evaluated in 2 separate categories as RW and NRW, while Ayeleru et al. collected daily and weekly wastes specific to the city and classified them into 9 different categories as paper and cardboard, glass, metal, plastic, textiles, organics, construction and demolition, special care waste, and other wastes.<sup>18</sup>

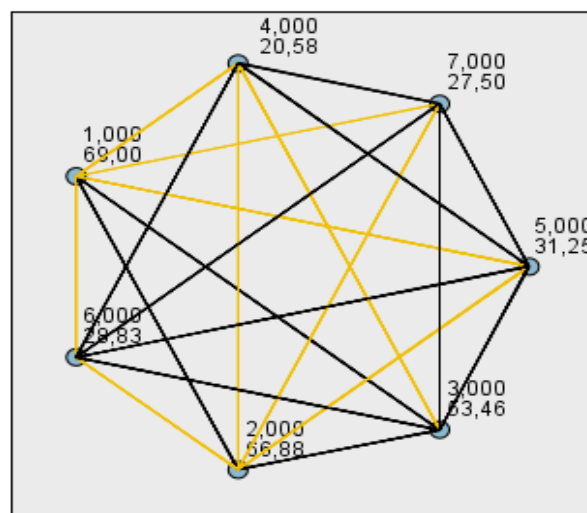


**Figure 5.** Differences of RW by Service Units

In the study, one-way analysis of variance (ANOVA), which was also used in this study, was used to control whether the wastes showed statistical differences according to summer and winter seasons. Since it is a city-specific study, Minitab Version 17 was used to evaluate whether the differences between waste data according to population, employment and number of households based on historical data covering summer and winter months are significant. As a result of the studies, it has been calculated that the highest waste composition among the daily collected wastes is plastic waste, which is 28% in summer and 26% in winter. Similarly, it was determined that organic wastes constitute the highest waste composition among the weekly collected wastes, with 28% in summer and 29% in winter, and it was argued that the difference between the wastes generated in the two seasons was not statistically significant (p>0.05). The common aim of both studies is to evaluate the appropriate ZWMS model by analyzing the information on waste data with statistical analysis methods.

#### 4. CONCLUSION

With increasing pressure on limited natural resources, it is clear that governing bodies around the world are increasingly interested in models, frameworks and approaches to sustainable development. Adoption of ZWMS in waste management has become a necessity rather than a choice for the transition to a low-carbon and less polluting economy, where emerging models such as circular economy principles are adopted in environmental management, which can alleviate increasing waste volumes. In this context, when the ZWMS applied in AMM Administrative Service Buildings is examined; It has been observed that waste management is carried out within the framework of the Zero Waste Management Regulation legislation provisions and within the scope of a certain hierarchy.<sup>19</sup>

DOI: <http://dx.doi.org/10.32571/ijct.992891>

E-ISSN: 2602-277X

As a result of the statistical studies, it has been determined that the Central Building and Additional Service Buildings have higher RWs than other service units. In the institutional sense, with the ZWMS application, it has been determined that the recovery target of the RWs in the waste is achieved here at best. It is thought that the fact that posters and information brochures about zero waste are used more widely in the Headquarters and Additional Service Buildings and that the personnel in this unit participate in zero waste trainings are effective in this situation. 119009 kg of the 137992 kg waste collected during the study was included in the urban waste collection system and sent to the integrated solid waste disposal facility, while 21983 kg was delivered to licensed companies as recyclable waste. Thus, it was possible to achieve an average recovery rate of 16% for the 12-month period. It is thought that this rate of gain obtained in the first year of the AMM ZWMS application will increase with the full adoption of the application by the institution and the awareness of the employees.

#### ACKNOWLEDGEMENTS

This study was produced from the master thesis of Çukurova University, Institute of Natural and Applied Sciences, Department of Environmental Engineering, No. 5896.

#### Conflict of interests

I declares that there is no a conflict of interest with any person, institute, company, etc.

#### REFERENCES

- Guerrero L. A.; Maas G., Hogland W. *Waste Management*, **2013**, 33, 220-232.
- Ulaşlı, K., 2018. Geri Kazanılabilir Atıkların ve Sıfır Atık Projesi Uygulamaları: Kadıköy Belediyesi. Masters Thesis [Online] Hasan Kalyoncu University, Gaziantep, <http://openaccess.hku.edu.tr/xmlui/handle/20.500.11782/1838> (accessed August 07, 2021)
- Er, M. K., 2012. Sıfır Atık Yönetimi ve Ofis Tipi Binalarda Uygulanması. Masters Thesis [Online], Istanbul Technical University, Istanbul, <https://polen.itu.edu.tr/handle/11527/609> (accessed May 15, 2020)
- Johnson, B. *Sıfır Atık Ev*. Sineksekiz Yayınevi, İstanbul, 2013.
- Kerdlap, P., Low, J., S., C.; Ramakrishna, S. *Conservation and Recycling* **2019**, 151, 104438.
- Soh, S.L., Ong, S.K., Nee, A.Y.C. *Procedia CIRP*, **2014**, 15, 407–412.
- FISSAC, 2020. Fostering Industrial Symbiosis For A Sustainable Resource Intensive Industry Across The Extended Construction Value Chain, <https://fissacproject.eu/tr> (accessed May 11, 2020).
- Çevre ve Şehircilik Bakanlığı, İdari ve Ticari Binalar İçin Sıfır Atık Uygulama Rehberi, Ankara, 2017.
- Yıldırım, Ö., 2017. Normal Dağılıma Sahip Olmayan Hata Terimli Zaman Serileri İçin Bir Yönlü Varyans Analizi: İşsizlik Oranı Verisine Uygulama. Masters Thesis [Online] Middle East Technical University, Ankara <http://etd.lib.metu.edu.tr/upload/12621242/index.pdf> (accessed August 05, 2021).
- Shirzadi, S., M., 2020. Kümeleme ve Anova (Varyans) Yöntemleri ile Erzincan Gümüşhane ve Bayburt İllerinin Kuraklık Analizi. Masters Thesis [Online] Binali Yıldırım University, Erzincan, <https://tez.yok.gov.tr/UlusalTezMerkezi/tezDetay.jspx?id=nIWtmqM2D14ZSqc0wGITpw&no=UdZ6Wf5Eomucko8hOKQ3VQ> (accessed August 05, 2021)
- Kolmogorov, A. *Inst. Ital. Attuari, Giorn.*, **1933**, 4, 83-91.
- Smirnov, N. *Recueil Mathematique*. **1939**, 6, 3-26.
- Levene, H. *Robust Tests For Equality Of Variances*; I. Olkin, S.G. Ghurye, W. Hoefding, W.G. Madow & H.B. Mann., Ed.; Stanford University Press: Carolina, 1960; pp. 278–292.
- Duncan, D.B. *Biometrics*, **1955**, 11, 1-42.
- Macunluoğlu, A., C., 2019. Bir Yönlü Varyans Analizine Alternatif Olan Parametrik ve Parametrik Olmayan K-Örneklem Test Prosedürlerinin Performanslarının Karşılaştırılması. Masters Thesis [Online] Uludağ University, Bursa, <https://acikerisim.uludag.edu.tr/bitstream/11452/15401/1/601611002%20Asl%C4%B1%20Ceren%20MACUNLUO%C4%9ELU.pdf> (accessed September 03, 2021)
- Elliott, A. C.; Woodward, W. A. *Statistical Analysis Quick Reference Guidebook: With SPSS Examples*. Sage Publications, Inc: Thousand Oaks, California, USA, 2007.
- Erdur, E., 2019. Türkiye'de Sıfır Atık Projesi ve Projenin Kamu Kurumlarında Uygulanması; Süleymanpaşa Belediyesi Örneği. Masters Thesis [Online] Gazi University, Ankara, <https://dspace.gazi.edu.tr/bitstream/handle/20.500.12>

[602/147719/?sequence=1&isAllowed=y](http://dx.doi.org/10.32571/ijct.992891) (accessed September 05, 2021).

18. Ayeleru, O. O., Okonta, F. N., Ntuli F. *Waste Management*, 2018, 79, 87-97.

19. Sıfır Atık Yönetmeliği, 2019. Resmi Gazete. Sayı: 30829, Yayın Tarihi: 12.07.2019.





## Comparison of quality properties of the Iranian Saffron (*Crocus sativus* L.) and Saffron grown in macro and micro locations in Turkey

Hasan ASİL<sup>1,\*</sup>, Ersen GÖKTÜRK<sup>2</sup>

<sup>1</sup>Medicinal and Aromatic Plants Program, Altınözü Vocational School of Agricultural Sciences, Hatay Mustafa Kemal University, 31001, Hatay, Turkey

<sup>2</sup>Department of Chemistry, Faculty of Science and Arts, Hatay Mustafa Kemal University, 31001, Hatay, Turkey

Received: 30 October 2021; Revised: 24 November 2021; Accepted: 25 November 2020

\*Corresponding author e-mail: hasan.asil@hotmail.com

**Citation:** Asil, H.; Göktürk, E. *Int. J. Chem. Technol.* 2021, 5 (2), 108-116.

### ABSTRACT

Volatile and bioactive compositions of saffron collected from different locations in Turkey and Iran were investigated using gas chromatography-mass spectrometry (GC-MS/FID and GC-MS/MS) for identification and quantification of volatile compounds. Ultrasound-assisted extraction method using methanol:ethyl acetate solvent mixture was used to isolate the volatile components of saffron. This study revealed that the amounts of the volatile and bioactive compounds of saffron varied between different geographical locations. The most important bioactive compounds of saffron, safranal, crocin and crocetin, were also quantitatively analyzed in all saffron samples. The highest amount of safranal and crocin were observed in Hatay Yayladağı saffron with 22532.97 mg kg<sup>-1</sup> and 647.26 mg kg<sup>-1</sup>, respectively. The highest amount of crocetin was obtained with 6.73 mg kg<sup>-1</sup> in Ankara Ayaş saffron. While Hatay kırıkhan saffron contained the highest fraction of fatty acid content with 23.56%, the highest fraction of bioactive components was discovered in Karabük Safranbolu ovacuma saffron with 90.84%. According to the obtained outcomes, the highest qualities saffron were determined to be observed in Hatay Yayladağı and Karabük Safranbolu ovacuma saffron, respectively.

**Keywords:** *Crocus sativus* L., GC-MS analysis, Saffron, ultrasound-assisted extraction, volatile components.

İran safranı (*Crocus sativus* L.) ile Türkiye'nin makro ve mikro lokasyonlarında yetiştirilen safranın kalite özelliklerinin karşılaştırılması

### ÖZ

İran ve Türkiye'nin farklı lokasyonlardan toplanan safranın uçucu ve biyoaktif bileşimleri, uçucu bileşiklerin tanımlanması ve miktar tayini için gaz kromatografisi-kütle spektrometrisi (GC-MS/FID ve GC-MS/MS) kullanılarak araştırılmıştır. Safranın uçucu bileşenlerini izole etmek için metanol:etil asetat çözücü karışımı kullanılarak ultrason destekli ekstraksiyon yöntemi kullanılmıştır. Bu çalışma, safranın uçucu ve biyoaktif bileşiklerinin miktarlarının farklı coğrafi konumlar arasında doğrulandığını ortaya koymak için yapılmıştır. Safran, safranal, krosin ve krosetin gibi en önemli biyoaktif bileşikler de tüm safran örneklerinde kantitatif olarak analiz edilmiştir. En yüksek safranal ve krosin sırasıyla 22532.97 mg kg<sup>-1</sup> ve 647.26 mg kg<sup>-1</sup> ile Hatay Yayladağı safranında gözlemlendi. En yüksek krosetin miktarı 6.73 mg kg<sup>-1</sup> ile Ankara Ayaş safranında elde edilmiştir. Yağ asidi içeriği en yüksek fraksiyon %23.56 ile Hatay Kırıkhan safranı içerirken, biyoaktif bileşenlerin en yüksek fraksiyonu %90.84 ile Karabük Safranbolu ovacuma safranında bulunmuştur. Elde edilen sonuçlara göre en yüksek kalite safranın Hatay Yayladağı ve Karabük Safranbolu ovacuma safranında gözlemlendiği belirlenmiştir.

**Anahtar Kelimeler:** *Crocus sativus* L., GC-MS analizi, Safran, ultrason destekli ekstraksiyon, uçucu bileşenler.

### 1. INTRODUCTION

Saffron (*Crocus sativus* L.) is a highly valued herb because of its stigmas, which are widely used as spice, medicinal drugs and food additives. Saffron has an

important pharmacological potential and is economically valuable spice. The saffron plant has a wide history of use in traditional medicinal treatment or prevention of different types of diseases, including cancer.<sup>1-3</sup> The dried saffron stigma contains crocin, safranal and picrocrocin,

and these photochemical substances are responsible for the color, aroma and taste of the saffron.<sup>4</sup> Crocetin is an aglycone part of naturally occurring crocin and is produced in biological systems as a hydrolytically bioactive metabolite.<sup>5,6</sup> Studies on the pharmacological activities of crocetin have shown that this aglycone is a therapeutically useful bioactive metabolite.<sup>6</sup>

The quality of saffron is chemically determined by the existence of three main secondary metabolites; crocin (water-soluble crocetin esters), picrocrocin (monoterpene glycoside and safranal precursor) and safranal (an important essential oil component) are responsible for colour and bitter taste of saffron. These metabolites are essential for the quality of saffron. The amounts of these metabolites in saffron vary according to the geography where saffron is grown, and therefore, geographical origin is very important for high quality saffron production.<sup>7,8</sup> To increase product profitability, many researchers are working on the evaluation of saffron by-products such as tepals, stamens, styles, leaves and corms.<sup>9,10</sup>

Saffron, which can be grown in tropical and subtropical climates in the northern hemisphere, is successfully grown in various ecologies up to 2000 m high altitude. One of the origins of saffron is Anatolian ecology. Although most of the parts of Turkey have suitable ecology for saffron cultivation, saffron is widely grown in safranbolu region.<sup>11</sup> There is no information about the first origin of saffron around the world, but Iran is reported to be the first origin for saffron production and then, it was spreaded out to Turkey and Greece. However, today saffron is successfully grown in Spain, Italy, France, Switzerland, Morocco, Egypt, Israel, Azerbaijan, Pakistan, India, New Zealand, Australia and Japan. Total saffron production around the world is about 205 tons; Iran 160 tons (~ 80%), India 8-10 tons (~ 5%), Greek 4-6 tons (~ 3%), Morocco 0.8-1 tons (~ 0.5%), Spain 0.3-0.5 tons (~ 0.25%) and the rest of it was produced by other countries.<sup>12,13</sup> According to the literature, location and saffron corms from different

## 2.2. Preparation of standard substances and extraction procedure

0.5 mg mL<sup>-1</sup> safranal, crocin ve crocetin standard solutions were prepared in ethanol, diluted with 10 - 2.000 ng mL<sup>-1</sup> concentrations and stored at 4 °C. The extractions of saffron stigma samples were accomplished using the ultrasonic-assisted solvent extraction method. 100 mg of stigma was grinded and put in a flask. 1.8–4.2 mL of methanol:ethyl acetate (30:70) mixture was then added to the flask. Obtained mixture was then sonicated in an ultrasonic bath for 15 min. After sonication, obtained extract was centrifuged for 3 min at 5000 rpm. This process was repeated three times and obtained supernatants were collected in a different flask. The

origins can have an impact on saffron productivity and quality.<sup>14</sup> Fatty acid components are analyzed by GC-MS and GC-MS FID.<sup>15,16, 17</sup>

Today, many researchers have focused on the identification of new volatile compounds in saffron and new analytical techniques. Sample characterization is generally neglected. Some researchers purchase saffron and analyze it without paying attention to its origin or originality.<sup>18</sup> The main objective of this study is to compare the qualities of saffron obtained from different locations. Specifically, it was aimed to compare the qualities of Iranian saffron, which is known to be the main production area of saffron around the World, and macro and micro-locations in Turkey. Saffron samples were collected from the different cities (macro) and their counties (micro) in Turkey. The amounts of safranal, crocin, crocetin, volatile compounds, fatty acids and bioactive components of the obtained samples were evaluated to discriminate the qualities of the collected saffron samples.

## 2. MATERIALS AND METHODS

Saffron samples were obtained from traditional production areas. The saffron stigmas were dried at room temperature for two days following harvest and placed in 1g glass jars with lids. samples were received from the production areas by cargo. Iranian saffron was obtained from the province of Rezevi Khorasani. Saffron stigma samples in Turkey were obtained from different locations including Hatay (Kırıkhan, Iskenderun, Hassa and Yayladağı counties), Karabük (Safranbolu county Yukarıbucak and Ovacuma villages), Ankara (Ayaş, Nallıhan and Polatlı counties), Çukurova region (Adana-Cukurova, Mersin-Tarsus and Osmaniye-Kadirli counties) and Antalya (Korkuteli county). The altitude and coordinate information of saffron production locations are given in Table 1. Safranal ≥90% stabilized, (W338907-Sample-K), crocetin dialdehyde (18804-10 MG) and crocin (17304-1G) standards were purchased from Sigma Aldrich and used as received.

solvent mixture was evaporated with a final volume of 1 mL and obtained extracts were stored at +4 °C in the dark for GC-MS analyses.<sup>4,19</sup>

## 2.3. Gas Chromatography- Tandem mass spectrometry (GC-MS/MS) analysis

Volatile components of saffron samples were identified by GC-MS/MS (Hewlett-Packard 6890) instrument equipped with HP-5MS fused silica column (5% phenyl methyl polysiloxane 30 m 0.25 mm i.d.. film thickness 0.25 µm) and Hewlett-Packard mass selective detector 6890. GC-MS/MS analyses were carried out under the same conditions reported in the literature.<sup>4, 19, 20</sup>

**Table 1.** Altitude and coordinate information of saffron production locations

Macro	Micro	Elevation	Longitude (E)	Latitude (N)
HATAY	Kırıkhan	122	36 36	31 22
	İskenderun	10	36 36	35 08
	Hassa	288	36 36	42 30
	Yayladağı	711	36 36	02 08
KARABÜK	Safranbolu Yukarıçiflik	829	41 32	17 43
	Safranbolu Ovacuma	376	41 32	27 45
ANKARA	Ayaş	902	40 32	01 18
	Nallıhan	596	40 31	09 20
	Polatlı	811	39 32	35 11
ÇUKUROVA	Adana Çukurova	95	37 35	06 09
	Tarsus	35	36 34	57 35
	Osmaniye Kadirli	94	37 36	23 04
ANTALYA	Korkuteli	871	37 30	03 19
IRAN	Rezaviye Horasani	955	36 59	16 36

#### 2.4. Gas Chromatography-Mass spectrometry flame ionization detector (GC-MS/FID) analysis

The amounts of safranal, crocin and crocetin were detected by GC-MS/FID (Hewlett-Packard 6890) instrument equipped with HP-88 fused silica column (100 m 0.25 mm i.d., film thickness 0.25  $\mu\text{m}$ ) and Hewlett-Packard mass selective detector 6890. The oven was heated to 60  $^{\circ}\text{C}$  and waited for 1 min at that temperature. Then, the temperature was raised to 100  $^{\circ}\text{C}$  by 5  $^{\circ}\text{C min}^{-1}$  and waited for 4 min. The temperature was increased by 5  $^{\circ}\text{C min}^{-1}$  to 135  $^{\circ}\text{C}$  and waited for 20 min. Finally, it was increased by 10  $^{\circ}\text{C min}^{-1}$  to 170  $^{\circ}\text{C}$  and waited for 22 min. The gas mixture to the flame was made of 60  $\text{mL min}^{-1}$  of  $\text{H}_2$  (UHP grade), 400  $\text{mL min}^{-1}$  air (zero grade), 10  $\text{mL min}^{-1}$  Helyum (99.9999%) as carrier gas. Injector temperature was kept at 200  $^{\circ}\text{C}$ .<sup>4, 19</sup>

### 3. RESULTS AND DISCUSSION

In this study, the quality of saffron samples obtained from different locations was evaluated using two different aspects. First, evaluation involved in some quality comparisons of saffron samples obtained from 13 different micro-locations in five different macro locations in Turkey and Iranian saffron. In both studies, the volatile components in the stigma samples were determined by GC-MS/MS analysis. The amount of active ingredients indicating the quality of saffron such as safranal, crocin and crocetin in the stigma were determined by GC-MS/FID analysis. Both analysis methods are explained comparatively.

#### 3.1. Comparisons of the qualities of saffron samples

Safranal fractions of Iranian saffron and saffron grown in different locations in Turkey and the amounts of safranal, crocin and crocetin in these saffron samples were summarized in Table 2. According to the Table 1, the highest fractions of safranal were obtained with the order by 86.88% Safranbolu Ovacuma saffron in Karabük, 75.48% Yayladağı saffron in Hatay, 70.23% Polatlı saffron in Ankara, 68.58% Osmaniye Kadirli in Çukurova. Safranal fraction in Iranian saffron was found to be 64.66%. When safranal fractions were compared, the highest amount of safranal was observed in Safranbolu Ovacuma saffron in Karabük with 86.88%. Safranal, which is the most abundant volatile component in saffron, was reported to constitute 60-70% of the volatile components in saffron in the literature.<sup>21</sup> In another report, it was reported that 93% of safranal was found in the saffron sample according to the olfactometric.<sup>22</sup>

In another study, the fractions of safranal in Spanish saffron collected from different locations were found to be 77.7% (SF-SP4), 73.2% (SF-SP3), 64.5% (SF-SP2), SF-SP6 (50.7%), 32.1% (SF-SP1) and 29.8% (SF-SP5). Significant differences on the safranal fractions were observed among the different locations. Such differences were reported to be due to different agricultural practices or drying methods of saffron.<sup>23</sup>

**Table 2.** Comparison of the safranal fractions and the amounts of safranal, crocin and crocetin compounds obtained from Iranian saffron and saffron from micro and macro locations in Turkey.

Location		GC-MS/MS	GC-MS/FID		
Macro	Micro	Safranal (%)	Safranal (mg/kg)	Crocine (mg/kg)	Crocetin (mg/kg)
HATAY	Kırıkhan	24.47	5422.74	379.84	1.30
	İskenderun	29.31	7828.07	91.80	5.98
	Hassa	28.56	3253.14	284.66	0.70
	Yayladağı	75.48	22532.97	647.26	3.40
KARABÜK	Safranbolu Yukarıçiflik	64.10	12095.55	77.56	0.20
	Safranbolu Ovacuma	86.88	21776.36	157.04	2.20
ANKARA	Ayaş	68.88	20609.74	526.04	6.73
	Nallıhan	66.97	14439.36	241.93	3.52
	Polatlı	70.23	16764.30	488.86	5.10
ÇUKUROVA	Adana Çukurova	65.53	14681.35	223.46	3.26
	Tarsus	57.48	15717.08	534.35	0.02
	Osmaniye Kadirli	68.58	14942.37	225.76	1.97
ANTALYA	Korkuteli	34.67	4450.01	221.23	2.20
IRAN	Rezevi Horasani	64.66	14678.80	358.38	5.80

The amounts of safranal significantly differed among the different locations. The highest amount of safranal was observed in the order by Yayladağı saffron with 22532.97 mg kg<sup>-1</sup>, Safranbolu Ovacuma saffron with 21776.36 mg kg<sup>-1</sup>, Ayaş saffron with 20609.74 mg kg<sup>-1</sup>, Tarsus saffron with 15717.08 mg kg<sup>-1</sup> and Korkuteli saffron with 4450.01 mg kg<sup>-1</sup>. The amount of safranal in Iranian saffron was 14648.80 mg kg<sup>-1</sup>. In the literature, the average amount of safranal in different locations was examined and results showed that safranal was obtained with 335.9 g kg<sup>-1</sup> in Spanish saffron and 488.6 g kg<sup>-1</sup> in Greek saffron. The geography plays an important role for the amounts of safranal found in saffron among different farming locations, especially in the regions of Greece, Iran, Italy and Spain, but no significant difference was observed between Iranian and Spanish saffron.<sup>24</sup> The amounts of safranal from 76 commercially available saffron samples in different countries varied between 1.35 and 10.56 g kg<sup>-1</sup> by the GC-MS/FID analysis.<sup>25</sup>

According to GC-MS/FID analysis results, the highest amounts of crocin in the macro locations was obtained in the order of Yayladağı saffron in Hatay with 647.26 mg kg<sup>-1</sup>, Tarsus saffron in Çukurova with 534.35 mg kg<sup>-1</sup>, Ayaş saffron in Ankara with 526.04 mg kg<sup>-1</sup>, Korkuteli saffron in Antalya with 221.23 mg kg<sup>-1</sup> and Safranbolu Ovacuma saffron in Karabük with 157.04 mg kg<sup>-1</sup> (Table 2). The amount of crocin in Iranian saffron was found to be 358.38 mg kg<sup>-1</sup>. As seen in the Table 2, the highest amount of crocin was observed in Hatay Yayladağı

saffron with 647.26 mg kg<sup>-1</sup>. Crocin amounts in some locations in Turkey, especially Yayladağı and Kırıkhan in Hatay, Ayaş and Polatlı in Ankara and Tarsus in Çukurova locations, are found to be higher compared to the Iranian saffron. In the literature, the amounts of crocin under different locations, drying conditions and 20 months storage period were reported to be 333.33 mg kg<sup>-1</sup> in Tehran and 293.33 mg kg<sup>-1</sup> in Alborz in Iran.<sup>26</sup> This study shows that the amounts of crocin obtained from Iranian saffron are very close to our findings. When the crocetin amounts were evaluated according to GC-MS/FID analysis results, the highest crocetin amounts were obtained in the order of Ayaş saffron in Ankara with 6.73 mg kg<sup>-1</sup>, Iskenderun saffron in Hatay with 5.98 mg kg<sup>-1</sup>, Adana Çukurova saffron in Çukurova with 3.26 mg kg<sup>-1</sup>, Safranbolu Ovacuma saffron in Karabük with 2.20 mg kg<sup>-1</sup> and Korkuteli saffron in Antalya with 2.20 mg kg<sup>-1</sup>. The amount of crocetin in Iranian saffron was 5.80 mg kg<sup>-1</sup>. The highest amount of crocetin was observed in Ayaş saffron in Ankara with 6.73 mg kg<sup>-1</sup>.

### 3.2. Evaluation of major components in saffron samples

Major components of saffron samples grown in Iran and different locations in Turkey are presented in Table 3. Six most abundant volatile components found in saffron samples identified by GC-MS/MS analysis are shown in Table 3.

**Table 3.** Major volatile components of saffron samples obtained in Iran and macro and micro locations in Turkey.

<b>The fractions (%) of major components observed in saffron grown in Hatay macro climate</b>						
	<b>Rt</b>	<b>Volatile components</b>	<b>Kırıkhan</b>	<b>İskenderun</b>	<b>Hassa</b>	<b>Yayladağı</b>
1	12.706	Safranal	24.47	29.51	28.56	75.48
2	38.696	Glyceryl Arachidate	20.71	20.16	15.48	5.32
3	33.429	Linoleic Acid	9.53	2.65	0.38	0.34
4	31.481	Palmitic Acid	5.47	3.52	4.95	1.89
5	33.302	Stearolic Acid	4.04	4.59	8.40	3.07
6	39.466	Oleoamide	2.79	7.13	2.65	0.90
			<b>67.01</b>	<b>67.56</b>	<b>60.42</b>	<b>87.00</b>
<b>The fractions (%) of major components observed in saffron grown in Karabük macro climate</b>						
				<b>Safranbolu Yukarıçiftlik</b>	<b>Safranbolu Ovacuma</b>	
1	12.706	Safranal		64.10		86.90
2	38.696	Glyceryl Arachidate		7.45		3.46
3	18.905	2,6,6-Trimethyl-4-Hydroxy-1-Cyclohexene-1-Carboxaldehyde		1.43		1.75
4	33.302	Stearolic Acid		3.06		1.23
5	31.481	Palmitic Acid		2.60		0.92
6	11.182	2,3-Dihydro-3,5-Dihydroxy-6-Methyl-4H-Pyran-4-One		0.73		0.69
				<b>79.37</b>		<b>94.95</b>
<b>The fractions (%) of major components observed in saffron grown in Ankara macro climate</b>						
			<b>Ayaş</b>	<b>Nallıhan</b>		<b>Polath</b>
1	12.706	Safranal	68.90	66.97		70.20
2	38.696	Glyceryl Arachidate	8.62	6.68		5.55
3	39.466	Oleoamide	3.56	1.10		1.18
4	33.302	Stearolic Acid	2.47	6.36		2.90
5	31.481	Palmitic Acid	1.65	2.67		0.00
6	33.465	Linolenic Acid Methyl Ester	1.44	2.05		0.18
			<b>86.64</b>	<b>85.83</b>		<b>80.01</b>
<b>The fractions (%) of major components observed in saffron grown in Çukurova macro climate</b>						
			<b>Adana Çukurova</b>	<b>Mersin Tarsus</b>		<b>Osmaniye Kadirli</b>
1	12.706	Safranal	65.5	57.5		68.6
2	38.696	Glyceryl Arachidate	6.98	7.48		6.94
3	33.302	Stearolic Acid	4.22	6.20		2.23
4	31.481	Palmitic Acid	2.40	0.00		1.94
5	5.098	Butenolide	2.36	0.63		0.33
6	11.182	2,3-Dihydro-3,5-Dihydroxy-6-Methyl-4H-Pyran-4-One	1.26	1.70		1.38
			<b>82.72</b>	<b>73.51</b>		<b>81.42</b>
<b>The fractions (%) of major components observed in saffron grown in Antalya macro climate</b>						
						<b>Korkuteli</b>
1	12.706	Safranal				68.6
2	38.696	Glyceryl Arachidate				6.94
3	33.302	Stearolic Acid				2.23
4	31.481	Palmitic Acid				1.94
5	17.661	Isopropylidencyclopropyl Methyl Ketone				1.63
6	11.182	2,3-Dihydro-3,5-Dihydroxy-6-Methyl-4H-Pyran-4-One				1.38
						<b>82.72</b>
<b>The fractions (%) of major components observed in saffron grown in Iran macro climate</b>						
						<b>Rezevi Horasam</b>
1	12.706	Safranal				64.7
2	38.696	Glyceryl Arachidate				7.10
3	33.429	Linoleic Acid				3.84
4	31.481	Palmitic Acid				2.46
5	33.302	Stearolic Acid				2.10
6	17.661	Isopropylidencyclopropyl Methyl Ketone				1.81
						<b>82.01</b>



These six components have been detected as major volatile components of the saffron stigmas. The second most abundant component of the saffron samples for all locations was found to be glyceryl arachidate. The highest amount of volatile components in saffron samples were observed in the order of Safranbolu Ovacuma saffron in Karabük with 94.95%, Hatay Yayladağı saffron with 87.00%, Ankara Ayaş Saffron with 86.64%, Adana Çukurova saffron with 82.72% and Antalya Korkuteli Saffron with 82.72%. The amount of major volatile components in the Iranian saffron was found to be 82.01%.

### 3.3. Evaluation of essential fatty acid components

According to the obtained results, saffron samples contained significant amounts of fatty acids as major components. It was observed that saffron samples contain very rich essential fatty acid compositions including palmitic acid, pentadecanoic acid, stearolic acid, linoleic acid, linolenic acid methyl ester, stearic acid and

oleoamide. These fatty acids found in saffron samples are shown in Table 4. The highest amounts of fatty acids found in saffron samples are observed with 23.56% from Kırıkhan saffron in Hatay, 13.79% from Antalya saffron, 13.40% from Nallıhan saffron in Ankara, 11.31% from Mersin Tarsus saffron and 9.76% from Safranbolu Yukarıçiftlik saffron in Karabük. The fatty acid fraction in the Iranian saffron is detected to be 10.36%. Table 4 shows that fractions of the volatile fatty acids in saffron stigmas are quite high, such amounts of fatty acids is considered to be very important for both human health and saffron quality. Tables 4 also shows that stearolic acid seems to be the most abundant fatty acid found in saffron stigmas for all locations. In the literature, differences between the amounts of saturated and unsaturated fatty acids in saffron pollens were found to be quite high. Omega acids (3,6,7,9) including linolenic acid have been reported to be found among the unsaturated fatty acids.<sup>9</sup>

**Table 4.** Volatile fatty acids obtained from Iranian saffron and saffron samples from micro and macro locations in Turkey.

Macro Locations	Micro Locations	Fatty acid fractions (%)							Total (%)
		Palmitic (%)	Pentadecanoic (%)	Stearolic (%)	Linoleic (%)	Linolenic Methyl Ester (%)	Stearic (%)	Oleoamide (%)	
HATAY	Kırıkhan	5.47	0.54	4.04	9.53	0.00	1.19	2.79	<b>23.56</b>
	İskenderun	3.52	0.54	4.59	2.65	0.00	1.13	7.13	<b>19.56</b>
	Hassa	4.95	0.00	8.40	0.38	0.00	1.39	2.65	<b>17.77</b>
	Yayladağı	1.89	0.00	3.07	0.34	1.12	0.52	0.90	<b>7.84</b>
KARABÜK	Safranbolu Yukarıçiftlik	2.60	0.41	3.06	0.31	1.98	0.00	1.40	<b>9.76</b>
	Safranbolu Ovacuma	0.92	0.19	1.23	0.00	0.00	0.31	0.49	<b>3.14</b>
ANKARA	Ayaş	1.65	0.00	2.47	0.23	1.44	0.00	3.56	<b>9.35</b>
	Nallıhan	2.67	0.23	6.36	0.22	2.05	0.77	1.10	<b>13.40</b>
	Polatlı	0.00	0.27	2.90	0.28	0.18	2.66	1.18	<b>7.47</b>
ÇUKUROVA	Adana Çukurova	2.40	0.00	4.22	0.29	0.00	1.23	0.99	<b>9.13</b>
	Tarsus	0.00	0.44	6.20	0.41	0.00	3.21	1.05	<b>11.31</b>
	Osmaniye Kadirli	1.94	0.39	2.23	0.36	0.00	0.74	0.91	<b>6.57</b>
ANTALYA	Korkuteli	0.00	0.63	0.00	0.56	4.25	7.14	1.21	<b>13.79</b>
IRAN	Rezevi Horasanı	2.46	0.33	2.10	3.84	0.00	0.94	0.69	<b>10.36</b>

### 3.4. Evaluation of the bioactive components

Comparison of the bioactive components (drug, food, pharmacological) of the Iranian saffron and saffron grown in different locations in Turkey are given in Table 5. Bioactive components were identified with literature searches (PubChem and Sigma Aldrich Research Databases). Volatile fatty acids found in saffron samples are already shown in Table 4 and therefore, they are not included in Table 4. Safranbolu Ovacuma saffron in Karabük had the highest amount of volatile compounds

(90.84%) with bioactive properties, followed in the order by 82.31% in Yayladağı saffron in Hatay, 79.31% in Ayaş saffron in Ankara, 77.03% in Osmaniye Kadirli saffron in Çukurova region and 55.28% in Korkuteli saffron in Antalya. The fraction of the bioactive volatile components found in the Iranian saffron was 74.41%. It has been reported in the literature that bioactive compounds may differ between dissimilar genotypes or genotypes collected from different geographic regions.<sup>27,28</sup> Therefore, none of the bioactive components were found at the same amount for all locations.<sup>24</sup> In a

study carried out with olfactometric technique, it was reported that 2,3-butanedione was found as a main flavor compound of Spanish saffron. In the same study, many bioactive components including safranal, isophorone,

and 4-ketoisophorone were found in the saffron samples.<sup>29</sup> Isophorones are known to be bioactive and have chemopreventive, antimicrobial and antioxidant activity properties.

**Table 5.** Bioactive components of saffron samples obtained in Iran and macro and micro locations in Turkey.

Macro Locations	Micro Locations	Butenolide (%)	Cyclopentanone (%)	Isophorone (%)	Ketosisophorone (%)	Safranal (%)	1-Phenylethanol (%)	Glycerol Palmitate (%)	Glycerol Arachidate (%)	Total (%)
HATAY	Kırıkhan	1.24	2.48	0.00	0.63	24.47	1.81	1.38	20.71	<b>52.72</b>
	İskenderun	1.74	1.20	1.44	0.64	29.51	0.46	1.37	20.16	<b>56.52</b>
	Hassa	1.49	1.46	1.68	0.40	28.56	0.00	1.34	15.48	<b>50.41</b>
	Yayladağı	0.85	0.19	0.00	0.00	75.48	0.00	0.47	5.32	<b>82.31</b>
KARABÜK	Safranbolu	1.33	0.25	0.86	0.83	64.1	0.89	0.00	7.45	<b>75.71</b>
	Yukarıçiflik Ovacuma	0.00	0.00	0.00	0.23	86.88	0.00	0.27	3.46	<b>90.84</b>
ANKARA	Ayaş	0.59	0.00	0.00	0.55	68.88	0.00	0.67	8.62	<b>79.31</b>
	Nallıhan	1.24	0.18	0.00	0.25	66.97	0.00	0.65	6.68	<b>75.97</b>
	Polatlı	0.20	0.00	0.00	0.27	70.23	0.00	0.53	5.55	<b>76.78</b>
ÇUKUROVA	Adana	2.36	0.00	0.00	0.66	65.53	0.00	0.61	6.98	<b>76.14</b>
	Çukurova	0.63	0.00	1.29	0.7	57.48	0.00	0.83	7.48	<b>68.41</b>
	Mersin Tarsus	0.33	0.00	0.00	0.61	68.58	0.00	0.57	6.94	<b>77.03</b>
ANTALYA	Korkuteli	2.30	0.00	2.61	0.83	34.67	0.00	1.24	13.63	<b>55.28</b>
	Rezevi Horasanı	1.24	0.00	0.00	0.63	64.66	0.00	0.78	7.10	<b>74.41</b>

#### 4. CONCLUSION

In this work, we studied the effects of different geographical locations on the kind and amounts of volatile and fatty acid components of saffron. The results showed a significant effect of the location on the volatile compounds of saffron. On the basis of the obtained results, saffron is an adaptable plant and can be efficiently produced in different geographical and climate conditions. Geographic origin, drying process and different agricultural processes play an important effect on the qualities of saffron and may result in significant differences in the amounts of volatile and bioactive components in saffron samples. According to the obtained outcomes, the highest qualities saffron were determined to be observed in Hatay yayladağı and Karabük safranbolu ovacuma saffron, respectively. Even though Hatay yayladağı and Karabük safranbolu stations located in different geographic regions, their altitudes are very close. Therefore, they probably have similar climate effects on the qualities of saffron.

#### Conflict of interest

Authors declare that there is no conflict of interest with any person, institute, company, etc.

#### REFERENCES

- Hire, R.R.; Srivastava, S.; Davis, M.B.; Konreddy, A.K.; Panda, D. Antiproliferative Activity of Crocin Involves Targeting of Microtubules in Breast Cancer Cells. *Sci Rep.* **2017**, 7(1): 44984.
- Khorasanchi, Z.; Shafiee, M.; Kermanshahi, F.; Khazaei, M.; Ryzhikov, M.; Parizadeh, M.R.; Kermanshahi, B.; Ferns, G.A.; Avan, A.; Hassanian, S.M. *Crocus sativus* a natural food coloring and flavoring has potent anti-tumor properties. *Phytomedicine.* **2018**, 43: 21-27.
- Mir, M.A.; Ganai, S.A.; Mansoor, S.; Jan, S.; Mani, P.; Masoodi, K.Z.; Amin, H.; Rehman, M.U.; Ahmad, P. Isolation, purification and characterization of naturally derived Crocetin beta-d-glucosyl ester from *Crocus sativus* L. against breast cancer and its binding chemistry with ER-alpha/HDAC2. *Suudi J Biol Sci.* **2020**, 27(3): 975-984.
- Asil, H. Farklı Depolama Sürelerinin Safranın (*Crocus sativus* L.) Farmakolojik Ajanlarına (Safranal, Crocin ve Crocetin) Etkisi ve Kalite Özellikleri Bakımından Değerlendirilmesi. Celal Bayar Üniversitesi

- Sağlık Bilimleri Enstitüsü Dergisi. **2021**, 8 (2) , 263-269. DOI: 10.34087/cbusbed.804112
5. Lautenschläger, M.; Sendker, J.; Hüwel, S.; Galla, H. J.; Brandt, S.; Düfer, M.; and Hensel, A. Intestinal formation of trans-crocetin from saffron extract (*Crocus sativus* L.) and in vitro permeation through intestinal and blood brain barrier. *Phytomedicine*. **2015**, 22(1), 36-44.
6. Reddy, C.N.; Bharate, S.B.; Vishwakarma, R.A.; Bharate, S.S. Chemical analysis of saffron by HPLC based crocetin estimation. *J Pharm Biomed Anal*. **2020**, 181: 113094.
7. Cardone, L.; Castronuovo, D.; Perniola, M.; Cicco, N.; Candido, V. Evaluation of corm origin and climatic conditions on saffron (*Crocus sativus* L.) yield and quality. *J. Sci. Food Agric*. **2019**, 99(13): 5858-5869.
8. Trimigno, A.; Marincola, F.C.; Dellarosa, N.; Picone, G.; Laghi, L. Definition of food quality by NMR-based foodomics. *Curr. Opin. Food Sci*. **2015**, 4: 99-104.
9. Chichiricò, G.; Ferrante, C.; Menghini, L.; Recinella, L.; Leone, S.; Chiavaroli, A.; Brunetti, L.; Di Simone, S.; Ronci, M.; Piccone, P.; Lanza, B.; Cesa, S.; Poma, A.; Vecchiotti, G.; Orlando, G. *Crocus sativus* by-products as sources of bioactive extracts: Pharmacological and toxicological focus on anthers. *Food Chem. Toxicol*. **2019**, 126: 7-14.
10. Lahmass, I.; Ouahhoud, S.; Elmansuri, M.; Sabouni, A.; Elyoubi, M.; Benabbas, R.; Choukri, M.; Saaloui, E. Determination of Antioxidant Properties of Six By-Products of *Crocus sativus* L. (Saffron) Plant Products. *Waste and Biomass Valorization*. **2018**, 9(8): 1349-1357.
11. Asil, H.; Ayanoglu, F. The Effects of Different Gibberellic Acid Doses and Corm Cutting Methods on Saffron (*Crocus sativus* L.) Yield Components in Turkey. *Fresenius Environ. Bull*. **2018**, 27(12A): 9222-9229.
12. Caballero-Ortega, H.; Pereda-Miranda, R.; Abdullaev, F.I. HPLC quantification of major active components from 11 different saffron (*Crocus sativus* L.) sources. *Food Chem*. **2007**, 100(3): 1126-1131.
13. Fernandez, J.A. Biology, biotechnology and biomedicine of saffron. Recent research developments in plant science. **2004**, 2: 127-159.
14. Ben El Caid, M.; Salaka, L.; El Merzougui, S.; Lachguer, K.; Lagram, K.; El Mousadik, A.; Serghini, M.A. Multi-site evaluation of the productivity among saffron (*Crocus sativus* L.) for clonal selection purposes. *J Appl Res Med Aromat Plants*. **2020**, 17: 100248.
15. Koçer, O, Ayanoglu, F . Dişi Defne (*Laurus nobilis* L.) Genotiplerinde Meyve Yağ Asitleri Kompozisyonlarının Belirlenmesi . *Uluslararası Doğu Anadolu Fen Mühendislik ve Tasarım Dergisi* , **2021**. 3 (1) , 72-88 . DOI: 10.47898/ijeased.843773.
16. Koçer, O.; Ayanoglu, F.; Konuşkan, D.B. Quality Characteristics of Bay laurel (*Laurus nobilis* L.) Fatty Oils Extracted by Different Methods, 4. International Symposium of Medicinal and Aromatic Plants, **2018**
17. Koçer, O.; Ayanoglu, F.; Konuşkan, D.B. Determination of Suitable Bay Laurel (*Laurus nobilis* L.) Genotypes for Fruit Growing and Effects of Different Harvest Periods on Fatty Oil Quality, 4. International Symposium of Medicinal and Aromatic Plants, **2018**
18. Carmona, M.; Zalacain, A.; Salinas, M.R.; Alonso, G.L. A new approach to saffron aroma. *Crit Rev Food Sci Nutr*. **2007**, 47(2): 145-159.
19. Gokturk, E.; Asil, H. Hatay/Kırıkhan'da Yetiştirilen Safran (*Crocus sativus* L.) Stigmasının Ekstraktının GC-MS analizi. *Türk Tarım ve Doğa Bilimleri Dergisi*. **2018**, 5(3): 317-321.
20. Koçer, O. Hatay Yöresinde Yetişen *Thymbra spicata* L. (Zahter/Karabaş Kekliği) Bitkisinin Uçucu Yağ Oran ve Bileşenlerinin Belirlenmesi . *Avrupa Bilim ve Teknoloji Dergisi* , **2021**. (27) , 446-449 . DOI: 10.31590/ejosat.963053
21. Rezaee, R.; Hosseinzadeh, H. Safranin: from an aromatic natural product to a rewarding pharmacological agent. *Iran. J. Basic Med. Sci*. **2013**, 16(1): 12-26.
22. Culleré, L.; San-Juan, F.; Cacho, J. Characterisation of aroma active compounds of Spanish saffron by gas chromatography–olfactometry: Quantitative evaluation of the most relevant aromatic compounds. *Food Chem*. **2011**, 127(4): 1866-1871.
23. Farag, M.A.; Hegazi, N.; Dokhalahy, E.; Khattab, A.R. Chemometrics based GC-MS aroma profiling for revealing freshness, origin and roasting indices in saffron spice and its adulteration. *Food Chem*. **2020**, 331: 127358.
24. Anastasaki, E.; Kanakis, C.; Pappas, C.; Maggi, L.; Del Campo, C.P.; Carmona, M.; Alonso, G.L.; Polissiou, M.G. Geographical differentiation of saffron by GC–MS/FID and chemometrics. *Eur. Food Res. Technol*. **2009**, 229(6): 899-905.
25. Bononi, M.; Milella, P.; Tateo, F. Gas chromatography of safranin as preferable method for the commercial grading of saffron (*Crocus sativus* L.). **2015**, *Food Chemistry*. 176: 17-21.

26. Rahimi, A.; Rezaee, M.B.; Jaimand, K.; Ashtiany, A.N. Effects of Storage and Cultivation on Crocin Content of Dried Stigma of Saffron *Crocus sativus* L. *Akademik Gıda*. **2014**, 12(1): 16-19.

27. Sampaio, B.L.; Edrada-Ebel, R.; Da Costa, F.B. Effect of the environment on the secondary metabolic profile of *Tithonia diversifolia*: a model for environmental metabolomics of plants. *Sci. Rep.* **2016**, 6(1): 29265.

28. Vahedi, M.; Kabiri, M.; Salami, S.A.; Rezaeost, H.; Mirzaie, M.; Kanani, M.R. Quantitative HPLC-based metabolomics of some Iranian saffron (*Crocus sativus* L.) accessions. *Ind Crops Prod.* **2018**, 118: 26-29.

29. Amanpour, A.; Sonmezdag, A.S.; Kelebek, H.; Selli, S. GC-MS-olfactometric characterization of the most aroma-active components in a representative aromatic extract from Iranian saffron (*Crocus sativus* L.). *Food Chem.* **2015**, 182: 251-256.



## Phytochemical and GCMS analysis on the ethanol extract of *Foeniculum Vulgare* and *Petroselinum crispum* leaves

Jamaluddeen MOHAMMED ABUBAKAR<sup>1</sup>, Great IRUOGHENE EDO<sup>1</sup>,

Nur PAŞAOĞLULARI AYDINLIK<sup>1,\*</sup>

<sup>1</sup>Faculty of Arts and Sciences, Department of Chemistry, Cyprus International University, Nicosia, Turkey

Received: 8 April 2021; Revised: 26 October 2021; Accepted: 27 October 2021

\*Corresponding author e-mail: [mailto:nurp@ciu.edu.tr](mailto:mailto:nurp@ciu.edu.tr)

**Citation:** Mohammed, Abubakar, J.; Iruoghene, Edo, G.; Paşaoğluları, Aydınlik, N. *Int. J. Chem. Technol.* 2021, 5 (2), 107-124.

### ABSTRACT

*Petroselinum crispum* (Parsley) and *Foeniculum vulgare* (Fennel) are aromatic herbs belonging to Apiaceae and Lamiaceae family. Phytochemical, GC-MS and FTIR properties of ethanolic extract of *Foeniculum vulgare* and *Petroselinum crispum* leaves investigated. Plant leaves were extracted based on separation using ethanol and subjected to phytochemical testing that revealed the presence of biologically active substances including terpenoids, steroids, flavonoids, alkaloids, tannins and cardiac glycosides. GC-MS evaluation of *Foeniculum vulgare* revealed two bioactive compounds (1,4 Cyclohexadiene and Metronidazole) and *Petroselinum crispum* revealed six bioactive compounds (Cineole, I-Limonene, Cyclohexane, Phenol, Neophytadiene and 9,12,15 octadecatrienoic). FTIR analysis of parsley displayed strong bands at 2915.50 cm<sup>-1</sup> which corresponds to C–H stretching and medium band at 1476.80 cm<sup>-1</sup> which corresponds to N-H stretching vibrations due to the presence of amino acids. Fennel displayed strong bands at 2832.61 cm<sup>-1</sup> which is equivalent to C–H showing saturated and unsaturated compounds and medium band at 1029.98 cm<sup>-1</sup> corresponds to C–O present in esters. Antibacterial activity of these plants confirmed their effectiveness in the traditional medicine.

**Keywords:** *Petroselinum crispum*, *foeniculum vulgare*, FTIR, medicinal plant, phytochemical, GC-MS.

### *Foeniculum vulgare* ve *Petroselinum crispum* yapraklarının etanol özündeki fitokimyasal ve GCMS analizi

#### ÖZ

*Petroselinum crispum* (Maydanoz) ve *Foeniculum vulgare* (Rezene) türleri sırasıyla Apiaceae ve Lamiaceae familyasına ait aromatik bitkilerdir. Bu çalışmada *Foeniculum vulgare* ve *Petroselinum crispum* yapraklarının etanolik ekstraktının fitokimyasal, GC-MS ve FTIR özelliklerinin araştırılması amaçlanmıştır. Her iki bitkinin yaprakları etanol kullanılarak ekstrakte edilip ayrıldı. Ayrılan bu ekstraktlar terpenoidler, steroidler, flavonoidler, alkaloidler, tanenler ve kardiyak glikozitler dahil biyolojik olarak aktif maddelerin varlığını ortaya çıkaran fitokimyasal testlere tabi tutuldu. GC-MS ölçümünde *Foeniculum vulgare*'nin değerlendirmesinde iki biyoaktif bileşik (1,4 Cyclohexadiene ve Metronidazole) ve *Petroselinum crispum* altı biyoaktif bileşik (Cineole, I-Limonene, Cyclohexane, Phenol, Neophytadiene ve 9,12,15 octadecatrienoic) ortaya çıkmıştır. Maydanoz'un FTIR analizinde, C–H gerilmesine karşılık gelen 2915.50 cm<sup>-1</sup>'de güçlü bantlar ve amino asitlerin varlığından dolayı N-H gerilme titreşimlerine karşılık gelen 1476.80 cm<sup>-1</sup>'de orta bantlar saptanmıştır. Rezenede sırasıyla doymuş ve doymamış bileşikler gösteren C–H'ye eşdeğer olan 2832.61 cm<sup>-1</sup>'de güçlü bantlar saptanmış ve 1029.98 cm<sup>-1</sup>'deki orta bant esterlerde bulunan C–O'ya karşılık gelmiştir. Bu bitkilerin antibakteriyel aktivitesi, geleneksel tıptaki etkinliklerini doğrulamıştır.

**Anahtar Kelimeler:** *Petroselinum crispum*, *foeniculum vulgare*, FTIR, tıbbi bitki, fitokimyasal, GC-MS.

### 1. INTRODUCTION

Plants and their derivatives have always been an important source of medication for our ailing conditions for centuries in the history of mankind.<sup>1</sup> The first understanding and the discovery of different healing

effects of plants was from ancient times. Over time, humans became interested in knowing the exact origins and what was responsible for most of the healing properties of the components of the plant.<sup>2</sup> Plants are the primary basis of pharmaceutical drugs, with a broad range of biological actions including antimicrobial,



antioxidants and anti-fungal properties.<sup>3,4</sup> Although, several microorganisms have formed resistance against antibiotics, leading to healing deficiency.<sup>5,6</sup> Current antibiotic treatments are also very costly. Plants can produce a large number of diverse bioactive compounds.<sup>7</sup> High concentrations of phytochemicals, which may protect against free radical damage, accumulate in fruits and vegetables. Plants containing valuable phytochemicals can complement the needs of the human body by acting as natural antioxidants.<sup>8</sup> Several studies have shown that many plants are rich source of antioxidants. This resulted in an increase in the use of plant extracts and their derivatives.<sup>9</sup> In early research, some botanical products have demonstrated the curative ability of severe illnesses including cancer, blood glucose, and inflammation.<sup>10,11</sup> These reports reveal that the plants however constitute significantly for the detection of innovative drugs and medicinal substances. *Foeniculum vulgare* is commonly referred to as fennel plant belonging to the *Lamiaceae* family originally cultivated mainly in the Mediterranean region, although it is currently being adapted and planted in most part of the world. Research has indicated that the fennel plant particularly its leaves contains various biologically active and phytochemical constituents.<sup>12</sup> In highly European countries, fennel is traditional utilized as a therapeutic herb with a recipe in local dishes.<sup>13</sup> In Cyprus, the leaves and flowers are also being used as dyes called Turkish brown or yellow dye.<sup>14</sup> It is an indigenous plant of Mediterranean region in southern Europe to be precise, but then owing to its therapeutic benefit and huge bioactive constituent, fennel become adopted virtually everywhere on the world right now.<sup>12</sup> Its fresh or dried leaves, roots, seed and fruit are used in cosmetic products, pharmaceutical and food industries.

*Petroselinum crispum* (Parsley) exists as a herb from the *Apiaceae* family, which is being used in food, medicinal products, cosmetic and perfume industry.<sup>15</sup> *Petroselinum crispum* may prove to be one of the world's most ancient medicinal plants used as a condiment in food.<sup>16</sup> Earlier research on the biochemical makeup of *Petroselinum crispum* have showed the existence of flavonoid compounds, terpenoids and 2H-chromen-2-one.<sup>17</sup> It is used for treating different illnesses like strokes, clotting, alzheimer and cardiovascular diseases. In traditional medicine, *Petroselinum crispum* is used as a treatment for hemorrhoids, the roots for treating urethral infection, kidney stones and enhancing brain operation and memory.<sup>18</sup> Furthermore, Parsley is being utilized as a hypoglycemic, abortifacient, hypolipidemic, carminative, anticoagulant, emmenagogic agent and antimicrobial agent.<sup>19</sup>

This research was aimed to investigate the phytochemical, GC-MS and FTIR properties of ethanolic extract of *Foeniculum vulgare* and *Petroselinum crispum* leaves.

## 2. MATERIALS AND METHODS

### 2.1. Extract preparation

*Foeniculum vulgare* and *Petroselinum crispum* leaves were acquired from a vegetable garden in Iefkosa, Cyprus. Both plant leaves were identified by a botanist from the Cyprus ministry of agriculture and natural resources. The collected leaves from both plant material was left dry at room temperature and later grounded in an electric power grinder. Consequently, 45 g of both plant leaves powder were extracted using 200 ml of ethanol in a Soxhlet system and both extracts were filtered using a Whatman filter paper. The amount of extracts obtained was weighed and the residue were kept in dark to be used further during the experiment.<sup>20</sup> The residue was kept in the dark to prevent changes in the nature of the plant's constituents.

### 2.2. Chemicals and materials

The chemicals used were all analytical grade reagents. The chemicals used were purchased from the Sigma-Aldrich chemical company (St. Louis, MO, USA). The Milli-Q purification system (Millipore, Bedford, MA, USA) was used for the refinement of water used in the research analysis.

### 2.3. Phytochemical screening

The qualitative phytochemical screening of the ethanolic extract of both plant leaves were subjected for the discovery of various phytochemicals produce in the ethanol extracts by using standard method proposed by Shahmokhtar and Farzaei.<sup>21,22</sup> The ethanol extract was evaluated for the presence and absence of Flavonoids, Tannins, Saponins, Steroids, Terpenoids, Cardiac glycosides and Alkaloids.

### 2.4. Saponins

5ml of distilled water (5ml) was mixed with 2 g of extract and shaken vigorously in a test tube for 45 s. The test tube was let to stand for 30 minutes in a vertical position. The honeycomb froth that persists for 15-20 minutes demonstrates the presence of saponins.

### 2.5. Alkaloids

2ml of 1% HCL was added to 1 g of extract and then moderately heated, then the reagents (Mayer and Wagner) were added at the same time to the mixture. Darkening of the resulting precipitate was regarded as the evidence for the presence of alkaloids.

### 2.6. Tannins

The ethanol extract (1g) was mixed with distilled water (15ml) inside a test tube and heated simultaneously with

the addition of ferric chloride solution (in drops) showing the presence of tannins when a brownish green color is observed.

### 2.7. Flavonoids

The ethanol extract (1g) was mixed with sodium hydroxide (4ml) and H<sub>2</sub>SO<sub>4</sub> (2 drops) showing the presence of flavonoids when a yellow coloration is formed.

### 2.8. Glycosides

Acetic acid (4ml) and chloroform (2ml) were mixed with ethanol extract (1g) forming a solution which was cooled and the addition of H<sub>2</sub>SO<sub>4</sub> showing the presence of glycosides when a green coloration is formed.

### 2.9. Steroids

Chloroform (2ml) was mixed with ethanol extract (1g) and then H<sub>2</sub>SO<sub>4</sub> (4ml) showing the presence of steroids when a reddish coloration is formed.

### 2.10. Terpenoids

Chloroform (4ml) and acetic anhydride (1ml) were mixed with ethanol extract (1g) and the addition of H<sub>2</sub>SO<sub>4</sub> (2ml) showing the presence of terpenoids when a reddish violet coloration is formed.

### 2.11. GC-MS analysis

GC has the ability to detect and resolve complex mixtures extracts containing many different compounds. Immediately the components exit the GC column, they are then ionized and separated as fragments by the mass spectrometer (MS) using chemical ionization sources. The *Foeniculum vulgare* and *Petroselinum crispum* leaves ethanol extracts were analyzed using a GC-MS system (GC-MSQP2010 SE plus Shimadzu Technology Japan) equipped with an HP-5MS capillary column (30m x 0.25 mm) to determine the active compound. The injection volume of each sample was 1 µL. Helium was used as a carrier gas with flow rate of 1 mL/min, the injection port temperature was 250°C and the program of the sample was set to a temperature range from 50°C to 300°C at a rate of 50°C/min and 10min hold at 300°C for non-volatile constituents. The GC-MS analysis was carried out in Chemistry Laboratory of Cyprus International University.

### 2.12. Identification of Compounds

The identification details of the separation between the volatile compounds was carried out via retention indices and mass spectrometry through a comparison using database of National Institute Standard and Technology (NIST), library 2008.

### 2.12. FTIR analysis

The Fourier-transform infrared spectroscopy (FTIR) method and technique was used for the determination and identification of various types of functional groups in each powdered leaf ethanol extract of the two plants used in the analysis as described by Hussein.<sup>4</sup> The absorbed light wavelength is a function of the chemical bond. By reading the infrared absorption spectrum, the chemical bonds within a molecule are determined. The infrared spectroscopy spectrum (IR) was obtained using the Fourier-transform infrared spectroscopy (Shimadzu Japan). The ethanol extract powdered (10mg) of both plant leaves was ground in an agate mortar, encapsulated in 100mg of KBr pellet, to prepare translucent sample disc and pestle in order to obtain a fine powdered sample and the obtained fine powder was subsequently used for the FTIR analysis.

## 3. RESULTS AND DISCUSSION

Qualitative analysis of some secondary metabolites was studied in *Foeniculum vulgare* and *Petroselinum crispum* leaves ethanol extract. Generally, the medicinal properties of pharmaceutical plants may be ascribed to the existence of a variety of phytochemicals such as Steroids, Tannins, Terpenoids etc. The various biological activities of all known phytochemicals including antioxidants, antifungals and antibacterial activity are recognized. The results showed that both plant extracts contain flavonoids, tannins, saponins, steroids, terpenoids, alkaloids and glycosides. Likewise, terpenoids were not present in *Petroselinum crispum* leaves ethanol extract. These phytochemicals indicated to offer exceptional pharmaceutical activities in both the conventional and traditional medicine. The unique healing and medicinal effects of plants is also dependent on the presence of their secondary metabolites. *Foeniculum vulgare* and *Petroselinum crispum* ethanol leaves extract, in accordance with the previous phytochemical study, have the same secondary metabolites such as flavonoids, tannins, saponins, steroids, terpenoids and glycosides.<sup>12,22</sup> The presence of organic nitrogen compounds with antibacterial properties is alkaloids. The core group of phenolic compounds acting as anti-inflammatory, antimutagenic, antioxidants and anticarcinogenic properties are flavonoids and tannins. hepatoprotective, antipyresis, antidiabetic, pain alleviation and relaxing therapies are found in terpenoids. Both plants have often been used as nausea, laxative and antitumor treatments for fever medications.<sup>23,24</sup> Analysis of phytochemistry of both leaves showed that both plants contain rich bioactive compounds as shown in Table 1 and Table 2. However, the leaves and stems are currently used in a limited number of current uses in conventional medicine, the lack of science reports on the leaf prompted us to carry out a methodical phytochemical analysis of the plant. Potential future research would certainly allow the positive properties to be highlighted, which may open

new pathways so that they can make effective use of the plant as a rich source of bioactive compounds in the pharmaceutical industry.

**Table 1.** phytochemical analysis results of *Foeniculum Vulgare* leaves ethanol extract.

Phytochemicals	<i>Foeniculum Vulgare</i> leaves
Flavonoids	+
Tannins	+
Saponins	+
Steroids	+
Terpenoids	+
Alkaloids	+
Glycosides	+

+ (present), - (absent)

**Table 2.** Phytochemical analysis results of *Petroselinum crispum* leaves ethanol extract.

Phytochemicals	<i>Petroselinum crispum</i> leaves
Flavonoids	+
Tannins	+
Saponins	+
Steroids	+
Terpenoids	-
Alkaloids	+
Glycosides	+

+ (present), - (absent)

Fourier Transform Infrared Spectrophotometer (FTIR) is one of the most important analytical tools for the determination and identifying the types of the functional group presents in a given compound. It is also a rapid technique used to synthesize and characterize organic cell properties and identify their functional group in molecules depending on their vibrating frequency at different wave number. The FTIR spectroscopy is an analytical tool used in identification of several functional groups responsible for medicinal properties in both plants. FTIR spectroscopy was used to determine some qualitative aspects of the organic compounds in *Foeniculum vulgare* and *Petroselinum crispum* leaves ethanol extract. The FT-IR spectrum shows the characteristics of the fingerprint. The infrared spectrum

can recognize and detect certain variations not only of the main inorganic materials. We confirm the presence of many characteristics functional groups as detected at different vibrational frequency band in the IR spectrum as shown in Figure 1 and Figure 2. The various functional groups observed using FTIR spectrum indicates the presence of O-H group (alcohol), carboxylic acid, amine, Sulphur derivatives, amino acid, and nitro - compounds among others as recorded in Table 3 and Table 4. The FTIR spectrum of *Petroselinum crispum* leaves displayed four different bands across the entire range observed. The frequency bands at 2915.50 cm<sup>-1</sup> and 3300.84 cm<sup>-1</sup> corresponds to C-H and O-H stretching present in hydrocarbons and benzene ring compounds (like ascorbic acid) respectively.<sup>25,26</sup>

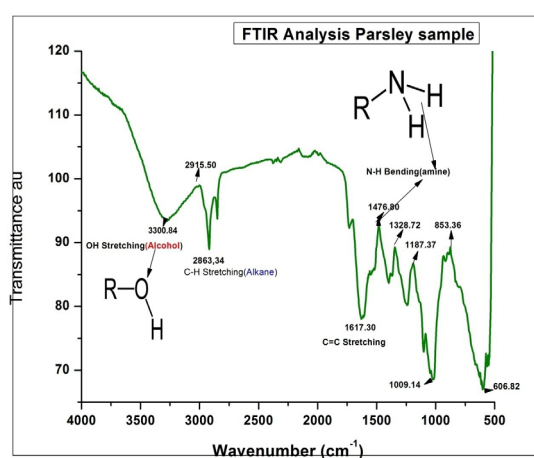


**Figure 1.** FTIR Spectrum of *Petroselinum crispum* leaves sample at solid state.

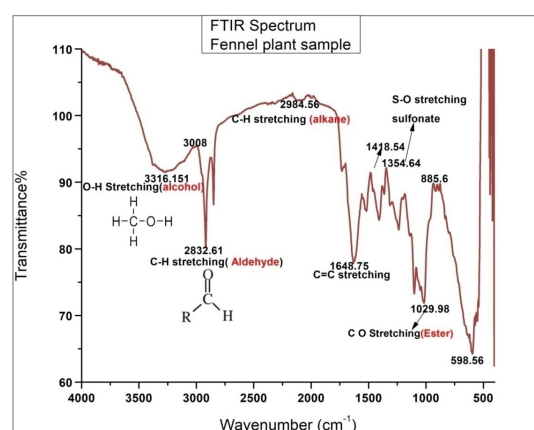


**Figure 2.** FTIR Spectrum of *Foeniculum Vulgare* leaves sample at solid state.

The absorption bands at 1476.80 cm<sup>-1</sup> which corresponds to N-H stretching vibrations may be due to the presence of amino acids.<sup>27</sup> The FTIR spectrum of *Foeniculum vulgare* leaves displayed six different bands across the entire range observed. The bands at 2832.61 cm<sup>-1</sup> and 2984.56 cm<sup>-1</sup> corresponds to C-H present in alkenes and

alkanes respectively and bands at 1029.98  $\text{cm}^{-1}$  corresponds to C–O present in esters.<sup>28</sup> The frequency bands at 3316.15  $\text{cm}^{-1}$  and 1354.64  $\text{cm}^{-1}$  corresponds to O–H stretching and SO stretching present in alcohol.<sup>25</sup>

**Table 3.** Absorption peak and functional group of *Petroselinum crispum* leaves sample (at solid state).

Absorption ( $\text{cm}^{-1}$ )	Functional Group	Peak Appearance
3300.84	OH Stretching (alcohol)	Medium
2915.50	CH Stretching (alkane)	Strong
1476.80	N-H Bending (amine)	Medium
1617.30	C=C Stretching	Medium

**Table 4.** Absorption peak and functional group of *Foeniculum Vulgare* leaves sample (at solid state).

Absorption ( $\text{cm}^{-1}$ )	Functional Group	Peak Appearance
3316.151	O-H Stretching (Alcohol)	Medium
2832.61	C-H Stretching (Alkene)	Strong
2984.56	C-H Stretching (Alkane)	Weak
1354.64	SO Stretching	Medium
1648.75	C=C Stretching	Strong
1029.98	C-O Stretching(ester)	Strong

GC-MS chromatogram is still the best instrument for the separation of organic chemical compounds while at the same time the identifying of such compounds through the use of mass spectroscopy. GC-MS analytical technique is usually seen as a common confirmation test. It is best used to make an effective chemical analysis. The analysis provides a representative spectral output of all the compounds that get separated from the sample. The initial involves injecting the sample to the injected port of the Gas chromatography (GC) device. Then the GC instrument separate and vaporizes the sample and analyses the various components. Each component was ideally producing a specific spectral peak that may be recorded on a paper chart electronically. The time elapsed between elution and injection is called the retention time. The peak is measured from the base to the tip of the peak. Interpretation of Mass-Spectrum was carried out by using the database of National institute

Standard and Technology (NIST) having more than 62,000 patterns. Where the spectrum of the unknown components is compared with the spectrum of known components which was stored in the NIST library. The name, chemical structure and molecular weight of the components of the test materials were determined. GC-MS analysis of ethanolic extract of *Foeniculum vulgare* and *Petroselinum crispum* leaves

In accordance with the present study, compounds of ethanol extracts of *Foeniculum vulgare* and *Petroselinum crispum* leaves have been identified with compounds name, retention time, peak area and its bio-active activities through GCMS evaluation. In the current research, some phytochemicals were identified from ethanol extracts by GCMS. *Foeniculum vulgare* and *Petroselinum crispum* leaves ethanol extract were subjected to GC-MS in order to recognize the phytochemical compounds. The biologically active compounds such as 1,4 Cyclohexadiene, Metronidazole, 1H-Purine-6 amine, I-Limonene which has been reported as hepatoprotective, antihistaminic, anti-eczemic, antimicrobial, anti-cancer, anti-arthritis, anti-asthma and antidiuretic activities.

Figure 3 and Figure 4 were the chromatogram of both extracts. The phytochemicals are believed to have been present between retention times 14.759 to 19.262 and 6.629 to 19.922 respectively. In *Foeniculum vulgare* leaves ethanol extract, two biologically active compounds have been detected and that this biologically active compounds name, retention time, peak area and its bio-active activities were presented in Table 5.

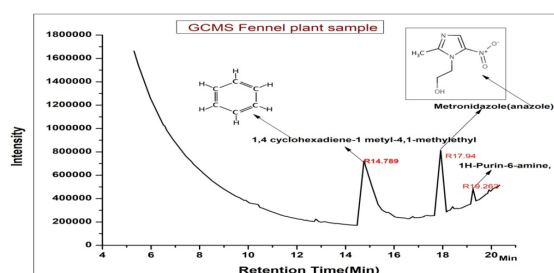


**Figure 3.** GC-MS chromatogram of Ethanolic extract of *Foeniculum Vulgare* leaves

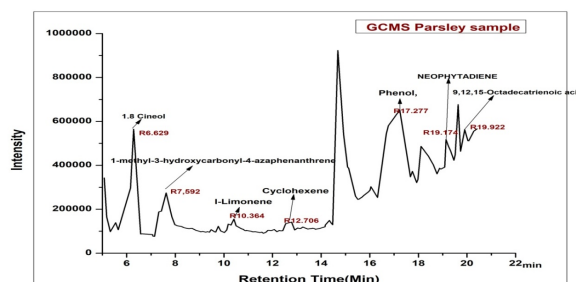


**Figure 4.** GC-MS chromatogram of Ethanolic extract of *Petroselinum crispum* leaves

The bioactive compounds are 1,4 Cyclohexadiene with the retention time at 14.759 and peak area of 3.4 has anti-cancer activity.<sup>29</sup> Metronidazole (anazole) with the retention time at 17.943 and peak area of 4.2 has Anti-bacterial activity.<sup>30</sup> 1H-Purine-6 amine at a retention time at 19.262 and a peak area of 0.96 displayed no biological activity that is linked to the compound until now.

In *Petroselinum crispum* leaves ethanol extract, six biologically active compounds have been detected and that this biologically active compounds name, retention time, peak area and its bio-active activities were presented in Table 6. The biologically active compounds are Cineole, with the retention time at 6.629 and peak area of 12.8 has anti-inflammatory, antioxidants and antimicrobial activities as well as, in the treatments of cardiovascular and respiratory disease.<sup>31</sup> I-Limonene

with the retention time at 10.364 and peak area of 3.21 has anti-microbial activities.<sup>32</sup> cyclohexane with the retention time at 12.706 and peak area of 2.4 has Anti-microbial activities which helps in many drug formulation procedure.<sup>33</sup> Phenol with the retention time at 17.277 and peak area of 14.3 has anti-inflammatory and antimicrobial activities.<sup>34</sup> Neophytadiene with the retention time at 19.174 and peak area of 15.2 has anti-inflammatory and antimicrobial activities as well as, in the treatment of skin disease and headache.<sup>35</sup> 9,12,15 octadecatrienoic with the retention time at 19.922 and peak area of 13.76 has hepatoprotective, antihistaminic, anti-eczemic, antimicrobial, anti-cancer, anti-arthritis, anti-asthma and antidiuretic activities.<sup>36</sup> 1 methyl 3 hydroxylcarbonyl at a retention time at 7.59 and a peak area of 8.34 displayed no biological activity that is linked to the compound until now.

**Table 5.** Bioactivities of phytocomponents identified in the Ethanol extract of *Foeniculum Vulgare* leaves by GC-MS.

SN	Retention Time	Name of the compounds	Peak Area	Biological Activity
1	14.759	1,4 Cyclohexadiene	3.4	Anti-cancer Agents
2	17.943	Metronidazole (anazole)	4.2	Anti-bacterial activity
3	19.262	1H-Purine-6 amine	0.96	NO Biological activity

**Table 6.** Bioactivities of phytocomponents identified in the Ethanol extract of *Petroselinum crispum* leaves by GC-MS.

SN	Retention Time	Name of the compounds	Peak Area	Biological Activity
1	6.629	Cineole	12.8	Anti-inflammatory, Antioxidants and Antimicrobial activity
2	7.592	1 methyl 3 hydroxylcarbonyl	8.34	NO Biological activity
3	10.364	I-Limonene	3.21	Anti- microbial activity
4	12.706	Cyclohexane	2.4	Anti-microbial activity
5	17.277	Phenol	14.3	Anti-inflammatory agents, and antimicrobial
6	19.174	Neophytadiene	15.2	Anti-inflammatory agents, and antimicrobial
7	19.922	9,12,15 octadecatrienoic acid	13.76	Hepatoprotective, Antihistaminic, Anti-eczemic, Antimicrobial, anti-cancer Anti-arthritis, anti-asthma and antidiuretic.



#### 4. CONCLUSIONS

Various phytochemicals and pharmacological studies have been performed on two different medicinal plants (*Foeniculum Vulgare* and *Petroselinum crispum* leaves) using analytical methods (GC-MS and FTIR analytical techniques) and phytochemical screening. The GC-MS chromatogram of the ethanol extract of the two selected plant samples showed the presence of eight therapeutic bioactive compounds. phytochemical screening of the ethanolic leave extract of the sample analyzed indicates the presence of many various secondary metabolites such as tannins, flavonoids, saponins, terpenoids and steroids among others. These plants are potential source of natural antioxidants that have great therapeutic property. However, the FTIR analysis showed the presence of characteristics functional groups such as amine, O-H group and Sulphur derivatives among others. Further studies may also be conducted in other to identify more bioactive compounds in *Foeniculum Vulgare* leaves.

#### Conflict of interests

Authors declare that there is no a conflict of interest with any person, institute, company, etc.

#### REFERENCES

- Josephine Ozioma, E.-O.; Antoinette Nwamaka Chinwe, O. In *Herbal Medicine*; IntechOpen, 2019.
- Petrovska, B. *Pharmacogn. Rev.* **2012**, 6 (11), 1.
- Parham, S.; Kharazi, A. Z.; Bakhsheshi-Rad, H. R.; Nur, H.; Ismail, A. F.; Sharif, S.; RamaKrishna, S.; Berto, F. *Antioxidants* **2020**, 9 (12), 1309.
- Hussein, J. H.; Mohammed, Y. H.; Imad, H. H. *J. Pharmacogn. Phyther.* **2016**, 8 (3), 60–89.
- Upadhyay, R. K. *Am. J. Plant Sci.* **2015**, 06 (07), 1058–1068.
- Marín, I.; Sayas-Barberá, E.; Viuda-Martos, M.; Navarro, C.; Sendra, E. C. *Foods* **2016**, 5 (4), 18. <https://doi.org/10.3390/foods5010018>.
- Altemimi, A.; Lakhssassi, N.; Baharlouei, A.; Watson, D.; Lightfoot, D. *Plants* **2017**, 6 (4), 42.
- Zhang, Y.-J.; Gan, R.-Y.; Li, S.; Zhou, Y.; Li, A.-N.; Xu, D.-P.; Li, H.-B. *Molecules* **2015**, 20 (12), 21138–21156.
- Cheesman, M.; Ilanko, A.; Blonk, B.; Cock, I. *Pharmacogn. Rev.* **2017**, 11 (22), 57.
- Drzewoski, J.; Hanefeld, M. *Pharmaceuticals* **2021**, 14 (2), 122.
- Onyibe, P. N.; Edo, G. I.; Nwosu, L. C.; Ozgor, E. *Biocatal. Agric. Biotechnol.* **2021**, 36, 102118.
- Badgujar, S. B.; Patel, V. V.; Bandivdekar, A. H. *Biomed Res. Int.* **2014**, 2014, 1–32.
- Renna, M.; Gonnella, M. *Int. J. Gastron. Food Sci.* **2012**, 1 (2), 111–115.
- Ozturk, M.; Uysal, I.; Guçel, S.; Altundag, E.; Dogan, Y.; Baslar, S. *Res. J. Text. Appar.* **2013**, 17 (2), 69–80.
- Ahmed, A. M. A.; Elkady, F. M. A.; Khalid, K. A. *Asian J. Plant Sci.* **2018**, 17 (2), 96–106.
- Pal, R. S.; Pal, Y.; Saraswat, N.; Wal, P. *Open Med. J.* **2020**, 7 (1), 1–6.
- Mara de Menezes Epifanio, N.; Rykiel Iglesias Cavalcanti, L.; Falcão dos Santos, K.; Soares Coutinho Duarte, P.; Kachlicki, P.; Ożarowski, M.; Jorge Riger, C.; Siqueira de Almeida Chaves, D. *Food Funct.* **2020**, 11 (6), 5346–5356.
- Chaves, D. S. A.; Frattani, F. S.; Assafim, M.; de Almeida, A. P.; Zingali, R. B.; Costa, S. S. *Nat. Prod. Commun.* **2011**, 6 (7), 1934578X1100600.
- Tang, E. L.; Rajarajeswaran, J.; Fung, S.; Kanthimathi, M. *J. Sci. Food Agric.* **2015**, 95 (13), 2763–2771.
- Mansoori, A.; Singh, N.; Dubey, S. K.; Thakur, T. K.; Alkan, N.; Das, S. N.; Kumar, A. *Front. Agron.* **2020**, 2.
- Shahmokhtar, M. K.; Armand, S. *Nat. Prod. Chem. Res.* **2017**, 05 (04).
- Farzaei, M. H.; Abbasabadi, Z.; Ardekani, M. R. S.; Rahimi, R.; Farzaei, F. *Parsley: J. Tradit. Chinese Med.* **2013**, 33 (6), 815–826.
- Hozayen, W. G.; El-Desouky, M. A.; Soliman, H. A.; Ahmed, R. R.; Khaliefia, A. K. *BMC Complement. Altern. Med.* **2016**, 16 (1), 165.
- Mousavi, M.; Zaiter, A.; Becker, L.; Modarressi, A.; Baudelaire, E.; Dicko, A. *Phytochem. Anal.* **2020**, 31 (2), 154–163.
- Abdul Elah Mohammad, D.; Mohammad Taher, E. *J. Phys. Conf. Ser.* **2019**, 1294, 062048.
- Roy, K.; Sarkar, C. K.; Ghosh, C. K. *Appl. Nanosci.* **2015**, 5 (8), 945–951.

27. El-Borady, O. M.; Ayat, M. S.; Shabrawy, M. A.; Millet, P. *Adv. Powder Technol.* **2020**, *31* (10), 4390–4400.
28. Bocco, A.; Cuvelier, M.-E.; Richard, H.; Berset, C. *J. Agric. Food Chem.* **1998**, *46* (6), 2123–
29. Akhbari, M.; Kord, R.; Jafari Nodooshan, S.; Hamedi, S. *Nat. Prod. Res.* **2019**, *33* (11), 1629–1632.
30. Diao, W.-R.; Hu, Q.-P.; Zhang, H.; Xu, J.-G. *Food Control* **2014**, *35* (1), 109–116.
31. Liberal, Â.; Fernandes, Â.; Polyzos, N.; Petropoulos, S. A.; Dias, M. I.; Pinela, J.; Petrović, J.; Soković, M.; Ferreira, I. C. F. R.; Barros, L. *Molecules* **2020**, *25* (23), 5606.
32. Aljanaby, A. A. *J. J. Res. Chem. Intermed.* **2013**, *39* (8), 3709–3714.
33. Linde, G. A.; Gazim, Z. C.; Cardoso, B. K.; Jorge, L. F.; Tešević, V.; Glamočlija, J.; Soković, M.; Colauto, N. B. *Genet. Mol. Res.* **2016**, *15* (3).
34. Aishwaya, J. A Review. *J. Complement. Med. Altern. Healthc.* **2018**, *7* (2).
35. da Costa, G. A. F.; Morais, M. G.; Saldanha, A. A.; Assis Silva, I. C.; Aleixo, Á. A.; Ferreira, J. M. S.; Soares, A. C.; Duarte-Almeida, J. M.; Lima, L. A. R. dos S. *Evidence-Based Complement. Altern. Med.* **2015**, *2015*, 1–8.
36. Sagar, R.; Sahoo, H. *Indian J. Pharmacol.* **2012**, *44* (3), 398.



## The role of *Lavandula* sp. extract for effective inhibiting the mild steel corrosion in the hydrochloric acid solution

Demet ÖZKIR<sup>1,\*</sup>

<sup>1</sup>Niğde Ömer Halisdemir University, Faculty of Arts & Sciences, Department of Chemistry, Niğde 51240, Turkey

Received: 26 May 2021; Revised: 16 July 2021; Accepted: 2 August 2021

\*Corresponding author e-mail: dozkir@ohu.edu.tr

**Citation:** Özkır, D. *Int. J. Chem. Technol.* 2021, 5 (2), 125-132.

### ABSTRACT

The role of lavender extract in the present study is to examine the effect of inhibiting the corrosion of mild steel in the ambient conditions with its green and eco-friendly effect. It was determined the influence of inhibitor using electrochemical impedance spectroscopy (EIS) in different immersion times. From the EIS measurement results, it was observed that as the concentration of *Lavandula* extract in the HCl solution increased, the polarization resistance ( $R_p$ ) values in the EIS diagram increased. Finally, scanning electron microscope (SEM) analysis was conducted to better clarify the surface inhibition of the electrode containing *Lavandula* sp. extract at the highest concentration, 0.500% (w/v), at the end of the 120 h immersion time. It has been observed that both the surface analysis and EIS findings are very compatible with each other.

**Keywords:** *Lavandula*, EIS, HCl corrosion, Green inhibitor, SEM.

Lavanta türü özütünün hidroklorik asit çözeltisindeki yumuşak çelik korozyonunu etkin önlemedeki rolü

### ÖZ

Bu çalışmadaki lavanta özütünün rolü, yeşil ve çevre dostu etkisi ile ortam koşullarındaki yumuşak çeliğin korozyonunu önleme etkisini incelemektir. İnhibitörün etkisi, elektrokimyasal impedans spektroskopisi (EIS) kullanılarak farklı daldırma sürelerinde belirlenmiştir. Bu ölçüm sonuçlarından, HCl çözeltisi içerisindeki lavanta ekstraktının derişimi arttıkça, EIS diyagramındaki polarizasyon direnci ( $R_p$ ) değerlerinin de arttığı gözükümüştür. Son olarak, en yüksek derişimde (% 0.500 (w/v)) lavanta özütü içeren elektrodun, 120 saat daldırma süresi sonundaki yüzey inhibisyonunu daha iyi açıklamak için taramalı elektron mikroskopu (SEM) analizi yapılmıştır. Hem yüzey analizlerinin hem de EIS bulgularının birbiriyle son derece uyumlu oldukları görülmüştür.

**Anahtar Kelimeler:** *Lavanta*, EIS, HCl korozyonu, Yeşil inhibitör, SEM.

### 1. INTRODUCTION

Water Industries using metallic materials are often subject to corrosion phenomena. It is for this reason that corrosion can cause an unexpected failure, which definitely causes to economic losses and can impress product quality.<sup>1</sup> Preserving metallic materials, in particular inhibiting corrosion of mild steel, apparently requires a constant endeavour between man and nature.<sup>2,3</sup> Metallic materials are often threatened by their nature, which significantly reduces their lifetime. Mild steel is generally known to be low cost and is one of the most common metals. In addition, it has a technological and economic disadvantage due to its prone to corrosion in various environments such as acidic, basic, atmospheric

and aqueous. For this reason, it is essential to use it in scientific corrosion research.

There are many corrosion protection methods available. Among these, the most effective and widely used one is inhibitor application. Both inorganic and organic compounds are used effectively as inhibitors. However, there may be harmful effects on the environment. Recently, the use of plant extracts for corrosion inhibition and control purposes, especially as “green inhibitors”, has attracted attention.<sup>4-8</sup> One of the important sources of environmentally friendly inhibitors is plants.<sup>9</sup> Extracts from bark, seeds, leaves, fruits and plant roots have been shown to contain mixtures of organic compounds containing N, S and O atoms in its chemical formula,

which are effectual inhibition on metal corrosion in aggressive solutions.<sup>10,11</sup> Plant extracts are extremely abundant resources of chemical compounds such as organic acids, amino, terpenoids, alkaloids, tannins and phenolic compounds that are naturally found and synthesized in the body, and many of them are known to have inhibitor effects.<sup>12-15</sup> *Lavandula* extract/oil is extensively used in the fragrance and the pharmaceutical industry and, more recently, in food production as a natural sweetener for ice cream, candies and beverages. Literature researches reveal that no study has been conducted on the inhibition performance of *Lavandula* extract on the corrosion of mild steel involved in this study.

Apart from some extracts, the extracts from the leaves were generally those that indicated understandably better preservation at comparatively low concentrations. The reason for this has been pointed out that leaves are the main resource of phytochemicals.<sup>16,17</sup> Extracts can be classified in two ways: aqueous medium or organic solvent. Extracts from both media are selected according to the areas to be applied. For example, in corrosion studies, it is preferred to use extracts obtained from an aqueous medium, since the conditions are generally carried out in an aqueous electrolyte solution. In general, aqueous solution extracts include polar phytochemicals, while organic solution extracts include non-polar phytochemicals.<sup>18,19</sup> Phytochemicals carrying polar groups such as amine (-NH<sub>2</sub>), hydroxyl (-OH), ester (-COOR), carboxylic acid (-COOH), acetyl chloride (-COCl) and amide (-CONH<sub>2</sub>) are the main elements that provide adsorption to the metal surface as corrosion inhibitors. There are some basic groups in phytochemicals that provide corrosion inhibition. The most important of these are: Glycosides, alkaloids, flavonoids, steroids, tannins, phytosterols, flobatannins, anthraquinones, amino acids, triterpenes and phenolic compounds.<sup>20,21</sup> Due to their biological origin, plant extracts are environmentally friendly and often exhibit high preservation efficiency even at much lower concentrations.

Plants are unparalleled beings that transform the solar energy into a resource of living via photosynthesis. The lavender plant has a wide range of uses. The fresh flowered branch tips of lavender are generally used in the perfume industry, while the dried flower and leaf parts are used in the cosmetics industry. It is a shrub-looking perennial plant. Lavender can be sized between 20 and 60 cm. In this study, the extract of "*Lavandula* sp." from Lamiaceae family was used and its inhibitor influence was examined. It is also especially significant study in terms of inhibiting the corrosion of the mild steel electrode in HCl solution. It was intended to examine the influence of the *Lavandula* extract as an inhibitor on the mild steel corrosion in hydrochloric acid solution by EIS experiments in different immersion periods with various

concentrations. As result, it has been argued that the non-toxic and eco-friendly *Lavandula* extract is a highly effective inhibitor for industrial applications.

## 2. MATERIALS AND METHODS

### 2.1. Plant material

Lavenders used in the study were was collected from Niğde-Bor, Bereket village, 37°43'50" N, 34°32'35"E, in July 2020.

### 2.2. The solutions of *Lavandula* extract

Chemicals used in electrochemical tests are of analytical grade. *Lavandula* samples were firstly dried in an oven for almost 1 hour at 80 °C for preparing the stock solution of this plant's flowers extract. The flowers of the plant dried were separated from their stems. Dried 10 g of the violet flowers samples were weighed (Figure 1) and was added in 250 mL distilled water and refluxed for 18 h.



Figure 1. Dried violet *Lavandula* specimens.

The refluxed solution was filtered. Photographs of the filtration and clear extract obtaining steps are presented in Figure 2.



Figure 2. Extract acquisition stages.



The concentration of the stock *Lavandula* solution studied was 1.376% (w/v). All solution concentrations were diluted from the stock *Lavandula* solution. Electrochemical experiments were performed in 1.0 M HCl solution for aggressive media.

### 2.3. Electrodes and EIS measurements

The electrochemical tests were obtained on the surface of mild steel electrodes. The chemical composition (wt.%) of working electrodes is given in Table 1.

**Table 1.** The chemical composition of the working electrodes samples.

Element	%	Element	%	Element	%
(C)	0.08400	(Si)	0.10200	(Mn)	0.40900
(P)	0.01100	(S)	0.01900	(Cr)	0.06030
(Mo)	0.01040	(Ni)	0.07890	(Al)	Trace
(Co)	0.00198	(Cu)	0.21700	(Nb)	0.00222
(Ti)	Trace	(V)	0.01100	(W)	Trace
(Pb)	Trace	(Sn)	0.01620	(Sb)	Trace
(Fe)	Remain				

The electrodes were placed in a mould including polyester mixture and a surface area of 0.5024 cm<sup>2</sup> of the electrodes was subjected to hydrochloric acid solution. The surfaces of the test electrodes were abraded with 150, 600 and 1000 grids of sandpaper and polished and cleaned with alumina solution and acetone, respectively before each electrochemical experiment. The conventional three electrode methods were applied for EIS experiments. The first electrode is the working electrode and mild steel is used. The second is the counter electrode and a Pt plate with a surface area of 1.0 cm<sup>2</sup> is used. The third and last electrode is the reference electrode and Ag/AgCl has been used for this. All potentials in the study were measured against this Ag/AgCl electrode.

EIS experiments were studied utilizing CHI 660B electrochemical analyser with a computer-controlled (Fig. 3).

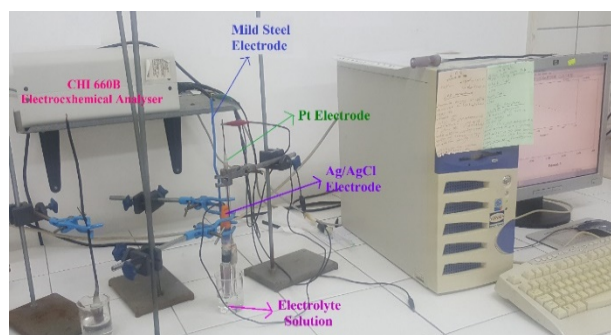


**Figure 3.** Photo of the experimental setup of a corrosion measurement with electrochemical analyser device in a laboratory area.

EIS measurements were performed in 1.0 M hydrochloric acid solution in with and without different *Lavandula* extract concentrations. The mild steel specimens were immersed in electrolyte solution for 1 h to equilibrate the corrosion potential ( $E_{corr}$ ) at the corrosion process prior to each EIS experiments. It was obtained on the corrosion potential at a frequency range of 10<sup>5</sup> to 5x10<sup>-3</sup> Hz with 5 mV amplitude carried out by EIS. One, 24 and 120 h experiments were performed to investigate immersion time EIS periods and it was compared that the inhibition efficiency values obtained by EIS at different exposure times. SEM (Zeiss SEM 500 with computer controlled) images were performed 120 h of immersion time in hydrochloric acid solution with and without *Lavandula* sp. extract at the highest concentration (0.500%). All experiments were realized at ambient temperature (298 K).

## 3. RESULTS and DISCUSSION

### 3.1. Evaluation of EIS findings

Impedance spectroscopy is one of the fastest and easiest methods that are often preferred in researching the protective properties of all these molecules on metals in aggressive solutions, whether the inhibitor used is organic molecules or inhibitors of plant origin.<sup>22-24</sup> For this reason, electrochemical behaviour of mild steel was evaluated by measuring with EIS at the end of one, 24 and 120 h immersion times in 1.0 M HCl solutions containing four different concentrations of *Lavandula* (0.100%, 0.050%, 0.300% and 0.500% (w/v)) and not containing inhibitor. The equivalent circuits of the corrosion process were constituted from these results by utilizing Zview2 software. The EIS parameters concerned to the corrosion process are also given in Table 2.

**Table 2.** The related data acquired from fitting EIS measurements for mild steel in acidic solution with *Lavandula* extract at various exposure time.

Time	C (w/v %)	CPE					$\eta$ (%)	
		$R_s$ ( $\Omega$ cm <sup>2</sup> )	$R_p$ ( $\Omega$ cm <sup>2</sup> )	$\mu F$ cm <sup>-2</sup>	$n$	$R_L$ ( $\Omega$ cm <sup>2</sup> )		$L$ (H)
<b>1 h</b>								
Blank		1.2	72	110	0.94	8	4	-
0.050		1.2	320	106	0.89	-	-	77.5
0.100		1.3	540	83	0.86	-	-	86.7
0.300		1.2	750	78	0.84	-	-	90.4
0.500		1.3	805	73	0.83	-	-	91.1
<b>24 h</b>								
Blank		1.2	11	2600	0.95	1.3	1.1	-
0.050		1.5	170	310	0.85	-	-	93.5
0.100		1.3	470	110	0.84	-	-	97.8
0.300		1.3	600	90	0.84	-	-	98.2
0.500		1.1	674	80	0.83	-	-	98.4
<b>120 h</b>								
Blank		1.4	4	36520	0.89	0.4	0.3	-
0.050		1.6	50	1647	0.83	-	-	92.0
0.100		1.1	186	360	0.60	-	-	97.9
0.300		1.1	251	290	0.48	-	-	98.4
0.500		1.1	486	274	0.35	-	-	99.2



Proposed equivalent electrical circuits for mild steel electrodes were inserted in Figure 4 and the Nyquist diagrams in HCl solution of the extract have been showed for different exposure time in Figure 4.

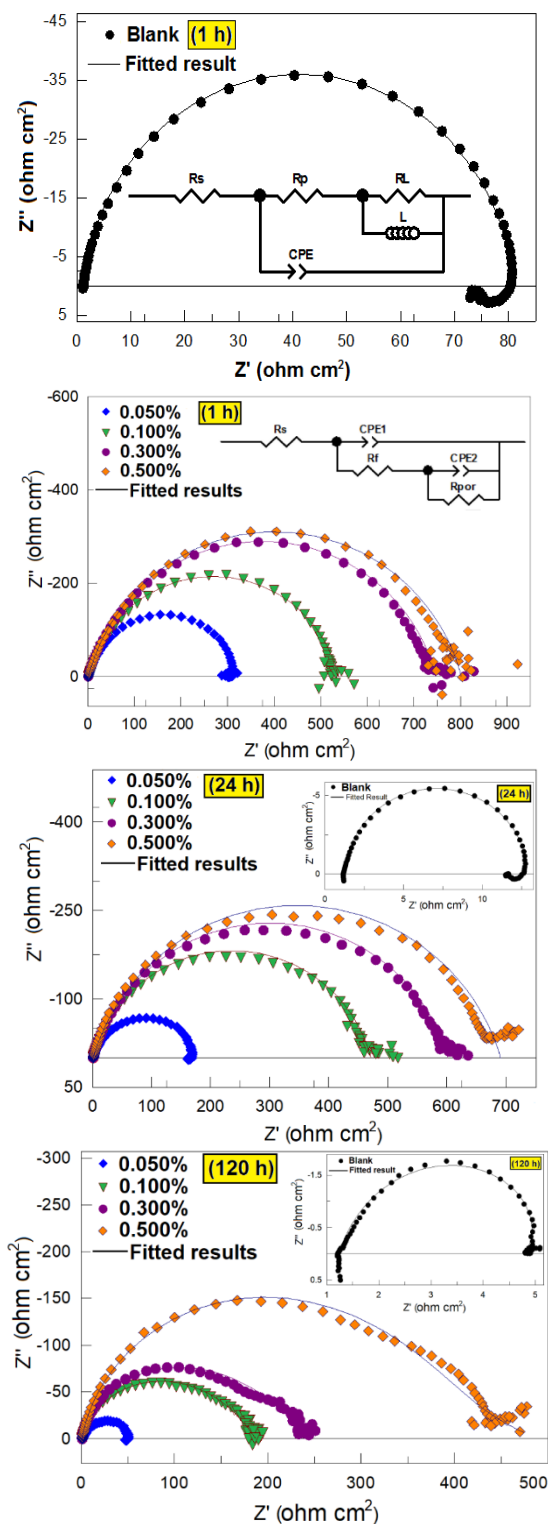


**Figure 4.** Fitted impedance curves for mild steel specimens in hydrochloric acid with and without various *Lavandula* extract concentrations for 1, 24 and 120h.

In the EIS diagram obtained for 1 h immersion period in Figure 4, it is viewed that the equivalent circuit model proposed for the inhibited solution is distinct from the one proposed for the uninhibited solution. One of the most obvious differences between the two is the adsorption film layer that comes into play in the inhibited solution. As can be clearly seen from Figure 4, the radii of the semicircles composed in the high frequency area in all inhibited solutions were greater than those in uninhibited ones, and the radii enhanced as the concentration of inhibitor enhanced.<sup>25-28</sup>

The “*n*” values shown in Table 2 are the surface roughness coefficient of the metal. As *Lavandula* extract solutions were added to the blank solution, the “*n*” values decreased, in other words, the surface roughness gradually diminished. “*R<sub>p</sub>*” is the polarization resistance, that is, the molecules of *Lavandula* extract are polarized by adsorption to the metallic surface in a corrosion process. While the *R<sub>p</sub>* value in the blank solution was 72 Ω cm<sup>2</sup>, as *Lavandula* was added to the medium at the last of each immersion period, the *R<sub>p</sub>* values increased. In addition, as the exposure period to the acidic solution increased, the *R<sub>p</sub>* values at each concentration gradually decreased as the corrosion process continued. Percent inhibition efficiency values (*η*%) calculated from *R<sub>p</sub>* values at the end of one-hour immersion time increased as *Lavandula* extract was added to the acidic solution, and this value provided a high inhibition rate of 91.1% at the highest *Lavandula* concentration (0.500%).

Another impedance parameter in Table 2 is the “*CPE*” value. *CPE* is the “constant phase element” in the electrical equivalent circuit and is conversely proportional to the *R<sub>p</sub>* value.<sup>29</sup> As the extract concentration increases in the solution medium, the *CPE* value decreases accordingly. In the EIS diagrams obtained in solutions containing *Lavandula* during each immersion period, it is viewed that the diameter of the capacitive loop increases significantly with the increase of the concentration. As can be seen in the Nyquist curve of the 120 h immersion time, where the exposure time to the acidic solution was the highest, the capacitive curves were gradually distorted. As a result of all these parameters and high inhibition values, it can be commented that as the concentration increases, the protective inhibitor film formed on the surface grows and the metal surface is well closed.

From all EIS diagrams, as the electrodes are exposed to acidic solutions, deviations from the semicircles, in other words frequency scattering, are clearly observed in the EIS plots. These scattering is actually caused by the increase of roughness on the metal surface due to prolonged exposure to the acidic solution. Among the

causes of high inhibition, which is also common in green type inhibitors, but involves almost all inhibitors, is the processes that occur in the high and low frequency regions of the Nyquist curves. Diffuse layer resistance ( $R_d$ ) and charge transfer resistance ( $R_{ct}$ ) play a role in the inhibition in the high frequency part, on the other hand, in the low frequency area, the film resistance ( $R_f$ ) in control of the film layer composed on the surface and all accumulated resistances ( $R_a$ ) that are present with corrosion products on the metal surface generally play a dominant role in a corrosion process.<sup>30</sup>

It can be said that percentages of inhibition in Table 2 are around 90% and above, except for a few values. In addition, the highest inhibition (99.2%) was obtained at the end of 120 h with the solution containing the highest amount of *Lavandula* extract. As can be seen from the results, it is possible to say that *Lavandula* molecules adsorb very well on the mild steel surface and cover the surface almost completely. Plant extracts called green usually involve complex secondary metabolites (phytochemicals) that can polarize certain functional groups and double bonds in their structures.<sup>31,32</sup> These functional groups and double bonds are regions rich in electron. For this reason, these parts, which are rich electron sources, facilitate the adsorption of phytochemical-containing plant extracts to the metal surface. Phytochemicals are natural and at the same time therapeutic compounds synthesized in plants as secondary metabolites. Its high inhibition effect on corrosion is caused by secondary metabolites (phytochemicals) well-known to include molecules such as nitrogenous compounds, phenolic compounds, flavonoids, terpenes and alkaloids. All of these compounds are also quite a source of  $\pi$ -electrons.

### 3.2. Evaluation of SEM images of mild steel electrodes

Present study investigating the effect of *Lavandula* extract on the surface of mild steel was carried out by examining the surface micrographs obtained by SEM technique. In the first stage, the mild steel electrodes were removed from the immersed solutions for 120 h, cleaned and dried. Afterwards, the SEM images obtained by cutting of 0.5 cm from the electrode surface with a hacksaw without waiting are given in Figure 5.

As can be easily seen from these surface micrographs, large black cavities in the form of recessions and pits are clearly monitored on the electrode surface kept in the blank solution. It can be said that the image of immersed in the blank solution is clearly oxidized and the surface is deteriorated. It is observed that the metal surface has a much smoother appearance, and the black cavities (pits)

are almost absent with the *Lavandula* extract added to the acidic solution. In other words, it can be clearly emphasized that the electrode surfaces are the roughest in the blank solution, the black spots are quite large and numerous, and they have the smoothest appearance at the highest concentration.<sup>33</sup> These results highly confirm each other with the long-term impedance results obtained with EIS.

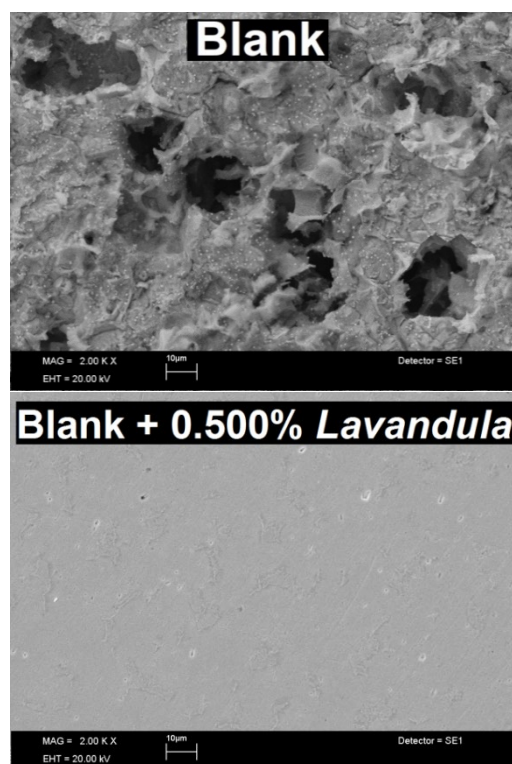


**Figure 5.** SEM images of electrodes immersed in hydrochloric acid solution for 120 h.

These results indicate high inhibition as a result of the *Lavandula* extract covering the surface of mild steel very well, and at the same time, the smoother the surface with the addition of the extract can be shown as another proof that it provides a very good inhibition.

## 4. CONCLUSIONS

In this current study conducted to define the electrochemical behavior of mild steel, experiments were made with EIS at last of one, 24 and 120 h of immersion in uninhibited and inhibited solutions and the results are summarized below:

- *Lavandula* extract, which is green and environmentally friendly, is intended to be used as an inhibitor for application at different immersion times against the mild steel corrosion in aggressive HCl solution and as a result, it has shown a very high inhibition performance.

- The impedance diagrams obtained at three different immersion times in both blank and inhibited solutions are in the form of a half ellipse. The radii of the semicircles in all inhibitor solutions are greater than those in the blank solution, and the radii enhanced as the inhibitor concentration raised.
- As the exposure time enhanced in inhibited solutions, the diameter of the capacitive loop decreased. In both non-inhibitor and inhibitor solutions, CPE values raised with enhancing immersion time and decreased with raising the concentration of *Lavandula* extract.
- Due to the increment in the inhibitor concentration, as the immersion time increased, the values of “the surface roughness coefficient: *n*” decreased, which can be interpreted as evidence of the adsorption of *Lavandula* extract molecules on the metallic surface.
- After one, 24 and 120 h exposure times of the mild steel electrodes to the acidic solution, the inhibition performance for *Lavandula* extract was approximately between 78% and 99%. This ratio is quite high and this has been suggested as evidence that the number of molecules in the *Lavandula* extract adsorbed on the mild steel surface increases due to the increment in *Lavandula* extract concentration.
- In the last stage of the study, the effect of *Lavandula* extract on the mild steel/solution interface was investigated using the SEM technique. On the electrode surface, which was kept in the acidic blank solution for 120 h, quite large and deep cavities (pits) were observed. On the contrary, when there is *Lavandula* extract in the acidic solution, it is very clear that these formed pits disappear or even become smaller. In other words, it was determined that the electrode surface in the blank solution was the roughest and the metal surface in the solution containing the *Lavandula* extract was the smoothest.
- SEM and EIS findings were also very compatible with each other.
- In the light of the results of this study, a plant extract called green inhibitor is a very useful and suitable inhibitor for the mild steel electrode in 1.0 M hydrochloric acid, moreover, it was concluded that such inhibitors should be

encouraged to increase their use because they are environmentally friendly and do not show toxic effects.

### Conflict of interest

*Author declares that there is no a conflict of interest with any person, institute, company, etc.*

### REFERENCES

1. Şahin, M.; Çadırlı, E.; Sürme, Y.; Özkır, D. Thermo-Electrical Properties in Pb-Sb Hypereutectic Alloy, *Met. Mater. Int.* **2013**, 19(3), 465-472.
2. Berrissoul A., Ouarhach A., Benhiba F., Romane A., Zarrouk A., Guenbour A., Dikici B., Dafali A., Evaluation of *Lavandula mairei* extract as green inhibitor for mild steel corrosion in 1 M HCl solution. Experimental and theoretical approach, *J. Mol. Liq.* **2020**, 313, 113493.
3. Loto C.A., Loto R.T., Effects of *Lavandula* and *Ricinus Communis* Oil as Inhibitors of Mild Steel Corrosion in HCL and H<sub>2</sub>SO<sub>4</sub> Media, *Procedia Manuf.* **2019**, 35, 407-412.
4. Loto C.A., Synergism of *Saccharum Officinarum* and *Ananas Comusus* Extract Additives on the Quality of Electroplated Zinc on Mild Steel, *Res. Chem. Intermed.* **2014**, 40, 1799-1813.
5. Aljuhani A., El-Sayed W.S., Sahu P.K., Rezki N., Aouad M.R., Salghi R., Messali M., Microwave-assisted synthesis of novel imidazolium, pyridinium and pyridazinium based ionic liquids and/or salts and prediction of physicochemical properties for their toxicity and antibacterial activity, *J. Mol. Liq.* **2018**, 249, 747-753.
6. Ameta G., Pathak A.K., Ameta C., Ameta R., Punjabi P.B., Sonochemical synthesis and characterization of imidazolium based ionic liquids: a green pathway, *J. Mol. Liq.* **2015**, 211, 934-937.
7. Abdel-Gaber A.M., Abd-El-Nabey B.A., Sidahmed I.M., El-Zayady A.M., Saadawy M., Inhibitive action of some plant extracts on the corrosion of steel in acidic media. *Corros. Sci.* **2006**, 48, 2765-2779.
8. Alibakhshi E., Ramezanzadeh M., Bahlakeh G., Ramezanzadeh B., Mahdavian M., Motamedi M., *Glycyrrhiza glabra* leaves extract as a green corrosion inhibitor for mild steel in 1 M hydrochloric acid solution: experimental, molecular dynamics, Monte Carlo and

- quantum mechanics study, *J. Mol. Liq.* **2018**, 255, 185-198.
9. Benabbouha T., Siniti M., El Attari H., Chefira K., Chibi F., Nmila R., Rchid H., Red algae *Halopitys incurvus* extract as a green corrosion inhibitor of carbon steel in hydrochloric acid, *J. Bio. Tribocorros.* **2018**, 4 (39), 1-9.
10. Odewunmi N.A., Umoren S.A., Gasem Z.M., Watermelon waste products as green corrosion inhibitors for mild steel in HCl solution, *J. Environ. Chem. Eng.* **2015**, 3, 286-296.
11. Mourya P., Banerjee S., Singh M.M., Corrosion inhibition of mild steel in acidic solution by *Tagetes erecta* (Marigold flower) extract as a green inhibitor, *Corros. Sci.* **2014**, 85, 352-363.
12. Halambek J., Berkovic' K., Vorkapić-Furać J., The influence of *Lavandula angustifolia* L. oil on corrosion of Al-3Mg alloy, *Corros. Sci.* **2010**, 52, 3978-3983.
13. Abiola O.K., James A.O., The effects of Aloe vera extract on corrosion and kinetics of corrosion process of zinc in HCl solution, *Corros. Sci.* **2010**, 52, 661-664.
14. Abdel-Gaber A.M., Khamis E., Abo-ElDahab H., Adeel S., Inhibition of aluminium corrosion in alkaline solutions using natural compound, *Mater. Chem. Phys.* **2008**, 109, 297-305.
15. Zerga B., Sfaira M., Rais Z., Touhami M.E., Taleb M., Hammouti B., Imelouane B., Elbachiri A., Lavender oil as an ecofriendly inhibitor for mild steel in 1 M HCl, *Mater. et Tech.* **2009**, 97, 297-305.
16. Schreiner M., Huyskens-Keil S., Phytochemicals in fruit and vegetables: health promotion and postharvest elicitors, *Crit. Rev. Plant Sci.* **2006**, 25, 267-278.
17. Alrefae S.H., Rhee K.Y., Verma C., Quraishi M.A., Ebenso E.E., Challenges and advantages of using plant extract as inhibitors in modern corrosion inhibition systems: Recent advancements, *J. Mol. Liq.* **2021**, 321, 114666.
18. Ji G., Shukla S.K., Dwivedi P., Sundaram S., Prakash R., Inhibitive effect of *Argemone mexicana* plant extract on acid corrosion of mild steel, *Ind. Eng. Chem. Res.* **2011**, 50, 11954-11959.
19. Krishnegowda P.M., Venkatesha V.T., Krishnegowda P.K.M., Shivayogiraju S.B., *Acalypha torta* leaf extract as green corrosion inhibitor for mild steel in hydrochloric acid solution, *Ind. Eng. Chem. Res.* **2013**, 52, 722-728.
20. Raja P.B., Fadaeinasab M., Qureshi A.K., Rahim A.A., Osman H., Litaudon M., Awang K., Evaluation of green corrosion inhibition by alkaloid extracts of *Ochrosia oppositifolia* and *isoreserpiline* against mild steel in 1 M HCl medium, *Ind. Eng. Chem. Res.* **2013**, 52, 10582-10593.
21. Oguzie E.E., Oguzie K.L., Akalezi C.O., Udeze I.O., Ogbulie J.N., Njoku V.O., Natural products for materials protection: Corrosion and microbial growth inhibition using *Capsicum frutescens* biomass extracts, *ACS Sustain. Chem. Eng.* **2013**, 1, 214-225.
22. Özkuş, D. The Electrochemical Variation of a Kind of Protein Staining and Food Dye as a New Corrosion Inhibitor on Mild Steel in Acidic Medium. *Int. J. Electrochem.* **2019**, 2019, 1-11.
23. Özkuş, D. A Newly Synthesized Schiff Base Derived from Condensation Reaction of 2,5-dichloroaniline and benzaldehyde: Its Applicability through Molecular Interaction on Mild Steel as an Acidic Corrosion Inhibitor by Using Electrochemical Techniques. *J. Electrochem. Sci. Technol.* **2019**, 10(1), 37-54.
24. Özkuş, D.; Ezer, T. A New Inhibitor Approach to the Corrosion of Mild Steel in Acidic Solution with Long-Term Impedance Tests: A New Application Area for *Hypnum cupressiforme* (Bryophyta), *Anatolian Bryology*, **2020**, 6(2), 119-128.
25. Sürme, Y.; Gürten, A.A. Role of polyethylene glycol tert-octylphenyl ether on corrosion behaviour of mild steel in acidic solution, *Corros. Eng. Sci. Techn.* **2009**, 44(4), 304-311.
26. Özkuş, D.; Kayakırılmaz, K. The Inhibitor Effect of (E)-5-[(4-(benzyl(methyl)amino)phenyl)diazenyl]-1,4-dimethyl-1H-1,2,4-triazol-4-ium zinc(II) Chloride, an Industrial Cationic Azo Dye, onto Reducing Acidic Corrosion Rate of Mild Steel, *J. Electrochem. Sci. Technol.* **2020**, 11(3), 257-272.
27. Özkuş, D.; Bayol, E.; Gürten, A.A.; Sürme, Y., Kandemirli, F. Effect of hyamine on electrochemical behaviour of brass alloy in HNO<sub>3</sub> solution, *Chem. Pap.* **2013**, 67(2), 202-212.
28. Kılınççeker, G.; Baş, M.; Zarifi, F.; Sayın, K. Experimental and Computational Investigation for (E)-2-hydroxy-5-(2-benzylidene) Aminobenzoic Acid Schiff Base as a Corrosion Inhibitor for Copper in Acidic

Media, *Iran. J. Sci. Technol. Trans. Sci.* **2021**, 45, 515-527.

29. Ongun Yüce, A.; Telli, E.; Doğru Mert, B.; Kardaş, G.; Yazıcı, B. Experimental and quantum chemical studies on corrosion inhibition effect of 5,5 diphenyl 2-thiohydantoin on mild steel in HCl solution, *J. Mol. Liq.* **2016**, 218, 384-392.

30. Yildiz, R.; Doğru Mert, B. Theoretical and experimental investigations on corrosion control of mild steel in hydrochloric acid solution by 4-aminothiophenol, *Anti-Corros. Method. M.* **2019**, 66(1), 127-137.

31. Palaniappan, N.; Cole, I.; Caballero-Briones, F.; Manickam, S.; Thomas, K.J.; Santos, D. Experimental and DFT studies on the ultrasonic energy-assisted extraction of the phytochemicals of *Catharanthus roseus* as green corrosion inhibitors for mild steel in NaCl medium, *RSC Adv.* **2020**, 10, 5399–5411.

32. Buchweishaija J. Phytochemicals as green corrosion inhibitors in various corrosive media: A review, *Tanz. J. Sci.* **2009**, 35, 77-92.

33. Keleş, H.; Keleş, M.; Sayın, K. Experimental and theoretical investigation of inhibition behavior of 2-((4-(dimethylamino)benzylidene)amino)benzenethiol for carbon steel in HCl solution, *Corros. Sci.* **2021**, 184, 109376.





## Synthesis, spectral characterization, DFT, and molecular docking studies of 2 - ((2,3-Dihydrobenzo [b] [1,4] dioxin-6-yl) (1H-indol-1-yl) methyl) phenol compound

Yeliz ULAŞ<sup>1,\*</sup>

<sup>1</sup>Uludağ University, Faculty of Arts & Sciences, Department of Chemistry, Bursa, 16000, Turkey

Received: 27 May 2021; Revised: 16 September 2021; Accepted: 19 September 2021

\*Corresponding author e-mail: yelizulas@uludag.edu.tr

**Citation:** Ulaş, Y. *Int. J. Chem. Technol.* 2021, 5 (2), 133-140.

### ABSTRACT

Synthesis of an alkylaminophenol compound used as a drug active material was carried out and the structural analysis of the compound was investigated experimentally and theoretically. For theoretical calculations, DFT / B3LYP method and 6-311 ++ G (d, p) set were used. Many properties of the compound; Spectral data, bond length, bond angle, dihedral angles, thermodynamic parameters, molecular surface, FMO analysis, nonlinear optical (NLO) properties and Natural Bond Orbital analysis were theoretically investigated. Also, a molecular docking study shows that the title compound might exhibit inhibitory activity against 2RAW protein.

**Keywords:** Alkylaminophenol, DFT, molecular docking, NBO, NLO

2- ((2,3-Dihydrobenzo [b] [1,4] dioksin-6-il) (1H-indol-1-il) metil) fenol bileşiğinin sentez, spektral karakterizasyon, DFT ve moleküler docking çalışmaları

### ÖZ

İlaç etken maddesi olarak kullanılan bir alkilaminofenol bileşiğinin sentezi gerçekleştirilmiş ve bileşiğin yapısal analizi deneysel ve teorik olarak incelenmiştir. Teorik hesaplamalar için DFT / B3LYP yöntemi ve 6-311 ++ G (d, p) seti kullanılmıştır. Bileşiğin birçok özelliği; Spektral veriler, bağ uzunluğu, bağ açısı, dihedral açılar, termodinamik parametreler, moleküler yüzey, FMO analizi, doğrusal olmayan optik (NLO) özellikler ve Natural Bond Orbital analizi teorik olarak incelenmiştir. Ayrıca, moleküler doking çalışmaları, başlık bileşiğinin 2RAW proteinine karşı inhibitör aktivite sergilediğini göstermektedir.

**Anahtar Kelimeler:** Alkylaminofenol, DFT, moleküler docking, NBO, NLO

### 1. INTRODUCTION

Alkylaminophenols are heterocyclic compounds containing hydroxyl and nitrogen in their structure.<sup>1-4</sup> It is found in the structures of drugs frequently used in cancer treatments. The compounds having antioxidant activity enables them to be used in chemotherapy.<sup>5,6</sup>

Although there are compounds synthesized in this field in recent years, the diversity of cancer types also accelerates the synthesis of new bioactive compounds. In addition, the fact that the radicals formed as a result of cancer cells become neutral and have antioxidant properties increase the importance of this compound

class. Although there are many methods in the literature for the synthesis of alkylaminophenols, the method using the petasis reaction was preferred in this study.<sup>7-11</sup> The reaction takes place by the amine and carbonyl compounds forming iminium ion and removing boric acid from the boronate complex formed by the added boronic acid. Studies on theoretical investigations of these compounds with quantum chemical calculations in the literature are quite limited.<sup>12</sup>

In order to ensure the diversity of alkylaminophenol type compounds, a new compound was synthesized in the study and then many properties of this compound were examined theoretically. Gaussian 09W software was

used for theoretical calculations and DFT/B3LYP/6-311++G(d,p) set was preferred for calculations.<sup>13-15</sup> Also, its biological significance was investigated by examining its effects on 2RAW protein with molecular docking studies.

## 2. MATERIALS AND METHODS

### 2.1 Experimental and Calculation methods

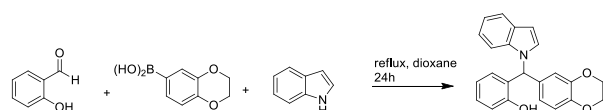


**Figure 1.** Synthesis of Alkylaminophenol Compound.

Synthesis was carried out according to the procedure in the literature (Figure 1).<sup>5</sup>

The chemicals used for synthesis were used directly without any extra purification. Structure analysis of the synthesized compound has been made by Bruker FT-IR spectrometer and Agilent 600 MHz NMR spectrometers. *2 - ((2,3-Dihydrobenzo [b] [1,4] dioxin-6-yl) (1H-indol-1-yl) methyl) phenol*: Verim 0.313 (87%), red brown solid, MP 75-76 °C. <sup>1</sup>H NMR (600 MHz, CDCl<sub>3</sub>): δ(ppm) = 2.07(s, 1H, indole), 3.72 (s, 1H, indole), 4.15-4.20 (m, 4H, dioxin), 5.58 (s, 1H, CH), 5.79 (s, 1H, Ar-OH), 6.63-6.68 (m, 3H, Ar-H), 6.76-6.88 (m, 3H, Ar-H), 7.14-7.21 (m, 2H, Ar-H), 7.30 (s, 1H, Ar-H), 8.03 (s, 1H, Ar-H), 8.08 (s, 1H, Ar-H). <sup>13</sup>C (CDCl<sub>3</sub>, 150 MHz): δ = 21.1 (indole); 42.3 (indole); 60.6 (dioxin); 67.6 (chiral carbon), 102.4 (Ar-); 111.1 (Ar-), 116.1 (Ar-); 116.9 (Ar-); 117.1 (Ar-); 117.2 (Ar-); 119.5 (Ar-); 119.9 (Ar-); 120.6 (Ar-); 122.3 (Ar-); 123.7 (Ar-); 124.0 (Ar-); 126.8 (Ar-); 130.0 (Ar-); 136.6 (Ar-); 142.1 (Ar-); 143.3 (Ar-); 153.5 (Ar-); 153.8 (C-OH). FT-IR ν (cm<sup>-1</sup>): 3409, 2978, 2815, 1705, 1589, 1501, 1453, 1281, 1254, 1190, 956, 825.

After the experimental characterization of structural, some properties of the compound was calculated with theoretical methods. Calculations include the B3LYP theory and 6-311 ++ G (d,p) set which is composed of Becke's three-parameter energy-functional hybrid approach and Lee-Yang and Parr's correlation function<sup>16</sup> in the Gaussian 09W program. Gauss-View 5.0 program was used for molecular modelling.<sup>17</sup>

## 3. RESULTS AND DISCUSSION

### 3.1 Molecular Geometry

The optimization process of the title compound synthesized using the Petasis reaction was carried out using the B3LYP / 6-311 ++ G (d, p) base set. The optimized form of the compound is given in Figure 2.

The bond length, bond angles and dihedral angles of the compound are comparatively given in Table 1.

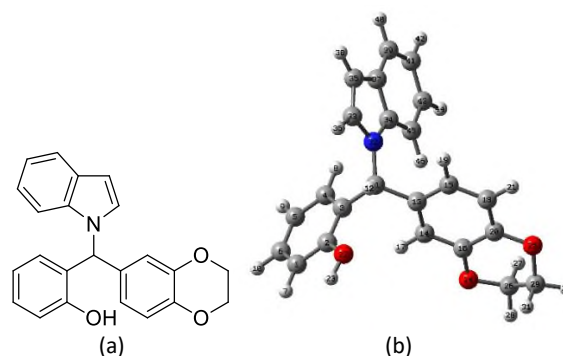


**Figure 2.** Molecular structure(a) and Optimized form(b) of 2 - ((2,3-Dihydrobenzo [b] [1,4] dioxin-6-yl) (1H-indol-1-yl) methyl) phenol compound.

**Table 1.** Some selected geometric parameters of Alkylaminophenol.

Bond Length(A <sup>0</sup> )	B3LYP	Bond Angles(°)	B3LYP
C1-C2	1.3947	C4-C3-C11	123.1
C2-C3	1.4038	C11-C3-C2	119.0
C3-C4	1.3956	C2-O22-H23	109.8
C4-C5	1.3942	C2-C1-H7	119.7
C5-C6	1.3919	C1-C6-C5	119.9
C4-H8	1.0827	H12-C11-C13	105.6
C1-H7	1.0864	C13-C15-H19	119.9
C2-O22	1.3726	C13-C14-H17	121.4
O22-H23	0.9627	C13-C14-C16	120.8
C3-C11	1.5263	C16-C20-C18	119.3
C11-H12	1.0933	C20-C18-H21	118.4
C11-C13	1.5324	C20-C16-O24	121.8
N32-C33	1.3863	C16-O24-C26	113.8
N32-C34	1.3905	O25-C29-C26	110.2
C34-C37	1.4246	O24-C26-H27	109.5
C33-C35	1.3661	H28-C26-C29	111.3
C11-N32	1.4707	C11-N32-C34	129.7
C37-C39	1.4042	C11-N32-C33	122.2
C34-C45	1.4001	N32-C33-H36	119.6
C45-C43	1.3884	N32-C34-C45	131.3
C39-C41	1.3857	C34-C45-H46	121.6
C33-H36	1.0794	C45-C43-H44	119.1
C45-H46	1.0813	C43-C41-C39	120.7
C13-C14	1.3911	C41-C39-C37	119.2
C13-C15	1.4011	C37-C34-C45	121.3
C15-H19	1.0841	C37-C35-C33	106.8
C14-H17	1.0829	Dihedral Angles	
C20-C16	1.3995	N32-C11-C3-C4	30.6
C16-O24	1.3753	N32-C11-C3-C2	-148.4
C20-O25	1.3739	C11-C3-C2-O22	-0.1
O24-C26	1.4294	H23-O22-C2-C1	0.3
O25-C29	1.4294	N32-C11-C13-C14	79.6
C26-C29	1.5174	N32-C11-C13-C15	55.1
C29-H30	1.0907	C16-O24-C26-C29	45.6
C25-H27	1.0966	H30-C29-O25-C20	165.7

The O-H bond length was experimentally and theoretically found to be 0.96 Å. While N32-C11 bond length was experimentally 1.47, it was calculated as 1.47 Å with the B3LYP method. In addition, the C = C bond length of 1.37 Å was calculated as 1.40 Å (B3LYP) for C13 = C15 atoms. Besides, the C-O-H bond angle, known to have an angle of 109.5 °, was calculated as 109.8 ° by the B3LYP method for C2-O22-H23. As a result; It can be said that there is a good agreement between the experimental bond length and bond angle values and the calculated values (Table 2).

### 3.2 NMR Studies

First of all, <sup>1</sup>H-NMR and <sup>13</sup>C-NMR values of the title compound were calculated with B3LYP / 6-311G ++(d,p). Then chemical shift values in CHCl<sub>3</sub> solvent medium and calculated by GIAO-NMR approach and IEFPCM method were compared with experimental values.

**Table 2.** Experimental and calculated <sup>1</sup>H and <sup>13</sup>C NMR chemical shifts (ppm).

Atoms	Experimental	B3LYP (CHCl <sub>3</sub> )
H23	5.79	4.39
H12	5.58	7.16
H27-H28		
H30-H31	4.15-4.20	4.19
H36	3.72	7.5
C35	21.1	105.5
C33	42.3	136.5
C26-C29	60.6	67
C13	136.6	140.2
C3	117.2	133.5
C11	67.6	65.0
C2	153.8	159.5

H12 and H23 peaks, which are one of the characteristic peaks of the compound, were experimentally observed at 5.58 ppm and 5.79, respectively, while calculations with the B3LYP method were found to be 7.16 ppm and 4.39 ppm. While our chiral carbon C11 was experimentally seen at 67.4, it was found to be 65.0 in our theoretical calculations.

In addition, the C2 carbon to which the hydroxyl group is attached has experimentally been found to have a value of 153.8 ppm, while theoretically, it has a value of 159.5 ppm. Although there are some deviations due to the presence of the OH group in the structure and intramolecular hydrogen bonds, it can be said that our theoretical data are compatible with the experimental data.

### 3.3 Mulliken Charge

The most common of the population analysis methods is the mulliken charge distribution. It is often used to make some qualitative estimates of the structure. Analysis; it was carried out with the B3LYP / 6-311G ++ (d, p) method and the results are given in Table 3. Mulliken charges are between -0.710 and 0.710. When we look at the atomic charges of alkylaminophenol, it is seen that the negative charge is around C39, C34, C11, C14, C5, C41 and C6 atoms, and the positive charge is around the N32, C3, C37, C13, H17, H23 atoms.

**Table 3.** Mulliken charges of the studied molecule.

Atoms	Mulliken (B3LYP)	Atoms	Mulliken (B3LYP)
C11	-0.517	C15	-0.138
C3	0.473	O25	-0.135
C2	-0.144	O24	-0.1
O22	-0.194	N32	0.710
H23	0.266	C33	0.051
C1	-0.228	H17	0.269
C5	-0.422	C34	-0.528
C6	-0.320	C37	0.469
C13	0.351	C39	-0.592
C14	-0.424	C41	-0.364

### 3.4 Frontier Molecular Orbitals (FMO)

FMO tells us about the reactivity of the compound. In order to determine the relevance of the compound to chemical reactions, we need to determine the energy values of the HOMO and LUMO orbitals. The structures showing the energy difference between HOMO and LUMO for our compound are given in Figure 3. HOMO and LUMO energies were calculated as -5.5287 and -0.7252, respectively. In this case, the ΔE energy difference is also calculated as 4.8035 eV. Physicochemical parameters of the compound by using HOMO and LUMO energy values are given in Table 4.

**Table 4.** HOMO, LUMO, ΔE, electronegativity (χ) chemical hardness (η), softness (S) and electrophilic index (χ) values of 2 - ((2,3-Dihydrobenzo [b] [1,4] dioxin-6-yl) (1H-indol-1-yl) methyl) phenol compound.

Physicochemical parameters	B3LYP/6-311++G(d,p)
E(HOMO, eV)	-5.5287
E(LUMO, eV)	-0.7252
ΔE(eV)	4.8035
χ	3.1270
η	2.4018
s	1.2009
ω	4.0711

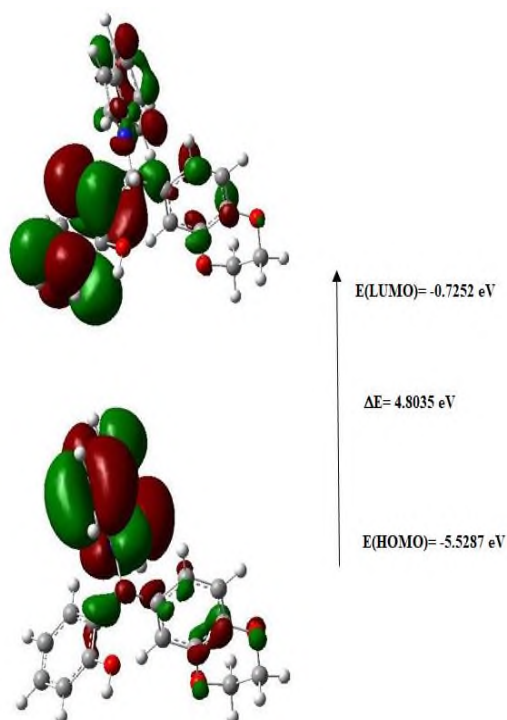


**Figure 3.** Frontier molecular orbitals, HOMO-LUMO energies.

### 3.5 Molecular Electrostatic Potential (MEP)

When looking at the three-dimensional molecular electrostatic potential surface of the compound (Figure 4), the energy scale is  $+6.476 \text{ e-}2 \text{ a.u.}$  and between  $-6.476 \text{ e-}2 \text{ a.u.}$  These values are; gives information about the chemical behaviour of the molecule. Looking at the structure, it is seen that the negative charge is

concentrated around the hydroxyl group and the positive part is concentrated on the nitrogen and phenyl protons. Determination of MEP surfaces; It is important in terms of providing information about intermolecular interactions and biological properties.

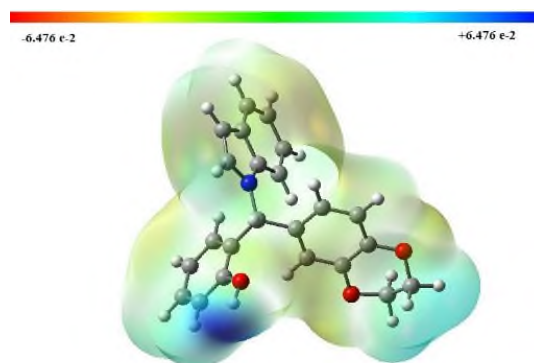


**Figure 4.** Molecular electrostatic potential surface and total electron density of 2 - ((2,3-Dihydrobenzo [b] [1,4] dioxin-6-yl) (1H-indol-1-yl) methyl) phenol.

### 3.6 Natural Bond Orbital (NBO) Analysis

NBO analysis is used to determine the electron density in all orbitals of the molecule.<sup>18,19</sup> A quadratic Fock matrix is used to evaluate the resulting donor-acceptor interactions. When each donor is defined as (i) and the recipient (j), delocalization is associated with  $i \rightarrow j$ , and the stability energy (E2) is expressed by the equation we define below.<sup>20</sup>

$$E(2) = \Delta E_{i,j} = q_i [F_{(i,j)}^2] / [E_i - E_j]$$

**Table 5.** NBO analysis using a quadratic Fock matrix for selected chemical bonds.

NBO(i) Donor	NBO(j) Acceptor	E(2) Kcal/mol	E(j)-E(i) a.u	F(i,j) a.u.	NBO(i) Donor	NBO(j) Acceptor	E(2) Kcal/mol	E(j)-E(i) a.u	F(i,j) a.u.
$\sigma(\text{C2-O22})$	$\sigma^*(\text{C1-C2})$	0.81	1.47	0.031	$\pi(\text{C1-C2})$	$\pi^*(\text{C1-C2})$	0.53	0.28	0.011
	$\sigma^*(\text{C1-C6})$	1.18	1.48	0.037		$\pi^*(\text{C3-C4})$	27.61	0.20	0.067
	$\sigma^*(\text{C2-C3})$	0.80	1.48	0.031		$\sigma^*(\text{C5-C6})$	21.81	0.29	0.072
	$\sigma^*(\text{C4-C8})$	5.10	0.29	0.035	$\pi(\text{C33-C35})$	$\sigma^*(\text{C11-H12})$	2.65	0.33	0.027
	$\sigma^*(\text{C16-C20})$	15.59	0.06	0.032		$\sigma^*(\text{C34-C45})$	1.57	0.49	0.026
	$\sigma^*(\text{C29-H31})$	1.43	0.98	0.034		$\sigma^*(\text{C33-C37})$	0.51	2.30	0.012

Table 5. Continued

$\sigma$ (C3-C11)	$\sigma^*$ (N32-C33)	1.09	1.08	0.031	$\sigma$ (C33-C35)	$\sigma^*$ (C4-C8)	212.67	0.07	0.109	
	$\sigma^*$ (C4-H8)	5900.53	0.01	0.226		$\sigma^*$ (C11-N32)	16.76	0.43	0.076	
	$\sigma^*$ (C26-H27)	25.83	0.65	0.116		$\sigma^*$ (C29-H31)	9.99	0.75	0.077	
	$\sigma^*$ (C29-H31)	51.55	0.69	0.169		$\sigma^*$ (C26-H27)	5.03	0.71	0.033	
	$\sigma^*$ (C34-C5)	3.15	0.82	0.048		$\sigma^*$ (C39-C41)	8.18	0.06	0.021	
	$\sigma^*$ (C34-C45)	7.45	0.87	0.072		$\sigma^*$ (C45-H46)	14.90	0.24	0.031	
	$\sigma^*$ (C43-C45)	11.04	0.22	0.048		LP(1) O22	$\sigma^*$ (C1-C2)	6.09	1.16	0.075
	$\sigma^*$ (C45-H46)	5.90	0.18	0.03			$\pi^*$ (C43-C45)	6.45	0.20	0.035
$\sigma$ (C11-C13)	$\sigma^*$ (C45-H46)	9.62	0.66	0.071	LP(2) O22	$\sigma^*$ (C45-H46)	6.90	0.17	0.030	
	$\sigma^*$ (C45-H46)	3.14	1.05	0.051		$\pi^*$ (C1-C2)	26.28	0.35	0.093	
	$\sigma^*$ (C45-H46)	2.05	0.84	0.037		$\pi^*$ (C3-C4)	0.50	0.27	0.011	
	$\sigma^*$ (C45-H46)	51.05	0.19	0.095	LP(1) O24	$\sigma^*$ (C11-N32)	3.68	0.07	0.014	
	$\sigma^*$ (C45-H46)	100.07	0.15	0.111		$\sigma^*$ (C16-C20)	4.50	1.09	0.063	
$\sigma$ (C11-N32)	$\sigma^*$ (C4-C5)	5.88	0.90	0.025	LP(2) O24	$\sigma^*$ (C29-H31)	10.25	0.62	0.072	
	$\sigma^*$ (C4-H8)	646.14	0.11	0.237		$\pi^*$ (C43-C45)	1.69	0.15	0.015	
	$\sigma^*$ (C11-H12)	6.48	0.81	0.065	$\sigma^*$ (C45-H46)	10683.23	0.04	0.569		
	$\sigma^*$ (C26-H27)	23.54	0.75	0.119	$\pi^*$ (C43-C45)	5180.26	0.07	0.572		



Table 5. Continued

	$\sigma^*(\text{C29-H31})$	34.51	0.79	0.148		$\sigma^*(\text{C35-C37})$	68.94	2.53	0.384
	$\sigma^*(\text{C43-C45})$	8.71	0.32	0.05		$\sigma^*(\text{C34-C45})$	119.08	0.73	0.270
LP(1) O25	$\sigma^*(\text{C43-C45})$	19797.48	2.17	5.885	LP(2) O25	$\sigma^*(\text{N32-C34})$	14853.90	2.28	5.201
	$\pi^*(\text{C43-C45})$	1916.29	6.09	3.300		$\sigma^*(\text{O24-C26})$	1437.84	4.73	2.227
	$\sigma^*(\text{C43-H46})$	2203.48	6.05	3.276		$\sigma^*(\text{C13-C14})$	2840.76	5.12	3.418
	$\sigma^*(\text{C34-C37})$	49110.31	0.93	6.049		$\pi^*(\text{C13-C14})$	32.19	6.54	0.448

When NBO analysis results are examined, it is seen that the atoms with the highest E (2) value are O22, O24, O25 atoms. It has been demonstrated by the data that these atoms (Table 5) are in strong interaction with phenyl rings. It can also be said that the chiral C11 atom is in strong interaction with the indole ring and phenyl rings to which it is attached with the N32 atom.

### 3.7 Nonlinear Optical Properties (NLO)

The NLO properties of the compound are due to its electrons. The presence of conjugation or donor groups in the structure changes many properties of the compound. Theoretical calculations made for this purpose give information about the electronic properties

of the compound. Calculations were made by selecting the *p*-nitroaniline compound used as a reference in the study. Isotropic linear polarization ( $\alpha$ ), anisotropic linear polarization ( $\Delta\alpha$ ), first-order hyperpolarization ( $\beta$ ) and total dipole moment ( $\mu$ ) values were calculated using the B3LYP method using the equations below.<sup>21</sup>

$$\mu = (\mu_x^2 + \mu_y^2 + \mu_z^2)^{1/2} \quad (1)$$

$$\langle\alpha\rangle = 1/3(\alpha_{xx} + \alpha_{yy} + \alpha_{zz}) \quad (2)$$

$$\Delta\alpha = [1/2((\alpha_{xx}-\alpha_{yy})^2 + (\alpha_{yy}-\alpha_{zz})^2 + (\alpha_{zz}-\alpha_{xx})^2)]^{1/2} \quad (3)$$

$$\langle\beta\rangle = [(\beta_{xxx} + \beta_{yyy} + \beta_{zzz})^2 + (\beta_{xyy} + \beta_{xzz})^2 + (\beta_{yyy} + \beta_{xxy} + \beta_{yzz})^2 + (\beta_{zzz} + \beta_{xxz} + \beta_{yyz})^2]^{1/2} \quad (4)$$

Table 6. NLO Analysis Results.

Property	<i>p</i> -NA	Alkylaminophenol	Property	<i>p</i> -NA	Alkylaminophenol
$\mu_x$	-7.4519	3.0798	$\beta_{xxx}$	-99.4560	178.3004
$\mu_y$	-0.001	3.0908	$\beta_{yyy}$	16.7004	9.9421
$\mu_z$	0.6869	0.1066	$\beta_{zzz}$	12.9992	10.6264
$\mu$	7.48 Debye	4.36 Debye	$\beta_{yyy}$	-0.0012	118.0253
$\alpha_{xx}$	-58.7480	-142.3714	$\beta_{xxy}$	-0.0004	-20.6859
$\alpha_{yy}$	-53.2767	-146.1486	$\beta_{yzz}$	0.0001	7.9136
$\alpha_{zz}$	-60.6128	-152.3852	$\beta_{zzz}$	0.4969	-5.5628
$\langle\alpha\rangle$	$-8.52 \times 10^{-24}$ esu	$-2.18 \times 10^{-23}$ esu	$\beta_{xxz}$	12.9100	23.8653
$\Delta\alpha$	$9.79 \times 10^{-25}$ esu	$1.3 \times 10^{-24}$ esu	$\beta_{yyz}$	0.4172	-5.5387
			$\langle\beta\rangle$	$8.99 \times 10^{-31}$ esu	$1.95 \times 10^{-30}$ esu

Looking at the NLO data (Table 6); it is seen that the dipole moment value of our alkylaminophenol compound is lower than *p*-NA. However, it is seen that the value of isotropic linear polarization, anisotropic linear polarization and first-order hyperpolarization is two times greater than *p*-NA. Based on these data, the

compound of 2 - ((2,3-Dihydrobenzo [b] [1,4] dioxin-6-yl) (1H-indol-1-yl) methyl) phenol has very high NLO properties in optoelectronics, laser technology, optical It appears to be a new compound that will contribute to many areas such as data storage.

### 3.8 Molecular Docking

Molecular docking studies were performed using Autodock Vina program.<sup>22</sup> The binding sites were centred on the Protein (PDB ID: 2RAW). Molecular docking techniques demonstrated that alkylaminophenol compound is Centromere-associated protein inhibitor. When looking at the 2D diagram (Figure 5), it was seen that there were alkyl-pi alkyl interactions and hydrogen bonds between the ligand and the protein. It was determined that there were interactions at a distance of 4.37 and 4.58 Å between alkyl and pi-alkyl. Hydrogen bond lengths were calculated to be 1.11, 1.86, 1.93 and 2.03 Å, respectively. The settlement score of the compound was determined to be -6.6 kcal/mol. This value clearly indicates that the alkylaminophenol compound has good biological activity (Table 7).

**Table 7.** Molecular Docking Results for Alkylaminophenol compound.

Protein ID	Binding Energy (Kcal/mol)	RMSD (Å)	Interactions	Distance (Å)
2RAW	-6.6	2.0	ABN A:118	1.11
				1.86
				1.93
				2.05
			LYS A:121	4.37
				4.58

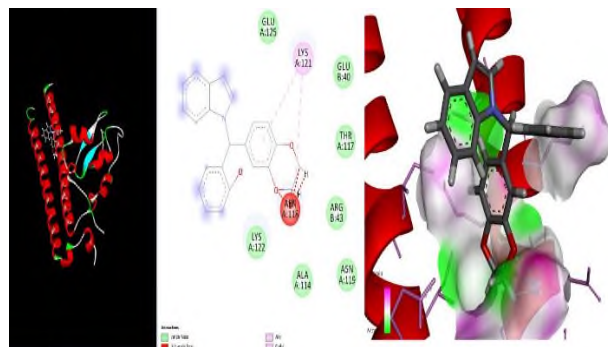


**Figure 5.** Docking analysis for the title compound.

### 4. CONCLUSION

In this study, the new alkylaminophenol type 2 - ((2,3-Dihydrobenzo [b] [1,4] dioxin-6-yl) (1H-indol-1-yl) methyl) phenol compound was synthesized with high yield for the first time. Structural analyzes of the compound were carried out experimentally and theoretically. Theoretical calculations were made by considering the DFT / B3LYP method and the 6-311 ++ G (d, p) base set. Many electronic properties of the compound (bond length, bond angle, dihedral angles) and the distribution of these electrons in orbitals (NBO) and chemical reactions have been calculated. Biological efficacy was predicted by molecular docking studies. In addition, it has been determined that NLO analysis can

be effective in optoelectronics other than medical applications.

### Acknowledgements

I would like to thank Melih ULAŞ for the optimization of the compound and Metin ULAŞ for bioinformatics contribution.

### Conflict of interests

Author declare that there is no a conflict of interest with any person, institute, company, etc.

### REFERENCES

- Wu, P.; Givskov, M.; Nielsen, T. E. *Chem. Rev.*, **2019**, 119(20), 11245–11290
- Neto, Í.; Andrade, J.; Fernandes, A. S.; Pinto Reis, C.; Salunke, J. K.; Priimagi, A.; Candeias, N. R.; Rijo, P. *ChemMedChem*, **2016**, 11, 2015–2023.
- Takahashi, N.; Ohba, T.; Yamauchi, T.; & Higashiyama, K. *Bioorg. Med. Chem.* **2006**, 14(17), 6089–6096.
- Liu, Y.; Wang, L.; Sui, Y.; Yu, J. *Chin. J. Chem.*, **2010**, 28(10), 2039–2044.
- Ulaş, Y.; Özkan, A. İ.; Tolan, V. *Ejosat*, **2019**, 16, 701–706.
- Doan, P.; Nguyen, T.; Yli-Harja, O.; Kandhavelu, M.; Yli-Harja, O.; Doan, P.; Nguyen, T.; Yli-Harja, O.; Candeias, N. R. *Eur J Pharm Sci*, **2017**, 107, 208–216.
- Ulaş, Y. *Ejosat*, **2019**, 16, 242–246.
- Petasis, N. A.; Goodman, A.; Zavialov, I. A. *Tetrahedron*, **1997**, 53(48), 16463–16470.
- Candeias, N. R.; Montalbano, F.; Cal, P. M. S. D.; Gois, P. M. P.. *Chem. Rev.*, **2010**, 110(10), 6169–6193.
- Hosseinzadeh, R.; Lasemi, Z.; Oloub, M.; Pooryousef, M.. *J. Iran. Chem. Soc.*, **2017**, 14(2), 347–355.
- Naskar, D.; Roy, A.; Seibel, W. L.; Portlock, D. E. *Tetrahedron Lett.*, **2003**, 44(31), 5819–5821.
- Ulaş, Y. *J. Comput. Biophys. Chem.*, **2021**, 20(3), 323-335 .

13. Muthu, S.; E. Porchelvi, E.; Karabacak, M.; Asiri, A. M.; Swathi, S. S. *J. Mol. Struct.*, **2015**, 1081, 400–412.
14. Suvitha, A; Periandy, S; Gayathri, P. *Spectrochim Acta A*, **2015**, 138, 357–369.
15. Suvitha, A.; Periandy, S; Govindarajan, M; Gayathri, P. (2015). *Spectrochim Acta A*, **2015**, 138, 900–912.
16. Becke, A. D. *Physical Review A*, **1988**, 38(6), 3098–3100.
17. Sivakumar, C.; Revathi, B.; Balachandran, V.; Narayana, B.; Vinutha V., S.; Shanmugapriya, N.; Vanasundari, K. *J. Mol. Struct.*, 2021, 1224 129286
18. S. P. P. Leela, J.; Hemamalini, R.; Muthu, S.; Al-Saadi, A. A. *Spectrochim Acta A*, **2015**, 146, 177–186.
19. Gültekin, Z.; Demircioğlu, Z.; Frey, W.; Büyükgüngör, O. *J. Mol. Struct.*, **2020**, 1199.
20. Ulaş, Y. *Int. J. Chem. Technol.* **2020**, 4 (2), 138-145
21. Raja, M.; Raj Muhamed, R.; Muthu, S., Suresh, M. *J. Mol. Struct.*, **2017**, 1141, 284–298.
22. Subashini, K.; Govindarajan, R.; Surendran, R.; Mukund, K.; Periandy, S.; *J. Mol. Struct.*, **2016**, 1125, 576-591.



## Antioxidant activity of silver nanoparticles synthesized from *Tagetes erecta* L. leaves

Ramazan ERENLER<sup>1,\*</sup>, Esmâ Nur GEÇER<sup>1</sup>, Nusret GENÇ<sup>1</sup>, Dürdane YANAR<sup>2</sup>

<sup>1</sup>Department of Chemistry, Faculty of Arts and Sciences, Tokat Gaziosmanpaşa University, 60250 Tokat, Turkey

<sup>2</sup>Department of Plant Protection, Faculty of Agriculture, Tokat Gaziosmanpaşa University, 60250 Tokat, Turkey

Received: 6 October 2021; Revised: 30 October 2021; Accepted: 10 November 2021

\*Corresponding author e-mail: [erenler@gmail.com](mailto:erenler@gmail.com)

**Citation:** Erenler, R.; Geçer, E. N.; Genç, N.; Yanar, D. *Int. J. Chem. Technol.* 2021, 5 (2), 141-146.

### ABSTRACT

*Tagetes erecta* leaves were extracted with deionized water at 55°C for around 3.0 hours and filtered. After removing of water from a quantity of solution by a rotary evaporator, the crude extract was obtained. The other filtrate was reacted with silver nitrate solution at 65°C for 2.5 hours to produce the silver nanoparticles (te-AgNPs). The structure of te-AgNPs was characterized by spectroscopic study. The characteristic hydroxyl vibrational of te-AgNPs was observed at 3214 cm<sup>-1</sup> in the Fourier Transform-Infrared Spectroscopy (FTIR). The maximum absorption was observed at 422 nm by Ultraviolet-Visible (UV-Vis) spectrophotometer. Scanning Electron Microscope (SEM) spectrum also proved the desired product with an average size of 46.26 nm. X-Ray Diffraction (XRD) spectrum revealed the te-AgNPs to be face-centered cubic crystalline structures. Antioxidant activity tests of extract and te-AgNPs were carried out and te-AgNPs displayed the significant antioxidant activity with the IC<sub>50</sub> values of 23.80 µg/mL, 4.46 µg/mL, and 2.79 µmol/mg sample corresponded to the 2,2-Diphenyl-1-picrylhydrazyl (DPPH), 2,2'-Azinobis(3-ethylbenzothiazoline-6-sulfonic acid) (ABTS) and Ferric ion Reducing Antioxidant Power) (FRAP) activities respectively.

**Keywords:** *Tagetes erecta* leaves, nanoparticles, spectroscopy, natural products, antioxidant activity.

### 1. INTRODUCTION

Aromatic and medicinal plants play a significant function in drug development as they contain bioactive compounds called secondary metabolites.<sup>1-4</sup>

Nanotechnology includes the physicochemical and biological process to construct nanomaterials, which are less than 100 nm and have unique properties.<sup>5</sup>

### *Tagetes erecta* yapraklarından sentezlenen nanopartiküllerin antioksidan aktivitesi

#### ÖZ

*Tagetes erecta* yaprakları yaklaşık saf su ile 55°C de 3.0 saat ısıtıldı ve daha sonra filtre edildi. Ham özüt elde etmek için süzölmüş çözeltinin bir miktarının çözücüsü döner buharlaştırıcı ile uzaklaştırıldı. Diğer filtre edilmiş çözelti, gümüş nitrat çözeltisi ile 65°C da 2.5 saat etkileştirilerek gümüş nanopartiküller (te-AgNPs) elde edildi. te-AgNPs yapısı spektroskopik yöntemlerle aydınlatıldı. te-AgNPs'in karakteristik hidroksil titreşimi, Fourier Transform Infrared Spektroskopisi (FTIR) spektrumunda 3214 cm<sup>-1</sup> de gözlemlendi. Ultraviolet-Visible (UV-Vis) spektrofotometre ile maksimum absorpsiyon 422 nm de gözlemlendi. Taramalı Elektron Mikroskop (SEM) spektral analizi ile de istenilen ürünün ortalama büyüklüğü 46.26 nm olarak belirlendi. X-Işını Kırınımı (XRD) spektrumu, te-AgNPs'in yüzey merkezli kübik kristal yapısında olduğunu ortaya koydu. Özüt ve te-AgNPs örneklerinin antioksidan aktivite testleri yapıldı ve te-AgNPs örneği, 23.80 µgml<sup>-1</sup>, 4.46 µgml<sup>-1</sup>, ve 2.79 µmolmg<sup>-1</sup> örnek<sup>-1</sup>, IC<sub>50</sub> değerleri ile sırasıyla önemli derecede 2,2-Difenil-1-pikrilhidraliz (DPPH), 2,2'-azinobis(3-etilbenzotiazolin-6-sulfonat) (ABTS) ve İndirgeyici Antioksidan Gücü (FRAP) aktivitesi gösterdi.

**Anahtar Kelimeler:** *Tagetes erecta* yapraklar, nanopartikül, spektroskopisi, doğal ürünler, antioksidan aktivite.

Nanotechnology has been used extensively in various fields such as nanomedicines, biomaterials, nanoelectronics, imaging, agriculture, environmental In medicine, it has been widely employed for diagnosis, and treatment of diseases, as well as drug delivery, and novel drug formulations.<sup>6</sup> Therefore, the synthesis of nanoparticles has attracted great interest and many synthesis pathways have been developed such as photochemical, radiation and electrochemical. Yet, the

corresponding methods cause pollution, toxicity and require drastic reaction conditions. So, natural products mediated synthesis of nanoparticles has opened a new era to this research area, since this method is eco-friendly, economical, and provides high efficiency with scale-up. Natural products like pure compounds, plant extracts, algae, enzymes, vegetable wastes, seaweed, arthropods have been used for nanoparticles production.<sup>7</sup> Natural products mediated synthesized nanoparticles displayed considerable biological actions such as anticancer, antioxidant, anti-inflammatory, antibacterial, antifungal, antiviral, acetylcholinesterase, mosquito larvicidal, photocatalytic.<sup>8-11</sup>

*Tagetes* genus belongs to Asteraceae family and includes 122 species. *Tagetes erecta* Linn. is an ornamental flower that is well-known as Marigold.<sup>12</sup> The corresponding plant has been employed as a traditional medicine for the therapy of colds, rheumatism, and bronchitis. Moreover, the juice of this plant has sudorific, vomitive, febrifuge, vermifuge, emetic properties. *Tagetes erecta* consists of lutein, xanthophyll.<sup>13</sup> Lutein is the responsible compound for the coloring of the *T. erecta*.<sup>14</sup> Besides, it has a protective effect against macular degeneration disease, cardiovascular disease, cancer, oxidative effects. The flower of *T. erecta* was reported to have anti-inflammatory, antimutagenic, antiviral, and antitumor effects.<sup>15,16</sup>

Reactive oxygen species are called free radicals that are essential for many reactions in the eukaryotic cell.<sup>17</sup> In some conditions like smoking, drugs, alcohol, bad lifestyle, excess free radicals are produced that harm to the lipid, protein, and nucleic acid leading to the diseases such as cancer, Alzheimer, and diabetes. Therefore, many antioxidant-based drugs, as well as food supplement containing antioxidant compounds, have been developed to combat the corresponding challenge.<sup>18</sup> Antioxidants are essential not only for humans but also to prevent food from spoiling.<sup>19</sup> Throughout the storage and dealing out of foods, lipids oxidation like enzymatic and auto oxidations are the main reactions that lead to food deterioration affecting the color, smell, taste, and nutritional value of foods. Hence, antioxidants are used for food to prevent radicalic reactions.<sup>20</sup> Synthetic antioxidants, such as butylated hydroxyl toluene (BHT) and butylated hydroxyl anisole (BHA) which are commonly used for food are restricted due to their toxic effect and possible carcinogens.<sup>21</sup> Therefore, the interest in natural antioxidants has been increased considerably by consumer preference and industries.<sup>22</sup>

Since the silver atoms are encapsulated and stabilized by bioactive compounds of the plants, the interest in nanoparticles for biological effects has been increased steadily. The nanoparticles using the medicinal plants were reported to display significant antioxidant activity.<sup>23</sup>

Herein, silver nanoparticles (te-AgNPs) were synthesized using *T. erecta* leaves and their structure was characterized by spectroscopic methods. Moreover, their antioxidant activity was accomplished using the DPPH<sup>•</sup> scavenging, ABTS<sup>•+</sup> radical cation scavenging, and reducing power assays.

## 2. MATERIALS AND METHODS

### 2.1. General

All chemicals and solvents utilized in nanoparticles synthesis and antioxidant activity tests were supplied from E. Merch (Darmstadt, Germany).

### 2.2. Plant material

*Tagetes erecta* L., a well-known plant was collected from the university campus during the maturation stage in August 2020.

### 2.3. Green synthesis of silver nanoparticles

*Tagetes erecta* leaves (40 g) was extracted with deionized water (500 mL) for 3 hours at 55°C. The solution was double filtered and divided equally into two pieces for crude extract and te-AgNPs. One solution (250 mL) was subjected to a rotary evaporator to produce crude extract (2.0 g). Another solution was used for the synthesis of te-AgNPs. *T. erecta* (250 mL) solution was reacted with AgNO<sub>3</sub> dissolved in deionized water (0.071 M, 100 mL) for 2.5 hours at 65°C. After the centrifugation at 4000 rpm for 15 min, silver nanoparticles were obtained, washed and lyophilized (0.75 g)<sup>24</sup> (Figure 1).

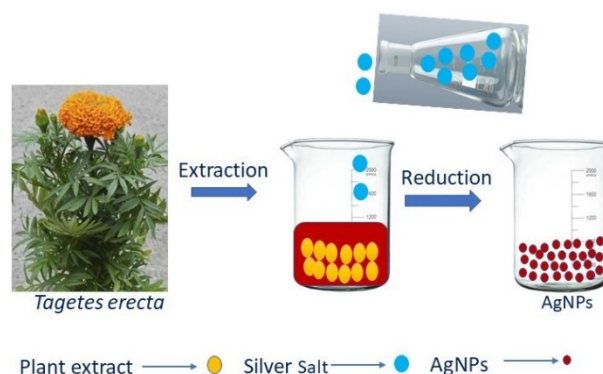


**Figure 1.** The green synthesis of te-AgNPs.

### 2.4. Characterization of silver nanoparticles

The structural elucidation of synthesized silver nanoparticles was carried out by fully spectroscopic analyses. Ultraviolet-visible, UV-2600 spectrophotometer was used to determine of maximum absorption of silver nanoparticles as well as antioxidant activity analyses. The functional groups of compounds that capped to the silver as well as stabilized the silver





between extract and te-AgNPs spectrum confirmed the formation of te-AgNPs (Figure 4). The vibrational signal at 3305 cm<sup>-1</sup> represented the OH of the flavonoid rings. CH stretching vibrational signals of alkanes appeared at 2973 cm<sup>-1</sup> and 2885 cm<sup>-1</sup>. The peak at 1574 cm<sup>-1</sup> corresponded to the double bond of an alkene. The vibrational signal at 1381 could be due to the CH bending of alkane. The signals observed at 1085 cm<sup>-1</sup>, 1047 cm<sup>-1</sup>, and 880 cm<sup>-1</sup> represented the CN stretching of amine, CN stretching of amine, and C=C bending of alkene respectively. The signals that appeared at 512 cm<sup>-1</sup> and 428 cm<sup>-1</sup> could be due to the silver oxide which accorded to the reported work.<sup>30</sup> Ag<sup>+</sup> ions might be reduced to Ag<sup>0</sup> by the secondary metabolites of plant extract, and consequently, the green synthesized AgNPs were capped and stabilized by functional groups of corresponding metabolites.<sup>31</sup>

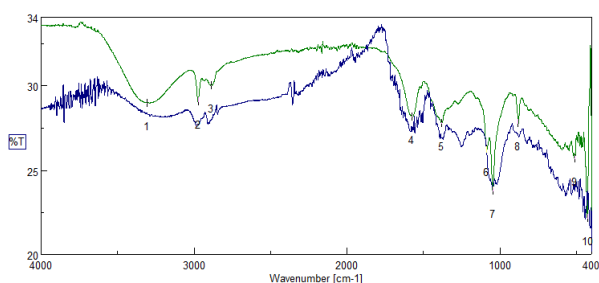


**Figure 4.** FTIR spectrum of extract (A) and AgNPs (B), 1: 3305, 2: 2973, 3: 2885, 4: 1574, 5: 1381, 6: 1085, 7: 1047, 8: 880, 9: 512, 10: 428

### 3.3. X-ray diffraction

The crystalline nature of te-AgNPs was determined by XRD analysis. Diffraction peaks at  $2\theta$  values of 38.1°, 44.3°, 64.4°, and 77.4° corresponded to the (111), (200), (220), and (311) reflections of the face-centered cubic crystalline (fcc) structure which was in accordance with the standard silver card values (JCPDS No. 87-0720). A previous study also confirmed the structure.<sup>32</sup> Debye-Scherrer formula was used for calculation of average crystalline size (1)

$$D = 0.9 \lambda / \beta \cos \theta \quad (1)$$

D represents the average crystalline size (°A),  $\lambda$  designates the x-ray wavelength (nm),  $\beta$  describes the angular line with at half maximum intensity (radians) and  $\theta$  is the angle (degree). The sharp diffraction peak in the XRD pattern displayed the crystalline properties of te-AgNPs. The impurity diffraction peaks were caused by the plant materials. The particle size was calculated as 46.26 nm (Figure 5).

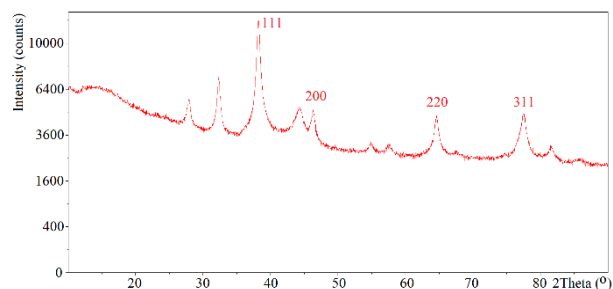


**Figure 5.** XRD pattern of te-AgNPs synthesized

### 3.4. Scanning Electron Microscope

The morphology of green synthesized te-AgNPs was presented by SEM analysis (Figure 6). SEM image revealed the dispersion of agglomerated clusters that were distributed over the surface. The energy dispersive analysis (EDX) verified the presence of NPs. Furthermore, the notable strong peak of Ag in synthesized NPs in the EDX spectrum at around 3 and 3.3 keV approved the structure of synthesized nanoparticles. In addition, elemental analysis proved the proposed structure as well (Figure 7).

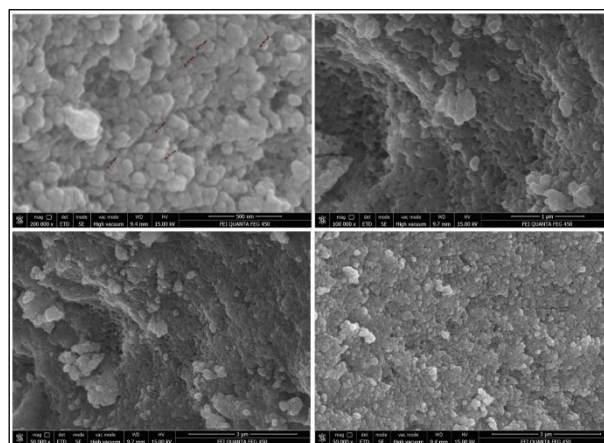


**Figure 6.** SEM images of te-AgNPs

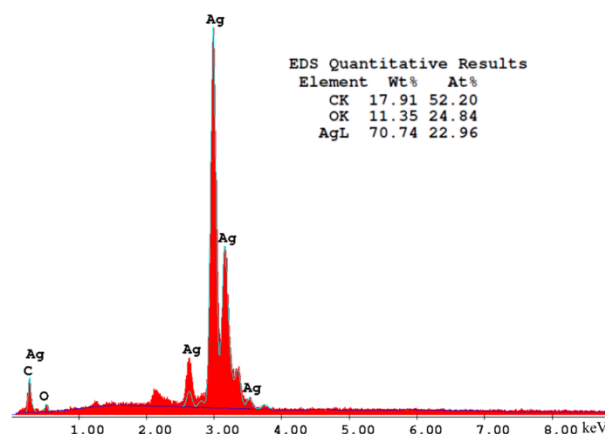


**Figure 7.** EDX spectrum and elemental analysis of te-AgNPs.

### 3.5. Antioxidant activity

Antioxidant activity of extract and silver nanoparticles from *T. erecta* leaves was achieved using DPPH, ABTS<sup>+</sup> and FRAP assays (Figure 8). In DPPH assay, AgNPs (23.8 µg/mL, IC<sub>50</sub>) revealed a higher effect than that of the extract (40.0 µg/mL, IC<sub>50</sub>) significantly. Yet, their radical scavenging effects were lower than the standards. In concerning the ABTS assay, AgNPs revealed excellent activity (4.5 µg/mL, IC<sub>50</sub>), even better than the standards BHT (7.3 µg/mL, IC<sub>50</sub>), and Trolox (5.7 µg/mL, IC<sub>50</sub>). However, the extract exhibited moderate activity (19.3 µg/mL, IC<sub>50</sub>). The same trend was observed in the FRAP assay. In FRAP assay, the effect of te-AgNPs (2.8 µmol TE/mg extract) was found higher than that of the extract (0.8 µmol TE/mg extract). Hence, te-AgNPs synthesized from *T. erecta* could be a promising antioxidant agent for the food and pharmaceutical industries. AgNPs synthesized from *T. erecta* was reported to have antibacterial activity against *Escherichia coli*, *Staphylococcus aureus* bacteria.<sup>33</sup> Moreover, AgNPs synthesized from *T. erecta* revealed improved photodegradation of Rhodamine B dye.<sup>34</sup> Nickel oxide nanoparticles prepared using *T. erecta* leaf extract exhibited significant photocatalytic, antibacterial activities as well as high sensitivity for glucose sensors.<sup>35,36</sup> te-AgNPs synthesized from *T. erecta* revealed the DPPH free radical scavenging effect, only DPPH assay was used for antioxidant activity and silver nanoparticles were synthesized at room temperature. Moreover, *T. erecta* was collected from India for the corresponding study.<sup>37</sup> However, in our study, *T. erecta* was collected in Tokat, DPPH, ABTS and FRAP assays were carried out for the antioxidant activity. Moreover, silver nanoparticles were synthesized at 65 °C. Silver nanoparticles synthesized from *T. erecta* leaves were reported to enhance the plant growth.<sup>38</sup> Another research presented that the AgNPs obtained from *T. erecta* leaves extract displayed the wound healing activity and anti-inflammatory activity in female Wistar albino rats.<sup>39</sup> In addition, Silver nanoparticles synthesized from *T. erecta* were reported to display supercapacitor and electrochemical sensing applications,<sup>40</sup> and amoxicillin detection.<sup>41</sup>

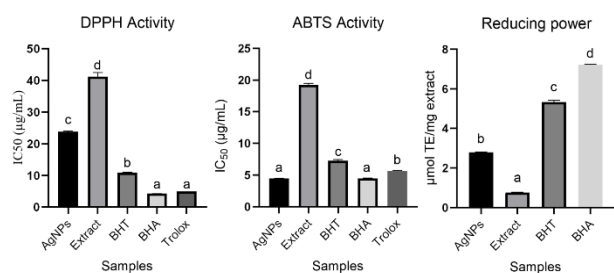


**Figure 8.** Antioxidant activity of te-AgNPs and extract. The results were reported as mean values  $\pm$  SDs of three independent assays ( $P < 0.05$ ). Values followed by the different letter are significantly different.

### 4. CONCLUSION

The synthesis of silver nanoparticles is one step, cheap, eco-friendly, and scale-up. The te-AgNPs synthesized from *T. erecta* leaves could be a promising material for the antioxidant agent. *T. erecta* includes significant bioactive compounds. Thus, the silver capped and stabilized by these compounds could be considered an effective material for the pharmaceutical and food industries. In other words, te-AgNPs synthesized from *T. erecta* are a promising agent that may offer a significant application in the treatment of oxidative stress-related diseases.

### Conflict of interest

The authors declare that *there is no a conflict of interest with any person, institute, company, etc.*

### REFERENCES

- Topçu, G.; Erenler, R.; Çakmak, O.; Johansson, C. B.; Çelik, C.; Chai, H.-B.; Pezzuto, J. M. *Phytochemistry* **1999**, 50 (7), 1195-1199.
- Elmastas, M.; Ozturk, L.; Gokce, I.; Erenler, R.; Aboul-Enein, H. Y. *Anal Lett* **2004**, 37 (9), 1859-1869.
- Demirtas, I.; Erenler, R.; Elmastas, M.; Goktasoglu, A. *Food Chem* **2013**, 136 (1), 34-40.
- Sahin Yaglioglu, A.; Akdulum, B.; Erenler, R.; Demirtas, I.; Telci, I.; Tekin, S. *Med Chem Res* **2013**, 22 (6), 2946-2953.
- Rama Krishna, A.; Espenti, C.; Rami Reddy, Y.; Obbu, A.; Satyanarayana, M. *J Inorg Organomet Polym Mater* **2020**, 30, 4155-4159.
- Aiswariya, K.; Jose, V. *J Inorg Organomet Polym Mater* **2021**, 31, 3111-3124.
- Lateef, A.; Ojo, S. A.; Elegbede, J. A. *Nanotechnol Rev* **2016**, 5 (6), 601-622.
- Bachheti, R. K.; Fikadu, A.; Bachheti, A.; Husen, A. *Saudi J Biol Sci* **2020**, 27 (10), 2551.
- Vanaraj, S.; Keerthana, B. B.; Preethi, K. *J Inorg Organomet Polym Mater* **2017**, 27 (5), 1412-1422.
- Erenler, R.; Dag, B. *Inorg Nano-Met Chem* **2021**, <https://doi.org/10.1080/24701556.2021.1952263>.
- Ravindra, S.; Mulaba-Bafubandi, A. F.; Rajinikanth, V.; Varaprasad, K.; Reddy, N. N.; Raju, K. M. *J Inorg Organomet Polym Mater* **2012**, 22 (6), 1254-1262.

12. Jiang, M.; Xu, Y.; Wang, L.; Liu, J.; Yu, J.; Chen, H. *Mitochondrial DNA Part B* **2020**, 5 (3), 2966-2971.
13. Hojnik, M.; Škerget, M.; Knez, Ž. *LWT-Food Science and Technology* **2008**; 41(10): 2008-2016.
14. Gau, W.; Ploschke, H.-J.; Wünsche, C. *J Chromatogr A* **1983**, 262, 277-284.
15. Chitrakar, B.; Zhang, M.; Bhandari, B. *Trends Food Sci Technol* **2019**, 89, 76-87.
16. Gansukh, E.; Mya, K. K.; Jung, M.; Keum, Y.-S.; Kim, D. H.; Saini, R. K. *Food Chem Toxicol* **2019**, 127, 11-18.
17. Erenler, R.; Sen, O.; Aksit, H.; Demirtas, I.; Yaglioglu, A. S.; Elmastas, M.; Telci, İ. *J Sci Food Agr* **2016**, 96 (3), 822-836.
18. Erenler, R.; Adak, T.; Karan, T.; Elmastas, M.; Yildiz, I.; Aksit, H.; Topcu, G.; Sanda, M. A. *The Eurasia Proceed Sci Tech Eng Math* **2017**, 1, 139-145.
19. Erenler, R.; Meral, B.; Sen, O.; Elmastas, M.; Aydin, A.; Eminagaoglu, O.; Topcu, G. *Pharm Biol* **2017**, 55 (1), 1646-1653.
20. Guzel, A.; Aksit, H.; Elmastas, M.; Erenler, R. *Pharmacogn Mag* **2017**, 13 (50), 316-320.
21. Sasaki, Y. F.; Kawaguchi, S.; Kamaya, A.; Ohshita, M.; Kabasawa, K.; Iwama, K.; Taniguchi, K.; Tsuda, S. *Mutat Res Genet Toxicol Environ Mutagen* **2002**, 519 (1-2), 103-119.
22. Elmastas, M.; Celik, S. M.; Genc, N.; Aksit, H.; Erenler, R.; Gulcin, İ. *Int J Food Prop* **2018**, 21 (1), 374-384.
23. Burlacu, E.; Tanase, C.; Coman, N.-A.; Berta, L. *Molecules* **2019**, 24 (23), 4354.
24. Genc, N.; Yildiz, I.; Chaoui, R.; Erenler, R.; Temiz, C.; Elmastas, M. *Inorg Nano-Met Chem* **2021**, 51 (3), 411-419.
25. Erenler, R.; Yilmaz, S.; Aksit, H.; Sen, O.; Genc, N.; Elmastas, M.; Demirtas, I. *Rec Nat Prod* **2014**, 8 (1), 32-36.
26. Erenler, R.; Telci, İ.; Ulutas, M.; Demirtas, I.; Gul, F.; Elmastas, M.; Kayir, O. *J Food Biochem* **2015**, 39 (5), 622-630.
27. Elmastaş, M.; Telci, İ.; Aksit, H.; Erenler, R. *Turk J Biochem* **2015**, 40 (6), 456-462.
28. Zuas, O.; Hamim, N.; Sampora, Y. *Mater Lett* **2014**, 123, 156-159.
29. Lu, H.; Yang, S.; Ma, H.; Han, Z.; Zhang, Y. *Anal Methods* **2016**, 8 (15), 3255-3262.
30. Iftikhar, M.; Zahoor, M.; Naz, S.; Nazir, N.; Batiha, G. E.-S.; Ilaq, R.; Bari, A.; Hanif, M.; Mahmood, H. M. *J Nanomater* **2020**, ID 8949674, <https://doi.org/10.1155/2020/8949674>.
31. Gecer, E. N.; Erenler, R.; Temiz, C.; Genc, N.; Yildiz, I. *Particul Sci Technol* **2021**, <https://doi.org/10.1080/02726351.2021.1904309>.
32. Beyene, H. D.; Werkneh, A. A.; Bezabh, H. K.; Ambaye, T. G. *Sust Mat Technol* **2017**, 13, 18-23.
33. Maji, A.; Beg, M.; Das, S.; Aktara, M. N.; Nayim, S.; Patra, A.; Islam, M. M.; Hossain, M. *Process Biochem* **2020**, 97, 191-200.
34. Katta, V.; Dubey, R. *Mat Today Proceed* **2021**, 45, 794-798.
35. Maji, A.; Beg, M.; Das, S.; Aktara, M. N.; Nayim, S.; Patra, A.; Islam, M. M.; Hossain, M. *Process Biochem* **2020**, 97, 191-200.
36. Likasari, I. D.; Astuti, R. W.; Yahya, A.; Isnaini, N.; Purwiandono, G.; Hidayat, H.; Wicaksono, W. P.; Fatimah, I. *Chem Phys Lett* **2021**, 780, 138914.
37. Tyagi, P. K.; Tyagi, S.; Gola, D.; Arya, A.; Ayatollahi, S. A.; Alshehri, M. M.; Sharifi-Rad, J. *J Nanomater* **2021**, 2021, ID 6515419.
38. Kumar, P.; Pahal, V.; Gupta, A.; Vadhan, R.; Chandra, H.; Dubey, R. C. *Sci. Rep.* **2020**, 10 (1), 20409.
39. Selvam, S. I.; Joicesky, S. M. B.; Dashli, A. A.; Vinothini, A.; Premkumar, K. *J Appl Nat Sci* **2021**, 13 (1), 343-351.
40. Salve, M.; Mandal, A.; Amreen, K.; Pattnaik, P. K.; Goel, S. *Microchem J* **2020**, 157, 104973.
41. ul Ain, N.; Anis, I.; Ahmed, F.; Shah, M. R.; Parveen, S.; Faizi, S.; Ahmed, S. *Sens Actuators B Chem* **2018**, 265, 617-624.





## Structural and spectral properties of 4-(4-(1-(4-Hydroxyphenyl)-1-phenylethyl)phenoxy)phthalonitrile: Analysis by TD-DFT method, ADME analysis and docking studies

Kenan ALTUN<sup>1</sup>, Ümit YILDIKO<sup>1</sup>, Aslıhan Aycan TANRIVERDİ<sup>2,\*</sup>, İsmail ÇAKMAK<sup>2</sup>

<sup>1</sup> Engineering and Architecture Faculty, Department of Bioengineering, Kafkas University, Kars, 36100, Turkey

<sup>2</sup> Faculty of Arts and Sciences, Department of Chemistry, Kafkas University, Kars, 36100, Turkey

Received: 3 October 2021; Revised: 3 December 2021; Accepted: 8 December 2021

\*Corresponding author e-mail: [t.aslihanaycan@gmail.com](mailto:t.aslihanaycan@gmail.com)

**Citation:** Altun, K.; Yıldiko, Ü.; Tanrıverdi, A. A.; Çakmak, İ. *Int. J. Chem. Technol.* 2021, 5 (2), 147-155.

### ABSTRACT

Since phthalonitrile compounds have become popular lately, the focus has been on the idea that these compounds should be investigated. A unique phthalonitrile compound, 4-(4-(1-(4-hydroxyphenyl)-1-phenylethyl)phenoxy)phthalonitrile (coded as PN) was selected and molecular modeling studies were carried out on this compound to be brought to the literature. First, time-dependent density functional theory (TD-DFT) calculations (Geometry optimization, HOMO-LUMO, dipole moment calculations, MEPS maps, Mulliken atomic charges, and NBO analysis) were performed for PN. In addition, in this section, absorption, distribution, metabolism, excretion, and toxicity (ADMET) analysis for the compound belonging to the phthalonitrile group was performed and the color regions were presented separately. Finally, molecular docking studies were performed for a compound separately with three different enzymes (AChE, BChE,  $\alpha$ -GLY), and docking scores and receptor models were presented.

**Keywords:** Phthalonitrile, TD-DFT, ADMET, molecular docking.

4-(4-(1-(4-Hidroksifenil)-1-feniletıl) fenoksi) ftalonitril'in yapısal ve spektral özellikleri: TD-DFT metodu ile analiz, ADME analizi ve doking çalışmaları

### ÖZ

Ftalonitril bileşikleri son zamanlarda popüler hale geldiğinden, bu bileşiklerin araştırılması gerektiği fikri üzerinde durulmuştur. Eşsiz bir ftalonitril bileşiği olan, 4-(4-(1-(4-hidroksifenil)-1-feniletıl)fenoksi)ftalonitril (PN olarak kodlanmıştır) seçilmiş ve literatüre kazandırılmak üzere bu bileşik üzerinde moleküler modelleme çalışmaları yapılmıştır. İlk olarak, PN için zamana bağlı yoğunluk fonksiyonel teorisi (TD-DFT) hesaplamaları (Geometri optimizasyonu, HOMO-LUMO, dipol moment hesaplamaları, MEPS haritaları, Mulliken atom yükleri ve NBO analizi) yapılmıştır. Ayrıca bu bölümde ftalonitril grubu bileşiğe ait absorpsiyon, dağılım, metabolizma, atılım ve toksisite (ADMET) analizleri yapılmış ve renk bölgeleri ayrı ayrı sunulmuştur. Son olarak, bir bileşik için ayrı ayrı üç farklı enzim (AChE, BChE,  $\alpha$ -GLY) ile moleküler doking çalışmaları yapılmış ve doking skorları ve reseptör modelleri sunulmuştur.

**Anahtar Kelimeler:** Ftalonitril, TD-DFT, ADMET, Moleküler doking.

### 1. INTRODUCTION

In the last few years, phthalonitriles (PNs) have remarked many attention for their extraordinary features. The enhanced heat resistance of phthalonitriles also shows other highly attractive performances such as an outstanding flame resistance, well mechanical properties at high temperature, low water uptake, outstanding

corrosion resistance, and developed UV protection behavior.<sup>1</sup> However, PN materials have brittleness property. Brittleness, an inherent property of PNs, results from the hardness of monomeric vanguards and the high degree of crosslinking of their cured versions.<sup>2</sup> Additionally, normal PN monomers require higher curing temperatures and a longer time to attain completely cured systems. Although the inset of multi



curing catalysts was contrived to enhance curing attitude to a significant rating, curing temperatures and times did higher than those of other high-performance thermosets.<sup>3,4</sup> The afore mentioned PN deficiencies were examined by researchers and many solutions were recommended. Introduced functionalities involved imide, alkene, bismaleimide, alkyl, benzoxazine, benzimidazole, novolac, and the like. Functionality election is often driven by targeted features. Other functions can ensure both improvements.<sup>5</sup> When the PN monomer does not encounter all the necessities for a particular application, forming blends and copolymers with another PN compound is the first choice before careful blending with other types of monomers.<sup>6</sup> The diversity of PN monomers present, involving typical, functional, and self-catalyzing PN monomers and oligomers with different features, may direction some of the limitations of a single PN monomer.<sup>7</sup>

Methods for predicting the 3-d structure of a protein generally fall into three categories: ab initio or de novo modeling, threading, and homology or comparative modeling. Ab initio modeling uses a combination of statistical analysis and physics-based energy function to estimate the natural multiple of a delivered sequence.<sup>8</sup> Ab initio modeling is favoured for estimating the structure of a sequence when no convenient template is found or when the query is common to use a particular fold than the envisaged template despite sequence similarity.<sup>9</sup> Various ab initio algorithms exercise statistical information, secondary structure, and part assemblage for folding forecast. Also common to all algorithms is the simplistic presentment of the protein to keep the forecast problem traceable. Reference is made to the reader for more information on the particular ab initio estimation methods.<sup>10,11</sup>

In this study, molecular modeling studies of a selected unique PN compound were carried out. TD-DFT studies were carried out to have information about the energy properties, electrical properties, and nonlinear optical properties of the compound. In addition, ADME analysis was carried out to investigate the ADMET properties of the compound. Finally, molecular docking studies have been carried out successfully to determine whether the PN compound will be compatible with the drug design phenomenon.

## 2. MATERIALS AND METHODS

### 2.1. Computer calculations

The PN molecule was first drawn in ChemBioDraw for TD-DFT calculations in the gaussian 09 program and minimized by the SYBL2 (mol2) method with the Chem3D program. Similarly, the drawn molecules were converted to 3D MOL2 files in Chem3D and transferred to GaussView 6.0. TD-DFT study<sup>12</sup> was calculated on 6-

311G basis set in B3LYP and LanL2DZ method and images of each calculation<sup>13</sup> (Geometry optimization, HOMO and LUMO analysis, Mulliken atomic charges and dipole moment, MEP analysis) were taken. Molecular docking was provided to investigate the exact binding site and binding mechanism of ligand-protein interactions. Schrödinger's Maestro Molecular Modeling platform (version 11.8).<sup>14</sup> Online servers such as SwissADME (<http://www.swissadme.ch/index.php>) were used for ADME analysis.<sup>15</sup> The LLC model was applied in the molecular docking approach. Crystal structures of human asetilkolinesteraz (AChE) (PDB ID: 4M0E), butirilkolinesteraz (BChE) (PDB ID: 6SAM) ve alfa-glukosidaz ( $\alpha$ -GLY) (PDB ID: 3A4A) enzymes were downloaded. All compounds were equipped as for that former studies with the Ligprep module. Ligand-protein docking studies were carried out with the glide docking module. The highest binding energies and binding conformations between enzymes and ligands were estimated.<sup>16</sup> The lowest energy positions show the highest binding affinities. Molecular docking study were visualized with Discovery Studio 2016 client (Visualizer 2005).

## 3. RESULTS AND DISCUSSION

The molecule belonging to the phthalonitrile group was first drawn in ChemBioDraw for theoretical calculations in the Gaussian 09 program and applied by the "PDB" format method with the Chem3D program. Applied molecules were given to the Gaussian 09 program and ab initio calculations were done for this structure.

### 3.1. TD-DFT Studies

#### 3.1.1. Geometry optimization of PN compound

The theoretically calculated values of some phthalonitrile compounds can give an idea about the geometry of molecular changes.<sup>17,18</sup> The optimized basic structure and total energy conversion of PN are given in Figure 1.

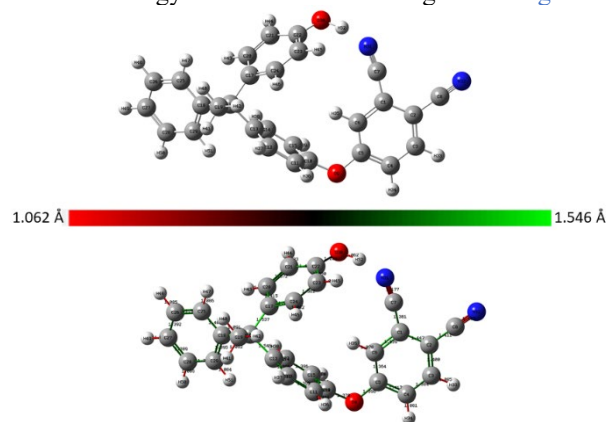


**Figure 1.** Optimized structure for PN using the TD-DFT method and the R3PW91 / TD-FC and RB3LYP/6-311G (d, p) basis set.

The optimized bond length parameters of the molecule calculated with the TD-FC basis set of R3PW91 and the 6-311G (d, p) basis set of RB3LYP in the PN TD-DFT method are shown in Figure 1 and listed in Table 1. There is very little difference between the R3PW91 and RB3LYP values. This means that the structure has minimum potential energy. A comparison of optimized two basis set of PN was studied. All bond lengths and

bond angles in phenyl rings are within the normal range. The C-C bond distances for R3PW91 are 1.361-1.545 Å, and the C-O bond distances for RB3LYP are 1.363-1.555 Å and 1.288-1.405 Å for the oxygen atom between the two phenyl rings. The C-H lengths in the aromatic ring are 1.076 - 1.091 Å. All C-C-C angles are between 112° and 123°. The C-C-H angle in the compound is 112° - 121°, C-C-O 115° -123°, and O-C-H 112-113°.

**Table 1.** The theoretically obtained bond lengths (Å), bond angles (°), and dihedral angles (°) of the molecule for PN.

Bond lengths (Å)			Bond Angles (°)		
Atom Groups	R3PW91	RB3LYP	Atom Groups	R3PW91	RB3LYP
C1-C2	1.44698	1.45150	C1-C2-C8	121.41592	121.39628
C1-C6	1.43875	1.44267	C1-C2-C3	118.48142	118.47263
C2-C3	1.39996	1.40259	C2-C8-N32	179.70130	179.64954
C2-C8	1.41060	1.41301	C1-C7-N31	172.70007	172.58947
C8-N32	1.16159	1.16117	C2-C3-H33	117.85024	117.85481
C3-H33	1.08452	1.08370	C1-C6-H35	117.99770	117.86282
C3-C4	1.38446	1.38648	C14-C15-H39	121.02220	120.94766
C4-H34	1.08135	1.08041	C6-C5-O9	122.93404	122.97260
C4-C5	1.41656	1.41929	C5-C4-H34	119.83494	119.82089
C5-C6	1.36368	1.36422	C5-O9-C10	115.62031	116.03688
C6-H35	1.07815	1.07656	C3-C4-C5	118.35084	118.31576
C5-O9	1.39623	1.40504	C10-C11-H36	119.07370	119.07862
C1-C7	1.38134	1.38401	C10-C11-C12	119.90458	119.94643
C7-N31	1.17695	1.17685	C10-C15-H39	119.21409	119.21882
O9-C10	1.36993	1.37458	C11-C12-C13	120.99433	121.05933
C10-C11	1.38872	1.39056	C12-C13-C16	122.38367	122.36303
C11-H36	1.08383	1.08296	C12-C13-C14	117.80020	117.64938
C10-C15	1.39258	1.39444	C13-C14-H38	119.74895	119.85308
C15-H39	1.08375	1.08282	C13-C16-C18	114.03440	114.08505
C14-C15	1.38572	1.38782	C13-C16-C19	112.51612	112.44122
C14-C13	1.40329	1.40569	C16-C19-H42	113.40299	113.42896
C14-H38	1.08491	1.08351	H40-C19-H41	107.79547	107.81048

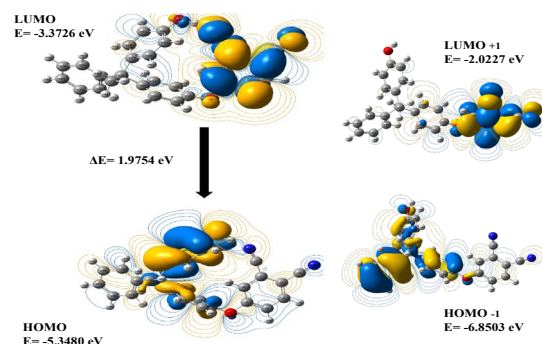
  

Dihedral Angles (°)			Dihedral Angles (°)		
Atom Groups	R3PW91	RB3LYP	Atom Groups	R3PW91	RB3LYP
C1-C2-C3-C4	0.46233	0.42841	C23-C22-O30-H52	17.82858	18.19702
C2-C1-C7-N31	179.01002	178.23777	H46-C24-C23-H45	0.04831	0.28348
C3-C4-C5-O9	179.66344	179.70866	C12-C13-C16-C18	133.08575	133.14003
H36-C11-C10-O9	4.56578	4.79244	H48-C26-C27-H49	0.29434	0.30255

### 3.1.2. Frontier molecular orbitals (HOMO-LUMO) and dipole moment calculations of the PN compound

The main electrical parameters regarding orbitals in a molecule are the highest occupied molecular orbital (HOMO) and lowest unoccupied molecular orbital (LUMO) and energy vacancies. HOMOs are the outermost (highest energy) orbital electrons that can act as electron donors. The LUMO is the innermost (lowest energy) orbital that has enough space to accept electrons and can act as an electron acceptor. The HOMO and LUMO orbitals determine the interaction of the molecule with other sort.<sup>19</sup> The orbital representation of HOMO and LUMO for density PN is shown in Figure 2. Calculated using the TD-DFT method from  $E_{\text{HOMO}} - 5.3480$  eV -  $E_{\text{LUMO}} - 3.3726$  eV for the TD-FC basis set of R3PW91 and  $E_{\text{HOMO}} - 5.3172$  eV -  $E_{\text{LUMO}} - 3.2913$  eV for the 6-311G (d, p) basis set of RB3LYP (Figure 2). The HOMO and LUMO orbitals determine how the molecule interacts with other species. It also helps characterize the

bandgap, chemical reactivity, and kinetic stability. A small border indicates the electronegativity, hardness, polarization, and other reactivity indices of a molecule with an orbital gap. Table 2 shows the chemical reactivity indices.



**Figure 2.** HOMO-LUMO energy maps and bandgap for PN using the TD-DFT method and the R3PW91/TD-FC basis set.

The dipole moment is an important property of the energy associated with the applied electric field of molecule.<sup>20</sup> The dipole moment consists of

intermolecular interactions involving Van der Waals type dipole-dipole forces and generates strong intermolecular attraction. Table 3 shows the calculated parameters, electronic dipole moment, and total dipole moment.

**Table 2.** Comparison of HOMO, LUMO, energy gaps (D), and PN-related (au) molecular properties for PN.

Molecular Energy	R3PW91	RB3LYP
E <sub>LUMO</sub>	-3.3726	-3.2913
E <sub>HOMO</sub>	-5.3480	-5.3172
E <sub>LUMO+1</sub>	-2.0227	-1.9617
E <sub>HOMO-1</sub>	-6.8503	-5.3172
Energy Gap ( $\Delta$ )  E <sub>HOMO</sub> - E <sub>LUMO</sub>	1.9754	2.0259
Ionization Potential (I = -E <sub>HOMO</sub> )	5.3480	5.3172
Electron Affinity (A = -E <sub>LUMO</sub> )	3.3726	3.2913
Chemical Hardness ( $\eta = (I - A)/2$ )	0.9877	1,0129
Global Softness ( $s = 1/2 \eta$ )	0.4938	0,5064
Chemical Potential ( $\mu = -(I + A)/2$ )	-4.3603	-4,3042
Electronegativity ( $\chi = (I + A)/2$ )	4.3603	4,3042
Global Electrophilicity ( $\omega = \mu^2/2 \eta$ )	9,6245	9,1453

**Table 3.** For PN, dipole moments (Debye), (au) polarizability,  $\beta$  components and value of  $\beta$  tot phthalonitrile are calculated by TD-DFT method for R3PW91/TD-FC and RB3LYP /6-311G (d, p) basis set.

Parameter	R3PW91	RB3LYP	Parameter	R3PW91	RB3LYP
$\mu_x$	-0.6581	-0.7534	$\beta_{xxx}$	-249.4849	-250.2618
$\mu_y$	-6.0908	-6.0036	$\beta_{xxy}$	-141.4082	-142.4993
$\mu_z$	0.5071	0.5107	$\beta_{xyy}$	-5.0885	-6.3562
$\mu(D)$	6.1472	6.0722	$\beta_{yyy}$	-61.7956	-59.9208
$\alpha_{xx}$	-192.7117	-195.1953	$\beta_{xxz}$	-32.4278	-29.7575
$\alpha_{yy}$	-195.0605	-196.8636	$\beta_{xyz}$	10.9778	11.3327
$\alpha_{zz}$	-178.1407	-179.7363	$\beta_{yyz}$	-1.9491	-1.5071
$\alpha_{xy}$	-25.0475	-24.9492	$\beta_{xzz}$	-5.1822	-3.1047
$\alpha_{xz}$	3.0576	3.0537	$\beta_{yzz}$	-12.0244	-11.4329
$\alpha_{yz}$	2.7554	2.8848	$\beta_{zzz}$	7.9632	6.9515
$\alpha(\text{au})$	-188.6376	-190,5984	$\beta(\text{esu})$	$3.3 \times 10^{-30}$	$3.0 \times 10^{-34}$

### 3.1.3. Molecular electrostatic potential surface (MEPS) maps of PN

The molecular electrostatic potential surface MEPS shows the size, shape, and electrostatic potential values of the molecule and is plotted for the phthalonitrile molecule. MEPS mapping is very beneficial in

investigating the physicochemical properties of molecular structure.<sup>21</sup> The green color indicates neutral electrostatic potential. Here, MEPS maps were mapped for PN as shown in Figure 3. In the case of phthalonitrile, the MEPS map shows negative potential regions around the nitrogen atoms, characterized by red color. It shows

an almost neutral potential as most of the aromatic ring region is represented by green.

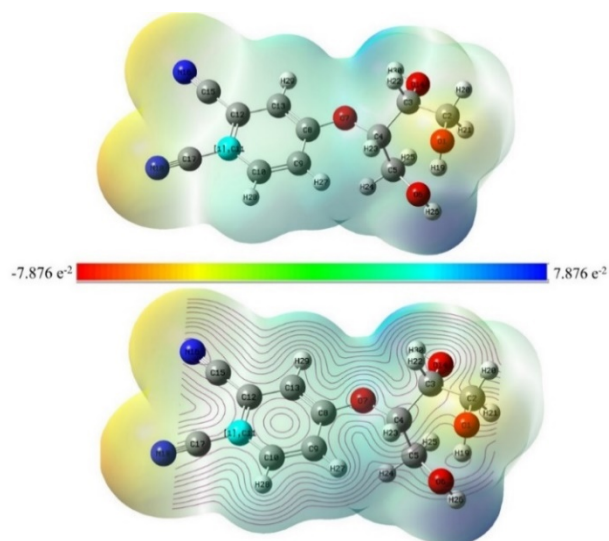


Figure 3. MEPS mappings for PN.

### 3.1.4. Mulliken atomic charges of PN

The calculation of Mulliken atomic charges plays an important role in applying quantum chemical calculations. Mulliken atom was calculated for PN on the basis set of R3PW91/TD-FC and RB3LYP/6-311G (d, p) by the TD-DFT method. The graph comparing the Mulliken atomic charges for PN is presented in Figure 4. The data obtained from the calculations are presented in Figure 5 and Table 4. The distribution of Mulliken charge is that the oxygen atom attached to the aromatic ring is O1 (-0.403) - (-0.500), O6 (-0.435) - (-0.539), O7 (-0.381) - (-0.359). It was observed that some C atoms were positive and some were negative.

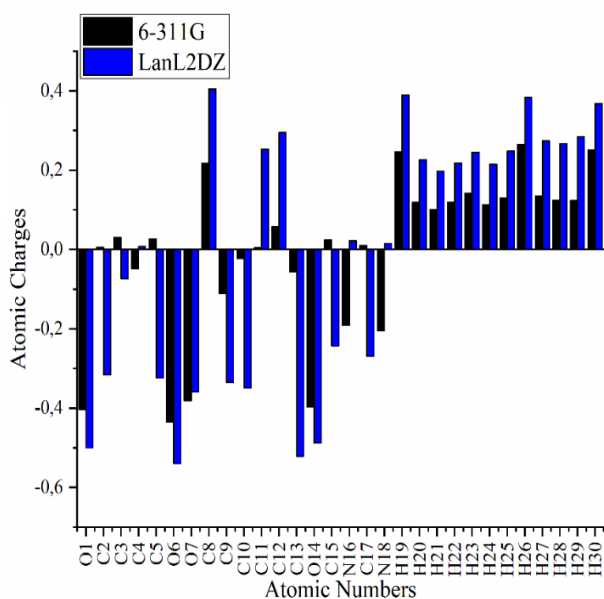


Figure 4. Comparison of Mulliken atomic charges for PN.

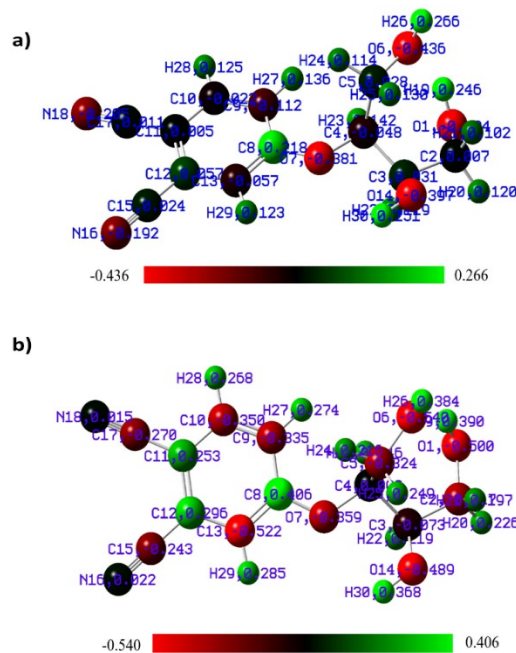


Figure 5. The Mulliken atomic charges of a) R3PW91 / TD-FC and b) RB3LYP/ 6-311G (d, p) basis set by TD-DFT method for PN.

### 3.1.5. NBO analysis of PN

NBO analysis provides research on the most accurate Lewis structure of the molecule, detailed electron density of all orbitals, NBO method is an evaluation of full and empty orbital interactions that provides information about both intermolecular and intermolecular interactions. A quadratic Fock matrix was constructed to evaluate the donor-receiver interactions in the NBO analysis of our compound. The result of the interaction is a loss of occupancy from a localized NBO of the idealized Lewis structure to an empty non-Lewis orbital. For each transmitter (i) and receiver (j), the stabilization energy associated with the displacement of  $i \rightarrow j$  is estimated as  $E(2)$ . NBO analysis was performed to explain charge transfer or charge displacement due to intramolecular interaction between bonds. These results are measurements of delocalization and hyperconjugation, the results analyzed for PN are given in Table 5.

Intramolecular interactions are observed as an increase in electron density (ED) in the antibody orbitals weakening the respective bonds (C - O), The electron density of the conjugated substituted bond (1.9938 au) indicates a strong dislocation, the occupancy rate of  $\Sigma$  bonds is higher than that of  $\sigma^*$  bonds. high, which provides greater localization. The intramolecular hyper conjugative interaction of the distribution to  $\pi$  (C8-C9)  $\pi$  electrons in the ring leads to stabilization of a portion of the ring, as seen in Table 5.  $\pi^*$  (C10-C11) and anti-Ring\* (C12-C13) lead to 25.61-18.56 kcal/mol stabilization. These values increased conjugation leading to strong localization.

### 3.2. ADME analysis of PN

Currently, ADME studies in drug manufacturing are used to select the most promising compounds and to minimize the risk of late-stage drug wear. With these studies, a balance between pharmacodynamic and pharmacokinetic properties can be determined as preliminary information.<sup>22</sup> Here, many parameters such as molecular properties, drug solubility S, cell permeability, HIA, polar surface area PSA, and drug similarity score were investigated by virtual scanning methods on small molecules. An existing oral drug selected according to

Lipinski's rule of 5 should have a molecular weight and LogP of no more than 500 and 5, respectively, less than 10 hydrogen bond acceptors, and less than 5 hydrogen bond donors.

Online servers such as SwissADME (<http://www.swissadme.ch/index.php>) were used. The results in Table 6 show that the compounds are coherent with MA 276.25-416.47 g/mol (<500), LogP values 1.54-4.99 (<5), and acceptor hydrogen bond (AHB) 4-6 (<10) according to Lipinski's rule. Topological PSA values are between 77.04 - 99.89 <140, A2 ABS is between 74.54-82.42% (Figure 6).

**Table 5.** Selected NBO results for PN were calculated for the R3PW91/TD-FC baseset by the TD-DFT method.

NBO(i)	Type	ED/e	NBO(j)	Type	ED//e	E(2) <sup>a</sup> (Kcal/mol)	E (j)-E(i) <sup>b</sup> (a,u)	F (i, j) <sup>c</sup> (a,u)
O1-C2	σ	1.99381	C3-O14	σ*	0.04747	1.31	1.11	0.034
O1-H19	σ	1.98833	C2-H20	σ*	0.02047	1.55	1.12	0.037
			C2-H21	σ*	0.02569	0.96	1.10	0.029
C2-C3	σ	1.97792	C3-C4	σ*	0.04747	0.72	0.96	0.024
			C3-H22	σ*	0.03218	0.55	1.01	0.021
			C4-O7	σ*	0.03349	2.51	0.86	0.042
			O14-H30	σ*	0.00765	1.73	1.03	0.038
C5-H24	σ	1.98516	C3-C4	σ*	0.04747	3.07	0.88	0.047
			C4-O7	σ*	0.03349	1.36	0.78	0.029
			C4-H23	σ*	0.02617	2.56	0.93	0.044
O6-H26	σ	1.98875	C4-C5	σ*	0.03155	2.10	1.08	0.043
O7-C8	σ	1.99010	C12-C13	σ*	0.02208	1.01	1.70	0.037
C8-C9	σ	1.97976	C8-C13	σ*	0.02054	4.03	1.24	0.063
			C9-C10	σ*	0.01337	2.82	1.27	0.054
			C10-H28	σ*	0.01201	2.51	1.15	0.048
			C10-C11	π*	0.38304	25.61	0.28	0.076
			C12-C13	π*	0.37067	18.56	0.27	0.064
C15-N16	σ	1.99344	C12-C15	σ*	0.03019	10.02	1.58	0.113
C17-N18	σ	1.99390	C11-C17	σ*	0.03091	9.28	1.57	0.108
			C10-C11	σ*	0.02334	3.20	0.85	0.047
			C11-C12	σ*	0.04047	3.89	0.79	0.050

**Table 6.** Physicochemical and lipophilicity of the most active compounds.

Code	Lipophilicity consensus log P	Physico-chemical properties								
		MA <sup>a</sup> g/mol	Heavy atoms	Aromatic heavy atoms	Rot. bond	H- bond acc.	H-bond don.	MR <sup>b</sup>	TPYA <sup>c</sup> (Å <sup>2</sup> )	% ABS <sup>d</sup>
PN	4.99	416.47	32	24	5	4	1	123.04	77.04	82.42

<sup>a</sup>MA, molecular weight; <sup>b</sup>MR, molar refractivity; <sup>c</sup>TPYA, topological polar surface area; <sup>d</sup>ABS%: absorption percentage (ABS% = 109 - [0.345 × TPYA]); <sup>e</sup>Quinic acid; <sup>f</sup>Quercitrin; <sup>g</sup>Miquelianin).



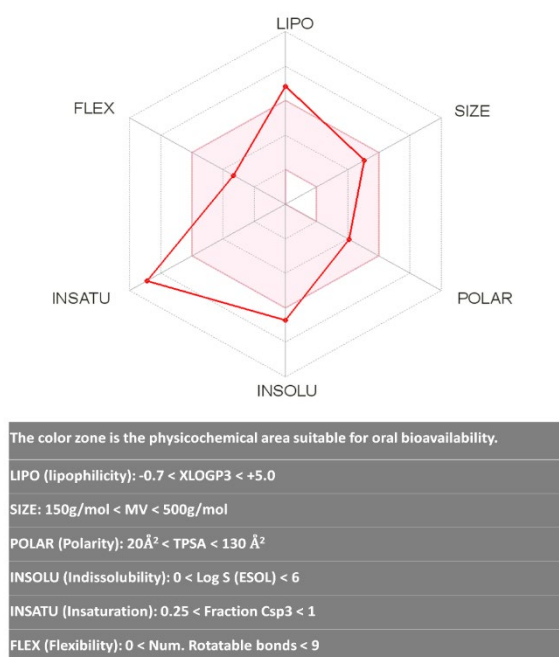


**Figure 6.** Color regions and physicochemical parameters of PN.

### 3.3. Molecular docking studies of PN

Molecular docking is useful for investigating the ligand-receptor binding mechanism and for learning about the interaction of binding modes at the molecular level.<sup>23,24</sup>

Molecular docking was performed to identify the selected binding sites of ligands with the receptor and to largely approve the experimental observations. In this study, which consisted of one compound and three enzyme sets, three good docking scores were found (Table 7). These ligands were docked to the catalytic active site of the enzyme and the docking results were examined on the basis of binding affinity and interaction mode. However, in terms of molecular structure, the best binding affinity score was seen in BchE enzyme.

**Table 7.** The best binding affinity scores (kcal/mol) of compounds in the catalytic sites of enzymes.

Phenolic Compound	Docking Score		
	AChE (PDB: 4M0E)	BChE (PDB:6SAM)	$\alpha$ -GLY (PDB:3A4A)
PN	-8.01	-8.332	-5.209

The similarity of the protein structure to the natural ligand increases this value because it is structural. The dynamics of the protein plays an important role in how proteins must interact with a number of derivatives to form complexes that can enhance or limit their biological functions. After choosing the best pose in the whole ligand-enzyme docking study, the binding modes were analyzed to comprehend the inhibition mechanisms. Figure 7 shows the 3D and 2D interaction as a result of the PN-AChE docking study. The affinity score for

binding affinity with PN-AChE was calculated as  $-8.01$  kcal/mol. Here, HOH-869 ( $1.76\text{\AA}$ ) hydrogen-bonded water hydrogen bond to phenol in the bonding mechanism, VAL-340 ( $3.07\text{\AA}$ ) bonded with hydrogen-bonded to phenol, Conventional Hydrogen Bond with PHE-295 ( $2.01\text{\AA}$ ) bound to the first Nitrogen of phthalonitrile and ( $2.81\text{\AA}$ ) bound to the second Nitrogen of TYR-337 phthalonitrile, VAL-294 ( $3.03\text{\AA}$ ) carbon-hydrogen bond attached to the first Nitrogen of phthalonitrile, TRP-286 ( $4.31\text{\AA}$ ) and TYR-341 ( $4.19\text{\AA}$ ) Pi-Pi stacking attached to the center of the phthalonitrile benzene ring, LEU-76 ( $5.44\text{\AA}$ ) Pi-Alkyl bonded to the center of the benzene ring, TYR-124 ( $5.66\text{\AA}$ ) are examples of Pi-Pi T-shaped bonded to the center of the benzene ring and other interactions are as in Figure 7.

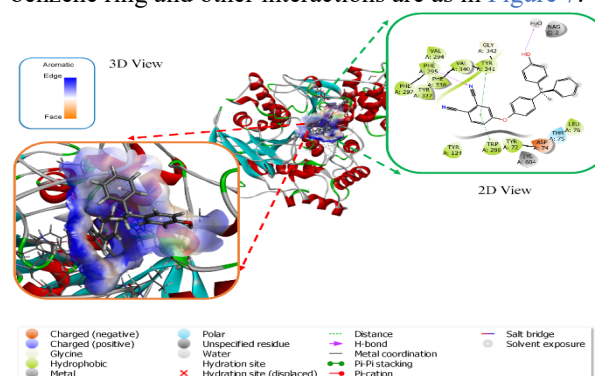


**Figure 7.** 3D view of the aromatic surface on the receptor and 2D view of PN-AChE enzyme interactions.

Figure 8 shows the 3D and 2D interaction as a result of the PN-BChE docking study. In binding affinity with PN-BChE, the highest affinity score was calculated as  $-8.332$  kcal/mol. Here, in the bonding mechanism, ALA-328 ( $2.72\text{\AA}$ ) and ASN-289 ( $2.14\text{\AA}$ ) hydrogen-bonded conventional hydrogen bond to phenol, PHE-329 ( $4.36\text{\AA}$ ) benzene ring bonded to center Pi-Pi stacking, and also ( $4.36\text{\AA}$ ) Pi-Pi T-shaped, TYR-332 ( $2.80\text{\AA}$ ) Pi-donor hydrogen bond to phenol hydrogen-bonded as well as ( $5.14\text{\AA}$ ) Pi-Pi T-shaped bonded to the center of the benzene ring and finally TRP-231 ( $5.90\text{\AA}$ ) are examples of Pi-Pi T-shaped bonds attached to the center of the benzene ring. Other interactions are as in Figure 8.

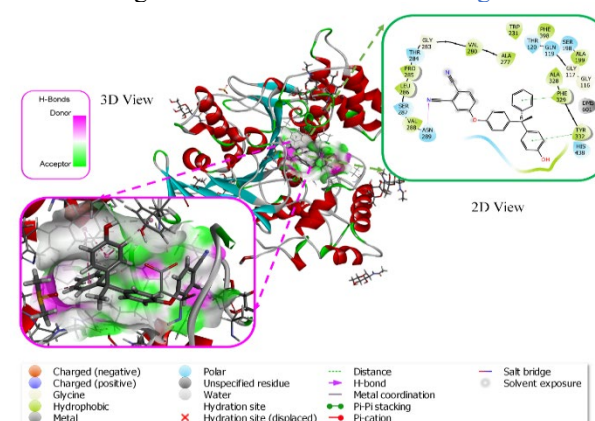


**Figure 8.** 3D view of hydrogen bond donor/acceptor surface on the receptor and 2D view of PN-BChE enzyme interactions.

Figure 9 shows the 3D and 2D interaction as a result of the PN- $\alpha$ -GLY docking study. The affinity score for binding affinity with PN- $\alpha$ -GLY was calculated as -5.209 kcal/mol. Here, the bonding mechanism is conventional Hydrogen Bonding HIS-112 (2.30 Å), GLN-182 (2.34 Å) bonded to nitrogen of phthalonitrile, and hydrogen-bonded to TYR-158 (2.35 Å) phenol. ASN-415 (2.37 Å) hydrogen-bonded incompatible donor-donor bond to phenol, ASP-215 (4.39 Å) and GLU-277 (4.72 Å) Pi-anion bonded to the center of the benzene ring, TYR-158 (4.52 Å) Pi-Pi T-shaped bond attached to the center of the benzene ring, PHE-178 (4.92 Å) Pi-Pi stacking connected to the center of the benzene ring, ARG-315 (4.04 Å) and VAL-216 (5.08 Å) Pi-alkyl bond attached to the center of the benzene ring, PHE-303 (5.28 Å) and HIS-280 (5.35 Å) are examples of Pi-alkyl bond attached to the methyl group and other interactions are as in Figure 9.

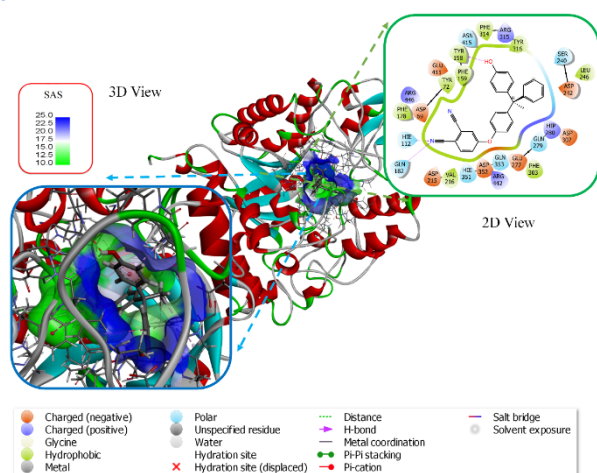


Figure 9. 3D view of the SAS surface on the receptor and 2D view of PN- $\alpha$ -GLY enzyme interactions.

#### 4. CONCLUSIONS

As a result, there was one caveat that users of docking software should constantly remind themselves: their embedded models should be analyzed with a skeptical eye. In the theoretical studies and findings section, the molecule of the phthalonitrile group was first drawn in ChemBioDraw for DFT calculations in the Gaussian 09 program and minimized by the SYBL2 (mol2) method with the Chem3D program. Minimized molecules were given to the Gaussian 09 program and TD-DFT calculations (Geometry optimization, HOMO-LUMO, dipole moment calculations, MEPS maps, Mulliken atomic charges, and NBO analysis) were made for the structure. In addition, in this section, ADME analysis was performed for the compound belonging to the phthalonitrile group, and the color regions were presented separately. Among all values, PN was found to have good permeability. Finally, molecular docking studies were carried out for PN with three different enzymes (AChE, BChE,  $\alpha$ -GLY) and docking scores and receptor models were presented. Although AChE and

BChE docking scores are the highest, they have very close values.

#### Conflict of interests

Authors declare that there is no a conflict of interest with any person, institute, company, etc.

#### REFERENCES

- Derradji, M.; Ramdani, N.; Zhang, T.; Wang, J.; Gong, L.-d.; Xu, X.-d.; Lin, Z.-w.; Henniche, A.; Rahoma, H.K.S.; Liu, W.-b. *Prog. Org. Coat.* **2016**, 90, 34-43.
- Dominguez, D.D.; Keller, T.M. *Polymer.* **2007**, 48, 91-97.
- Keller, T.M. *J Polym. Sci. A Polym. Chem.* **1988**, 26, 3199-3212.
- Tomoda, H.; Saito, S.; Ogawa, S.; Shiraishi, S. *Chem. Lett.* **1980**, 9, 1277-1280.
- Derradji, M.; Wang, J.; Liu, W. *In Phthalonitrile Resins and Composites*, Eds.: William Andrew Publishing, 2018, pp 107-174.
- Derradji, M.; Wang, J.; Liu, W. *In Phthalonitrile Resins and Composites*, Eds.: William Andrew Publishing, 2018, pp 175-239.
- Sastri, S.B.; Keller, T.M. *J Polym. Sci. A Polym. Chem.* **1998**, 36, 1885-1890.
- Keller, T.M.; Dominguez, D.D. *Polymer.* **2005**, 46, 4614-4618.
- Brunovska, Z.; Ishida, H. *J. Appl. Polym. Sci.* **1999**, 73, 2937-2949.
- Hardin, C.; Pogorelov, T.V.; Luthey-Schulten, Z. *Curr. Opin. Struct. Biol.* **2002**, 12, 176-181.
- Warzel, M.L.; Keller, T.M. *Polymer.* **1993**, 34, 663-666.
- Brémond, É.A.G.; Kieffer, J.; Adamo, C. *J. Mol. Struct. THEOCHEM.* **2010**, 954, 52-56.
- Guillaumont, D.; Nakamura, S. *Dyes. Pigm.* **2000**, 46, 85-92.
- Gilad, Y.; Senderowitz, H. *J. Chem. Inf. Model.* **2014**, 54, 96-107.
- Ekins, S.; Waller, C.L.; Swaan, P.W.; Cruciani, G.; Wrighton, S.A.; Wikel, J.H. *J. Pharmacol. Tox. Met.* **2000**, 44, 251-272.

16. Kaya, E.D.; Türkhan, A.; Gür, F.; Gür, B. *J. Biomol. Struct. Dyn.* **2021**, 1-14.

17. Yıldiko, Ü.; Ata, A. Ç.; Tanriverdi, A. A.; Çakmak, İ. *Bull. Mater. Sci.* **2021**, 44, 186.

18. Ağırtaş, M.S.; Cabir, B.; Yıldiko, Ü.; Özdemir, S.; Gonca, S. *Chem. Pap.* **2021**, 75, 1749-1760.

19. Güngördü, Solğun, D.; Yıldiko, Ü.; Özkartal, A.; Ağırtaş, M.S. *Chem. Pap.* **2021**,

20. Bhuvaneswari, R.; Bharathi, MD.; Anbalagan, G.; Chakkaravarthi, G.; Murugesan, K.S. *J. Mol. Struct.* **2018**, 1173, 188-195.

21. Vanasundari, K.; Balachandran, V.; Kavimani, M.; Narayana, B. *J. Mol. Struct.* **2017**, 1147, 136-147.

22. Tuntland, T.; Ethell, B.; Kosaka, T.; Blasco, F.; Zang, RX.; Jain, M.; Gould, T.; Hoffmaster, K. *Front. Pharmacol.* **2014**, 5, 174.

23. Adiguzel, R.; Türkan, F.; Yildiko, Ü.; Aras, A.; Evren, E.; Onkol, T. *J. Mol. Struct.* **2021**, 1231, 129943.

24. Aras, A.; Türkan, F.; Yildiko, U.; Atalar, M.N.; Kılıç, Ö.; Alma, M.H.; Bursal, E. *Chem. Pap.* **2021**, 75, 1133-1146.



## Resorcinol derivatives as human acetylcholinesterase inhibitor: An *In Vitro* and *In Silico* study

Uğur GÜLLER<sup>1,\*</sup>

<sup>1</sup>*Iğdır University, Faculty of Engineering, Department of Food Engineering, Iğdır 76000, Turkey*

Received: 29 May 2021; Revised: 4 August 2021; Accepted: 5 August 2021

\*Corresponding author e-mail: [ugur.guller@igdir.edu.tr](mailto:ugur.guller@igdir.edu.tr)

**Citation:** Güller, U. *Int. J. Chem. Technol.* 2021, 5 (2), 156-161.

### ABSTRACT

Inhibitors of Acetylcholinesterase (Acetylcholine acetylhydrolase, AChE, E.C.3.1.1.7) are highly significant in the therapy of a chronic illness such as Alzheimer's disease (AD) due to the deep relationship with memory and acetylcholine. So investigation of natural AChE inhibitors having minimal side effects has become important. In this paper human erythrocytes AChE enzyme (0.032 EU mg<sup>-1</sup> protein) was partially isolated by using DE-52 anion exchange chromatography. Then, primer effects of resorcinol derivatives on the enzyme activity were studied and IC<sub>50</sub> values were found in the range of 2.74-363.61 μM. Besides, inhibition profiles were elucidated by molecular docking and the highest inhibition potency was observed in 4-hexylresorcinol with the free binding energy of -6.16 kcal mol<sup>-1</sup>. In conclusion, it was found that 4-hexylresorcinol had the highest inhibitory potential on human AChE. So, this compound may be used in drug design in memory-lost diseases.

**Keywords:** Acetylcholinesterase, resorcinol, inhibition, molecular docking.

### İnsan asetilkolinesteraz inhibitörü olarak resorsinol türevleri: Bir *In Vitro* ve *In Silico* çalışma

#### ÖZ

Asetilkolinesteraz inhibitörleri (Asetilkolin asetilhidrolaz, AChE, E.C.3.1.1.7), hafıza ve asetilkolin ile derin ilişkisi nedeniyle Alzheimer hastalığı (AD) gibi kronik bir hastalığın tedavisinde oldukça önemlidir. Bu nedenle minimal yan etkiye sahip doğal AChE inhibitörlerinin araştırılması önem kazanmıştır. Bu çalışmada insan eritrosit AChE enzimi (0.032 EU mg<sup>-1</sup> protein) DE-52 anyon değiştirme kromatografisi kullanılarak kısmen izole edilmiştir. Daha sonra resorsinol türevlerinin enzim aktivitesi üzerindeki primer etkileri incelenmiş ve IC<sub>50</sub> değerleri 2.74-363.61 μM aralığında bulunmuştur. Ayrıca inhibisyon profilleri moleküler docking ile aydınlatılmış ve en yüksek inhibisyon gücü -6.16 kcal mol<sup>-1</sup> serbest bağlanma enerjisi ile 4-heksilresorsinolde gözlenmiştir. Sonuç olarak, 4-heksilresorsinolün insan AChE üzerinde en yüksek inhibitör potansiyele sahip olduğu bulunmuştur. Bu nedenle, bu bileşiğin hafıza kaybı olan hastalıklarda ilaç tasarımında rehberlik edebileceği düşünülmektedir.

**Anahtar Kelimeler:** Asetilkolinesteraz, resorsinol, inhibisyon, moleküler docking.

### 1. INTRODUCTION

Alzheimer's disease (AD), the cause of about 60-70% of dementia cases, is a chronic neurodegenerative disease, and its incidence accelerates exponentially with age. AD, which initially shows symptoms of short-term memory loss and mental dysfunction, as it progresses it leads to mood swings, loss of motivation, inability to manage personal care and behaviour, physical dysfunction and eventually death. Approximately 24 million people

suffered from AD in 2018, and it is estimated that this number will quadruple in 2050.<sup>1-3</sup> Although the pathogenesis of AD has not been fully clarified, there are some hypothesis on pathophysiology of AD such as cholinergic hypothesis, β-amyloid (AP) peptide theory, irregularity on energy metabolism, and oxidative stress.<sup>4-7</sup> One of the most common studied of these is cholinergic hypothesis and this hypothesis is generally based on the treatment of AD. The cholinergic system plays a role in the transport of impulses between central



and peripheral nervous system cells, and the decline of cholinergic neurons and loss of neurotransmission have been reported to be the main causes of decreased cognitive function in patients with AD. The cholinergic hypothesis explains the main cause of AD with a decrease in the synthesis of acetyl choline (ACh).<sup>8</sup> ACh, an important neurotransmitter involved in signal transduction, is synthesized in the cholinergic neurons of the brain. It has been reported that ACh decreases in some neurodegenerative diseases.<sup>9-12</sup>

In a healthy brain, in the reaction catalysed by Acetylcholinesterase (AChE, E.C. 3.1.17) approximately 80% of ACh hydrolyses to acetate ions and choline.<sup>11, 13</sup> This enzyme is mainly localized in the synaptic cavities of the central and peripheral nervous system and red cell membranes. It plays a key role in nerve conduction as it terminates the stimuli in cholinergic pathway with ACh hydrolysis.<sup>11, 14-15</sup> It has been declared that inhibition of AChE can significantly reduce behavioural disorders of patients with AD. Therefore, the cholinergic hypothesis based on inhibiting the activity of acetylcholinesterase (AChE) is used in development of therapeutic strategies<sup>16</sup> and this led to the discovery of the first 4 drugs (tacrine, donepezil, rivastigmine, and galantamine) certified by FDA.

Moving on the advantages of AChEIs in the treatment of AD, in the current study, it was aimed to investigate the effects of resorcinol derivatives (Figure 1) on the activity of AChE. Besides, the interactions between compounds and the enzyme were clarified by the molecular docking method in order to understand the inhibition mechanism more clearly. In some research, alkylresorcinols have been reported to have some biological activities, such as antioxidant, anticancer, antimicrobial, antiparasitic, antifungal activities, and enzyme inhibition potency.<sup>17-18</sup>

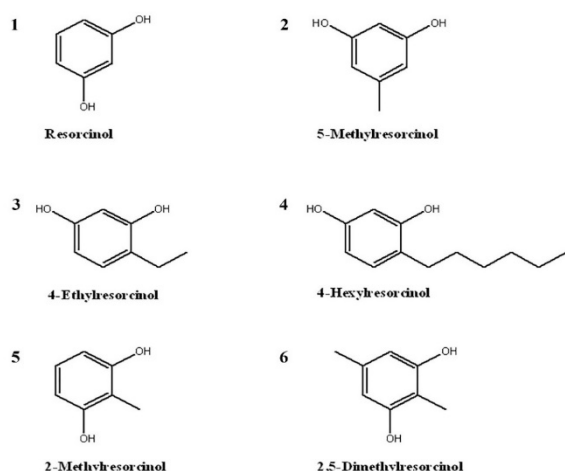


**Figure 1.** The chemical structures of resorcinol derivatives used in this study.

## 2. MATERIALS AND METHODS

### 2.1. Chemicals

All chemicals used in the isolation and activity determination of enzyme were procured from E. Merk AG. The erythrocyte of waste human blood was taken from the Turkish Red Crescent, Erzurum, Turkey.

### 2.2. Enzyme assay and Quantitative Protein Determination

AChE activity was measured spectrophotometrically at 436 nm according to Worek et al.'s method, modified from Ellman procedure which is more sensitive than Ellman's method.<sup>19</sup> In this method, during the reaction, the yellow-colored anion 2-nitro-5 thiobenzoate (TNB) formed from the 5,5'-dithiobis-(2-nitrobenzoic acid) (DTNB) in the presence of the acetylthiocholine iodide. At 436 nm increased absorbance is recorded and used in activity calculations. The protein amount of enzyme samples was analysed according to the Bradford method at 595 nm by using bovine serum albumin (BSA, 1 mg ml<sup>-1</sup>) as standard protein.<sup>20</sup>

### 2.3. Partial purification of acetylcholinesterase from human erythrocytes by DE-52 anion exchange chromatography

Erythrocytes were haemolysis by stirring with ice water in a ratio of 1:5. Then the haemolysed erythrocyte sample was centrifuged at 5 000 g for 15 minutes and pH of it was increased to 7.8 with 0.05 M K<sub>2</sub>HPO<sub>4</sub> solution and AChE was isolated by DE-52 anion exchange chromatography, equilibrated with phosphate buffer at pH 7.5, as reported in Guller and co-workerset.<sup>21</sup> The AChE was eluted with the increasing salt gradient in the equilibration buffer. All these operations were carried out at about +4°C.

### 2.4. Inhibition studies

For examining the effects of resorcinols, activity determinations were performed at the different amount of compounds and at least five various inhibitor concentrations were chosen. Enzyme activity measured without resorcinols was taken as 100%. Activities determined in the presence of each compound calculated as activity%. Then activity% - [resorcinol derivatives] graphs were drawn using Microsoft Office 2016 Excel, and concentrations of compound that inhibited 50% of the activity (IC<sub>50</sub>) were calculated from these graphs.<sup>21-22</sup>

### 2.5. Analysis of bindings models

The crystal structure of the acetylcholinesterase enzyme (PDB code: 4EY7)<sup>23</sup> was downloaded from the RSCB Protein Data Bank (PDB) with 2.0 Å resolution. Molecular structures of the derivatives were gotten by



ChemDraw Professional 15.0 and Avogadro software \*.pdb file. Receptor protein and ligands were prepared by using Autodock4.2 tool.<sup>24</sup> Finally, the grid box dimension (80 × 80 × 80 Å), grid spacing (0.375 Å), and grid boxes centres (x= -2.980, y= -40.109, z= 30.750) were adjusted to provide optimum binding poses. The Lamarckian genetic algorithm was used to determine the appropriate binding positions of ligands. The binding positions and interactions of ligand-receptor complexes were viewed using Discovery Studio Visualizer.

### 3. RESULT AND DISCUSSION

The role of acetylcholine (ACh), a neurotransmitter, is to ensure the neural impulses reach the muscles or related tissues after being released into the synaptic space by the nerve cells. In diseases related to memory loss, ACh reported to break down in a very short time. Therefore, it is used in the diagnosis and treatment of Alzheimer's disease (AD) today.<sup>25</sup> It was determined that ACh levels in normal-aged control groups' brain are different from normal-aged AD patients' brain around 50%.<sup>25-27</sup> When ACh is hydrolysed by Acetylcholinesterase (AChE), its role in neurotransmission ends. It has been determined that the transmission among nerves is strengthened by inhibition of AChE.<sup>28</sup> Besides, it has been seen that anticholinesterase drugs provide a significant regression in behavioural disorders in patients with memory-related diseases.<sup>29</sup> Considering the above-mentioned importance of AChE inhibition in treatment of memory lost diseases, in this study primer effects of resorcinols on enzyme activity were investigated. Also, inhibition mechanisms were clarified by molecular docking. Firstly, 0.032 EU mg<sup>-1</sup> AChE was isolated from human erythrocytes by DE-52 anion exchange chromatography as described in method section. Then, *in vitro* inhibition studies of compounds on enzyme activity were performed spectrophotometrically. Activity%-[inhibitor] graphs were plotted (Figure 2). From the equations of these exponential graphs, the concentrations of compounds that inhibits the activity by half was calculated.

As seen from the Table 1, IC<sub>50</sub> values of compounds found in range between 2.74-363.61 μM. Most effective inhibitor was determined as 4-hexylresorcinol (4) with the IC<sub>50</sub> value of 2.74 μM. The IC<sub>50</sub> value of tacrine, used as a standard inhibitor, was found to be 0.013 μM. The inhibition potency of the studied compounds was found to be lower than the standard inhibitor (IC<sub>50</sub> values were higher). The previous researcher described that so many compounds such as N-(4-methoxyphenethyl)-N-(substituted)-4-methylbenzenesulfonamides, carbamate substituted coumarin derivatives, salicylanilide and 4-chlorophenol-based N-monosubstituted carbamates, tacrine hybrids with carbohydrate derivatives, bivalent β-carboline derivatives, N-arylisomaleimides, and benzylidenemalononitrile derivatives, carbazole-coumarin hybrids, azoderivatives.<sup>30-38</sup>

**Table 1.** Results of *in vitro* and molecular docking studies of resorcinol derivatives on hAChE.

Compounds	IC <sub>50</sub> (μM)	R <sup>2</sup>	Estimated Free Energy of Binding (kcal/mol)	Estimated K <sub>i</sub> constant (μM)
1	363.16	0.93	-4.96	231.63
2	345	0.98	-5.09	187.20
3	36.31	0.95	-5.52	89.32
4	2.74	0.98	-6.16	30.33
5	3.2	0.94	-4.93	243.77
6	57.5	0.92	-5.26	139.53
Tacrin	0.013	0.96	-7.49	3.26

IC<sub>50</sub> values of N-(4-methoxyphenethyl)-N-(substituted)-4-methylbenzene sulfonamides on human erythrocytes AChE were found in range of 0.0751- 22.549 μM.<sup>30,39</sup> determined that donepezil-flavonoid hybrids inhibited human erythrocytes AChE with IC<sub>50</sub> values of 0.021-7.49 μM. It was seen that inhibition potencies of compounds 4 and 5 in the current study were almost similar those of the studies conducted by Abbasi and co workers<sup>30</sup> and Valencia and co workers.<sup>39</sup> When compared with resorcinol, that the inhibitory effect of 4-hexylresorcinol (4), derived from C 4, was found 132.5 times higher. Güller and co workers<sup>38</sup> reported that 4-hexylresorcinol inhibited the human glutathione reductase (GR) higher than other derivatives. Studies examining the enzyme inhibition effect of resorcinols showed that; resorcinols derived from the 4<sup>th</sup> and 5<sup>th</sup> positions exhibited significant inhibition effect on cytochrome P450 and GR.<sup>18,40</sup>

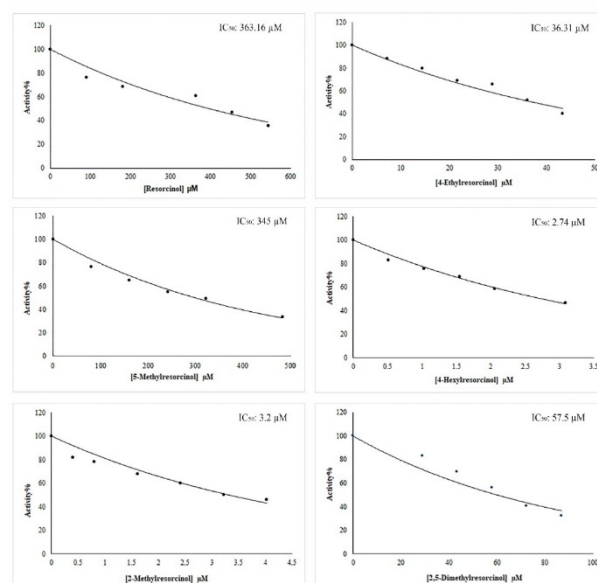


**Figure 2.** Activity%-[inhibitor] graphs of resorcinol derivatives.

After *in vitro* inhibition, molecular docking studies were performed by AutoDock 4.2 to clarify the inhibition mechanism. Estimated Binding Energies were predicted in a computer-aided manner and summarized in Table. Results of molecular docking studies were found to be consistent with *in vitro* inhibition results. The lowest binding energy was estimated for Compound 4 with  $-6.16$  kcal mol<sup>-1</sup>. However, all of the compounds had lower inhibition effects than the standard inhibitor. Free energy of binding was predicted for tacrine as  $-7.49$  kcal mol<sup>-1</sup>. When the inhibition mechanism inspected closer, it was seen that Try337 residue of hAChE receptor showed pi-sigma interaction with tacrine (Figure 3). Benzene moieties of compound had pi-alkyl interactions with Val294, Phe338, and Tyr341 residues. Compound formed pi-pi stacked interaction with phenyl group of Phe338 and pi-donor hydrogen bond with Phe295. Besides, tacrine had several van der Waals interactions with Gly122, Tyr124, Trp286, Ser293, Arg296, and Phe297 amino acids.

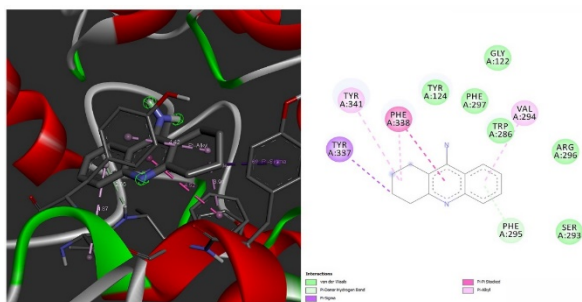


**Figure 3.** Potential binding modes and 2D ligand-receptor interaction diagrams of tacrine with hAChE receptor.

Compound 4 showed pi-sigma interaction with AChE in the same manner with tacrine (Figure 4). Tyr72, Asp74, and Tyr124 residues showed hydrogen bonds with -OH group of compound. It was observed that there was a pi-pi stacked interaction between the benzene ring of the molecule and the phenyl ring of Tyr124. Compound 4 had several van der Waals interaction with active site residues.

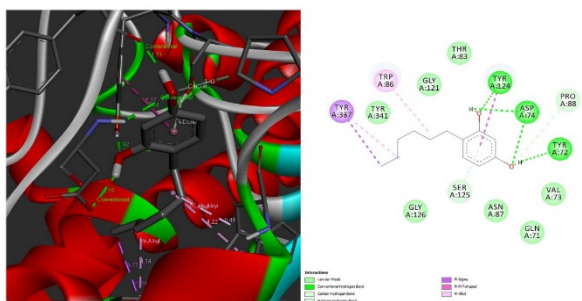


**Figure 4.** Potential binding modes and 2D ligand-receptor interaction diagrams of the most effective compound, 4-hexylresorcinol with hAChE receptor.

The interactions of compound 4 with hAChE receptor were found to be similar to those for the best inhibitors in the studies of Zhang and co workers<sup>41</sup> and Fernandes and co workers.<sup>42</sup>

#### 4. CONCLUSIONS

Consequently, in this study, inhibition potential of resorcinol derivatives on human erythrocyte AChE were investigated and mechanism were clarified. The inhibition of AChE is widely used in the treatment of illnesses of which symptoms are memory loss. As a result of *in vitro* inhibition studies, it was seen that most effective inhibitor of hAChE is compound 4 (4-hexylresorcinol) with the IC<sub>50</sub> of 2.74 μM. Also, molecular docking studies predict docking score as  $-6.16$  kcal mol<sup>-1</sup>. The results of both the *in vitro* and *in silico* approaches were seen to support each other. The results of the current paper may contribute to the studies regarding the design of new therapeutics targeting the activity of hAChE.

#### ACKNOWLEDGMENTS

There is no clinical application so, no animals or humans were used in this study. Human blood used for enzyme isolation was the waste blood that brought from the Turkish Red Crescent (Erzurum branch).

#### Conflict of interest

I declares that there is no a conflict of interest with any person, institute, company, etc.

#### REFERENCES

1. Blennow, K.; de Leon, M. J.; Zetterberg, H. *Lancet (London, England)* **2006**, 368 (9533), 387-403.
2. Burns, A.; Iliffe, S. *BMJ (Clinical researched)* **2009**, 338:b158.
3. Reitz, C.; Mayeux, R. *Biochemical pharmacology* **2014**, 88 (4), 640-651.
4. Baptista, F. I.; Henriques, A. G.; Silva, A. M.; Wiltfang, J.; da Cruz e Silva, O. A. *ACS chemical neuroscience* **2014**, 5 (2), 83-92.
5. Du, X.; Wang, X.; Geng, M. *Translational neurodegeneration* **2018**, 7 (1), 1-7.
6. Hardy, J.; Selkoe, D. J. *science* **2002**, 297 (5580), 353-356.
7. Tang, B. L.; Kumar, R. *Ann Acad Med Singapore* **2008**, 37 (5), 406-5.

8. Coyle, J. T.; Price, D. L.; DeLong, M. R. *Science* **1983**, *219* (4589), 1184-1190.
9. Blokland, A., *Brain Research Reviews* **1995**, *21* (3), 285-300.
10. Francis, P. T.; Palmer, A. M.; Snape, M.; Wilcock, G. K. *Journal of Neurology, Neurosurgery & Psychiatry* **1999**, *66* (2), 137-147.
11. H Ferreira-Vieira, T.; M Guimaraes, I.; R Silva, F.; M Ribeiro, F. *Current neuropharmacology* **2016**, *14* (1), 101-115.
12. Pope, C. N.; Brimijoin, S. *Biochemical pharmacology* **2018**, *153*, 205-216.
13. Greig, N. H.; Utsuki, T.; Yu, Q.-s.; Zhu, X.; Holloway, H. W.; Perry, T.; Lee, B.; Ingram, D. K.; Lahiri, D. K. *Current medical research and opinion* **2001**, *17* (3), 159-165.
14. Ahmad, B.; Mukarram Shah, S.; Khan, H.; Hassan Shah, S. *Journal of enzyme inhibition and medicinal chemistry* **2007**, *22* (6), 730-732.
15. Colovic, M. B.; Krstic, D. Z.; Lazarevic-Pasti, T. D.; Bondzic, A. M.; Vasic, V. M. *Current neuropharmacology* **2013**, *11* (3), 315-335.
16. Sun, Y.; Lai, M. S.; Lu, C. J.; Chen, R. C. *European journal of neurology* **2008**, *15* (3), 278-283.
17. Kozubek, A.; Tyman, J. H. P. *Chem Rev* **1999**, *99* (1), 1-25.
18. Srimai, V.; Ramesh, M.; Parameshwar, K. S.; Parthasarathy, T. *Medicinal Chemistry Research* **2013**, *22* (11), 5314-5323.
19. Worek, F.; Mast, U.; Kiderlen, D.; Diepold, C.; Eyer, P. *Clinica Chimica Acta* **1999**, *288* (1-2), 73-90.
20. Bradford, M. M. *Anal Biochem* **1976**, *72* (1-2), 248-254.
21. Guller, U.; Guller, P.; Ciftci, M. *Altern Ther Health Med* **2020**.
22. Adem, S.; Akkemik, E.; Aksit, H.; Guller, P.; Tufekci, A. R.; Demirtas, I.; Ciftci, M. *Medicinal Chemistry Research* **2019**, *28* (5), 711-722.
23. Cheung, J.; Rudolph, M. J.; Burshteyn, F.; Cassidy, M. S.; Gary, E. N.; Love, J.; Franklin, M. C.; Height, J. J. *Journal of medicinal chemistry* **2012**, *55* (22), 10282-10286.
24. Morris, G. M.; Huey, R.; Lindstrom, W.; Sanner, M. F.; Belew, R. K.; Goodsell, D. S.; Olson, A. J. *J Comput Chem* **2009**, *30* (16), 2785-2791.
25. Geula, C.; Mesulam, M. M. *Cholinergic Systems in Alzheimer's Disease, Alzheimer Disease*. 2 ed.; Lippincott, Williams and Wilkins: Philadelphia, PA, 1999.
26. Dhanasekaran, S.; Perumal, P.; Palayan, M. *Journal of Applied Pharmaceutical Science* **2015**, *5* (02), 012-016.
27. Forette, F. B. Alzheimer Hastalığında İlaç Geliştirilmesi: Tarihçesine Bakış ve Geleceğine İlişkin Öngörüler. In *Alzheimer Hastalığının Farmakoterapisi*, Gauthier, S., Ed. Yelkovan Yayıncılık: İstanbul, 2000; pp 1-5.
28. Bores, G. M.; Huger, F. P.; Petko, W.; Mutlib, A. E.; Camacho, F.; Rush, D. K.; Selk, D. E.; Wolf, V.; Kosley, R.; Davis, L. *Journal of Pharmacology and Experimental Therapeutics* **1996**, *277* (2), 728-738.
29. Giacobini, E. Cholinesterase Inhibitors. In *Enzymes of the cholinesterase family*, Springer: 1995; pp 463-469.
30. Abbasi, M. A.; Hassan, M.; Siddiqui, S. Z.; Shah, S. A. A.; Raza, H.; Seo, S. Y. *PeerJ* **2018**, *6*, e4962.
31. Biscussi, B.; Sequeira, M. A.; Richmond, V.; Mañez, P. A.; Murray, A. P. *Journal of Photochemistry and Photobiology A: Chemistry* **2021**, 113375.
32. Song, M.-q.; Min, W.; Wang, J.; Si, X.-X.; Wang, X.-J.; Liu, Y.-W.; Shi, D.-H. *Journal of Molecular Structure* **2021**, *1229*, 129784.
33. Zhao, Y.; Ye, F.; Xu, J.; Liao, Q.; Chen, L.; Zhang, W.; Sun, H.; Liu, W.; Feng, F.; Qu, W. *Bioorganic & medicinal chemistry* **2018**, *26* (13), 3812-3824.
34. Lopes, J. P. B.; Silva, L.; da Costa Franarin, G.; Ceschi, M. A.; Lüdtke, D. S.; Dantas, R. F.; de Salles, C. M. C.; Silva-Jr, F. P.; Senger, M. R.; Guedes, I. A. *Bioorganic & medicinal chemistry* **2018**, *26* (20), 5566-5577.
35. Krátký, M.; Štěpánková, Š.; Vorčáková, K.; Vinšová, J. *Bioorganic chemistry* **2018**, *80*, 668-673.
36. Guevara, J. A.; Trujillo, J. G.; Quintana, D.; Jiménez, H. A.; Arellano, M. G.; Bahena, J. R.; Tamay, F.; Ciprés, F. J. *Medicinal Chemistry Research* **2018**, *27* (3), 989-1003.
37. Kurt, B. Z.; Gazioglu, I.; Kandas, N. O.; Sonmez, F. *ChemistrySelect* **2018**, *3* (14), 3978-3983.

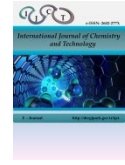
38. Güller, P.; Dağalan, Z.; Güller, U.; Çalışır, U.; Nişancı, B. *Journal of Molecular Structure* **2021**, *1239*, 130498.

39. Valencia, M. E.; Herrera-Arozamena, C.; de Andrés, L.; Pérez, C.; Morales-García, J. A.; Pérez-Castillo, A.; Ramos, E.; Romero, A.; Viña, D.; Yáñez, M. *European journal of medicinal chemistry* **2018**, *156*, 534-553.

40. Güller, P. *Journal of Molecular Structure* **2021**, *1228*, 129790.

41. Zhang, X.-Z.; Xu, Y.; Jian, M.-M.; Yang, K.; Ma, Z.-Y. *Medicinal Chemistry Research* **2019**, *28* (10), 1683-1693.

42. Fernandes, T. B.; Cunha, M. R.; Sakata, R. P.; Candido, T. M.; Baby, A. R.; Tavares, M. T.; Barbosa, E. G.; Almeida, W. P.; Parise-Filho, R. *Archiv der Pharmazie* **2017**, *350* (11), 1700163.



## Comparison of chemical composition and nutritive values of some clover species

İbrahim ERTEKİN<sup>1,\*</sup><sup>1</sup>Hatay Mustafa Kemal University, Agricultural Faculty, Field Crops Department, Hatay 31060, Turkey

Received: 3 October 2021; Revised: 26 October 2021; Accepted: 27 October 2021

\*Corresponding author e-mail: [ibrahim.ertkn@hotmail.com](mailto:ibrahim.ertkn@hotmail.com)Citation: Ertekin, İ. *Int. J. Chem. Technol.* 2021, 5 (2), 162-166.

## ABSTRACT

This study was carried out to compare the chemical composition and nutritive value of some clover species, especially common in the rangelands of the Mediterranean region. For this purpose, clover species (*Trifolium angustifolium*, *Trifolium cherleri*, *Trifolium hybridum*, *Trifolium lappaceum*, *Trifolium nigrescens*, *Trifolium pilulare*, *Trifolium resupinatum*, *Trifolium scabrum*, *Trifolium spumosum* and *Trifolium tomentosum*) were collected from ten different points in Hatay Mustafa Kemal University campus pasture. To determine the chemical composition of collected clover species, crude ash (CA), crude protein (CP), neutral detergent fiber (NDF), acid detergent fiber (ADF), acid detergent lignin (ADL), hemicellulose (Hcel) and cellulose (Cel) contents were investigated. In addition, dry matter digestibility (DMD), dry matter intake (DMI), relative feed value (RFV) and net energy lactation (NEL) characteristics were calculated in order to determine the nutritional value of clovers. Differences among species in terms of all features examined were found to be statistically significant. CA, CP, NDF, ADF, ADL, Hcel and Cel contents of species varied between 5.36% and 9.85%, 18.47% and 22.05%, 30.31% and 49.80%, 21.32% and 34.28, 3.25% and 5.04, 8.99% and 15.97% and 18.07% and 30.38, respectively. It was determined that the values of DMD, DMI, RFV and NEL properties calculated for the nutritive values of these plants varied between 62.20-72.29%, 2.41-3.97%, 116.20-222.18 and 1.40-1.74%, respectively. When the results obtained from the study were evaluated collectively, it was determined that *T. resupinatum* and *T. hybridum* offered a superior nutrient content and nutritional value compared to other species.

**Keywords:** Chemical Composition, Nutritional Value, Clover Species, Rangeland, Forage.

## Bazı üçgül türlerinin kimyasal kompozisyonu ve besin değerlerinin karşılaştırılması

## ÖZ

Bu çalışma özellikle Akdeniz iklim bölgesi meralarında yaygın bir şekilde bulunan bazı üçgül türlerinin kimyasal kompozisyonunu ve besin değerini karşılaştırmak için yürütülmüştür. Bu amaçla Hatay Mustafa Kemal Üniversitesi kampüs merasında on farklı noktadan üçgül (*Trifolium angustifolium*, *Trifolium cherleri*, *Trifolium hybridum*, *Trifolium lappaceum*, *Trifolium nigrescens*, *Trifolium pilulare*, *Trifolium resupinatum*, *Trifolium scabrum*, *Trifolium spumosum* ve *Trifolium tomentosum*) türleri toplanmıştır. Toplanan bu üçgül türlerinde kimyasal kompozisyonu belirlemek için ham kül (HK), ham protein (HP), nötr ortamda çözünmeyen lif (NDF), asitli ortamda çözünmeyen lif (ADF), asitli ortamda çözünmeyen lignin (ADL), hemiselüloz (Hsel) ve selüloz (Sel) içerikleri incelenmiştir. Ayrıca besin değerini belirlemek için kuru madde sindirimi (KMS), kuru madde tüketimi (KMT), nispi yem değeri (NYD) ve net enerji laktasyon (NEL) özellikleri hesaplanmıştır. Tek yıllık üçgül türlerinde incelenen tüm bu özellikler istatistiki açıdan önemli bulunmuştur. Türlerin HK, HP, NDF, ADF, ADL, Hsel ve Sel içerikleri sırasıyla %5.36-9.85, %18.47-22.05, %30.31-49.80, %21.32-34.28, %3.25-5.04, %8.99-15.97 ve %18.07-30.38 arasında değişiklik göstermiştir. Bu bitkilerin besin değerleri için hesaplanan KMS, KMT, NYD ve NEL özelliklerine ait değerlerin sırasıyla %62.20-72.29, %2.41-3.97, 116.20-222.18 ve %1.40-1.74 arasında değiştiği belirlenmiştir. Çalışmadan elde edilen bulgular topluca değerlendirildiğinde *T. resupinatum* ile *T. hybridum* türlerinin diğer türlere kıyasla üstün bir besin madde içeriği ve besin değerlerine sahip olduğu belirlenmiştir.

**Anahtar Kelimeler:** Kimyasal Kompozisyon, Besin Değeri, Tek Yıllık Üçgül Türleri, Mera, Yem.

## 1. INTRODUCTION

In general, legumes are widely used as green fodder, silage, ornamental plant, soil improvement, pollen and

nectar source and grazing plant in pasture vegetation.<sup>1</sup> Legume forage crops offer significant advantages in replanting winter pastures in arid regions.<sup>2</sup> In addition, nitrogen fixation to the soil where legumes grown can



provide nitrogen to many grasses.<sup>3</sup> Among the perennial forage crops, perennial legumes are considered the main roughage source for livestock and are cultivated worldwide.<sup>1</sup> Clover species are accepted as very valuable plants especially in many countries where Mediterranean climate prevails.<sup>2</sup> These plants are especially common in the pastures of our Mediterranean climate regions in which the pastures stated that the plant material collected from.

One of the most important criteria affecting forage quality in legume forage crops is species diversity. Species-dependent variation is primarily due to the morphology of shoot growth.<sup>4</sup> The difference in forage quality between species may also be caused by the difference in leaf and stem ratios of plant species.<sup>5</sup> Knowing the feed quality and acting with this awareness can increase the final animal productivity.<sup>6</sup>

The most commonly used analysis methods for the determination of feed quality can be listed as raw ash, which gives an idea about the mineral content of the feed, nitrogen determination that shows the protein content, insoluble fiber in neutral medium, insoluble fiber in acidic medium, and insoluble lignin in acidic medium.<sup>6-8</sup> Based on these analyzes, the nutritional value of the feeds is calculated and presented as various characteristics theoretically.<sup>9</sup> Thus, it is possible to have an idea about the nutrient content and feed quality of the roughage obtained from forage plants.

In this study, the chemical composition and nutritive value of some clover species, which are especially common in the rangelands of the Mediterranean climate regions, were investigated and the plant species were compared in terms of these characteristics.

## 1. MATERIALS AND METHODS

In this study, some clover species (*Trifolium angustifolium*, *Trifolium cherleri*, *Trifolium hybridum*, *Trifolium lappaceum*, *Trifolium nigrescens*, *Trifolium pilulare*, *Trifolium resupinatum*, *Trifolium scabrum*, *Trifolium spumosum* and *Trifolium tomentosum*) were used as plant material. These plant species were collected from Hatay Mustafa Kemal University campus pasture from 30 March to 15 April from 10 different points during the flowering period by cutting from a height of 5 cm from the soil surface. The same plant species collected from the different points were mixed and left to

dry in a hot air forced oven at 65 °C for 48 hours with three repetitions. The dried plant samples were theoretically ground at a diameter of 1 mm in the mill to make them ready for chemical analysis. Dry matter was determined in the dried samples in ground air. For the determination of dry matter (DM), 1 g of ground plant samples were weighed and dried in porcelain crucibles in a hot air blowing oven at 105 °C for at least 4 hours,<sup>10</sup> and dry matter determination was calculated. All feed quality and nutritional value criteria given in % symbol were calculated on the basis of dry matter. Crude protein (CP) and crude ash (CA) contents of clover species were determined according to the method of AOAC.<sup>10</sup> The Kjeldahl method was applied to determine the nitrogen content and it was multiplied by 6.25 to calculate the crude protein content.<sup>10</sup> The ground plant samples, which were weighed into porcelain crucibles as 1 g for CA analysis, were burned in a muffle furnace at 550 °C. Based on the analysis of neutral detergent fiber (NDF), acid detergent fiber (ADF) and acid detergent lignin (ADL), cell wall components of clover species were determined according to the method of Van Soest et al.<sup>11</sup> In addition, hemicellulose (Hcel) and cellulose (Cel) were calculated using the difference between NDF and ADF and the difference between ADF and ADL in these plant species.<sup>11</sup> According to Van Dyke and Anderson,<sup>9</sup> the dry matter digestibility (DMD), dry matter intake (DMI), relative feed value (RFV) and net energy lactation (NEL) characteristics of clover species were calculated with the following formulas.

$$\text{DMD} = 88.9 - (0.779 \times \% \text{ADF})$$

$$\text{DMI} = 120 / \% \text{NDF}$$

$$\text{RFV} = \% \text{DMD} \times \% \text{DMI} \times 0.775$$

$$\text{NEL} = (1.044 - (0.0119 \times \% \text{ADF})) \times 2.205$$

ANOVA test was applied to all numerical data obtained from this study and the features found to be significant ( $p \leq 0.05$ ) as a result of this test were grouped with Tukey pairwise test.

## 2. RESULTS AND DISCUSSION

The F values and significance levels of the chemical composition and nutritional value properties of some clover species were given in Table 1. As seen from Table 1, among the clover species, all the properties examined in terms of chemical composition and nutritional value were found to be statistically significant.

**Table 1.** ANOVA test results of chemical composition and nutritional value properties of some clover species.

	DM	CA	CP	NDF	ADF	ADL	Hcel	Cel	DMD	DMI	RFV	NEL
F	14.02	548.21	72.33	68.03	316.13	30.23	10.81	309.52	319.00	53.44	76.73	288.26
P	<.001	<.001	<.001	<.001	<.001	<.001	<.001	<.001	<.001	<.001	<.001	<.001
CV	0.21	1.00	1.08	2.63	1.35	4.41	8.15	1.54	0.45	2.59	2.80	0.69

Data on DM, CA, CP, NDF, ADF and ADL characteristics of some clover species and mean comparison test results were given in Table 2. The DM contents of the clover species evaluated in this study

varied between 94.84% and 96.74%. The highest DM was detected in *T. angustifolium* and the lowest in *T. resupinatum*. It has been reported in many studies that DM contents vary depending on plant species.<sup>12-14</sup>

**Table 2.** Mean comparison test results of DM, CA, CP, NDF, ADF and ADL traits in some clover species.

Clover species	DM %	CA %	CP %	NDF %	ADF %	ADL %
<i>T. angustifolium</i>	96.74±0.29 <sup>a</sup>	7.65±0.02 <sup>e</sup>	19.30±0.08 <sup>e</sup>	43.71±0.08 <sup>e</sup>	30.71±0.23 <sup>c</sup>	4.54±0.02 <sup>bc</sup>
<i>T. cherleri</i>	95.70±0.08 <sup>b</sup>	7.58±0.07 <sup>e</sup>	19.41±0.17 <sup>e</sup>	49.80±0.71 <sup>a</sup>	34.28±0.33 <sup>a</sup>	3.90±0.05 <sup>cde</sup>
<i>T. hybridum</i>	95.85±0.08 <sup>b</sup>	9.85±0.05 <sup>a</sup>	21.93±0.09 <sup>ab</sup>	38.60±1.59 <sup>d</sup>	28.07±0.35 <sup>d</sup>	5.43±0.26 <sup>a</sup>
<i>T. lappaceum</i>	95.87±0.05 <sup>b</sup>	5.36±0.07 <sup>f</sup>	18.47±0.14 <sup>f</sup>	48.56±0.10 <sup>ab</sup>	32.59±0.32 <sup>b</sup>	3.63±0.21 <sup>de</sup>
<i>T. nigrescens</i>	96.19±0.13 <sup>ab</sup>	8.94±0.04 <sup>c</sup>	20.90±0.09 <sup>cd</sup>	37.29±0.38 <sup>de</sup>	26.20±0.13 <sup>e</sup>	4.39±0.08 <sup>bc</sup>
<i>T. pilulare</i>	95.67±0.16 <sup>b</sup>	7.47±0.01 <sup>e</sup>	19.37±0.10 <sup>e</sup>	45.37±0.49 <sup>bc</sup>	31.68±0.20 <sup>bc</sup>	5.04±0.07 <sup>ab</sup>
<i>T. resupinatum</i>	94.84±0.09 <sup>c</sup>	8.41±0.11 <sup>d</sup>	22.05±0.26 <sup>a</sup>	30.31±0.85 <sup>f</sup>	21.32±0.17 <sup>g</sup>	3.25±0.09 <sup>e</sup>
<i>T. scabrum</i>	95.97±0.14 <sup>b</sup>	9.27±0.04 <sup>b</sup>	21.23±0.11 <sup>bc</sup>	39.40±0.14 <sup>d</sup>	27.38±0.14 <sup>de</sup>	3.90±0.08 <sup>cde</sup>
<i>T. spumosum</i>	96.22±0.08 <sup>ab</sup>	8.60±0.03 <sup>d</sup>	21.00±0.11 <sup>cd</sup>	37.34±1.07 <sup>de</sup>	24.31±0.23 <sup>f</sup>	3.27±0.11 <sup>e</sup>
<i>T. tomentosum</i>	96.28±0.05 <sup>ab</sup>	9.04±0.01 <sup>bc</sup>	20.43±0.12 <sup>d</sup>	33.95±0.40 <sup>ef</sup>	23.15±0.12 <sup>f</sup>	4.18±0.07 <sup>cd</sup>

DM: Dry matter, CA: Crude ash, CP: Crude protein, NDF: Neutral detergent fiber, ADF: Acid detergent fiber, ADL: Acid detergent lignin

<sup>a-f</sup>Data with different letters in the same column are different from each other.

CA contents were determined between 5.36% and 9.85% in clover species. While the highest CA content was determined in *T. hybridum*, the lowest was determined in *T. lappaceum*. CA contents varied significantly among the species. As a matter of fact, many researchers have reported that plant mineral matter contents vary significantly among the species.<sup>15-18</sup> CP contents of clover species varied between 18.47 and 22.05% and these values are quite good in terms of nutrient content. The highest CP content was found in *T. resupinatum* while the lowest CP content was found in *T. lappaceum*. It was determined that there was no statistical difference between *T. resupinatum* and *T. hybridum* species. Tekeli and Ates<sup>19</sup> found in their study that CP contents of some clover species vary from species to species and they determined that CP contents varied between 19.01 and 24.51%. As a matter of fact, the CP content results obtained from this study were similar to the results of Tekeli and Ates.<sup>19</sup> Among the clover species, NDF contents varied between 30.31 and 49.80%, the highest value was determined in *T. cherleri* and the lowest in *T. resupinatum*. *T. cherleri* and *T. lappaceum* species were placed statistically in the same group. Similarly, *T.*

*resupinatum* and *T. tomentosum* species were also included in statistically similar groups. Pereira and co-workers<sup>20</sup> studied in some clover species with 316 samples and as a result of this study, they determined that the NDF contents were between 14.54 and 51.58%. The NDF contents obtained from this study were within the ranges reported by Pereira-Crespo.<sup>20</sup> ADF contents of clover species were found to be between 21.32% and 34.28%. Similar to NDF contents, the highest and lowest values in ADF contents were determined in *T. cherleri* and *T. resupinatum* species, respectively. Pereira and co-workers<sup>20</sup> found the ADF contents of some clover species to be between 11.55 and 44.35%, which supports the ADF results obtained from our study. ADL contents of clover species varied between 3.25 and 5.04%. The highest ADL content was determined in *T. hybridum* and the lowest in *T. resupinatum* species. High lignin content is an undesirable feature in feeds<sup>21</sup> and in this respect, the *T. resupinatum* species came to the fore.

Data on Hcel, Cel, DMD, DMI, RFV and NEL characteristics of some clover species and mean comparison test results were given in Table 3.

**Table 3.** Mean comparison test results of Hcel, Cel, DMD, DMI, RFV and NEL traits in some clover species.

Clover species	Hcel %	Cel %	DMD %	DMI %	RFV	NEL %
<i>T. angustifolium</i>	13.00±0.31 <sup>ab</sup>	26.17±0.25 <sup>c</sup>	64.98±0.18 <sup>e</sup>	2.75±0.00 <sup>de</sup>	138.27±0.19 <sup>d</sup>	1.50±0.01 <sup>e</sup>
<i>T. cherleri</i>	15.53±0.44 <sup>a</sup>	30.38±0.38 <sup>a</sup>	62.20±0.26 <sup>e</sup>	2.41±0.04 <sup>e</sup>	116.20±2.11 <sup>e</sup>	1.40±0.01 <sup>g</sup>
<i>T. hybridum</i>	10.53±1.31 <sup>bc</sup>	22.63±0.28 <sup>de</sup>	67.03±0.27 <sup>d</sup>	3.12±0.12 <sup>c</sup>	162.09±6.95 <sup>c</sup>	1.57±0.01 <sup>d</sup>
<i>T. lappaceum</i>	15.97±0.34 <sup>a</sup>	28.96±0.14 <sup>b</sup>	63.51±0.25 <sup>f</sup>	2.47±0.00 <sup>e</sup>	121.63±0.51 <sup>de</sup>	1.44±0.01 <sup>f</sup>
<i>T. nigrescens</i>	11.09±0.41 <sup>bc</sup>	21.81±0.10 <sup>ef</sup>	68.49±0.10 <sup>c</sup>	3.22±0.03 <sup>bc</sup>	170.85±1.75 <sup>c</sup>	1.62±0.00 <sup>c</sup>
<i>T. pilulare</i>	13.69±0.67 <sup>ab</sup>	26.64±0.26 <sup>c</sup>	64.22±0.15 <sup>ef</sup>	2.65±0.03 <sup>e</sup>	131.65±1.16 <sup>de</sup>	1.47±0.01 <sup>ef</sup>
<i>T. resupinatum</i>	8.99±0.70 <sup>c</sup>	18.07±0.18 <sup>g</sup>	72.29±0.13 <sup>a</sup>	3.97±0.11 <sup>a</sup>	222.18±6.41 <sup>a</sup>	1.74±0.01 <sup>a</sup>
<i>T. scabrum</i>	12.02±0.06 <sup>bc</sup>	23.48±0.14 <sup>d</sup>	67.57±0.10 <sup>cd</sup>	3.04±0.01 <sup>cd</sup>	159.48±0.78 <sup>c</sup>	1.58±0.00 <sup>cd</sup>
<i>T. spumosum</i>	13.03±0.92 <sup>ab</sup>	21.05±0.20 <sup>f</sup>	69.96±0.17 <sup>b</sup>	3.22±0.09 <sup>bc</sup>	174.56±5.23 <sup>c</sup>	1.67±0.01 <sup>b</sup>
<i>T. tomentosum</i>	10.80±0.36 <sup>bc</sup>	18.97±0.19 <sup>g</sup>	70.87±0.10 <sup>b</sup>	3.54±0.04 <sup>b</sup>	194.20±2.38 <sup>b</sup>	1.69±0.00 <sup>b</sup>

Hcel: Hemicellulose, Cel: Cellulose, DMD: Dry matter digestibility, DMI: Dry matter intake, RFV: Relative feed value, NEL: Net energy lactation

<sup>a-g</sup>Data with different letters in the same column are different from each other.

Hcel contents of clover species were determined between 8.99 and 15.97%. The highest Hcel content was found in *T. lappaceum* and the lowest in *T. resupinatum*. High Hcel content increases the daily dry matter intake in cows and negatively affects digestibility.<sup>22,23</sup> Cel content of clover species was determined between 18.07 and 30.38%. The highest Cel content was determined in *T. cherleri* and the lowest in *T. resupinatum*. Tekeli and Ates<sup>19</sup> determined the crude fiber contents of clover species in a study they conducted, similar to the results obtained in this study. DMD, DMI, RFV and NEL values of clover species varied between 62.20 and 72.29%, 2.41 and 3.97%, 116.20 and 222.18 and 1.40 and 1.74%, respectively. In terms of these properties, the highest value was obtained from *T. resupinatum* and the lowest from *T. cherleri* species. If the RFV value calculated based on the DMD and DMI characteristics is above 150, the feed is said to be of the best quality.<sup>24</sup> The DMD, DMI and RFV values obtained from this study were similar to the results of Gürsoy and Macit<sup>25</sup> studying with some pasture legumes. Therefore, it was determined that very good quality roughage can be obtained from other clover species except *T. cherleri*, *T. lappaceum* and *T. pilulare*. In addition, *T. resupinatum* was statistically significantly separated by RFV. It was determined that the highest energy can be obtained from *T. resupinatum* in the lactation period of dairy cows. *T. resupinatum* was leading in terms of many features examined.

### 3. CONCLUSION

This study was carried out to compare the chemical composition and nutritional value of some clover species, especially grown in Mediterranean pastures. According to the results of this study, *T. resupinatum* was found to be superior in many features. However, when the results obtained from the study were evaluated collectively, it was determined that *T. resupinatum* and *T. hybridum* offered a superior chemical composition and nutritional value compared to other species. *T. cherleri*, *T. lappaceum* and *T. pilulare* species were found to provide lower quality roughage compared to other species. As a result, it can be said that a pasture dominated by *T. resupinatum* and *T. hybridum* species can provide better quality roughage compared to other species.

### Conflict of interest

I declare that there is no a conflict of interest with any person, institute, company, etc.

### REFERENCES

1. Ates, S.; Feindel, D.; El Moneim, A.; Ryan, J. Grass Forage Sci, 2014, 69, 17-31.

2. Can, E.; Çeliktaş, N.; Hatipoğlu, R.; Avcı, S. Turk J Field Crops, 2009, 14, 72-78.
3. Brahim, K.; Smith, S.E. J. Ran Manage, 1993, 46, 21-25.
4. Evers, G.W. Crop Sci, 2011, 51, 403-409.
5. Brink, G.E.; Fairbrother, T.E. Crop Sci, 1992, 32, 1043-1048.
6. Rocateli, A.; Zhang, H. Oklahoma Cooperative Extension Service, Division of Agricultural Sciences and Natural Resources, 2015, PSS-2117.
7. Yavuz, M. GOÜ Ziraat Fak Derg, 2005, 22, 93-96
8. Fulgueira, C.L.; Amigot, S.L.; Gaggiotti, M.; Romero, L.A.; Basílico, J.C. Fresh Prod, 2007, 1, 121-131.
9. Van Dyke, N.J.; Anderson, P.M. Alabama Cooperative Extension System, 1998, ANR-890.
10. AOAC. Association of Official Analytical Chemists, 1990, 66-88.
11. Van Soest, P.J.; Robertson, J.B., Lewis, B.A. J Dairy Sci, 1991, 74, 3583-3597.
12. Wilson, P.J.; Thompson, K.; Hodgson, J.G. New Phytol, 1999, 143, 155-162.
13. Shipley, B.; Vu, T.T. New Phytol, 2002, 153, 359-364.
14. Palacio, S.; Milla, R.; Albuixech, J.; Pérez-Rontomé, C.; Camarero, J.J.; Maestro, M.; Montserrat-Martí, G. New Phytol, 2008, 180, 133-142.
15. Harrington, K.C.; Thatcher, A.; Kemp, P.D. N Z Plant Prot, 2006, 59, 261-265.
16. Khan, Z.I.; Ashraf, M.; Valeem, E.E. Pak J Bot, 2006, 38, 1043-1054.
17. Lee, M.A. J Plant Res, 2018, 131, 641-654.
18. Mayer, J.A.; Cushman, J.C. J Agron Crop Sci, 2019, 205, 625-634.
19. Tekeli, A.S.; Ates, E. Cuban J Agric Sci, 2006, 40, 93-98.
20. Pereira-Crespo, S.; Valladares, J.; Flores, G.; Fernández-Lorenzo, B.; Resch, C.; Piñeiro, J.; Díaz, N.;

González-Arráez, A.; Bande-Castro, M.J.; Rodríguez-Diz, X. *CIHEAM*, 2012, 241-244.

21. Fracchiolla, M.; Lasorella, C.; Laudadio, V.; Cazzato, E. *Agric*, 2018, 8, 313.

22. Oba, M.; Allen, M.S. *J Dairy Sci*, 1999, 82, 589-596.

23. Budak, F.; Budak, F. *Türk Bil Der Derg*, 2014, 7, 1-6.

24. Undersander, D. *California Alfalfa Symposium*, 2003, 100-104.

25. Gürsoy, E.; Macit, M. *Anadolu Tar Bil Derg*, 2017, 32, 407-412.



## Variation of components in laurel (*Laurus nobilis* L.) fixed oil extracted by different methods

Musa TÜRKMEN<sup>1</sup>, Oğuzhan KOÇER<sup>2,\*</sup>

<sup>1</sup>Field Crops Department, Faculty of Agriculture, Hatay Mustafa Kemal University, Antakya, Hatay 31000, Turkey

<sup>2</sup>Pharmacy Services, Vocational School of Health Services, Osmaniye Korkut Ata University, Osmaniye 80000, Turkey

Received: 7 October 2021; Revised: 24 December 2021; Accepted: 24 December 2021

\*Corresponding author e-mail: [oguzhankocer@hotmail.com](mailto:oguzhankocer@hotmail.com)

**Citation:** Türkmen, M.; Koçer, O. *Int. J. Chem. Technol.* 2021, 5 (2), 167-171.

### ABSTRACT

In the study, it was aimed to determine the constituents of laurel fixed oil obtained from the different genotypes of laurel (*Laurus nobilis* L.), which is one of the natural plants of the region and which is widely found in the flora of Hatay, by traditional, cold press and soxhlet extraction methods. When the GC/MS analysis results of these obtained oils were examined, the main components of the fixed oils in the traditional method were found as capric acid (2.49%), lauric acid (1.17%), myristic acid (0.16%), palmitic acid (13.69%), stearic acid (2.39%), oleic acid (55.01%), linoleic acid (10.56%) and linolenic acid (0.11%). In cold press method, fixed oil components were capric acid (0.24%), lauric acid (9.24%), myristic acid (0.98%), palmitic acid (18.41%), stearic acid (2.84%), oleic acid (38.59%), linoleic acid (23.67%) and linolenic acid (2.19%), while it was determined as capric acid (0.46%), lauric acid (11.16%), myristic acid (1.54%), palmitic acid (18.39%), stearic acid (3.58%), oleic acid (36.92%), linoleic acid (23.02%) and linolenic acid (2.54%) in soxhlet extraction method. As a result, while the components of laurel fixed oil did not change according to the fixed oil extraction methods, the amounts of these components changed. Therefore, it was determined that the method of oil extraction in laurel was important.

**Keywords:** Laurel, *Lauris nobilis* L., GC-MS, Hatay, aromatic.

### Farklı yöntemlerle çıkarılan defne (*Laurus nobilis* L.) sabit yağ bileşenlerindeki değişim

#### ÖZ

Çalışmada Hatay florasında yoğun bir şekilde bulunan ve bölgenin doğal bitkilerinden biri olan defne (*Laurus nobilis* L.) genotiplerinden geleneksel, soğuk sıkım ve soxhlet ekstraksiyonu yöntemleri ile elde edilen defne sabit yağı bileşenlerinin belirlenmesi amaçlanmıştır. Elde edilen bu yağların GC/MS analiz sonuçları incelendiğinde sabit yağların ana bileşenleri geleneksel yöntemde, kaprik asit (%2.49), laurik asit (%1.17), myristic asit (%0.16), palmitik asit (%13.69), stearik asit (%2.39), oleik asit (%55.01), linoleik asit (%10.56), linolenik asit (%0.11), soğuk preste, kaprik asit (%0.24), laurik asit (%9.24), myristic asit (%0.98), palmitik asit (%18.41), stearik asit (%2.84), oleik asit (%38.59), linoleik asit (%23.67) ve linolenik asit (%2.19) ve soxhlet ekstraksiyonunda kaprik asit (%0.46), laurik asit (%11.16), myristic asit (%1.54), palmitik asit (%18.39), stearik asit (%3.58), oleik asit (%36.92), linoleik asit (%23.02) ve linolenik asit (%2.54) olduğu tespit edilmiştir. Sonuç olarak defne sabit yağının bileşenleri sabit yağ çıkarma yöntemlerine göre değişmezken bu bileşenleri miktarları değişiklik göstermiştir. Bu yüzden defnede yağ çıkarma yönteminin önemli olduğu tespit edilmiştir.

**Anahtar Kelimeler:** Defne, *Laurus nobilis* L., Hatay, aromatik.

### 1. INTRODUCTION

From the past to present, people have used plants for therapeutic purposes either by chance or as a result of curiosity, in order to find a cure for diseases. In recent years, medicinal and aromatic plants, which have created awareness all over the world, have become an important

focus of attention in Turkey as well. Medicinal and aromatic plants produce active substances that provide drugs to humans to prevent diseases, maintain health, and treat ailments. Essential and fixed oils obtained from leaves and fruits are used in domestic and foreign markets rather than the direct use of bay leaves and fruits, which have an important place in our foreign trade. Laurel and



its products are used in many fields such as food, medicine, cosmetics and chemistry. In addition, both domestic and foreign trade of laurel products is increasing recently in Turkey.<sup>1</sup>

Bay leaves has compelling features as antioxidant, antiseptic, antibacterial, anti-inflammatory, anticonvulsant, antifungal, analgesic, diaphoretic, anti-migraine, relieving stomach ailments and treating diabetes. In addition, It has been shown in many studies that the laurel plant is also good for diseases such as weakness, indigestion, insomnia, menstrual irregularities and rheumatism.<sup>2-9</sup> The fixed oil extracted from the anthocyanin fruit of the laurel is used in cosmetic medicine and food industries. It is also considered as a natural dyestuff.<sup>10-13</sup> The origin of the laurel plant is the Mediterranean countries according to some references while in some references its origin is Minor Asia (Anatolia) and Balkans. Our country is very suitable for the cultivation of many cultural plants in terms of climatic conditions, in addition, the rugged topography contributed to the crop aroma, taste, quality and yield characteristics of plants.<sup>14-17</sup> There are 45 genera and 1000 species in the Lauraceae family. There are 2 species belonging to the genus *Laurus* and they are *L. nobilis* and *L. angustifolia* and *L. angustifolia* has 4 subspecies.<sup>18-21</sup>

Turkey is a country with a significant potential to meet the demand for laurel oil production and its products. Laurel fruit oil is commonly produced in Hatay and exported abroad, either directly as oil or to be used in soap making. 20% of the production of laurel berry oil, which contains some volatile components and is called fixed oil and used in the soap industry.<sup>1,22</sup>

Hafizoglu and Reunanen<sup>23</sup> stated that there are more than 20 fatty acids in laurel fruits and the main components are lauric acid (54.2%), oleic acid (15.1%) and linoleic acid (17.2%). Ayanoglu and co-workers<sup>24</sup> determined that average value of lauric acid was 16.57%, palmitic acid was 18.57%, oleic acid was 38.08%, and linoleic acid was 23.90% in the fruits of 145 female laurel plants collected from different locations in Hatay. Beis and Dunford<sup>25</sup> used supercritical and petroleum ether extracts of laurel fruit oils obtained from Turkey, and the main components were found as lauric acid (43.1-44.8%), oleic acid (37.2 – 37.3%) and linoleic acid (14.7%-13.3%). On the other hand, Yazıcı (2002) determined that components of laurel fixed oil extracted using hexane as a solvent were lauric acid (12.31-14.96%), oleic acid (44.12-45.90%), linoleic acid (21.97-23.05%) and palmitic acid (14.39-14.86%) . The researcher also reported that as the altitude increases in the region, the ratio of saturated fatty acids decreased, while the ratio of unsaturated fatty acids increased. Timur<sup>26</sup> determined that laurel fixed oil components were 8.5-13.0% for lauric acid, 13.1-20.8% for palmitic acid, 36.3-48.3% for oleic acid and 52.8-29.9 for linoleic acid. Castilho and

co-workers<sup>27</sup> reported that laurel fruit contains 30% oleic acid, 20% linoleic acid, 18% lauric acid to 22.5% palmitic acid and 84%  $\beta$ -sterol. In a study conducted by Erden<sup>28</sup>, laurel fruits were harvested every week from October to December and dried in the sun to extract the oil by Soxhlet extraction method. Petroleum ether was used as solvent in this study, and the highest oil yield was obtained at the end of December with 25.55% (mass/mass). Nurbaş and Bal<sup>29</sup> investigated the effects of hexane, petroleum ether, carbon sulfide and benzene used as solvents on the efficiency of the Soxhlet extraction method in oil extraction from laurel fruit. In the trials, used hexane as solvent has the highest efficiency value with 32.12% fixed oil rate. Koçer and Ayanoglu<sup>9</sup> determined that the main components of fruit and seed fixed oils of laurel found as lauric acid, oleic acid, palmitic acid and linoleic acid. They reported that lauric acid was not found in fruit flesh.

## 2. MATERIALS AND METHODS

In this study, fruit fixed oil of laurel genotypes was extracted by traditional, cold pressing and Soxhlet extraction methods. The traditional method was made according to the boiling method performed by the region villagers. For the cold pressing and extraction method, laurel fruits were firstly dried in an oven at 70 °C. In the study, the extraction method is based on the principle of removing the solvent as a result of the extraction of the sample with solvent (hexane) and weighing the remaining residue (fixed oil). The laurel fruits, which were dried in an oven, were ground by a grinder and 5 g of sample was used in the extraction method. Hexane was used as the solvent in the extraction method. At the end of the extraction, the beaker containing oil was taken and kept in an oven set at 80 °C for 1 hour.<sup>30,31</sup>

100  $\mu$ l of oils obtained from laurel fruits were taken, 3 ml of N-Heptane and 400  $\mu$ l of 2N methanolic KOH solution were added and esterification was applied, and the components of the oils were analyzed by GC/MS. Determination of fixed oil components was performed with Thermo Scientific ISQ Single Quadrupole model gas chromatography device under the following conditions. TR-FAME MS model, 5% Phenyl Polysilphenylene-silohexane, 0.25 mm inner diameter x 60 m length, 0.25  $\mu$ m film thickness was used. Helium (99.9%) was used as the carrier gas at a flow rate of 1 mL/min. The ionization energy was set to 70 eV, the mass range m/z 1.2-1200 amu. Scan mode was used for data collection. The MS transfer line temperature was 250°C, the MS ionization temperature was 220°C, the injection port temperature was 220°C, the column temperature was initially 120°C and kept there for 1 min. It was increased to 175 °C by increasing 10 °C per minute and kept there for 10 minutes. It was increased to 210 °C by increasing 5 °C per minute and kept there for 5 minutes. Then, it was increased to 230 °C by increasing 5 °C per minute, and the analysis was concluded by

keeping it here for 6 minutes. The total analysis time is 38.5 minutes. The structure of each compound was defined using the Xcalibur program using mass spectra (Wiley 9).<sup>32</sup>

### 3. RESULTS AND DISCUSSION

#### 3.1. Traditional Method

When the fatty acid components of the oils extracted by the traditional boiling method from the laurel fruits (seeds) by the villagers living in Hatay were examined, 8 main components were determined (Table 1). The chromatogram of these components is shown in Figure 1. The highest value among these components was found as oleic acid with a rate of 55.01%. Also, other components were determined as palmitic acid (13.69%), linoleic acid (10.56%), capric acid (2.49%), stearic acid (2.39%), lauric acid (1.17%), myristic acid (0.16%) and linolenic acid (0.11%).

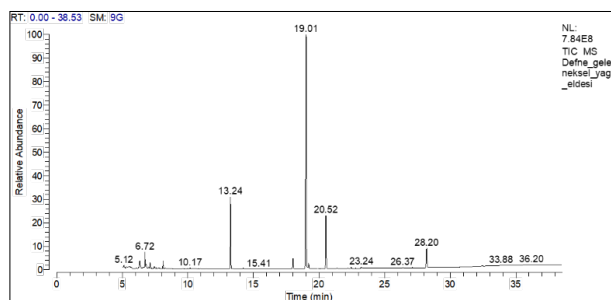


**Figure 1.** *Laurus nobilis* L. (Laurel) fixed oil chromatogram obtained by traditional method.

**Table 1.** *Laurus nobilis* L. (Laurel) fixed oil components and values obtained by traditional method.

RT	Compound Name	CAS	Area (%)
6:72	Kaprik asit, C10	110-42-9	2.49
8:10	Laurik asit, C12	111-82-0	1.17
10:17	Myristic asit, C14	124-10-7	0.16
13:24	Palmitik asit, C16	112-39-0	13.69
18:01	Stearik asit, C18:0	112-61-8	2.39
19:01	Oleik asit, C18:1	112-62-9	55.01
20:52	Linoleik asit C18:2	112-63-0	10.56
22:20	Linolenik asit, C18:3	301-00-8	0.11

As seen in Table 1, Laurel fixed oil components and their quantities were similar to literature reports.<sup>9,23-26</sup> In addition fixed oil component quantities was different from each other. The reason for this may be that lauric acid is found in the fruit seed, as stated in previous studies, and that the fixed oil in the fruit seed cannot be completely removed in the traditional method.

#### 3.2. Cold Press method

When the fatty acid components of the oils extracted from laurel fruits by cold pressing method were examined, 8 main components were determined (Table 3). The chromatogram results of these components is shown in Figure 3. The highest value among these components was found as oleic acid with a rate of 38.59% similar to the traditional method. However, oleic acid ration in cold pressing method was lower than traditional method. Other main components in cold pressing method were determined as linoleic acid (23.67%), palmitic acid (18.41%), lauric acid (9.54%), stearic acid (2.84%), linolenic acid (2.19%), myristic acid (0.98%) and capric acid (0.24%). In cold pressing method, some components were lower than traditional method while some components was higher.

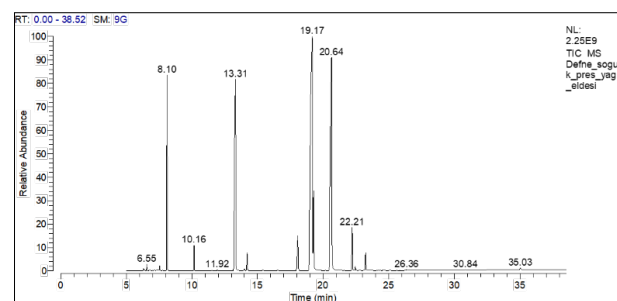


**Figure 2.** *Laurus nobilis* L. (Laurel) fixed oil chromatogram obtained by cold press method.

**Table 2.** *Laurus nobilis* L. (Laurel) fixed oil components and values obtained by cold press method.

RT	Compound Name	CAS	Area (%)
6:55	Kaprik asit, C10	110-42-9	0.24
8:10	Laurik asit, C12	111-82-0	9.54
10:16	Myristic asit, C14	124-10-7	0.98
13:31	Palmitik asit, C16	112-39-0	18.41
18:06	Stearik asit, C18:0	112-61-8	2.84
19:16	Oleik asit, C18:1	112-62-9	38.59
20:63	Linoleik asit C18:2	112-63-0	23.67
22:21	Linolenik asit, C18:3	301-00-8	2.19

As seen in Table 2, laurel fixed oil extracted by cold press method was similar to some research findings.<sup>9,23-26</sup> On the other hand, component quantities were different from each other. The difference in the amounts of the components can be attributed to both plant genetic structures and climatic conditions.

#### 3.3. Soxhlet extraction

When the fatty acid components of the oils extracted from the laurel berries were examined, 8 main

components were found (Table 3). The chromatogram results of these components are shown in Figure 3. The highest value among these components was found as oleic acid with a rate of 36.92% similar to the traditional and extraction methods. But, oleic acid value changed according to the methods. Other main components were determined as linoleic acid (23.02%), palmitic acid (18.39%), lauric acid (11.16%), stearic acid (3.58%), linolenic acid (2.54%), myristic acid (1.54%) and capric acid (0.46%).

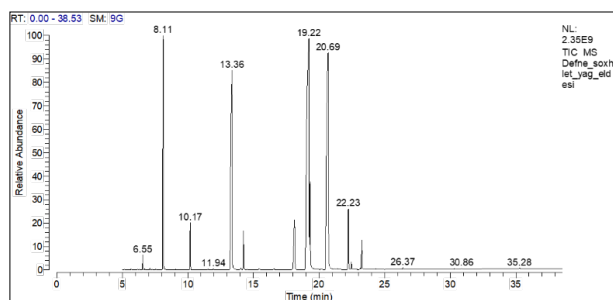


**Figure 3.** Fixed oil chromatogram of *Laurus nobilis* L. (Laurel) obtained by soxhlet extraction method.

**Table 3.** *Laurus nobilis* L. (Laurel) fixed oil components and values obtained from soxhlet extraction.

RT	Compound Name	CAS	Area (%)
6:55	Kaprik asit, C10	110-42-9	0.46
8:11	Laurik asit, C12	111-82-0	11.16
10:17	Myristic asit, C14	124-10-7	1.54
13:36	Palmitik asit, C16	112-39-0	18.39
18:12	Stearik asit, C18:0	112-61-8	3.58
19:22	Oleik asit, C18:1	112-62-9	36.92
20:69	Linoleik asit C18:2	112-63-0	23.02
22:23	Linolenik asit, C18:3	301-00-8	2.54

As seen in Table 3, laurel fixed oil components were similar to literature reports<sup>9,23-26</sup> and component quantities were different from each other. The difference in the amounts of the components can be attributed to both plant genetic structures and climatic conditions.

#### 4. CONCLUSION

When the GC/MS analysis results of traditional cold pressing and soxhlet extraction methods are examined, the main components of fixed oils were determined as capric acid (2.49-0.24-0.46%, respectively), lauric acid (1.17-9.54-11.16%, respectively), myristic acid (0.16-0.98-1.54%, respectively), palmitic acid (13.69-18.41-18.39%, respectively), stearic acid (2.39-2.84-3.58%, respectively), oleic acid (55.01-38-59-36.92%, respectively), linoleic acid (10.56-23.67-23.02%, respectively), linolenic acid (0.11-2.19-2.54%, respectively).

When these results were investigated, it was seen that the amount of lauric acid was less and the amount of oleic acid was higher in the traditional method compared to the other methods. The reason for this is thought to be due to the absence of lauric acid in the fruit flesh and for this reason, not all of the fixed oil in the fruit could be extracted with the traditional method. Since the laurel plant is not cultivated, the production of standard raw materials from this plant is restricted. In addition, unconscious harvesting and excessive slaughter also lead to the destruction of genetic resources.

The production of laurel, which is an important export product, should be increased and its planting should be encouraged for a quality production. Especially in the new afforestation areas, the laurel plant should be emphasized in the re-establishment of the degraded and burned forest areas. In the new agricultural facilities to be established for the production of laurel oil and laurel leaves, as well as in the reforestation of forest areas, plantings should be made with selected, high-quality types, and laurel leaf production.

#### Conflict of interest

The authors declare that there is no conflict of interest.

#### REFERENCES

- Koçer, O. 2021: *TURAN-CSR*. **2021**, 13(50), 465-469.
- Baytop, T. İ.Ü., *eczacılık fakültesi yayınları: Türkiye’de bitkiler ile tedavi*, No:40, İstanbul, 1984.
- Acartürk, R. *Ovak yayınları: şifalı bitkiler, flora ve sağlığımız*, Yayın No:1, Ankara, 1997.
- Duke, J.A. *CRC pres inc: CRC handbook of medicinal herbs*, Florida, 1987.
- Özhatay, N.; Koyuncu, M.; Atay, S.; Byfield, A. *Doğal hayatı koruma derneği: Türkiye’nin doğal tıbbi bitkilerinin ticareti hakkında bir çalışma*, ISBN:975-96081-9-7, İstanbul, 1997.
- Sayyah, M.; Valizadeh, J.; Kamalinejad, M. *Phytomedicine*. **2002**, 9, 212-216.
- Sayyah, M.; Saroukhani, G.; Peirovi, A.; Kamalinejad, M. *Phytother res*. **2003**, 17, 733-736.
- Simic, M.; Kundakovic, T.; Kovacevic, N. *Fitoterapia*. **2004**, 74(6), 613-616
- Rodilla, J. M.; Tinoco, M. T.; Morais, J. C.; Gimenez, C.; Cabrera, R.; Benito, D. M.; Castillo, L.; Gonzalez-

- Coloma, A. *Biochemical systematics and ecology*. **2008**, 36, 167-176.
10. Özer, S. *Orman genel müdürlüğü yayını: ülkemizdeki bazı önemli orman tali ürünlerinin teşhis ve tanıtım klavuzu*, Yayın No: 659, Seri No: 18, Ankara, 1987.
11. Hammer, K.A.; Carson, C.F.; Rley, T.V. *Journal of Applied Microbiology*. **1999**, 86, 985-990.
12. Driver, C.; Arroy, G. *Phytochemistry*. **2001**, 56, 229-236.
13. Longo, L.; Vasapollo, G. *J. Agric. Food Chem.* **2005**, 53, 8063-8067.
14. Kuzucu, M. *Fresen Environ Bull.* **2017**, 26 (12): 7521-7528.
15. Kuzucu, M. *JMEST*. **2018**, 5(12): 9303-9307.
16. Kuzucu, M. *Fresen Environ Bull.* **2019**, 28(1): 446-451.
17. Kuzucu, M. *IJENT*. **2021**, 5 (1):16-27 ISSN: 2602-4160.
18. Baydar, H. Süleyman Demirel Üniversitesi Ziraat Fakültesi Yayınları. **2009**, No. 51, Isparta, 234-235.
19. Kayacık, H. *Orman ve park ağaçlarının özel sistematigi*: Cilt II, 1977.
20. Boza, A. (2011). Karaburun Çeşme ve Dilek Yarımadası'nda Bulunan Doğal Defne (*Laurus nobilis* L.) Populasyonları Üzerinde Araştırmalar. Phd Dissertation, Ege Üniversitesi Fen Bilimleri Enstitüsü, Bahçe Bitkileri Anabilim Dalı, İzmir.
21. Seçmen, Ö.; Gemici, Y.; Leblebici, E.; Görk, G.; Bekat, L. *Ege üniversitesi fen fakültesi kitaplar serisi: tohumlu bitkiler sistematigi*, No: 116, İzmir, 1992.
22. Konukçu, M. *Devlet planlama teşkilatı yayın ve temsil dairesi başkanlığı: ormanlar ve ormancılığımız*. Yayın No. DPT: 2630, Ankara, 2001.
23. Hafizoglu, H.; Reunanen, M. *Lipid-Fett*. **1993**, 95:304--308.
24. Ayanoğlu, F.; Mert, A.; Kaya, D. A.; Köse, E. *Hatay yöresinde doğal olarak yetişen defne (Laurus nobilis L.) bitkisinin kalite özelliklerinin belirlenmesi ve seleksiyonu*. Tübitak Proje No: 108O878, 2010.
25. Beis, S.H.; Dunford, N.T. *Seed Oil. JAOCS*. **2006**, Vol. 83, no. 11, 953-957.
26. Timur, M. Defne Meyvesi Yağ Veriminin Arttırılması ve Bileşiminin Gaz Kromatografi Cihazı ile Belirlenmesi. Yüksek Lisans Tezi, Mustafa Kemal Üniversitesi, 2001
27. Castilhoa, P.; C.; Costaa, M.; Rodriguesb, A.; Partidáriooc, A. *Portugal. Jaocs*. **2005**, Vol. 82, no. 12 pg 863-867
28. Erden, Ü. 2005. Akdeniz Defnesi'nde (*Laurus nobilis* L.) Mevsimsel Varyabilite ve Optimal Kurutma Yöntemlerinin Araştırılması. Yüksek Lisans Tezi, Çukurova Üniversitesi, 2005.
29. Nurbaş, M. ve Bal, Y., 2005. *Eskişehir Osmangazi Üniversitesi Mühendislik ve Mimarlık Fakültesi Dergisi*. **2005**, 18 (2), 15-24.
30. Koçer, O.; Ayanoğlu, F. *IJEASED*. **2021**, 3 (1) , 72-88 . DOI: 10.47898/ijeased.843773
31. Ayanoğlu, F.; Kaya, D. A.; Koçer, O. *Int. J. Chem. Technol*. **2018**, 2(2): 167-161.
32. Türkmen, M.; Mert, A. *MKU. Tar. Bil. Derg*. **2020**, 25(3): 309-315. DOI: 10.37908/mkutbd.731874



## Production of organic light-emitting diode with fluorescence featured quinoline derivative

Mustafa DOĞAN<sup>1,\*</sup>, Ümit ERDEM<sup>1</sup>, Salih ÖKTEN<sup>2</sup>

<sup>1</sup>Scientific and Technological Research Application and Research Center, Kırıkkale University, Yahşihan, Kırıkkale 71450, Turkey

<sup>2</sup>Department of Mathematics and Science Education, Faculty of Education, Kırıkkale University, Yahşihan, Kırıkkale 71450, Turkey

Received: 19 October 2021; Revised: 12 November 2021; Accepted: 23 November 2021

\*Corresponding author e-mail: mustafadoga@gmail.com

**Citation:** Doğan, M.; Erdem, Ü.; Ökten, S. *Int. J. Chem. Technol.* 2021, 5 (2), 172-177.

### ABSTRACT

High-priced coating devices limit producing electronic devices and circuit applications widely in laboratories. Simply In this study spin coating technique was used to create surface thin films. Also with this method, an OLED (Organic Light Emitting Diode) device was practically produced. OLED device includes mainly HTL (hole transfer layer), fluorescent layer (light-emitting layer), and an ETL (electron transfer layer). Light-emitting layers in OLED experimental studies are frequently done with commercially produced expensive fluorescence polymers. As an example, MEH-PPV (Poly[2-methoxy-5-(2'-ethyl-hexoxy)-1,4-phenylenevinylene]), Alq3 (Tris-(8-hydroxyquinolinato) aluminum) are mostly known and used fluorescent semiconductor polymers. Alternative to these fluorescent polymers, three different produced quinoline ligand products has fluorescent feature were evaluated. After comparing the fluorescence yields of the produced three complexes, it was seen that 5,7-dibromo-8-hydroxyquinoline has the highest fluorescent response from the others. OLED device production was done with a commercial MEH-PPV (commercial) fluorescent product, and produced (5,7-dibromo-8-hydroxyquinoline). Designed OLED device illumination spectrum was found in the UV (ultraviolet) region. It was concluded that this quoniline product can use as a fluorescent material to produce an OLED device.

**Keywords:** thin film, OLED, fluorescence, UV, 8-hydroxyquinoline.

### Floresans özelliklere sahip kinolin türevi kullanılarak organik ışık yayan diyot üretimi

#### ÖZ

Bu çalışmada ışık yayan diyot üretimi için spin kaplama tekniği kullanılarak yüzeyde ince filmler oluşturulmuştur. Bu yöntemle pratik olarak bir OLED (Organik Işık Yayan Diyot) cihazı üretilmiştir. OLED cihazı temel olarak HTL (delik transfer katmanı), floresan katmanı (ışık yayan katman) ve bir ETL (elektron transfer katmanı) içerir. OLED deneysel çalışmalarında ışık yayan tabakalar genellikle ticari olarak üretilen fiyatları yüksek olan, floresans özelliklere sahip polimerler kullanılarak yapılır. Bu floresan özelliklere sahip yarıiletken polimerlere alternatif olarak üretilen ve floresan özelliğine sahip kinolin ligand ürünü incelenmiştir. Üretilen üç kinolin kompleksinin floresan verimleri karşılaştırıldıktan sonra 5,7-dibromo-8-hidroksikinolin ürününün diğer iki sentezlenen üründen daha yüksek floresan tepkisine sahip olduğu görülmüştür. OLED cihaz üretimi için sentezlenen bu floresan özellikli kinolin türevi (5,7-dibromo-8-hidroksikinolin) ve MEH-PPV (ticari) floresans özellikli ürün kullanılmıştır. Tasarlanan OLED cihazının aydınlatma spektrumu UV (ultraviyole) bölgesinde olduğu görülmüştür. Bu çalışma sonucunda ince film kaplama ile OLED üretilebileceği görülmüştür. Ayrıca üretilmiş kinolin türevinin bir OLED cihazı üretmek için floresan ara katman malzemesi olarak da kullanılabilirliği sonucuna varılmıştır.

**Anahtar Kelimeler:** ince film, OLED, floresans, UV, 8-hidroksikinolin.

### 1. INTRODUCTION

The development of semiconductor polymer-based products has significant application potential in the scientific and industrial fields. This technology finds application areas from the production of optoelectronics based organic light-emitting diodes, mobile phone

screens, new-generation high-resolution television screens to the photovoltaic cells that generate electricity with solar energy. After the 2000 years of discovering and developing the conductive polymers,<sup>1</sup> innovative studies were increased on organic electronics particularly the semiconducting polymers that were used in optoelectronic devices; such as organic light-emitting



diodes (OLEDs) and organic photovoltaic cells (OPVs). A luminescent layer between the anode ITO (indium tin oxide) coated glass) and the cathode (aluminum, Ga-In-Eu alloys) forms an OLED device. Applying a voltage (3V to 15V) between anode and cathode would give a characteristic light. Light spectrum is directly with luminescent material's bandgap. A band model can be used to describe the OLEDs working principle. When a potential difference is applied between the anode and the cathode; molecules would electrically be transferred into an excited state. In OLED device this excited state would return to the ground state by illumination. The color of the emitted light is determined by the scale of energy gap ( $E_g$ ) between the HOMO (highest occupied molecule orbital) and LUMO (lowest unoccupied molecule orbital) levels. Photochemical basics of luminescence were explained in the literature.<sup>2,3</sup> For the emission of light electric potential must drift charges through the coated polymer layers.

When the band structure is investigated; firstly electrons are injected into the LUMO of molecules close to the cathode and holes are injected into the HOMO of molecules close to the anode. For this process, it is crucial, that the Fermi levels of the electrodes fit well to the energy levels of the polymer layer. Also, intimate contact between all layers is necessary for charge transport. Injected charges drift through the polymer layer from molecule to molecule in opposite directions. These hopping processes are necessary because there are energetic barriers between the molecules, which the electrons have to overcome for an efficient current flow.<sup>4</sup> For the emission of light, a thin layer of the electroluminescent polymer has to be placed in a diode between a transparent ITO anode (indium tin oxide) and a low work function metal cathode. Polymer-based new generation semiconductors can be used instead of high-priced commercially used electro-optic materials such as gallium arsenide (GaAs), cadmium telluride (CdTe), and CdSe (Cadmium Selenide).<sup>4</sup> The development of new organic-based materials will also contribute greatly to the development of electro-optical device technology and sensor technology.<sup>5</sup> For this purpose in this study hydroxyquinoline derivative materials were produced. Synthesized material was used to make an OLED device.

When 8-hydroxyquinoline (8-HQ) complex evaluated it would be seen that, it has got large application fields from medical usage to chemical process applications.<sup>6</sup> 8-Hydroxyquinoline (8-HQ), an important quinoline derivative known as oxine, has been used as a fungicide in agriculture and a preservative in the textile, wood, and paper industries.<sup>7</sup> 8-HQ possesses potent coordinating ability and good metal recognition properties, which means it is widely used for analytical and separation purposes as well as for metal chelation.<sup>8</sup> Its aluminium complex is a common component of organic light-emitting diodes (OLEDs).

Variations in the substituents on the quinoline rings effect its luminescence properties.<sup>9</sup> In the photochemically induced excited-state ionic isomers are formed in which the hydrogen atom is transferred from oxygen to nitrogen.<sup>10</sup> The complexes as well as the heterocycle itself exhibit antiseptic, disinfectant, and pesticide properties<sup>11</sup> functioning as a transcription inhibitor. On the other hand, 5,7-dibromo-8-hydroxyquinoline has effective antibacterial, antiprotozoal, antiamebic, antifungal, bacteriostatic and fungistatic activities, particularly used in treating the intestinal amebiasis.<sup>12</sup> As well as its pharmaceutical importance, 5,7-dibromo-8-hydroxyquinoline is also used in spectrophotometric study and solvent extraction process.<sup>13</sup>

By this article a preliminary study was described which was performed using organic fluorescence coated surfaces. Synthesized 5,7-dibromo-8-hydroxyquinoline, has shown good fluorescence properties. It was seen that this quinoline product can be used successfully in semiconductor diode device production, after coated as a thin film.

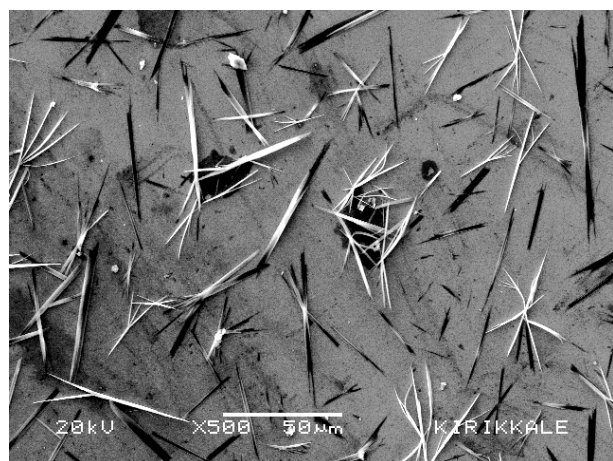
## 2. MATERIALS AND METHODS

High luminescence efficiency fluorescent products such as MEH-PPV (Poly[2-methoxy-5-(2-ethylhexyloxy)-1,4-phenylenevinylene]), Alq<sub>3</sub> (tris-(8-hydroxyquinoline)aluminum) materials are widely used as an efficient luminescent layer material. In this comparison, OLED device with MEH-PPV product over the PEDOT-PSS ((Poly (3, 4-ethylenedioxythiophene): polystyrene sulfonate) hole transfer layer was also produced. Basically, the OLED circuit is produced over a glass substrate, the ITO (indium tin oxide) layer serves as an anode and there is a luminescent fluorescence coated material over it, at last layer lithium fluoride (LiF) the electron transfer layer coated to increase the device luminescence efficiency. The lithium fluoride layer is an electron transfer layer. This thin layer was coated by dropping the LiF-water (0.7 mg/100 mL) solution over the surface and evaporating the water ingredient from the surface in a 70 degree heated incubator for one hour. Finally negative electrical connection was attached over the electron transfer layer. Gallium Indium Eutectic, known as wood metal (at liquid form), is used as the cathode connection contact, which facilitates to use over glass surface layer (Figure 1c).

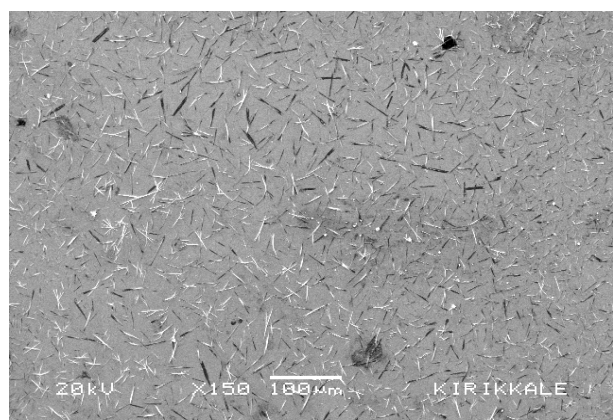
### 2.1 Chemicals and reagents

MEH-PPV, "Poly[2-methoxy-5-(2-ethylhexyloxy)-1,4-phenylenevinylene]" was purchased from Sigma-Aldrich, MEH-PPV which has got 2.3 eV band gap, average molecular weight is between 40,000-70,000. Fluorescence wavelength is between 493 nm and 554 nm. Orbital energy HOMO is -5.3 eV and LUMO is -3 eV. Electron transfer layer LiF with 99.995% purity was purchased from Sigma-Aldrich. Poly(3,4-

ethylenedioxythiophene) polystyrene sulfonate (PEDOT-PSS) is a widely used (HTL: Hole Transfer Layer) conductive polymer (3-4)% in water. It is widely used in sensor and OLED production stages. This product was also purchased from Sigma-Aldrich. ITO (indium tin oxide) coated glasses with 10 ohm/cm surface resistivity was also used for anode main substrate part, which purchased from Sigma-Aldrich. Liquid metal (Gallium-Indium eutectic, Sigma-Aldrich) was also used for cathode electrical contact connections to work OLED device.



(a)



(b)

**Figure 1.** Pictures of the spin coated 5,7 dibromo-8-hydroxyquinoline over PEDOT-PSS, ITO glass taken under 500 a) and 150 b) magnifications are shown.

## 2.2 Preparation of quinoline derivatives

1,2,3,4-tetrahydroquinoline-6,8-dicarbonitrile was synthesized via nucleophilic substitution reactions reported by previous related publications.<sup>14, 15</sup> The 5,7 dibromo-8-hydroxyquinoline was prepared according to literature reports isolated compounds were fully characterized with melting point, elemental analysis, FT-IR, <sup>1</sup>H, <sup>13</sup>C, HMBC and HETCOR spectroscopy in these paper.<sup>15,16</sup> Also, 8-nitroquinoline was purchased commercially from Sigma Aldrich.

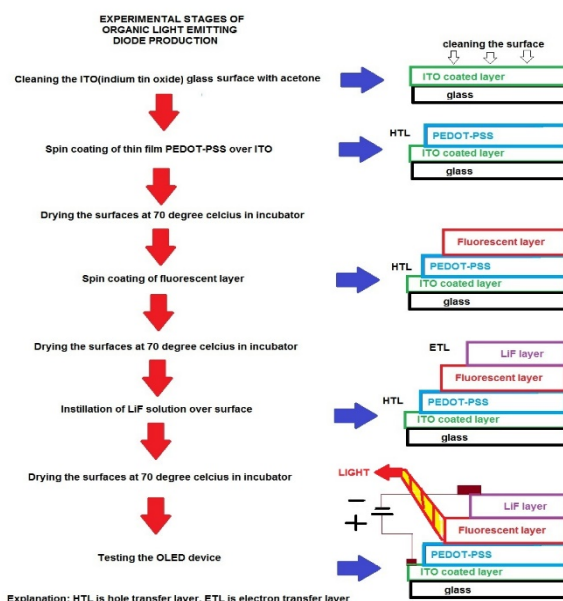
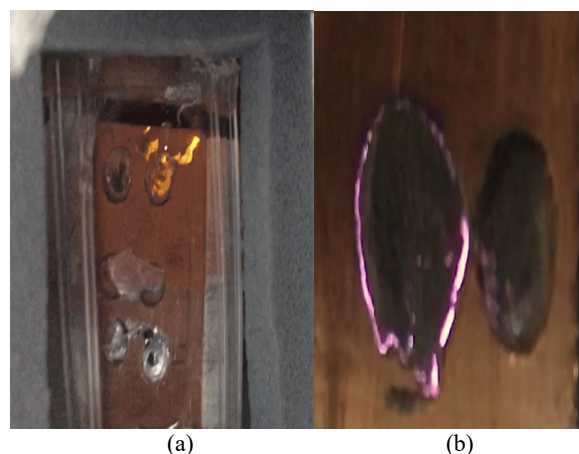
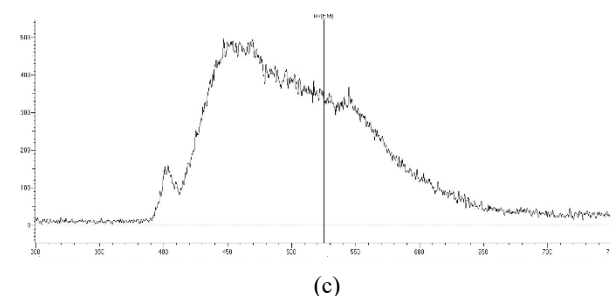


**Figure 2.** Experimental stages of OLED device production and explanations, ladder type coating prevents short circuit.



(a)

(b)



(c)

**Figure 3.** a) OLED device produced by MEH-PPV with luminescence light b) OLED diode circuit made with synthesized 5,7 dibromo-8-hydroxyquinoline and its operation c) 5,7-dibromo-8-hydroxyquinoline OLED device illumination spectrum.

## 3. RESULTS AND DISCUSSION

### 3.1 Chemistry

Quinoline derivatives, determined of their photophysical properties were prepared in recent papers. In brief, 5,7-

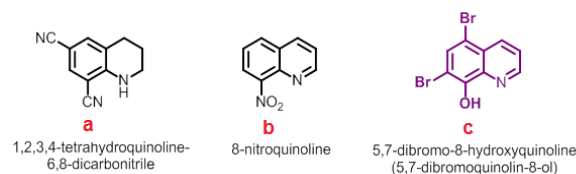
dibromo-8-hydroxyquinoline (c) **Figure 4** was obtained by treatment of 8-hydroxyquinoline and molecular bromine in ionic reaction conditions.<sup>6</sup> As seen in **Figure 4**; 6,8-dicyano-1,2,3,4-tetrahydroquinoline (a) was synthesized by  $S_NAr$  reactions in reflux temperature.

### 3.2 OLED device production

Organic light emitting device experimental sequences were explained in **Figure 2**. At first stage all surfaces must be cleaned; surfaces were cleaned with acetone and dried in incubator. Coatings were done using a ladder type passing and coating to prevent short circuit between all previous and subsequent layers. Spin coating device was designed with an 12 volt working fan. At second experimental stage PEDOT-PSS polymer layer was spin coated and dried in incubator at 70 degree celcius. At third stage fluorescent layer was coated with spin coating. After drying surfaces at 70 degree celcius LiF layer was coated. LiF is soluble in water this solution was dropped over the fluorescent layer and dried in incubator at 70 degree celcius. After all coatings completed, OLED device was tested and photographed (**Figure 3**).

When the surface resistance is measured with a multimeter device, it is seen that the bare resistance of the surface with just ITO (indium tin oxide) coated glass is 36 ohm/cm. An home made spin coating device was used for thin film coating over ITO glass surfaces. After the spin-coating of organic quinoline material; surface coating resistance was measured and found as 40 ohm/cm. With the spin coating system application, the homogenous surface coating was achieved. The new coating system was provided a 46 ohm/cm surface resistance on the glass. The surface coating was also examined with the SEM (JEOL-3010) electron microscope system. (**Figure 1a, b**) Unlike commercial OLED polymers, the newly synthesized 5,7-dibromo-8-hydroxyquinoline (c) was prepared by reaction of 8-hydroxyquinoline with 2 equivalent moles of  $Br_2$  under mild conditions.<sup>6</sup> Also final product 5,7-dibromo-8-hydroxyquinoline solution was prepared with chloroform solvent to coat surfaces. As an OLED substrate; ITO (indium tin oxide) coated glasses were used. PEDOT-PSS second coated layer was used as a hole transfer layer. As the third layer 5,7-dibromo-8-hydroxyquinoline layer was coated over the PEDOT-PSS layer. When the device was completed as explained; for as a test contact to which the negative voltage (cathode) will be given, the circuit was completed and operated with a smooth surfaced aluminum metal surface on the 5,7-dibromo-8-hydroxyquinoline fluorescent layer material. In subsequent tests, it was noticed that the surface should not be scratched. Instead of the aluminum cathode; Ga-In-Eu (wood metal - this is in liquid form) is used to prevent deterioration of the coating. Since this material, which is a liquid metal like mercury, cannot be held by a hand, a pit is formed over the circuit boards in the form

of a cavity, and wood metal was placed in it. With this setup on copper, the negative voltage was given over from Ga-In-Eu metal and positive voltage was given over the anode ITO layer. Three different compounds were produced for OLED purposes. These compounds are 6,8-dicyano-1,2,3,4-tetrahydroquinoline (**Figure 4a**), 8-nitroquinoline (**Figure 4b**) and another is 5,7-dibromo-8-hydroxyquinoline (**Figure 4c**).

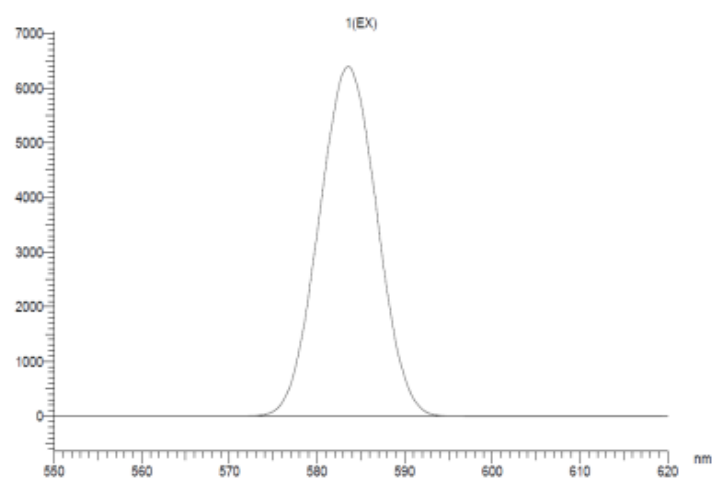
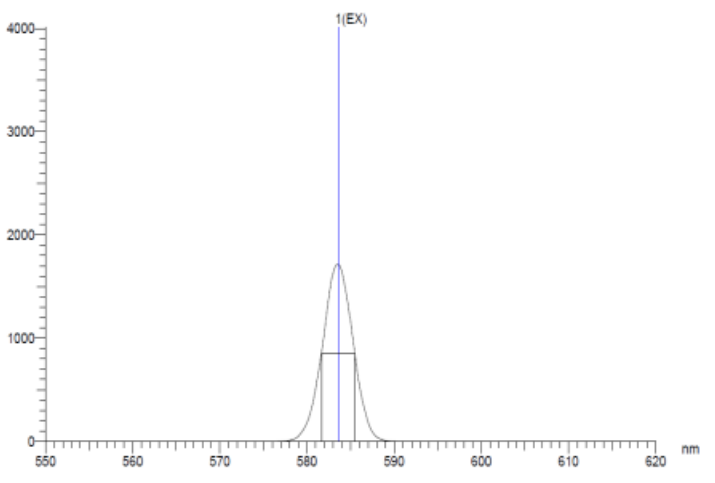
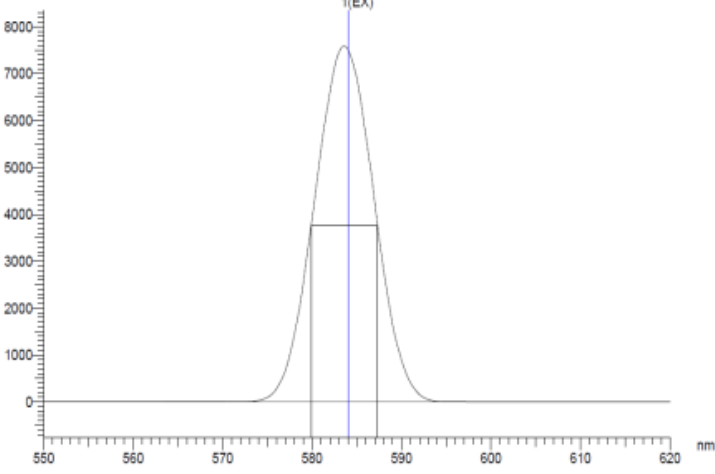


**Figure 4.** Main structures of substituted quinoline derivatives. Fluorescences yield of synthesized three heterocyclic organic ligand substances was compared for production of OLED.

The fluorescence properties of these produced products were examined with a Hitachi-7000 spectro fluorometer device. The experimental parameters used for the measurement are High voltage 900V, scan speed 60 nm/min, Ex-slit 5 nm and Em-slit 5 nm. Fluorescence measurement were found between the 575 nm to 593 nm wavelengths in all three samples. The phosphorescence material named 1,2,3,4-tetrahydroquinoline-6,8-dicarbonitrile (a), the second sample, showed slightly more phosphorus property than the 8-nitroquinoline (b). The first sample had a peak at height of 6300 (arbitrary units) while the second sample showed a phosphorus signal at 7300 (arbitrary units) level. The third sample phosphorus signal peak height exceeded the 10000 limit level in the same measurement parameters, and the Ex-slit and Em-slit setting were reduced from 5 nm to 2.5 nm. In this way, the phosphorus radiation completely measured with the photomultiplier tube of the Hitachi 7000 system. Signal numerical value was reduced and the measurement signal at 1700 was found. The third example 5,7-dibromo-8-hydroxyquinoline (c) with the highest luminescence property of these produced samples was used to made an OLED device.

The phosphorescence peaks of all three produced products are shown in **Figure 5** above. The experimental parameters used are High voltage: 700V, Ex -slit = 5 nm, Em-slit = 5 nm, scan speed 60 nm / min. It showed fluorescence in all three materials produced. In 5,7 dibromo-8-hydroxyquinolin sample, the fluorescence spectrum taken between 580 nm and 620 nm was at the highest level (**Figure 4**). By creating an OLED circuit with this material, it was desired to see the glow of the luminescence led circuit. Prior to this study, the OLED circuit was created using the material Poly [2-methoxy-5- (2-ethylhexyloxy) -1,4-phenylenevinylene], which was commercially available from Sigma-Aldrich, and operated by oled.



Fluorescence Intensity (Y axis) vs Wavelength (X axis)	Material	Fluorescence intensity (A.U.)
	8-nitroquinoline	6300 Slit 5nm
	6,8-dicyano-1,2,3,4-tetrahydroquinoline	1700 Slit 5nm
	5,7-dibromo-8-hydroxyquinoline  This quinoline ligand has the maximum fluorescence response from the others, <b>This ligand was used for OLED device production</b>	7300 Slit 2.5nm

**Figure 5.** Fluorescence measurement peaks of polymer materials produced a) 8-nitroquinoline (b), b) 1,2,3,4-tetrahydroquinoline-6,8-dicarbonitrile (a), c) 5,7-dibromo-8-hydroxyquinoline (c).

Luminescent light was taken with MEH-PPV product in Figure 4a. This luminescence light worked optimally at 12-13Volt values. When the value of 15Volt is reached, the OLED circuit is broken. Bare ITO surface resistance value is around 10 ohm / cm. After spin coating process over the surface coating was controlled relating the electrical resistance. The electrical conductivity of the 5,7-dibromo-8-hydroxyquinoline coated surface was measured with a multimeter. Surface conductivity was changed between 46 ohm / cm and 40 ohm / cm values over the surfaces. 5,7-dibromo-8-hydroxyquinoline OLED device has opened and experimental picture was showed in Figure 4b. OLED diode light response was defined in the UV (ultraviolet) region and recorded with HITACHI 7000 spectrofluorometer. (Figure 4c). Nowadays similar UV light sources production are necessary to simulate degradation of materials after sun exposure.<sup>17</sup>

#### 4. CONCLUSION

The OLED circuit has also been successfully run. It was seen that surfaces of coated layers are very sensitive to deterioration. Scratching the surface in OLED circuits can cause damaging of the thin coated surfaces and the circuit would not to work. Therefore, taking electrical contact with liquid metals such as Gallium or Gallium Indium Eutectic will also ensure that the circuit is tested without deterioration. Crystal and polymer applications for new generation OLED coating would give the way for applications to be made with these devices as sensors. This preliminary study has shown that the OLED device can produce with limited laboratory equipments. The production of electronic components with high purity semiconductors using p and n type silicon wafers, thin-film coating systems and lithography-based manufacturing techniques require laboratories and production facilities with very high costs today. With polymer coating and using spin coating systems; device production would be easier. High school and university students would have an opportunity to produce electronic devices with the way explained, also using the practical coating techniques explained in this study. Also known or synthesized luminescent materials can be investigated by these methods even within limited laboratory equipments or devices.

#### ACKNOWLEDGEMENTS

This work was supported by Scientific Research Projects Coordination Unit of Kırıkkale University (Project number 2016/076).

#### Conflict of interests

*There is no conflict of interest with any person, institution or company, etc.*

#### REFERENCES

- Jonas, F.; Heywang, G. *Electrochim. Acta* **1994**, *39* (8–9), 1345–1347.
- O'Hara, P. B.; St. Peter, W.; Engelson, C. *J. Chem. Educ.* **2005**, *82* (1), 49.
- Banerji, A.; Tausch, M. W.; Scherf, U. *Educ. química* **2013**, *24* (1), 17–22.
- Rehahn, M. *Chemie unserer Zeit* **2003**, *37* (1), 18–30.
- Doğan, M. *J. Mater. Sci. Mater. Electron.* **2021**, *32* (17), 22506–22516.
- Ökten, S.; Çakmak, O.; Saddiqa, A.; Keskin, B.; Özdemir, S.; İnal, M. *Org. Commun.* **2016**, *9* (4).
- Short, B. R. D.; Vargas, M. A.; Thomas, J. C.; O'Hanlon, S.; Enright, M. C. *J. Antimicrob. Chemother.* **2006**, *57* (1), 104–109.
- Albrecht, M.; Fiege, M.; Osetska, O. *Coord. Chem. Rev.* **2008**, *252* (8–9), 812–824.
- Montes, V. A.; Pohl, R.; Shinar, J.; Anzenbacher Jr, P. *Chem. Eur. J.* **2006**, *12* (17), 4523–4535.
- Bardez, E. *Isr. J. Chem.* **1999**, *39* (3–4), 319–332.
- Isshiki, K.; Tsuji, F.; Kuwamoto, T.; Nakayama, E. *Anal. Chem.* **1987**, *59* (20), 2491–2495.
- Lakshmi, A.; Balachandran, V.; Janaki, A. *J. Mol. Struct.* **2011**, *1004* (1–3), 51–66.
- Ahmed, M. J.; Haque, M. E. *Anal. Sci.* **2002**, *18* (4), 433–439.
- Ökten, S.; Cakmak, O.; Erenler, R.; Şahin, Ö. Y.; Tekin, Ş. *Turkish J. Chem.* **2013**, *37* (6), 896–908.
- Ökten, S.; Cakmak, O. *Tetrahedron Lett.* **2015**, *56* (39), 5337–5340.
- Ökten, S.; Cakmak, O.; Tekin, S.; Koprulu, T. K. *Lett. Drug Des. Discov.* **2017**, *14*(12), 1415-1424.
- Doğan, M. *Microsc. Res. Tech.* **2021**, *84*(11),2774–2783.